University of Michigan
EECS517 / NERS 578 Physical Processes in Plasmas Handouts
Fall 2010
Prof. Mark J. Kushner mjkush@umich.edu

Revision Schedule:

Version	Date	Comment
1	30 Aug 2010	Initial distribution
2	6 Sept 2010	Updated Class Schedule with Alternate Class times and locations

EECS 517 (NERS 578). Physical Processes in Plasmas
Fall 2010 - TuTh 10:30 AM - 12:00 PM - 1012 EECS

Instructor: Mark J. Kushner
2236 EECS Building (734-647-8148)
Office Hours: Afternoons or by appointment
e-mail: mjkush@umich.edu

Grader-Teaching Assistant: To be announced

Goals of Course: This course addresses the fundamental science and the technology of low temperature, partially ionized, non-equilibrium plasmas. This class of plasmas is used, for example, for etching and deposition of materials, surface treatment, lighting sources, flat panel displays, welding, laser ablation, lasers and biomedical applications. These plasmas are also naturally occurring, such as the aurora, shock waves and lightning. The objectives of this course are to first provide a foundation of the fundamentals of electron-atom collisions, electron and ion transport and the different ways in which low temperature plasmas are created. After providing this foundation, the course will apply those fundamentals to study of technologies which use partially ionized plasmas, with examples taken from lasers, plasma materials processing, lighting sources and plasma medicine.

Grading Policy: The field of low temperature plasmas is intrinsically interdisciplinary. The linkages between the supporting fields are best appreciated by problem solving in a real-world context. As a result, one will not be able to fully benefit from the course without putting a good-faith effort into the homeworks. To acknowledge the importance of homework, it is being heavily weighted in the grading policy. The grading policy will be:

Homework	30%
Mid-Term Exam	30%
Final Project	30%
Instructor's discretion	10%

Instructor's discretion includes my qualitative assessment of students' effort towards the course (e.g., class attendance and participation).

Texts:

Required: M. Lieberman, Principles of Plasma Discharges and Material Processing, 2nd Edition (Wiley, New Jersey, 2005)

Optional Text: A. Friedman and L. A. Kennedy, Plasma Physics and Engineering (Taylor and Francis, New York, 2004)

Note that both of these texts are available electronically through a subscription by the UM Engineering Library.

"Principles of plasma discharges and materials processing" can be accessed online at http://proxy.lib.umich.edu/login?url=http://www.myilibrary.com?id=25507

"Plasma physics and engineering" can be accessed online at http://proxy.lib.umich.edu/login?url=http://www.myilibrary.com?id=34790

Course Website: The course website will be located at "http://uigelz.eecs.umich.edu → Classes → EECS 517 ". The materials that will be posted on the website include:

1. Introductory materials
2. Homework assignments
3. Handout Packages (Note that some, but NOT ALL of the handouts can also be downloaded individually!)
4. Class announcements (such as cancellations, rescheduled classes, exam dates)

Course Map

"Gaseous Electronics is the study partially ionized gases and their application to technologically relevant devices."

MICROSCOPIC → **MACROSCOPIC**

Electron collisions

Cross sections, rate coefficients

Gas discharge theory
Electron production, loss
Sheaths
Electron distribution functions
Transport coefficients

Low pressure dc discharge devices

High pressure discharges and
e-beam pumped plasmas

rf and microwave discharges

Diagnostics

Applications:
Plasma etching
Toxic Gas Remediation
Special Topics

EECS 517/NERS 578 Fall 2010

Syllabus and Reading Assignments (Version 01)

Reading assignments in Lieberman are required. Others are recommendations for background.

Unit	Topic	Reading Assignments (Chapters or sections)	
		Lieberman	Fridman
I.	Introduction	1	1
II.	Electron Collisions	3,8 Appendix A	2,3
III.	Cross Sections and Rate Coefficients	3,8	2,3
IV.	Gas Discharges	2	7
V.	Electron Continuity Equation, Diffusion, Production, Loss	2,5	4.5
VI.	Sheaths	6.1-6.5 Handouts	6.1
VII.	Electron Distribution Functions	2, Appendix B	4.1-4.2
VIII.	Transport Coefficients	5	6
IX.	Low Pressure DC Discharges	10,14	7.12-7.8
X.	High Pressure Discharges and Electron Beam Pumped Plasmas	Handouts	12
XI.	RF and Microwave Discharges	11,12	10.5-10.6, 10.9
XII.	Fully Ionized Plasmas	4, Handouts	
XIII.	Magnetic Fields in Discharges	4	6.2
XIV.	Inductively Coupled Plasmas	12	10.7
XV.	Diagnostics	6.6	
XVI.	Applications and Special Topics (to be selected by class)		
	a. Plasma Etching/Deposition/Surface Chemistry	7 , 9, 15, 16	
	b. ECR and Helicon	13.1,13.2	10.8
	c. Plasmas in Liquids	Handouts	
	d. Plasma Medicine	Handouts	
	e. Dielectric Barrier Discharges	Handouts	

Required: M. Lieberman, Principles of Plasma Discharges and Material Processing, 2nd Edition (Wiley, New Jersey, 2005)

Optional Text: A. Friedman and L. A. Kennedy, Plasma Physics and Engineering (Taylor and Francis, New York, 2004)

Class Schedule (Version 02)

The class schedule is listed below. Due to my travel commitments this Fall, we have scheduled alternate makeup lectures on Friday afternoons. The times and locations of the alternate classes are:

Alternate Classes:

Date		Time	Room
17	Sept.	4:00 – 5:30 pm	DOW 1018
24	Sept.	4:00 – 5:30 pm	DOW 1018
1	Oct.	4:00 – 5:30 pm	DOW 1018
15	Oct.	4:00 – 5:30 pm	EECS 1012
29	Oct.	4:00 – 5:30 pm	EECS 1012
5	Nov.	4:00 – 5:30 pm	EECS 1012

Class Schedule:

Class	Day	Date		Comment	Approximate (!) Topic (See Syllabus for Reading Assignment)
1	T	7	Sept.		Introduction
2	Th	9	Sept.		Electron Collisions
3	T	14	Sept.		Electron Collisions
4	Th	16	Sept.		Cross Sections and Rate Coefficients
5	F	17	Sept.	Alternate Class	Cross Sections and Rate Coefficients
	T	21	Sept.	MJK Travel	
	Th	23	Sept.	MJK Travel	
6	F	24	Sept.	Alternate Class	Gas Discharges
7	T	28	Sept.		Electron Continuity, Diffusion, Sources
	Th	30	Sept.	MJK Travel	
8	F	1	Oct.	Alternate Class	Electron Continuity, Diffusion, Sources
	T	5	Oct.	MJK Travel	
	Th	7	Oct.	MJK Travel	
9	T	12	Oct.		Electron Continuity, Diffusion, Sources
10	Th	14	Oct.		Sheaths
11	F	15	Oct.	Alternate Class	Electron Energy Distributions
	T	19	Oct.	Fall Study Break	
	Th	21	Oct.	MJK Travel	
12	T	26	Oct.		Electron Energy Distributions
13	Th	28	Oct.		Transport Coefficients
14	F	29	Oct.	Alternate Class	Low Pressure DC Discharges
15	T	2	Nov.		Low Pressure DC Discharges
16	Th	4	Nov.		High Pressure and e-beam pumped plasmas
17	F	5	Nov.	Alternate Class	High Pressure and e-beam pumped plasmas
18	T	9	Nov.		RF Discharges
19	Th	11	Nov.		RF Discharges

20	T	16	Nov.		Fully Ionized Plasmas
21	Th	18	Nov.		Magnetic Fields in Discharges
22	T	23	Nov.		Magnetic Fields in Discharges
	Th	25	Nov.	Thanksgiving Recess	
23	T	30	Nov.		Inductively Coupled Plasmas
24	Th	2	Dec.		Diagnostics
25	T	7	Dec.		Special Topics – or Project Presentations
26	Th	9	Dec.		Special Topics – or Project Presentations
	M	13	Dec.	Final Project Due (5:00 pm)	

Supplementary Texts and References
**= On Reserve at UM Engineering Library

J. R. Roth **Industrial Plasma Engineering. Vol 1 & 2** **
Practical view of low temperature plasma physics from an engineering perspective.

A. Fridman and L. A. Kennedy **Plasma Physics and Engineering** **
Comprehensive text on low temperature plasmas

A. Fridman **Plasma Chemistry** **
Physics of low temperature plasmas and application to gas phase and surface chemistry.

*C. K. Birdsall and A. B. Langdo*n **Plasma Physics via Computer Simulation** **
Introductory text on the use of Particle-in-Cell simulations for modeling plasmas.

M. Mitchner **Partially Ionized Gases** **
Mostly for fully ionized plasmas but good treatment of sheaths, continuity equations, and electron-ion collisions.

G. Bekefi **Principles of Laser Plasmas**
Specialty items such as recombination, discharge stability and vibrational excitation.

L. M. Biberman, et al. **Kinetics of Nonequilibrium Low-Temperature Plasmas**
Good general reference but difficult to read.
(Russian Translation)

S. C. Brown **Basic Data of Plasma Physics**
Classic text for most topics.

B. Chapman **Glow Discharge Processes**
Good "gut level" monograph. Good source for RF discharges.

F. F. Chen **Introduction to Plasma Physics**
Fully ionized plasmas with good treatment of Debye lengths, and magnetic field effects.

B. Cherrington **Gaseous Electronics and Gas Lasers**
Good basic introduction.

J. Cobine **Gaseous Conductors**
Extremely empirical treatment of topics but good presentation. (You can learn something from this book on the first reading.)

L. Huxley **Diffusion and Drift of Electrons in Gases**
Advanced monograph on Boltzmann Equation and Transport Coefficients.

U. Kortshagen **Electron Kinetics and Applications of Glow Discharges**
Proceedings of NATO Workshop. Very good overview articles

L. Loeb **Basic Processes of Gaseous Electronics**
Classic and comprehensive text.

D. Manos and *D. Flamm* **Plasma Etching: An Introduction**
Compilation on methods in plasma processing.

T. Mark **Electron Impact Ionization**
Thorough treatment of electron impact collisions producing ionization

E. McDaniel **Ion Molecule Reactions**
Advanced monograph on reactions between ions and neutral atoms/molecules. Good tables of reaction rate coefficients.

L. C. Pitchford, et al. **Swarm Studies and Inelastic Electron-Molecule Collisions**
Compilation of papers on fundamental studies in nonequilibrium electron transport and obtaining cross sections from swarm data.

Y. Razier **Gas Discharge Physics**
If you are going to buy a second text, get this one. It has all the material that's important, but is difficult to read.

Y. Razier **Radio Frequency Capacitive Discharges**
Exhaustive treatment of this important discharge device for plasma etching.

S. Rossnagel **Handbook of Plasma Processing Technology**
Compilation of papers on basics of plasma etching and deposition.

B. M. Smirnov **Physics of Ionized Gases**
Good general reference but difficult to read. (Russian Translation)

A. von Engel **Ionized Gases**
Collection of lectures given at Oxford.
Considered a classic for introduction to field.

A. von Engel **Electric Plasmas; Their Nature and Uses**
Simplified view of gas discharges but good introduction.

J. Waymouth **Electric Discharge Lamps**
Defining text for fluorescent lamp physics.

Projects

In lieu of a final exam, there will be a final project. The project should consist of developing a model for, or performing an in depth analysis of, a low temperature plasma or electric discharge system. Some possible choices of electric discharge systems are:

- Plasma processing reactors
- Fluorescent lamps
- He-Ne, excimer, CO_2 lasers
- Sputter deposition reactors
- E-beam pumped systems
- Arc jets and plasma thrusters

The project should include a literature search to provide you with background on how these devices operate and to see how other researchers have analyzed them. Some of the models which appear in the literature are quite involved and complex. The intent of the project is not for you to duplicate the complexity of those models. Rather, the intent is to give you some sense of how the device and the "final product" (e.g., laser power, deposition rate, etch rate) scales. Your model should have at least the degree of sophistication of our homework assignments but should include real device parameters. For example, use the actual gas pressures, gas mixtures, dimensions, cross sections, currents, and voltages. (Note, you can obtain the real cross sections for the majority of cases of interest by request from M. Kushner.)

Your final project deliverables will consist of the written report and, optionally, a presentation to the class. The limit on length is 25 pages, though 25 pages are not required. (Fewer pages of higher quality are preferred.) Please include a description of the discharge system, how you have analyzed it, the scaling laws you developed and a discussion of what you have learned. Generously use plots to display parametric results. Your analysis might include issues such as:

- Electron densities
- Electron and ion temperatures
- Current density, power deposition, operating E/N
- Etch or deposition rates
- Electron or ion energy distributions
- Efficiency of producing the "product"
- Densities of excited states.
- Spectrum of emitted light.

Due dates: Optional Oral presentations: December 7 & 9, 2010
Report: Monday, December 13, 2009, 5:00 PM
Paper copy to Prof. Kushner office, PDF copy to mjkush@umich.edu

Units and Best Practice

Units prove to be a confusing aspect of this course. The units which are *commonly in use* in the field are the "standard" for this course. Unfortunately, the units are "mixed" (that is, a mixture of cgs and mks). Some useful conversion factors are listed below. Some best practices you should follow are:

1. ALWAYS perform a units analysis and perform a "sanity" check to determine that your answer is reasonable. In most cases, "unreasonable" answers are a result of unit problems. For example, if your answer is that the argon ion density in a plasma etching reactor is 10^{50} ions/cm^3, your answer is unreasonable and you probably have a units problem. You know your answer is unreasonable since if the density is really 10^{50} argon ions/cm^3, the mass of 10 cm^3 of the plasma would be equal to twice the mass of the earth.

2. **Never, ever be confused by expressing temperature in Energy Units (or vice-versa). Temperature in Energy Units ALWAYS Means**

$$T\ (eV) \equiv kT\ (eV)$$

3. Unless specified otherwise, you final answers in homework problems should be expressed in the following units.

Electron energies or temperatures	eV
Atomic or molecular energies or temperatures	K or eV
Lengths	cm
Electron, atomic or molecular masses	AMU or g
Electron, atomic or molecular speeds	cm/s
Cross sections	cm^2 or A^2
Mobilities	cm^2/V-s
Diffusion coefficients	cm^2/s
Rates coefficients (1st, 2nd, 3rd order)	s^{-1}, cm^3/s, cm^6/s
Electric fields	V-cm^{-1}
Normalized Electric Fields	V-cm^{-2} or Td (10^{-17} V-cm^2)
Densities	cm^{-3}
Power	W
Power deposition (specific)	W-cm^{-3}
Current density	Amps-cm^{-2}

Useful Conversion Factors

$k = 1.38 \times 10^{-16}$ erg/K $= 1.38 \times 10^{-23}$ J/K

1 eV $= 1.6 \times 10^{-12}$ ergs $= 1.6 \times 10^{-19}$ J $\equiv$ 11,594.2 K

$q = e = 1.6 \times 10^{-19}$ C (coulomb) $= 4.8 \times 10^{-10}$ esu

1 V = 1 J/C $= 10^{7}$ erg/C

$\varepsilon_o = 8.85 \times 10^{-12}$ [F/m or C^2/m-J] $= 8.85 \times 10^{-14}$ [F/cm or C^2/cm-J]

m_e (electron mass) $= 0.911 \times 10^{-27}$ g $= 0.911 \times 10^{-30}$ kg

E/N: 1 Td (Townsend) $= 10^{-17}$ V-cm^2 $= 10^{-21}$ V-m^2 = 0.354 V/cm-Torr at (T = 273 K)

1 $Å^2$ $= 10^{-16}$ cm^2 $= 10^{-20}$ m^2

1 atm = 760 Torr = 1.013 bar

Gas Density: $N = \frac{P}{kT} = 9.654 \times 10^{18} \frac{P(\text{Torr})}{T(K)}$ cm^{-3}

1 m^3 $= 10^6$ cm^3

Useful Relationships

Electron speed for energy ε : $v = \left(\frac{2\varepsilon}{m_e}\right)^{1/2} = 5.93 \times 10^7 \, (\varepsilon(\text{eV}))^{1/2}$ cm/s

Average electron thermal speed for temperature T_e: $v = \left(\frac{8kT_e}{\pi m_e}\right)^{1/2} = 6.69 \times 10^7 \, (T_e(\text{eV}))^{1/2}$ cm/s

Debye Length: $\lambda_D = \underset{\text{mks}}{\left(\frac{\varepsilon_o kT_e}{n_e q^2}\right)^{1/2}} = \underset{\text{cgs}}{\left(\frac{kT_e}{4\pi n_e q^2}\right)^{1/2}} = 743\left[\frac{T_e(eV)}{n_e\left(cm^{-3}\right)}\right]^{1/2} cm$

Plasma Frequency:

$$\omega_p \text{ (radian/s)} = \underset{\text{mks}}{\left(\frac{n_e q^2}{m_e \varepsilon_o}\right)^{1/2}} = \underset{\text{cgs}}{\left(\frac{4\pi n_e q^2}{m_e}\right)^{1/2}} = 5.64 \times 10^4 \left[n_e\left(cm^{-3}\right)\right]^{1/2} \frac{radians}{s}$$

Rate coefficient: $k\left(\frac{cm^3}{s}\right) = \langle \sigma \bullet v \rangle$ (e.g. (e.g. $\frac{\partial N}{\partial t} = n_e k N$))

σ = cross section cm^2 v = velocity cm/s

Conductivity: $\sigma = \frac{n_e q^2}{m_e \nu_m} = 2.81 \times 10^{-4} \frac{n_e\left(cm^{-3}\right)}{\nu_m\left(s^{-1}\right)} \frac{1}{\Omega - cm}$

ν_m = electron momentum transfer collision frequency

Electron Mobility: $\mu_e = \frac{q}{m_e \nu_m} = \frac{1.756 \times 10^{15}}{\nu_m\left(s^{-1}\right)} \frac{cm^2}{V - s}$

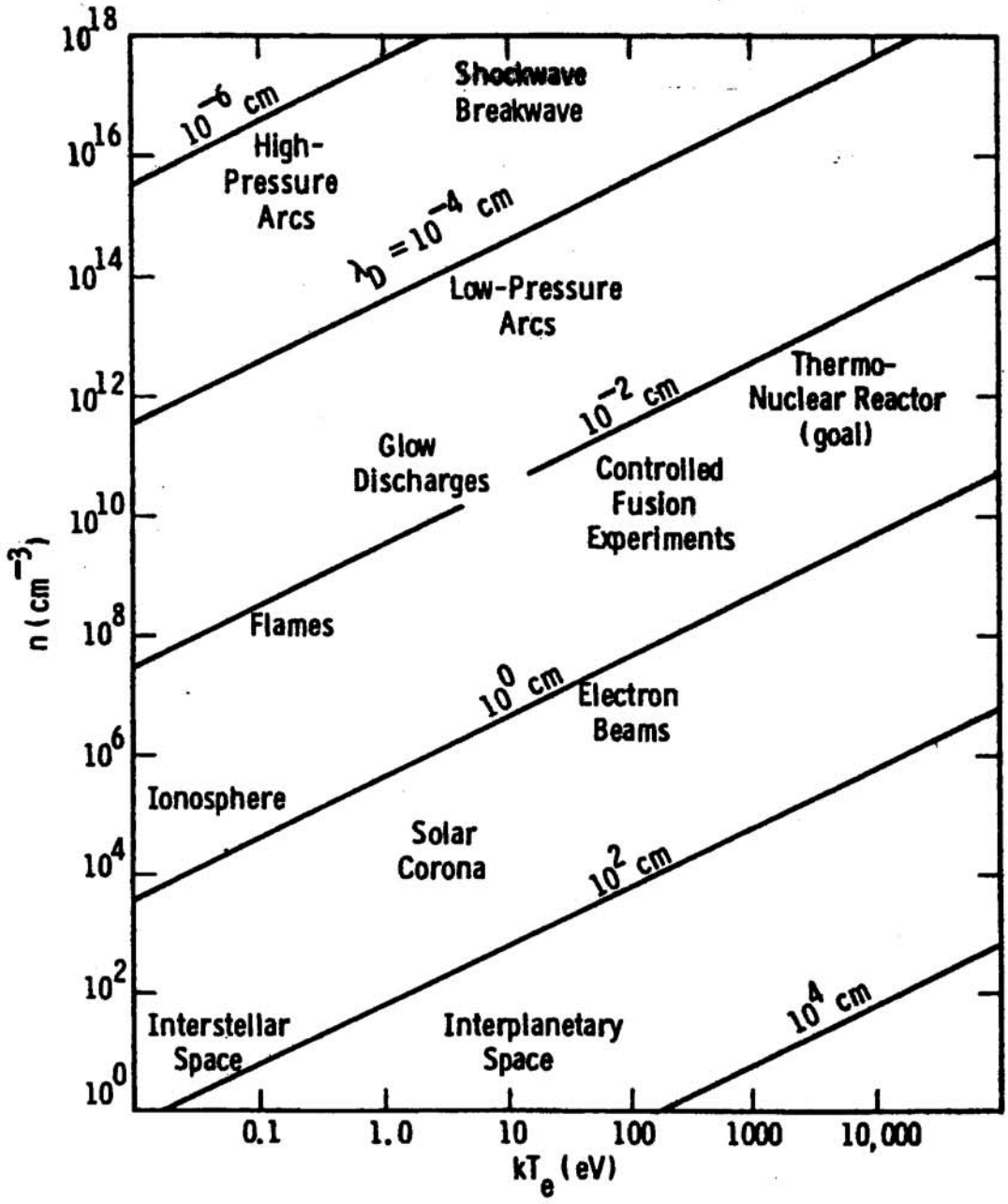

Fig. 1. Typical plasmas characterized by their electron energy and density [2].

Reference: Cobine

COPPER VAPOR LASER

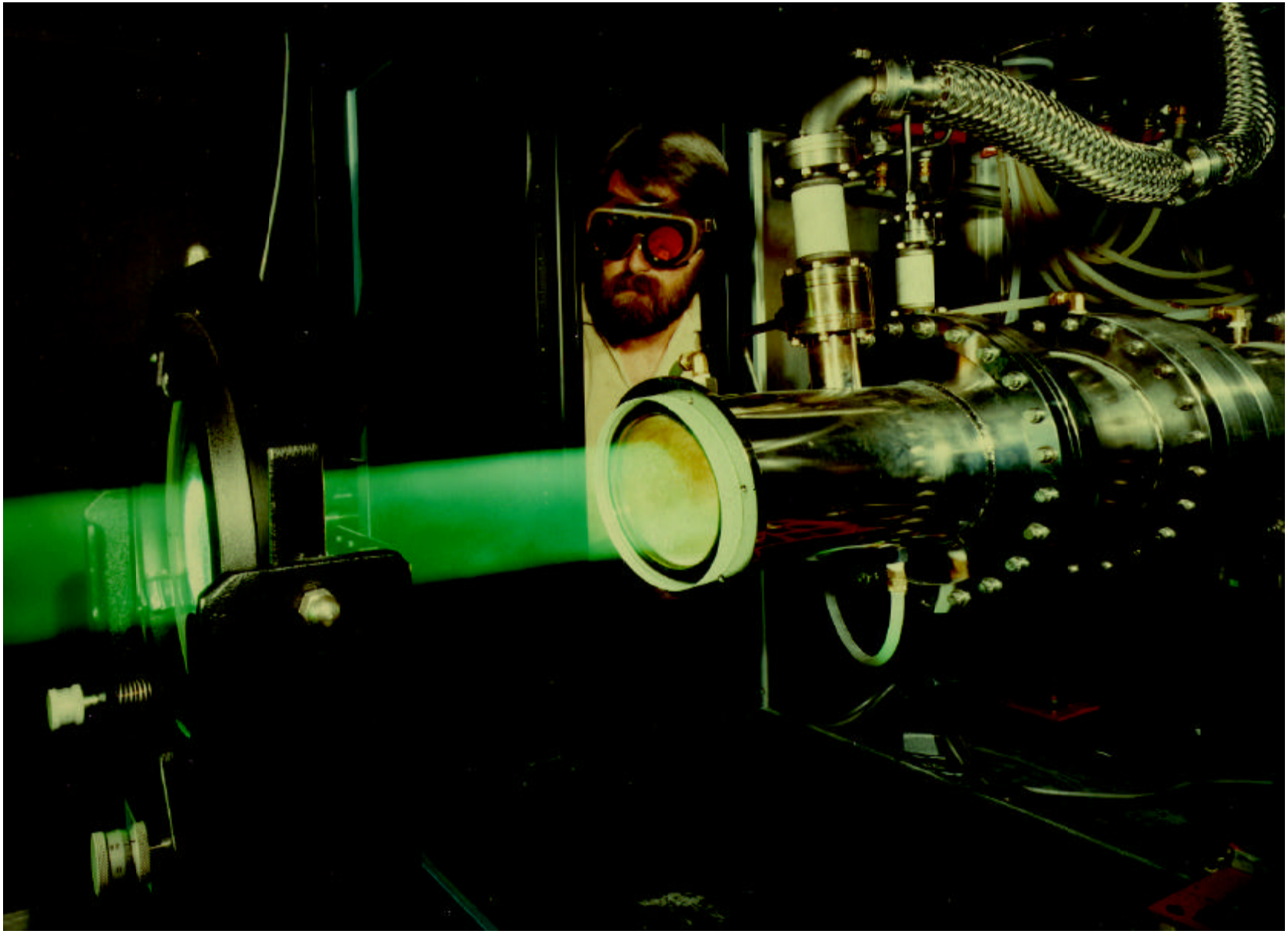

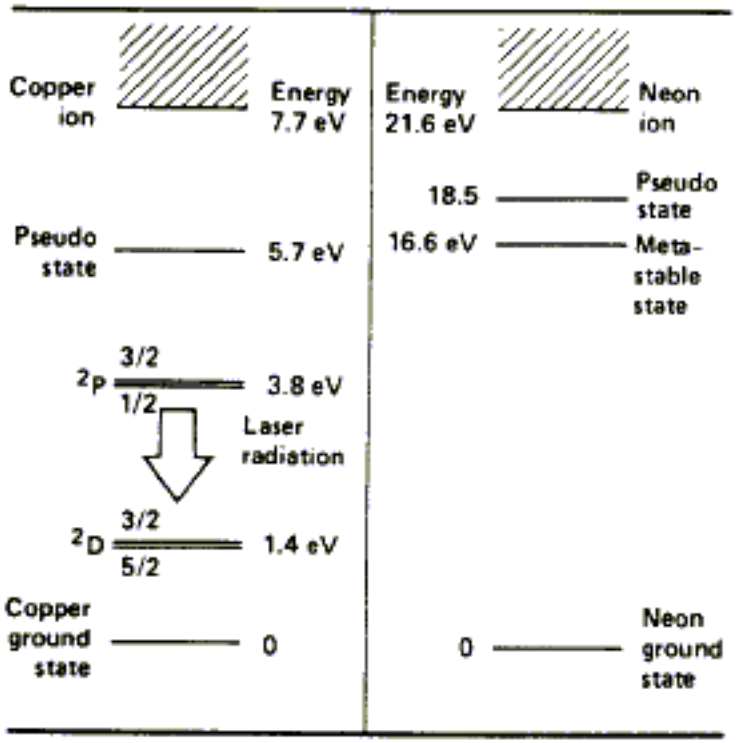

Copper and Neon Energy Levels

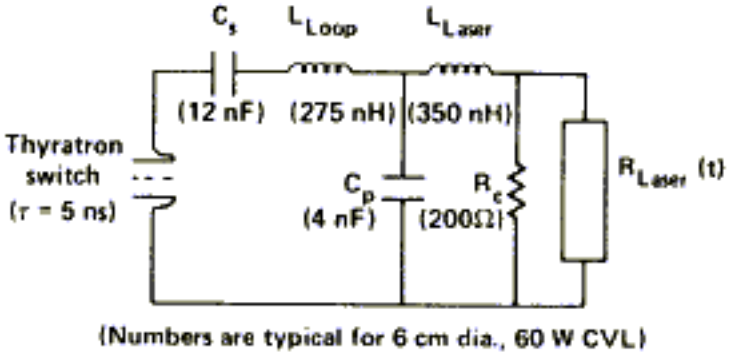

Typical Pulsed Power Circuitry

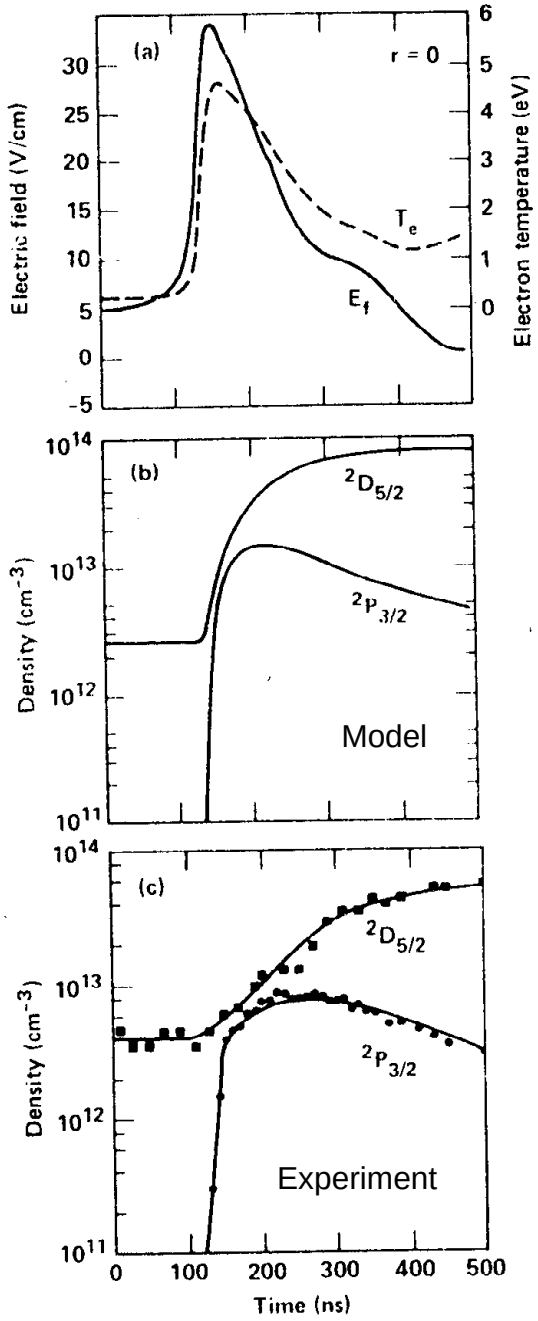

Laser Parameters During Discharge Current Pulse

cvl parameters

Gaseous Electronics Conference Reference Cell

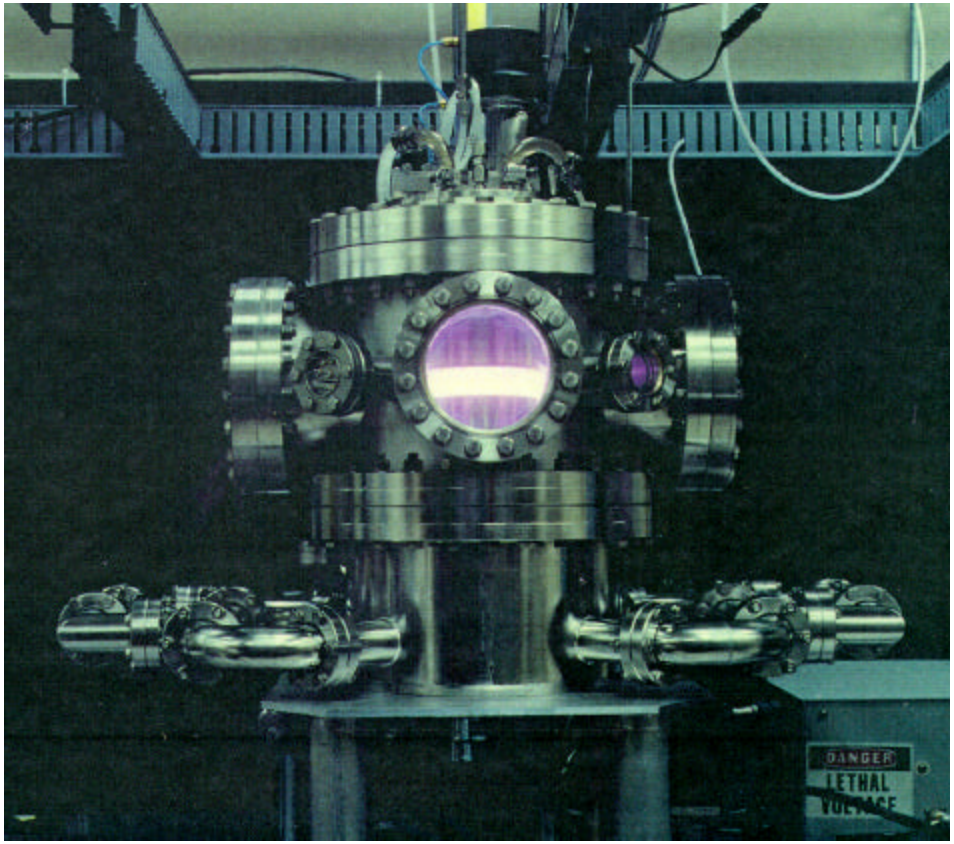

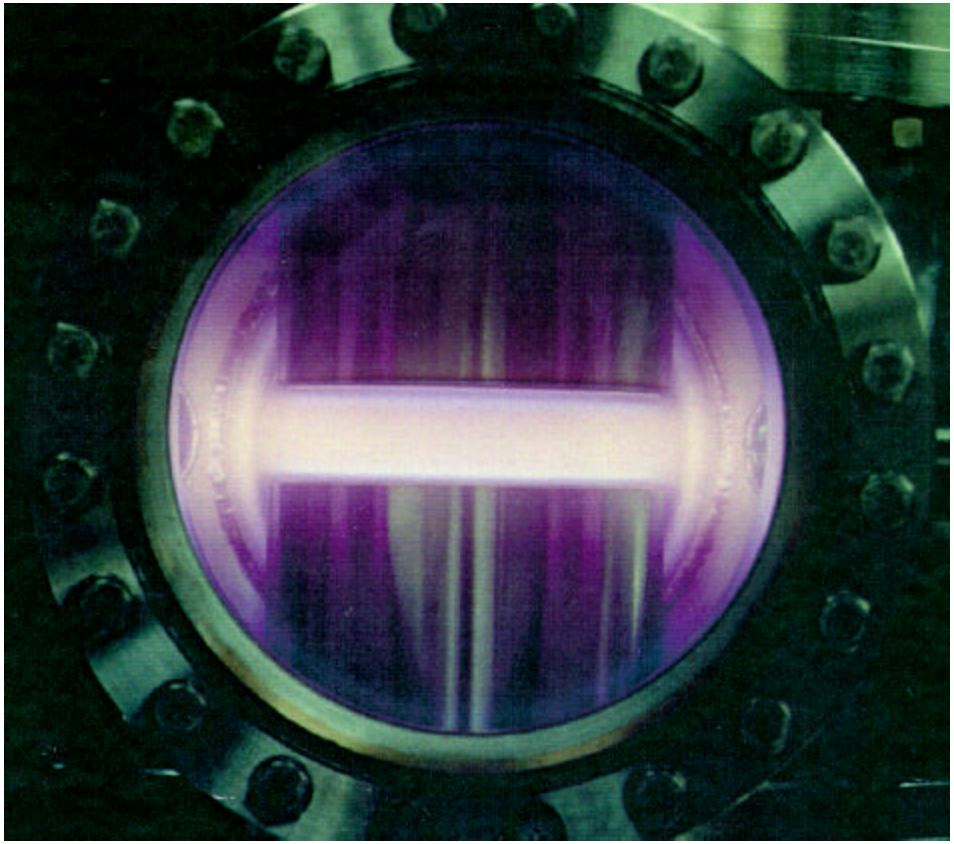

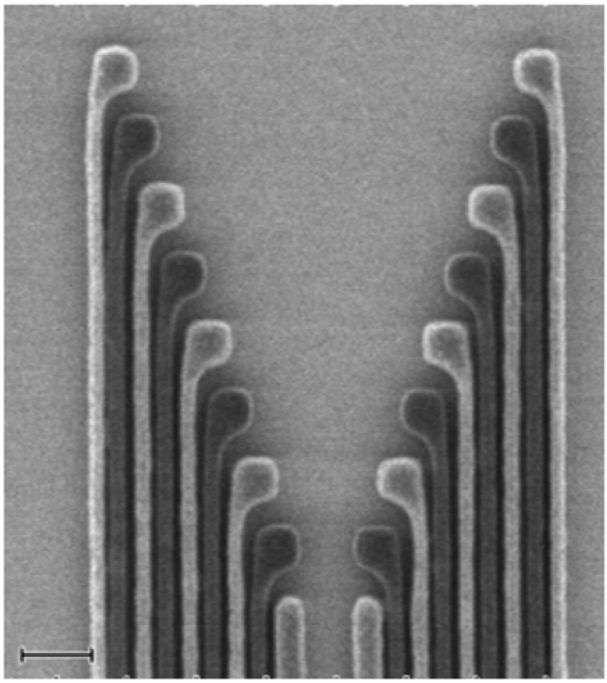

32nm half pitch poly Si gates plasma etched using a double pattering lithography technique.

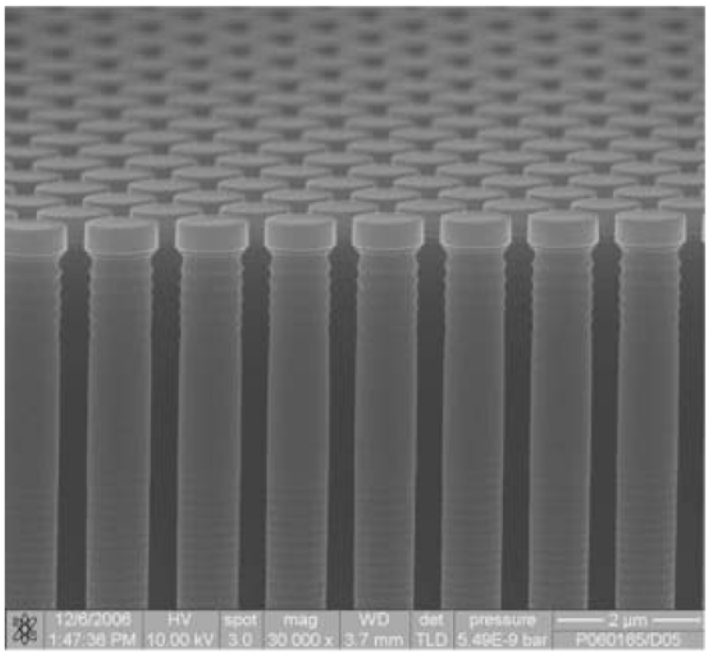

Deep Si etching for a liquid separation device.

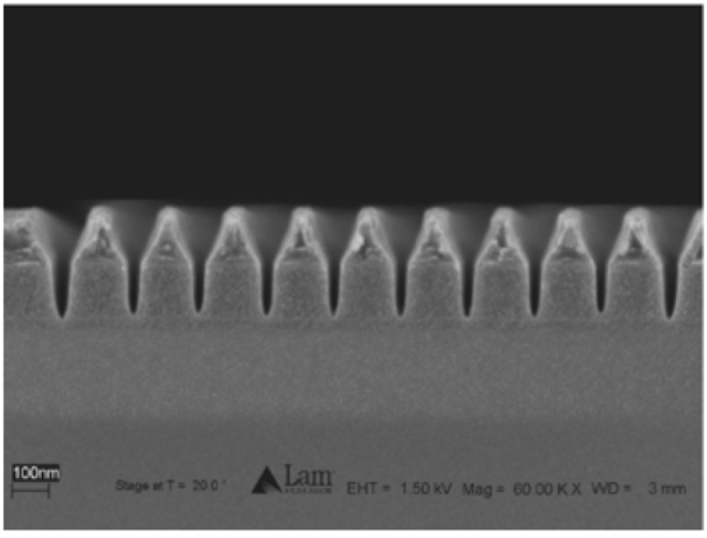

Etch of 30-nm wide trenches in a k=3.0 low-k material, using a next-generation patterning technique.

IMEC 2006 Scientific Report, http://www2.imec.be/

M. A. Vyvoda et al, "Effects of plasma conditions on the shapes of features etched in Cl_2 and HBr plasmas: I. Bulk crystalline silicon etching", J. Vac. Sci. Tech. A **16**, 3247 (1998)

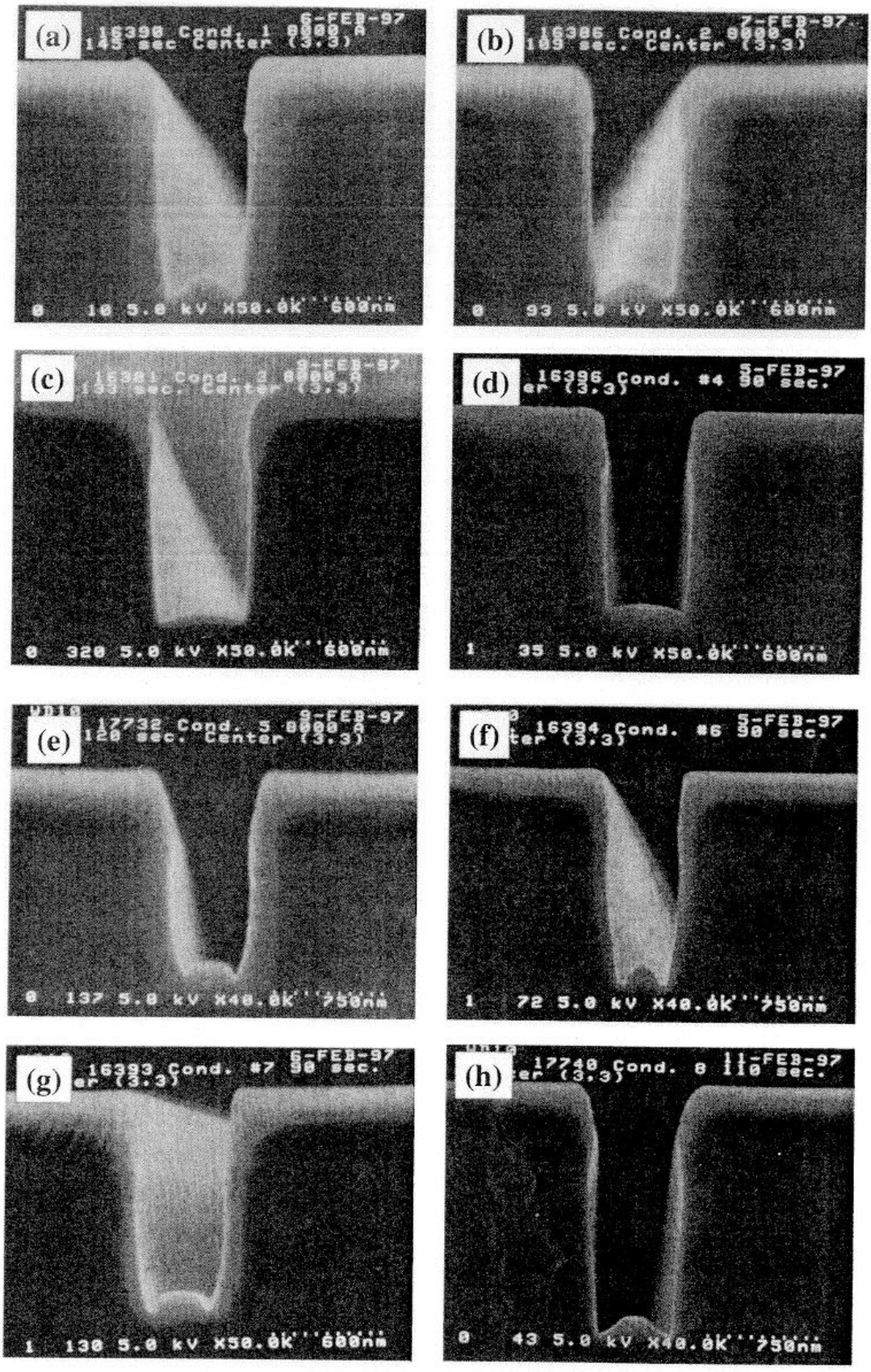

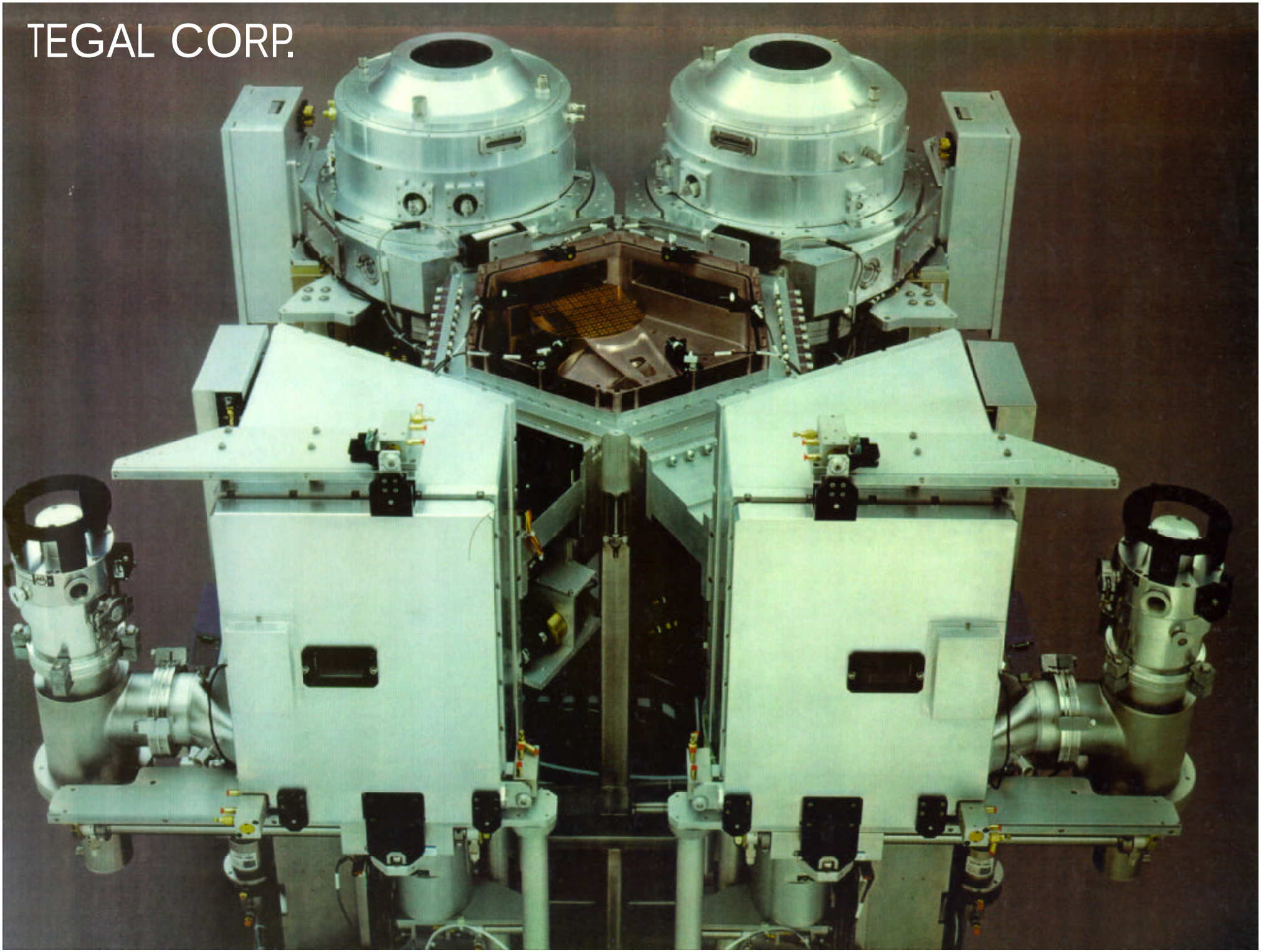
TEGAL CORP.

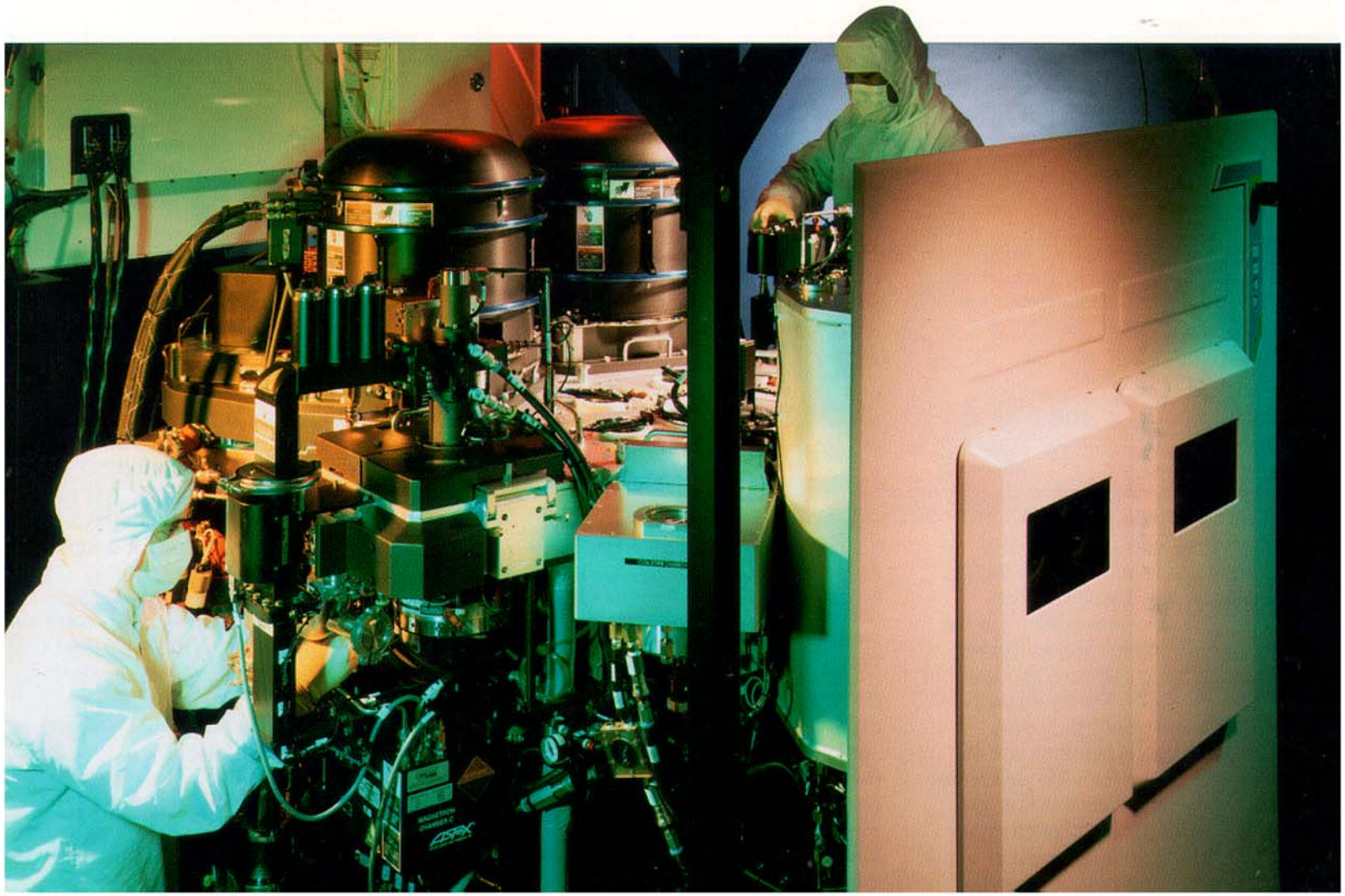

Applied Materials, Inc. - DPS (Decoupled Plasma Source)

Ref: Applied Materials, Inc.

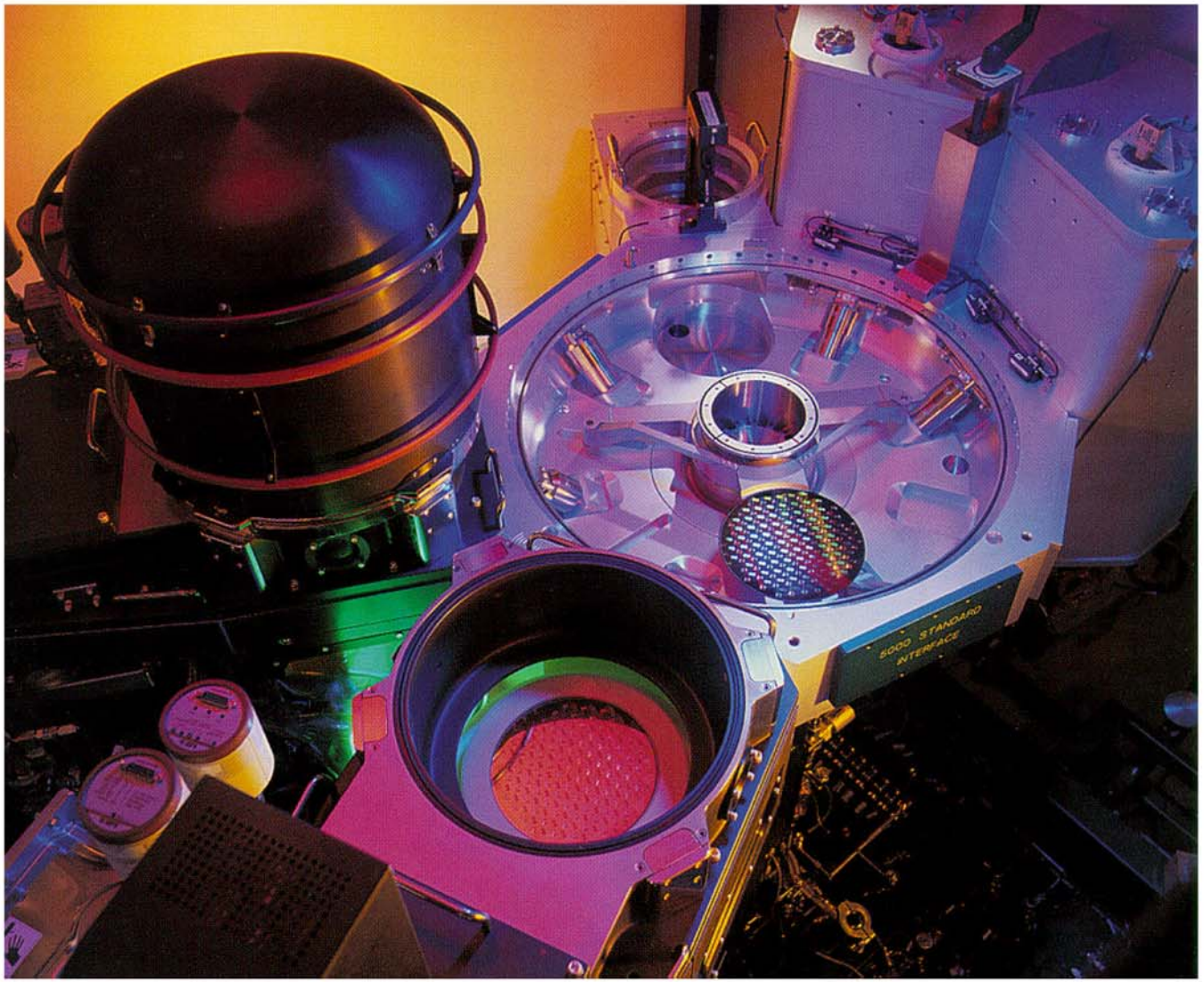

Applied Materials, Inc. - DPS (Decoupled Plasma Source)

Ref: Applied Materials, Inc.

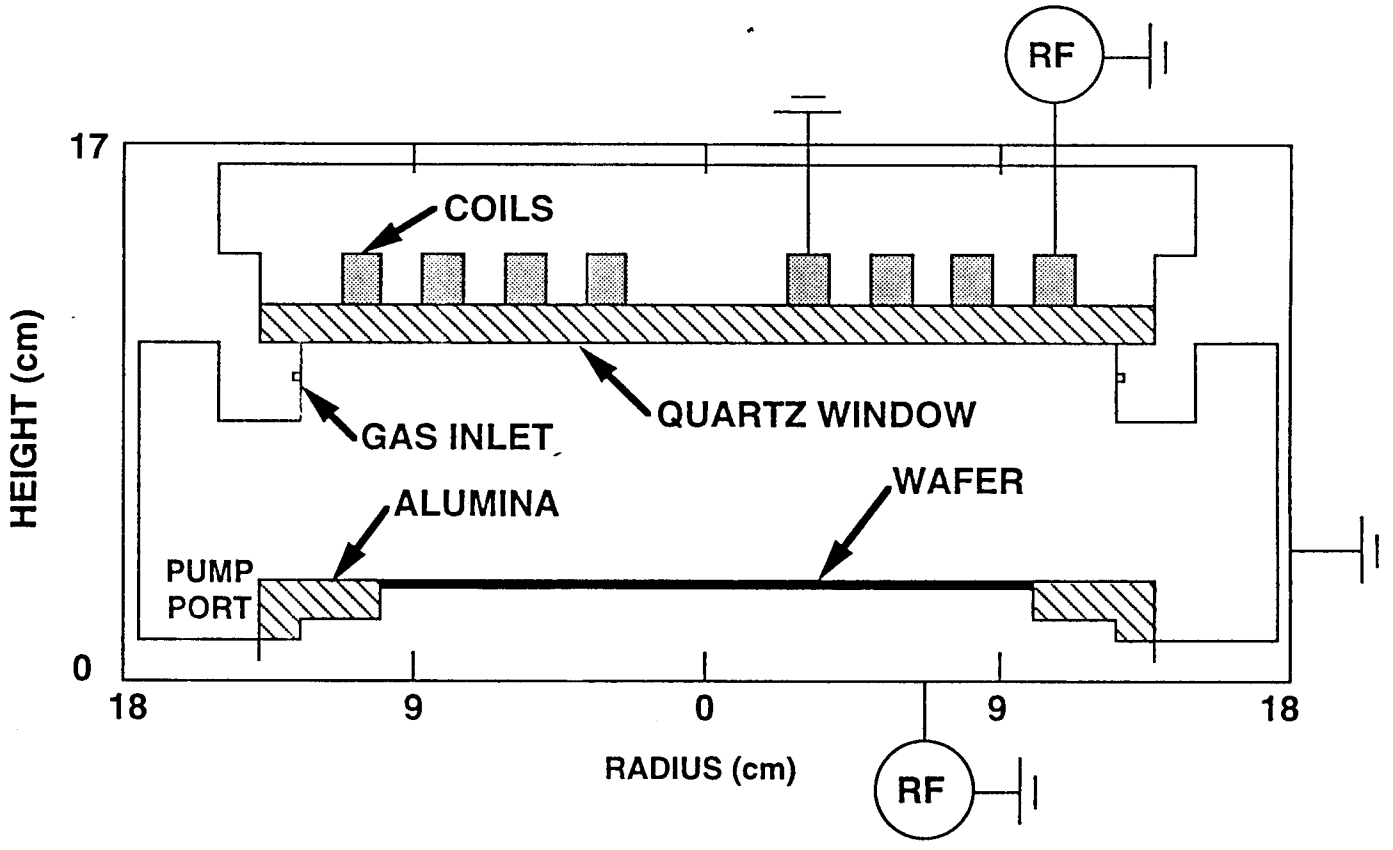
RF
17
COILS
HEIGHT (cm)
GAS INLET
QUARTZ WINDOW
WAFER
ALUMINA
PUMP
PORT
0
18
9
0
9
18
RADIUS (cm)
RF

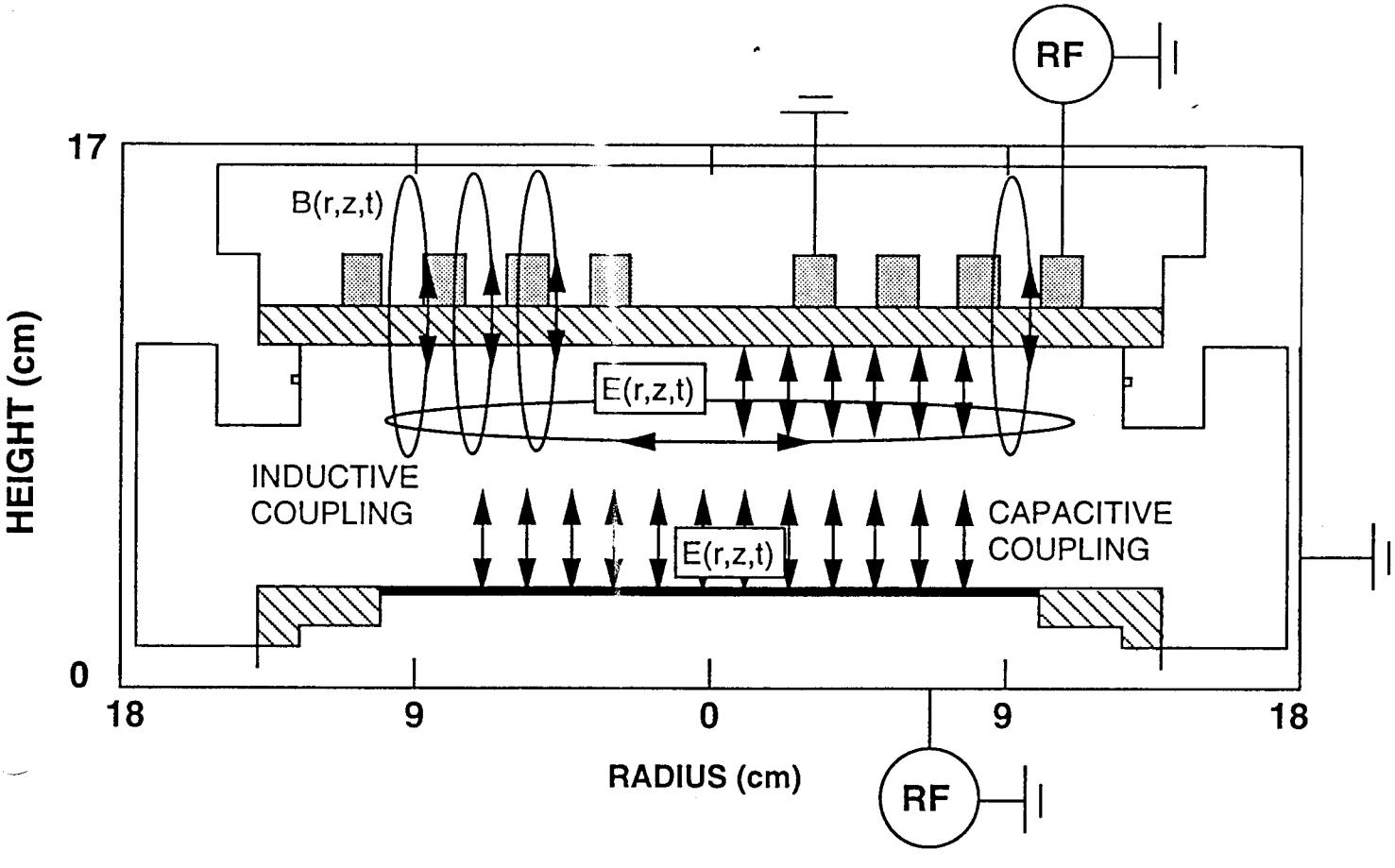
RF
17
B(r,z,t)
HEIGHT (cm)
E(r,z,t)
INDUCTIVE
COUPLING
E(r,z,t)
CAPACITIVE
COUPLING
0
18
9
0
9
18
RADIUS (cm)
RF

300 mm ETCH TOOL: ELECTRIC FIELD, POWER, ION DENSITIES

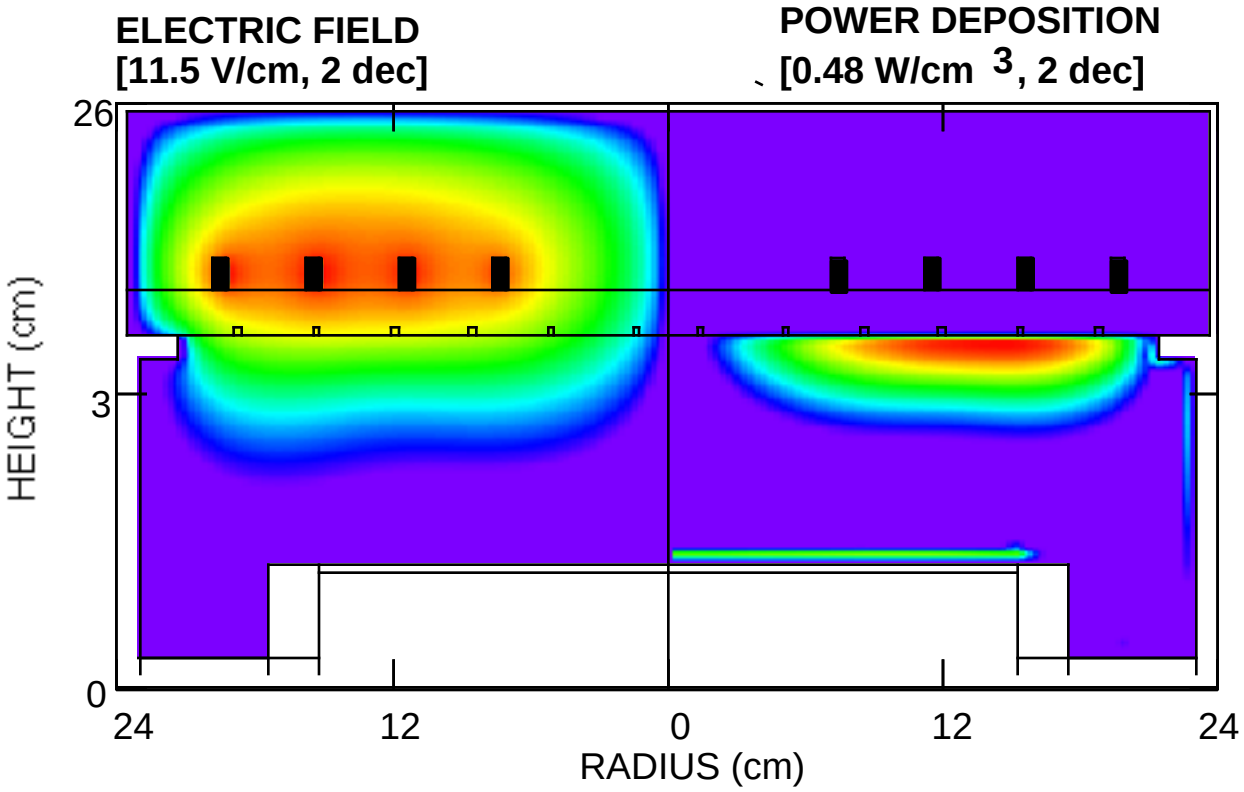

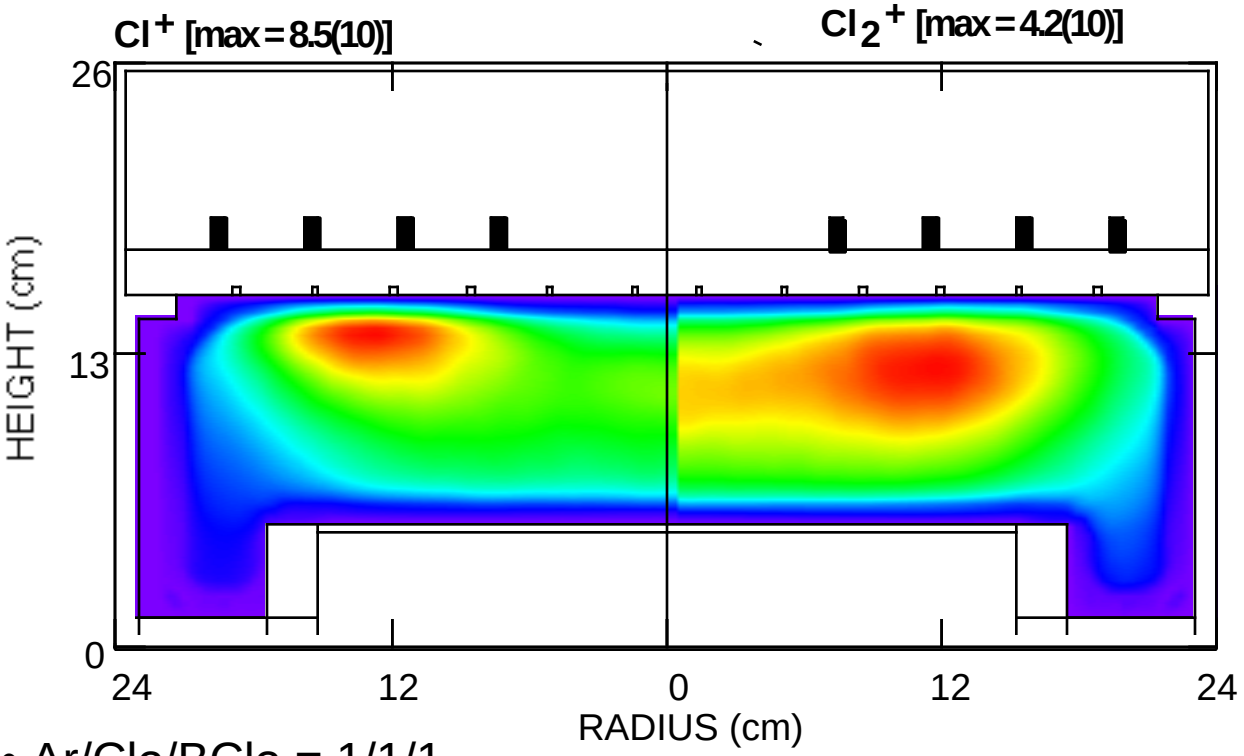

- $Ar/Cl_2/BCl_3$ = 1/1/1, 10 mTorr, 600 W ICP, 100 V bias, 150 sccm

300 mm ETCH TOOL: PRECURSORS, ETCH PRODUCTS

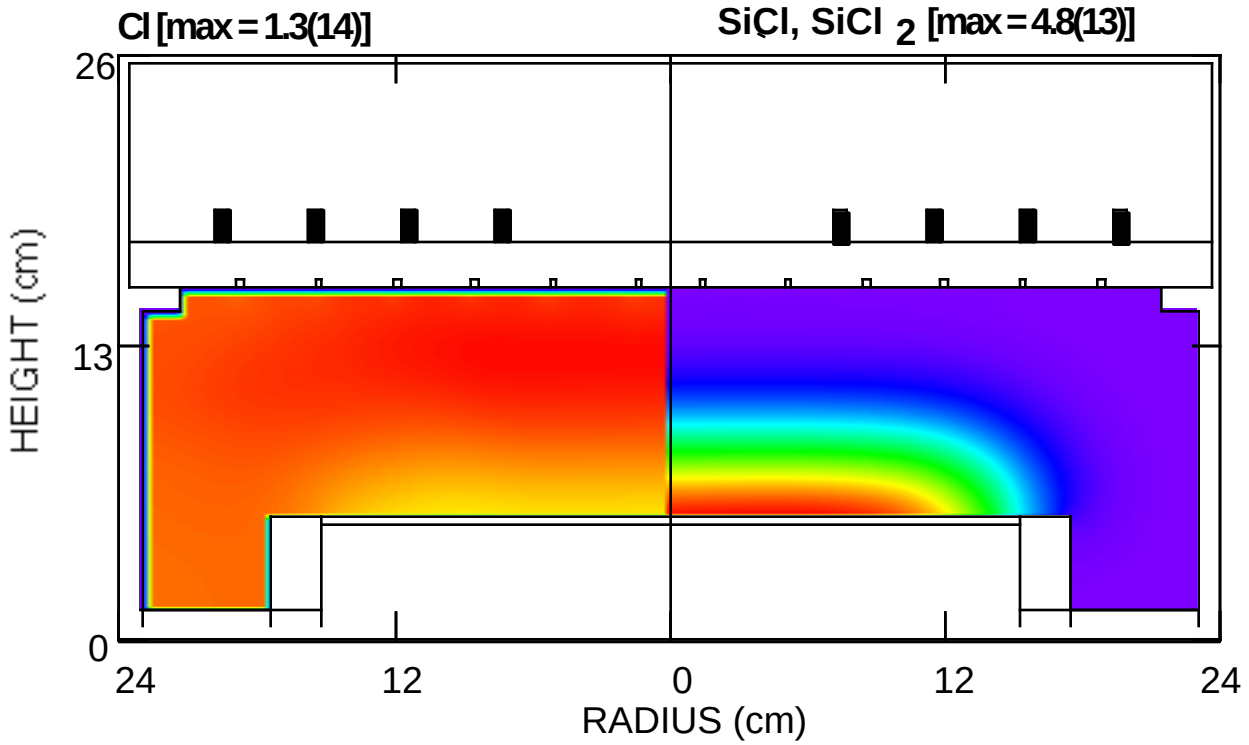

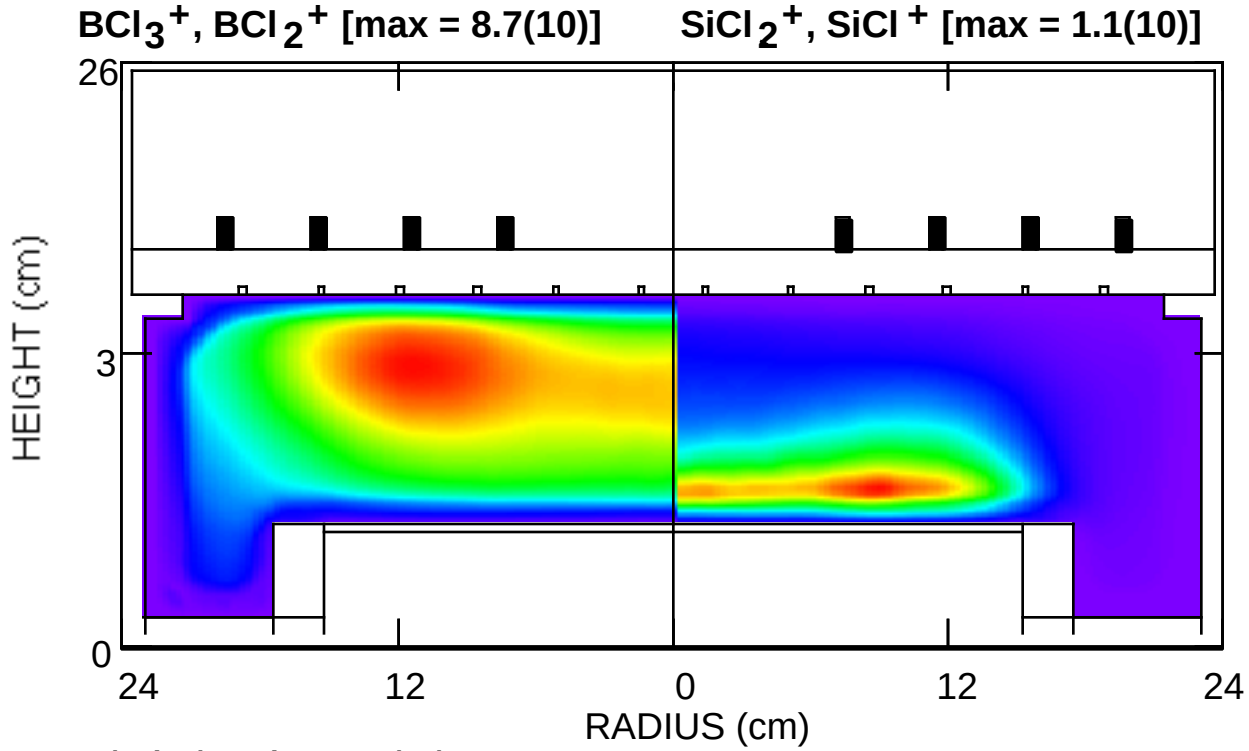

- $Ar/Cl_2/BCl_3$ = 1/1/1, 10 mTorr, 600 W ICP, 100 V bias, 150 sccm

UNIVERSITY OF ILLINOIS
OPTICAL AND DISCHARGE PHYSICS

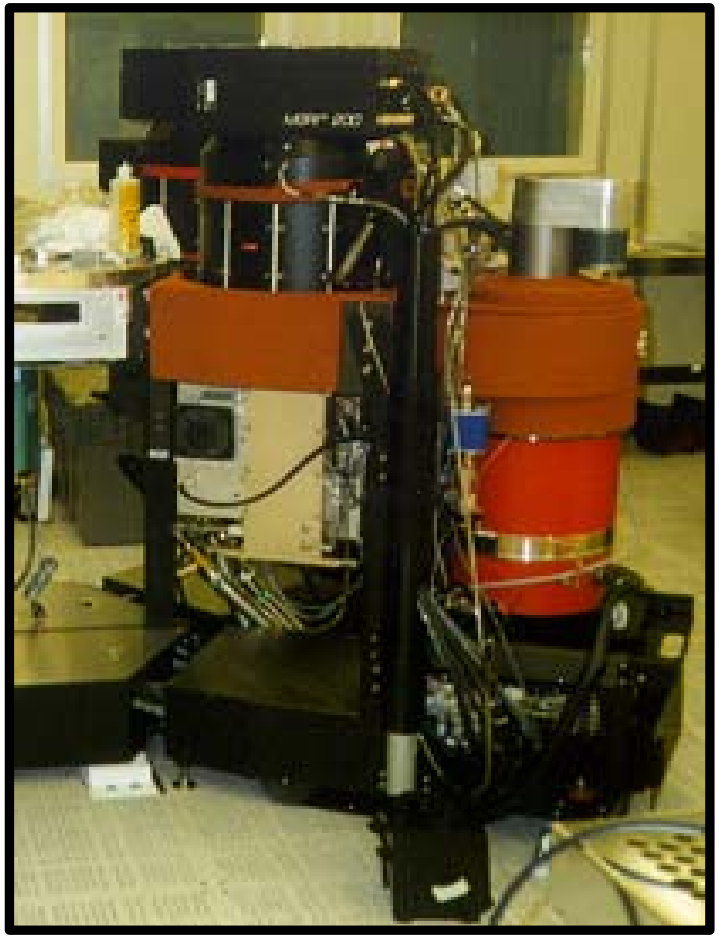

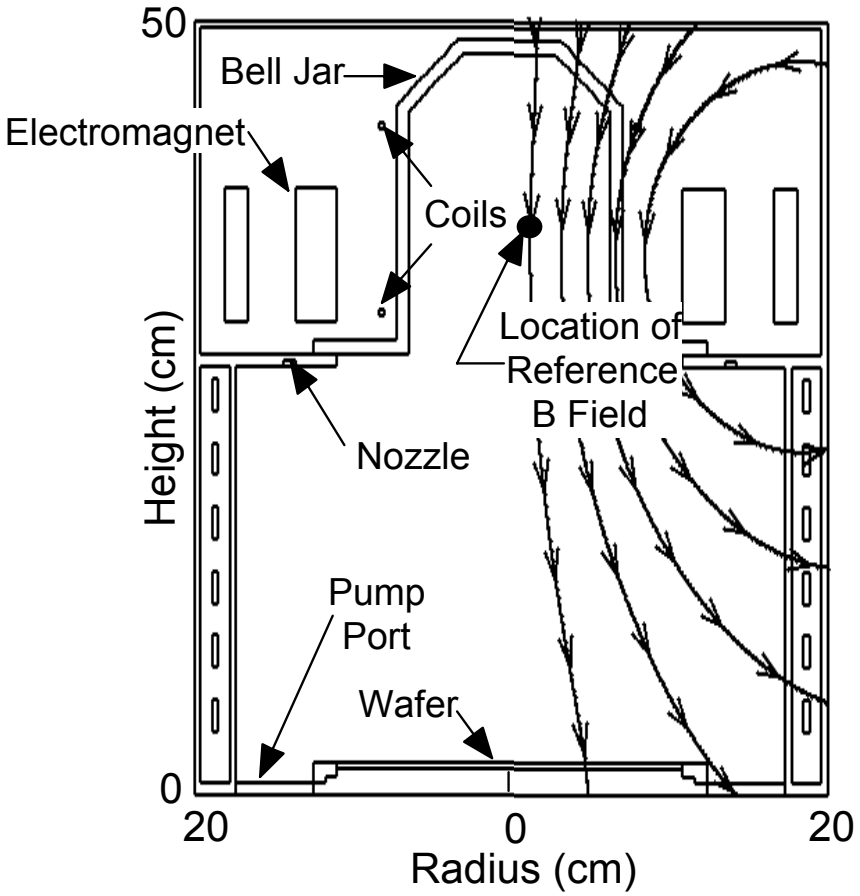

Trikon MORI Helicon Plasma Etching Tool

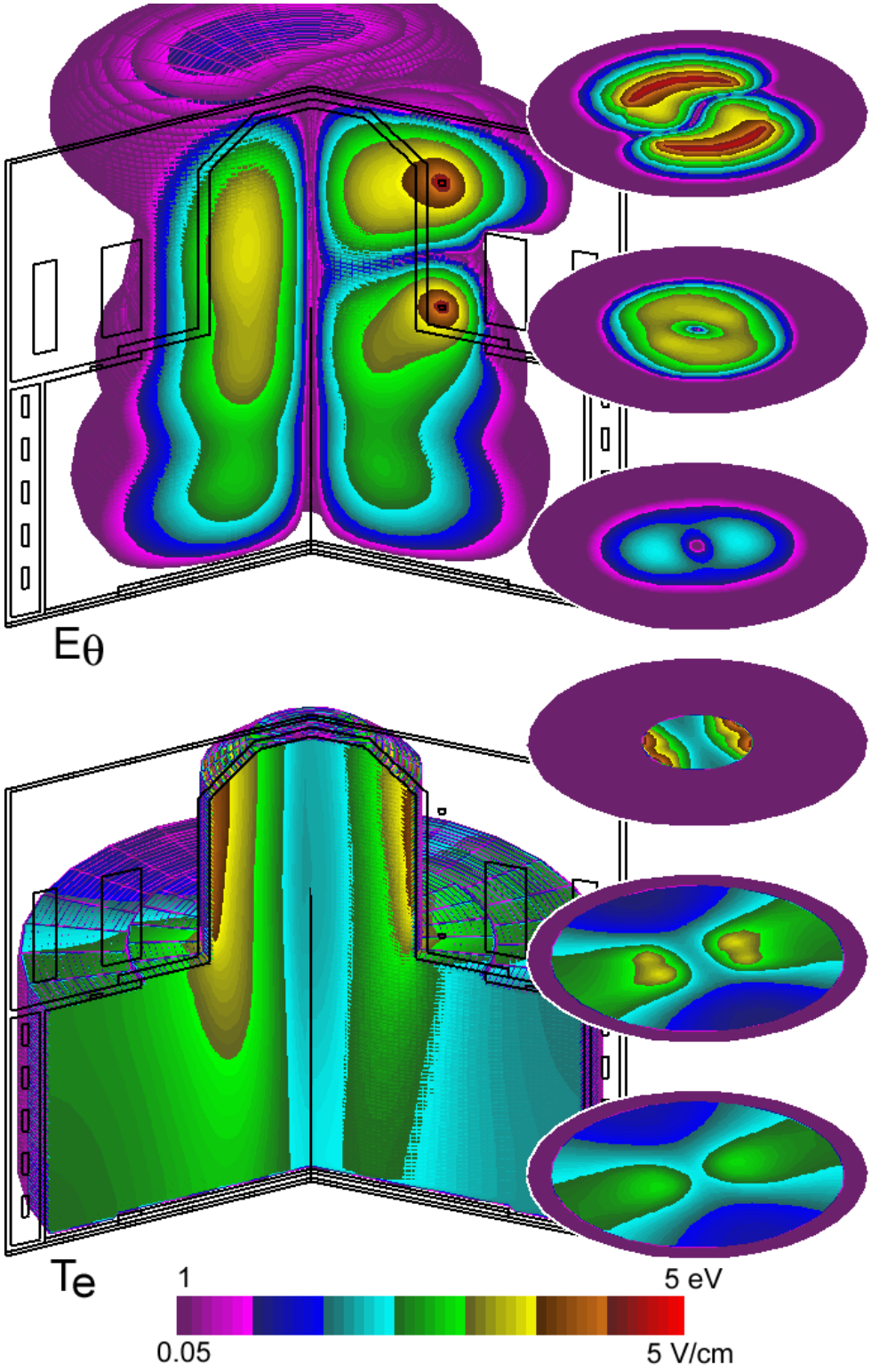

Electric field (top) and electron temperature (bottom) in a helicon plasma tool operating in 10 mTorr of Ar.

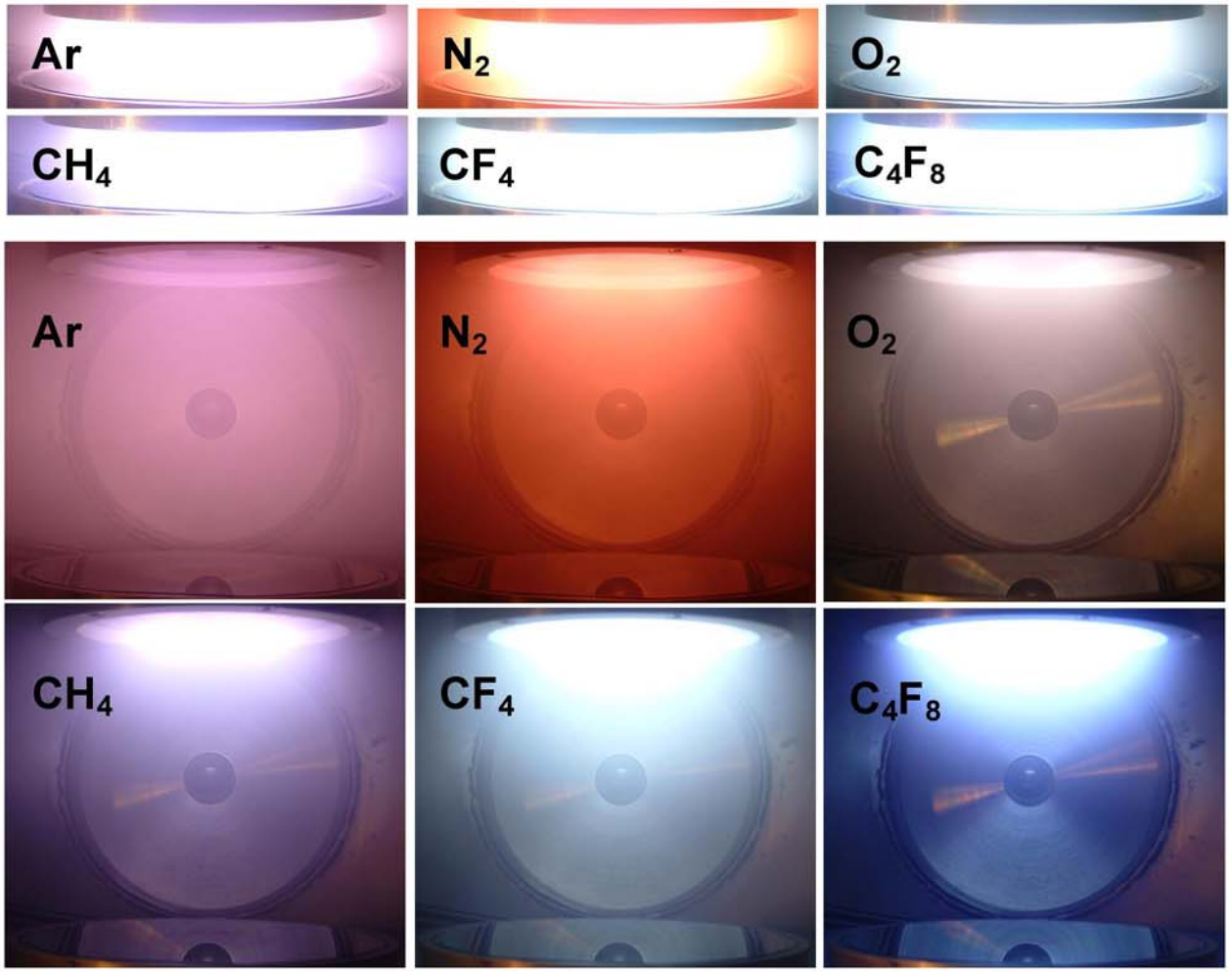

Inductively Coupled Plasma (40 mTorr, 400W)

M. J. Goeckner et al, Trans. Plasma Sci. 36, 996 (2008)

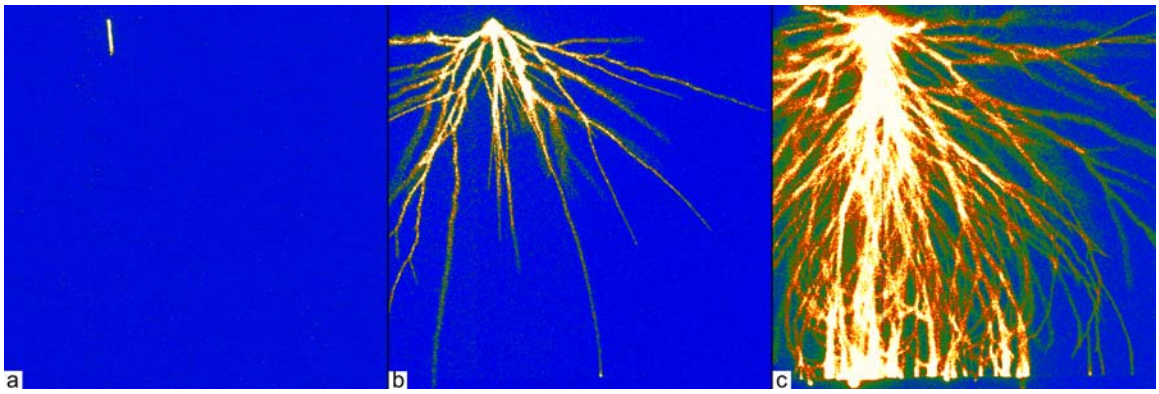

6 kV, 12.5 kV, 25 kV

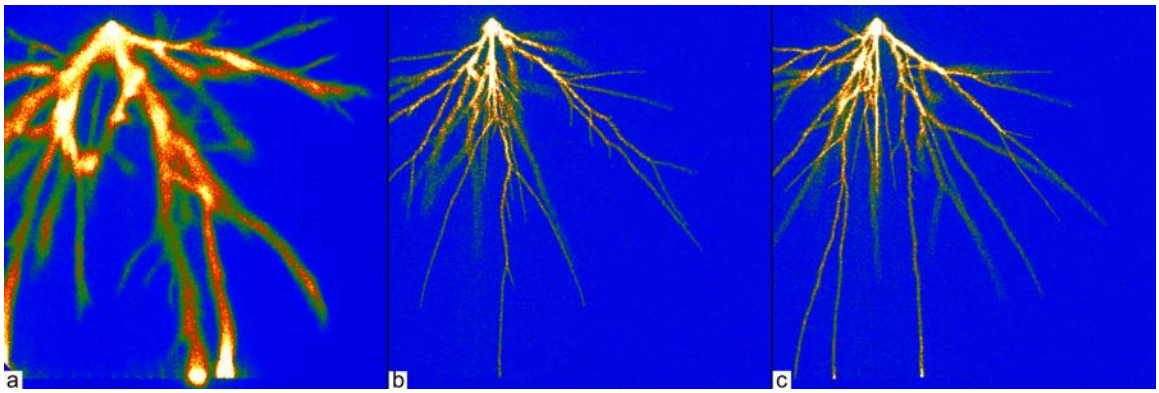

25 kV

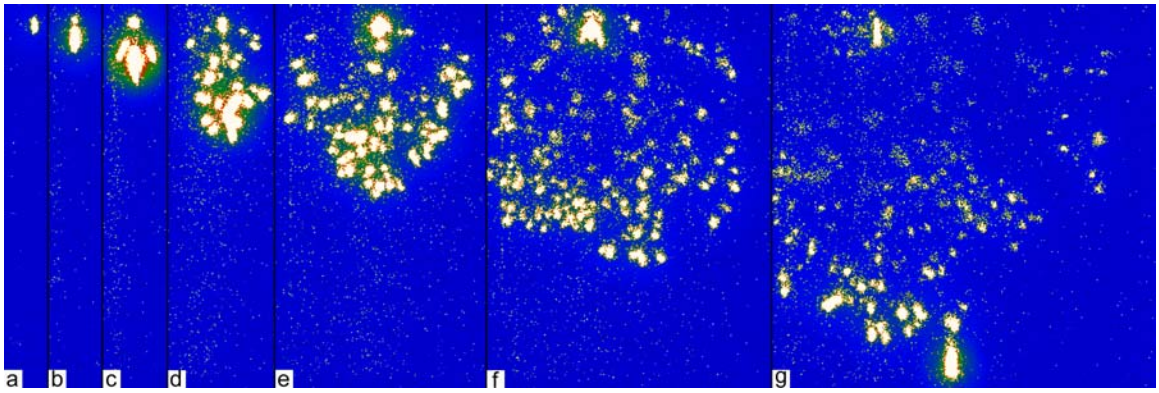

25 kV (0.8 ns resolution)

Streamers in a 25 mm air gap

(Ref: E. M. van Veldhuizen, P. C. M. Kemps and W. R. Rutgers)

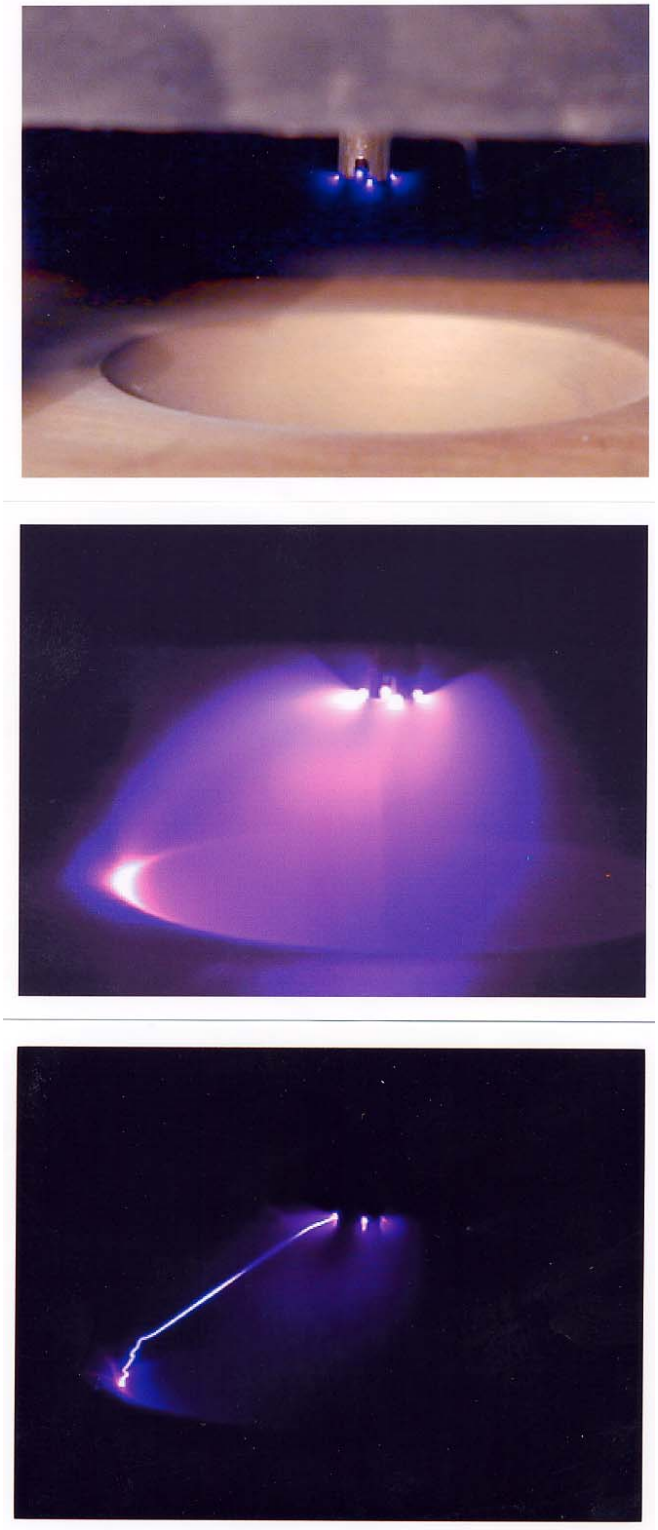

Discharges in Air: (top) negative glow, (middle) glow, (bottom) spark

(Ref: O. Goossens, T. Callebaut, Y. Akishev, A. Napartovich, N. Trushkin and C. Leys)

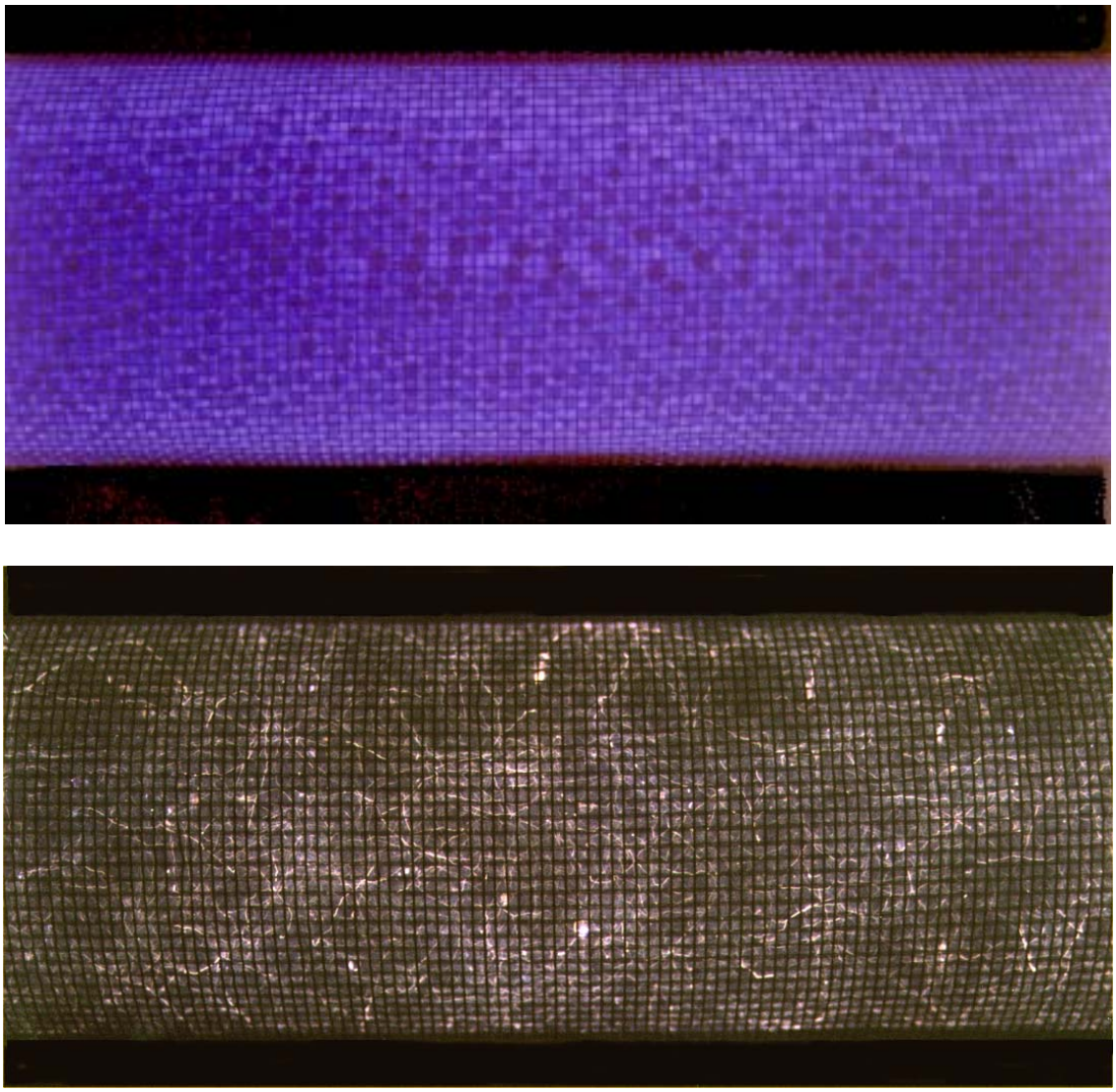

Glass Sphere Dielectric Barrier Discharge for Ozone Production
(top) 4 mm gap, 3 mm spheres, (bottom) 10 mm gap, 2 mm spheres

(Ref: A. B. Murphy and R. Morrow)

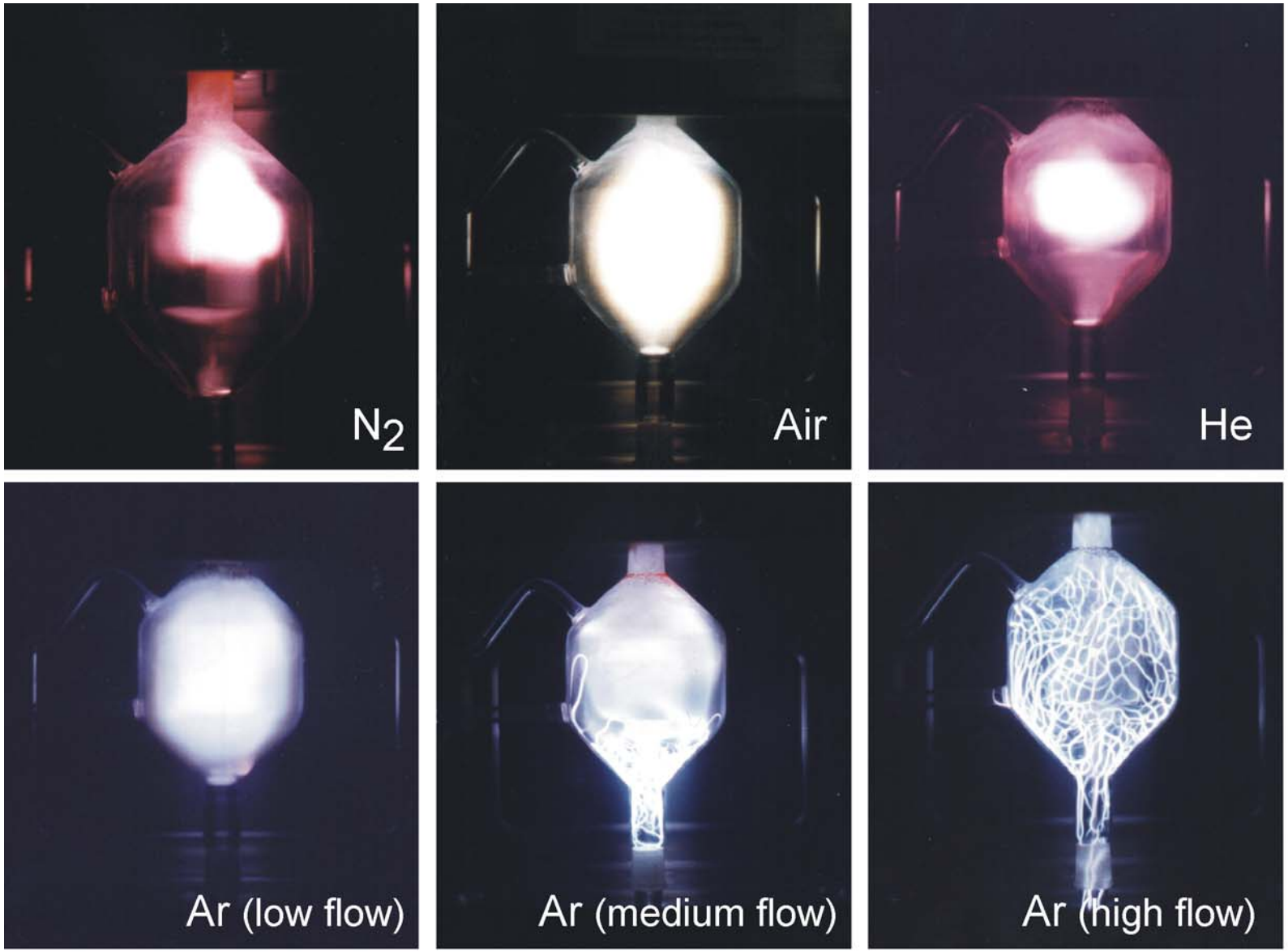

Microwave (2.45 GHz) Atmospheric Pressure Plasmas

M. J. Shenton and G. C. Stevens, Trans. Plasma Sci. 30, 184 (2002)

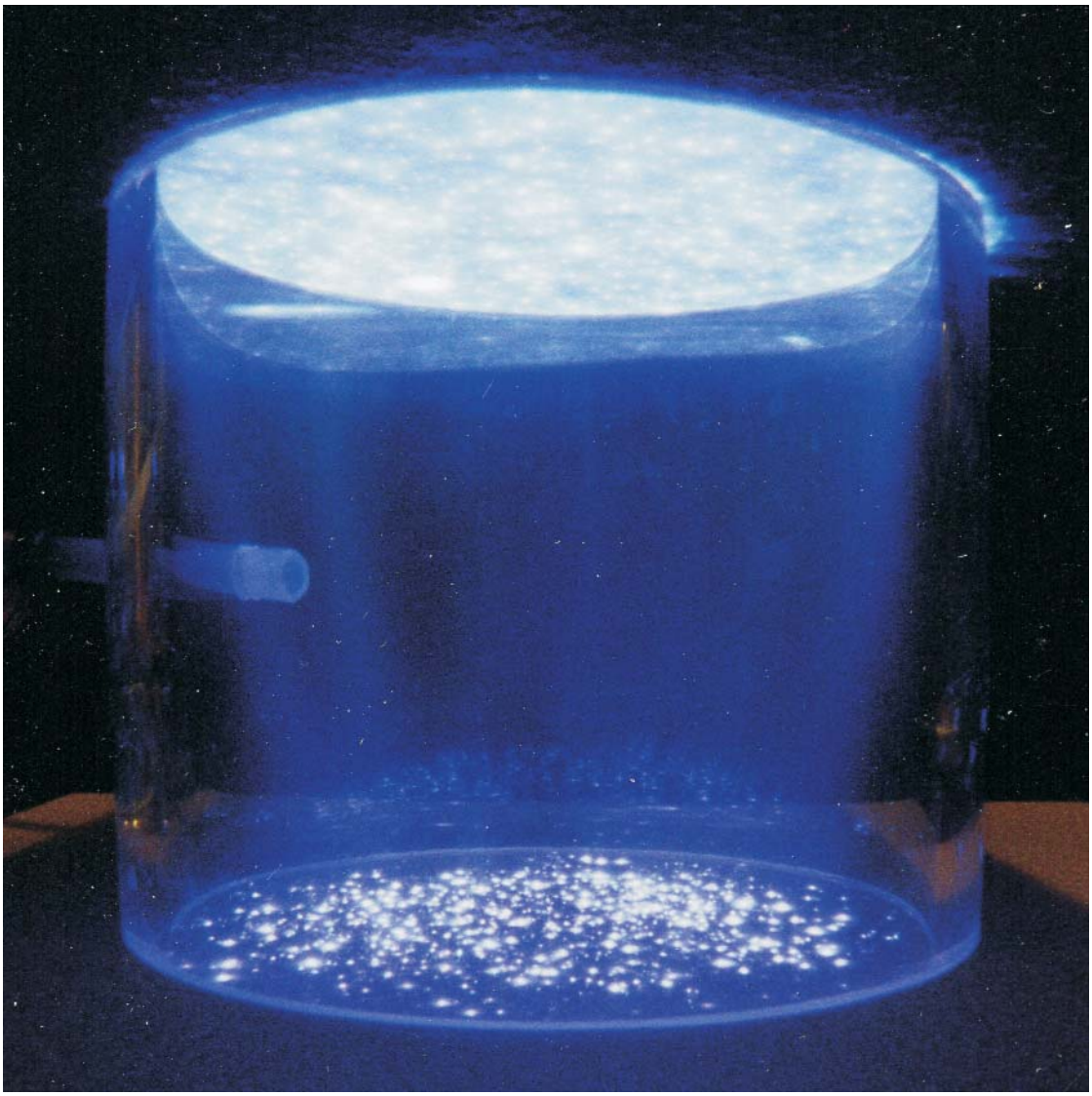

Atmospheric Pressure dc Discharge in He

I. Alexeff and M. Laroussi, Trans. Plasma Sci. 30, 174 (2002)

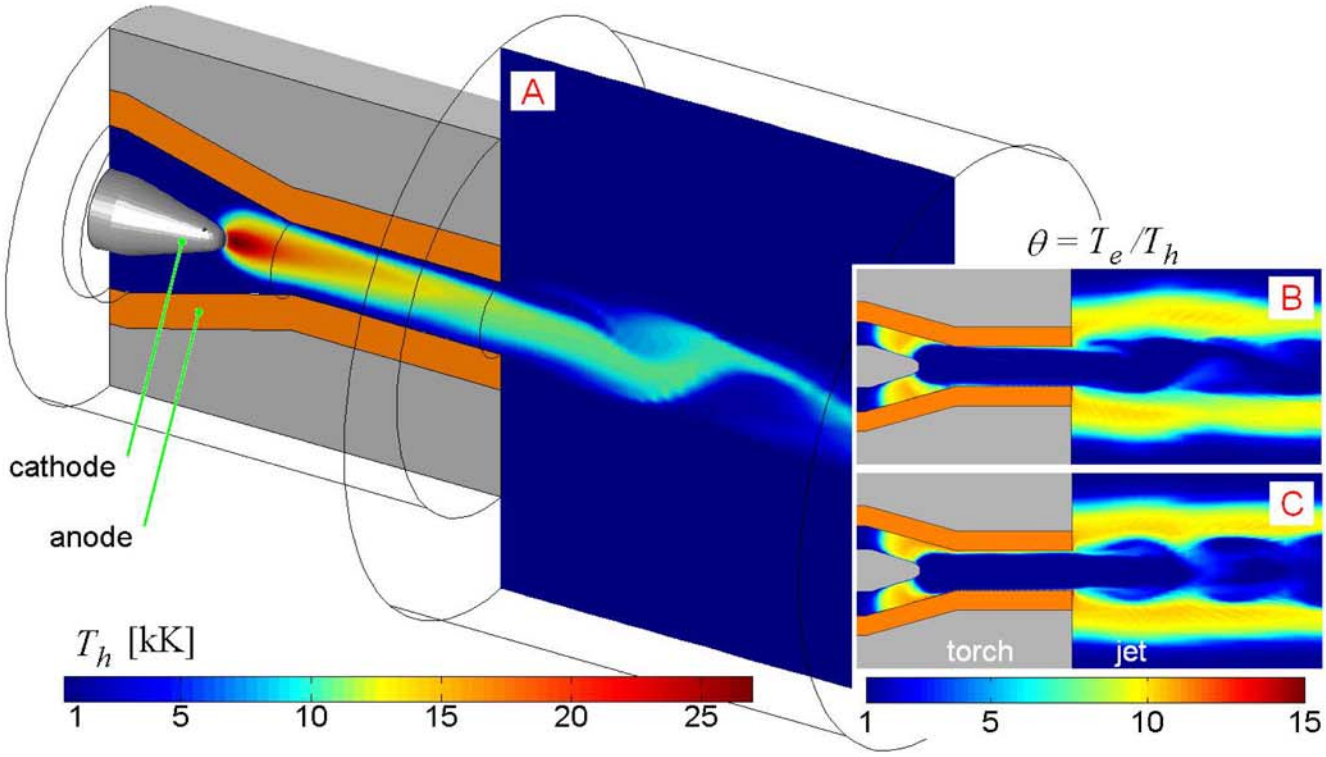

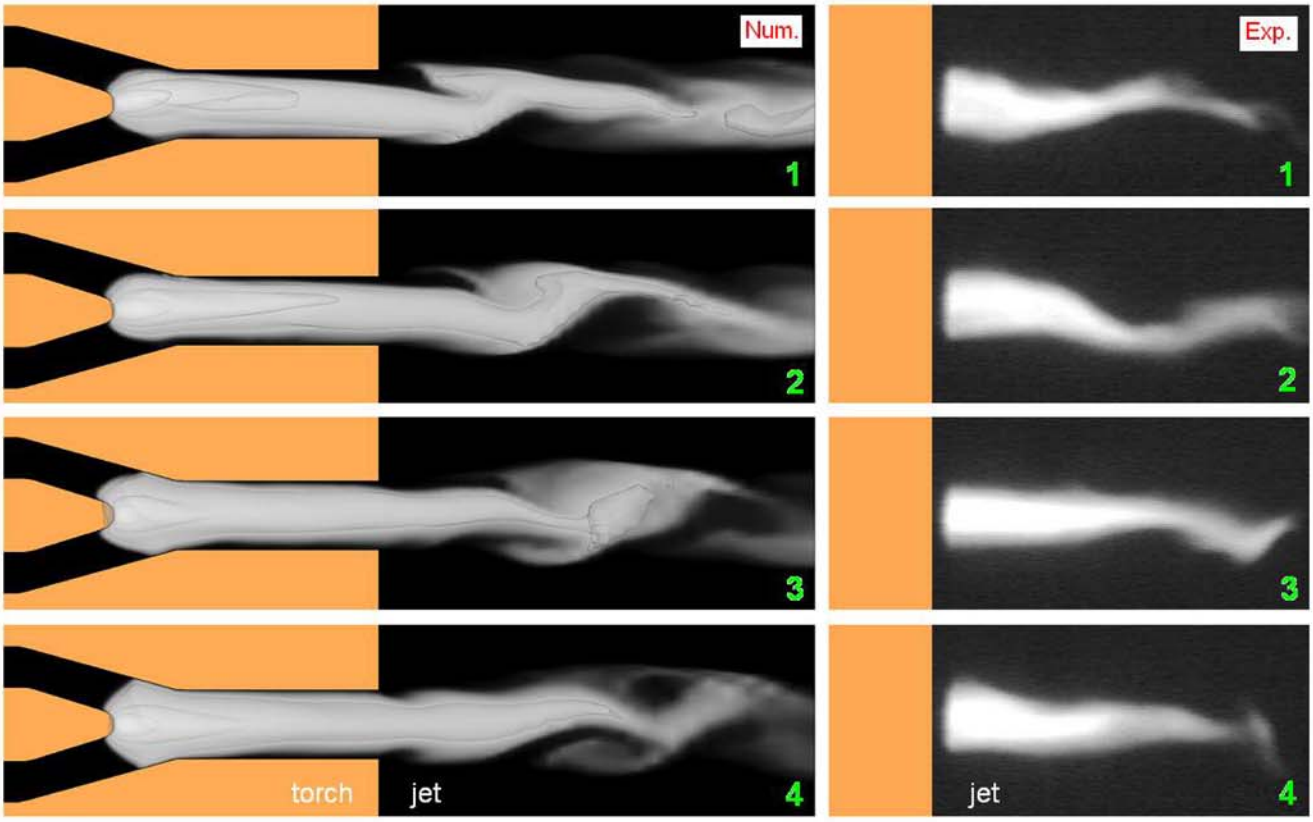

Arc Plasma Jet
(top) Calculated heavy particle temperatures (Ar, 400A)
(bottom) Model and experiment of plasma emission.

J. P Telles, et al. Trans Plasma Sci. 36, 1026 (2008)

PLASMA DISPLAY PANEL

Mitsubishi "Leonardo" 40-inch Plasma Display Panel

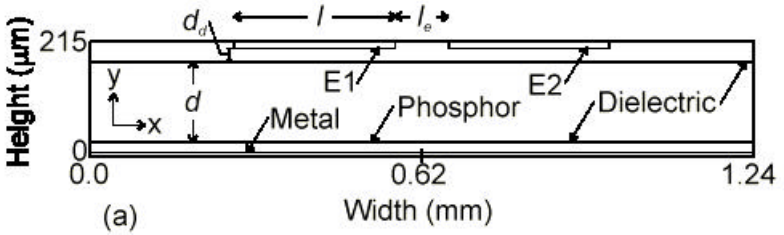

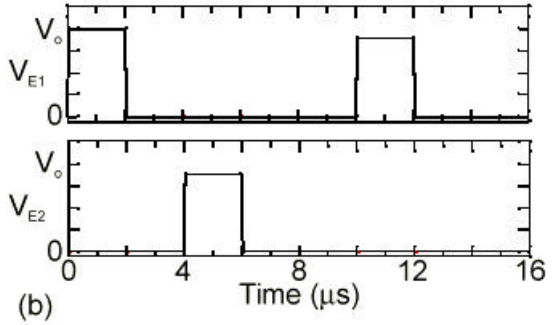

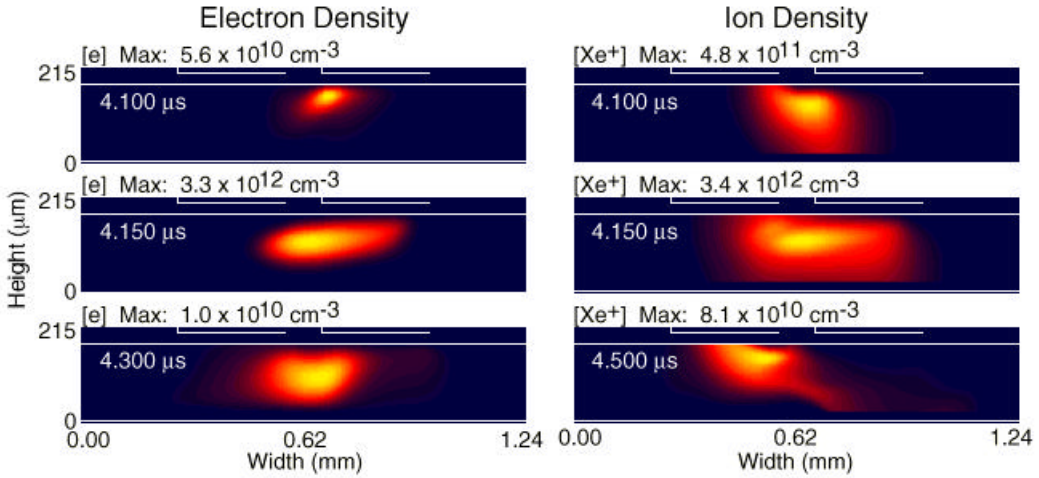

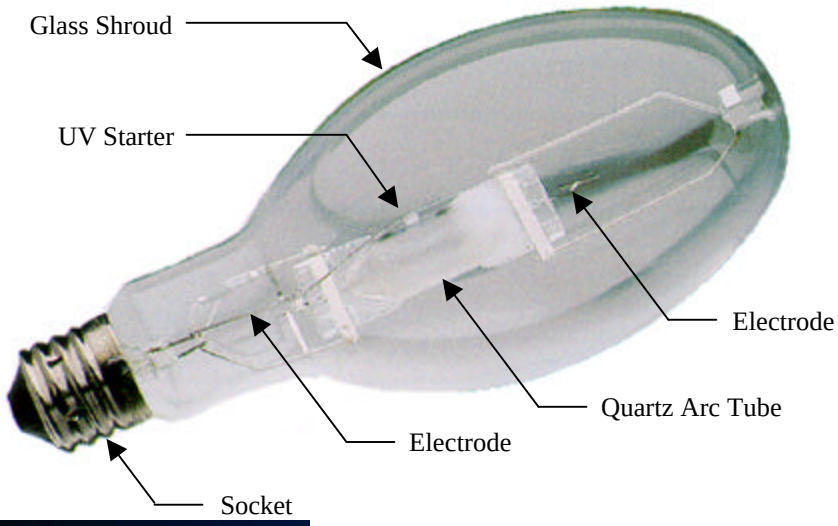

Osram-Sylvania - Metal Halide Lamp

Osram Sylvania "Metalarc Pro-Tech MP-175"

Osram-Sylvania Compact Fluorscent Lamp

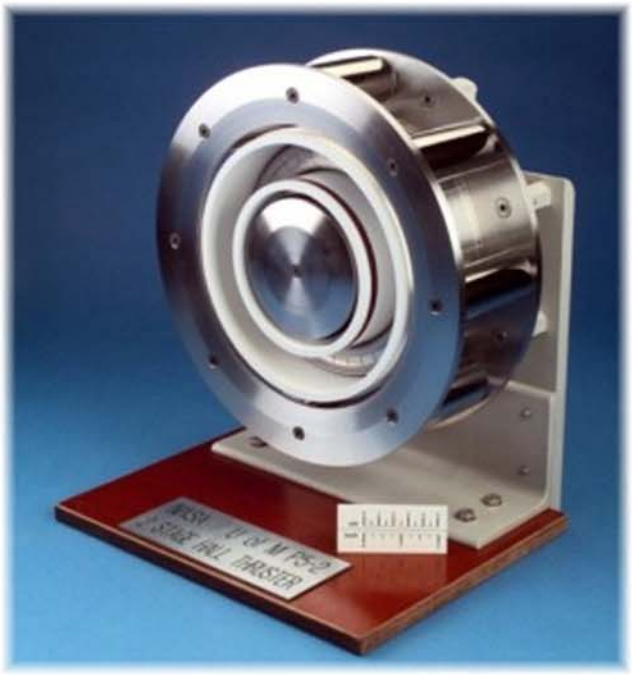

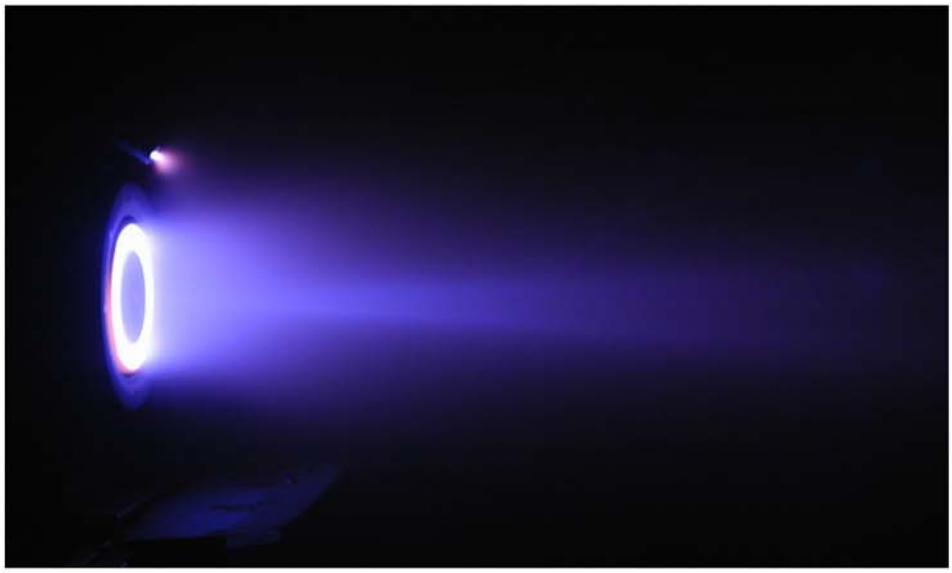

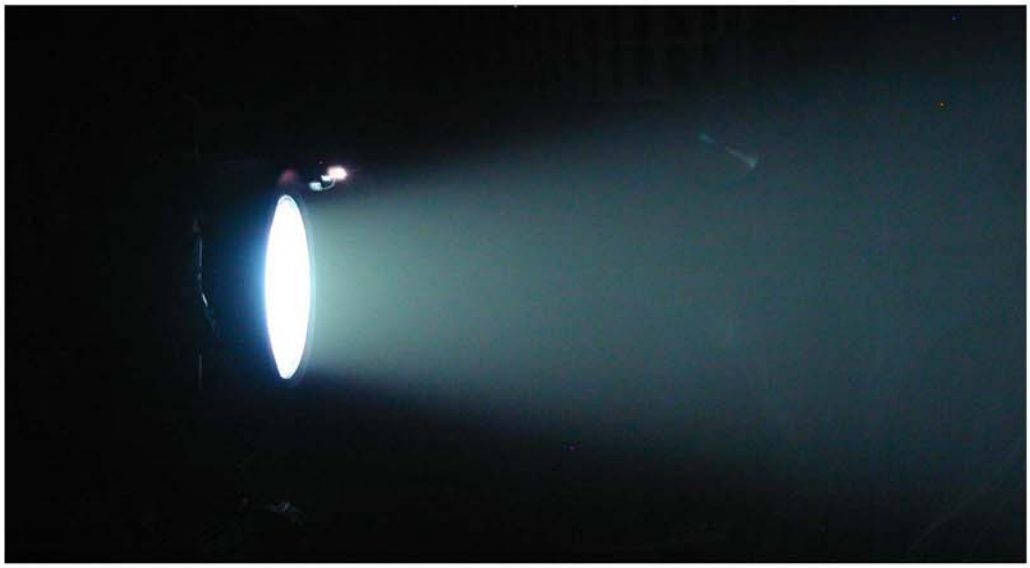

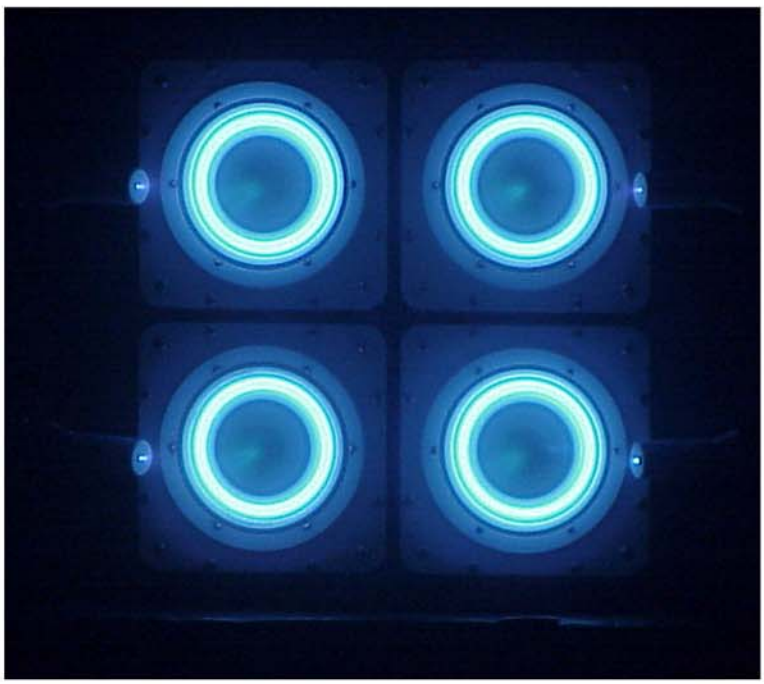

Hall Thrusters for Spacecraft Propulsion (Ref: A. Gallimore, UMich)

LARGE AREA PLASMA PROCESSING SYSTEM (LAPPS)-AGILE MIRROR (NAVAL RESEARCH LAB)

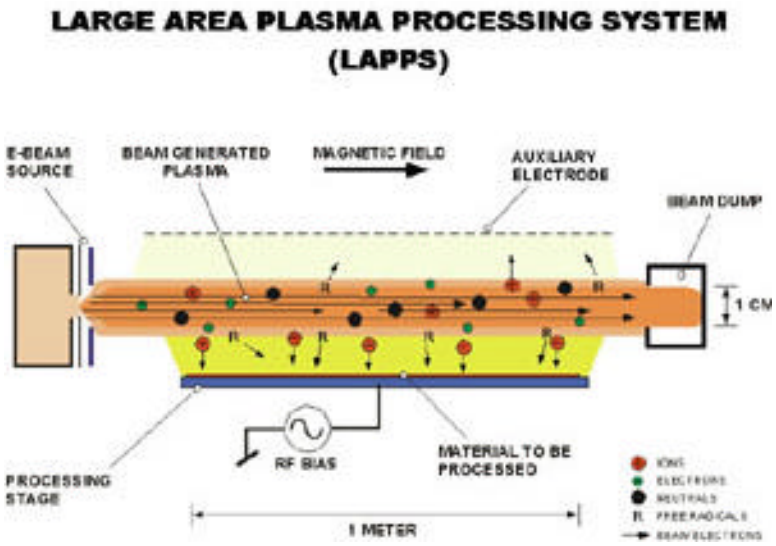

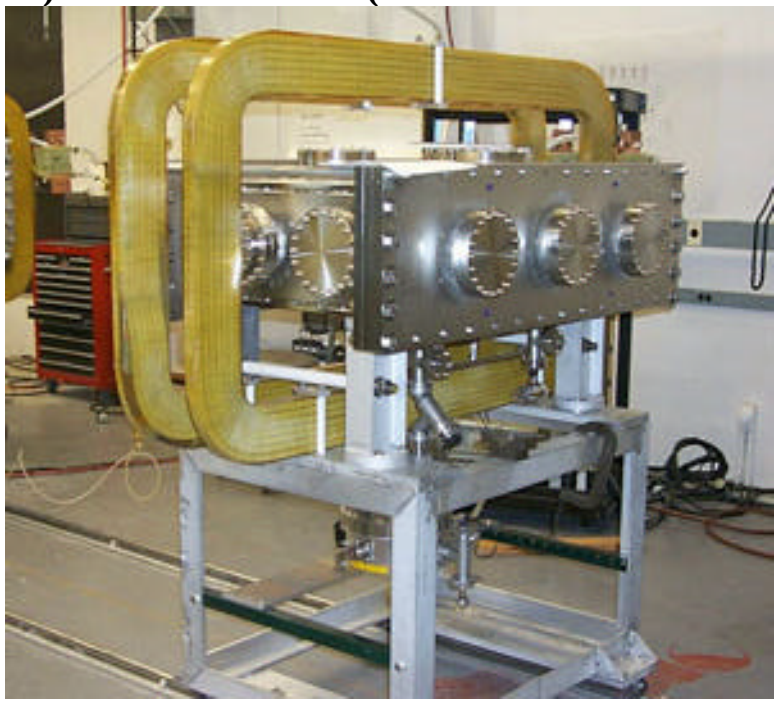

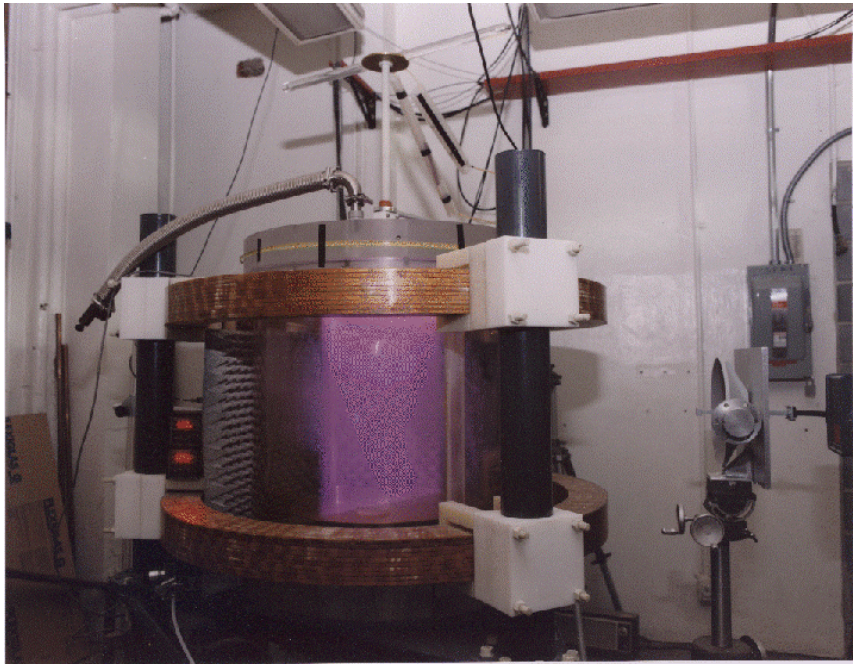

A low pressure (10s - 100s mTorr) chamber is placed in a solenoid to produce an axial magnetic field. A low plasma is produced by a cold-cathode electron beam alinghed with the magnetic field. A planar, low temperature plasma is produced.

Top left - Schematic of LAPPS system

Top right: LAPPS apparatus

Bottom left: Earlier version of LAPPS used as an agile microwave mioor. Agile mirror is shown in its low pressure chamber with the magnetic field coils. The 50 cm x 50 cm x 1 cm plasma distribution has a density sufficient to reflect 10 GHz microwaves fed by the antenna on the right.

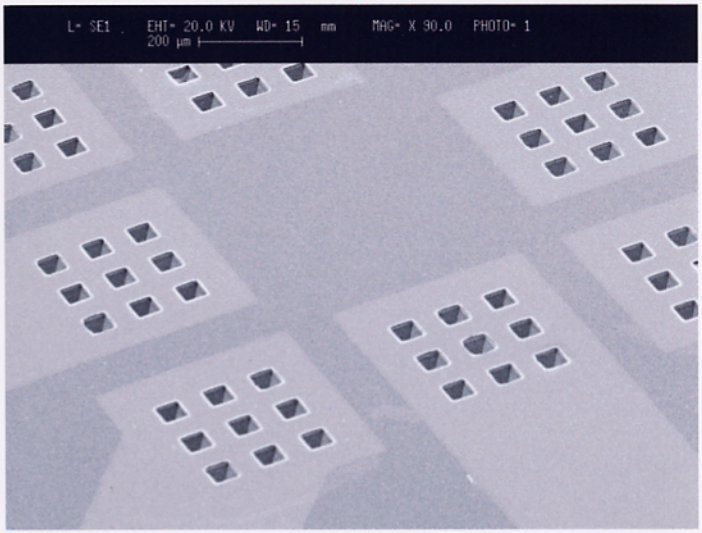

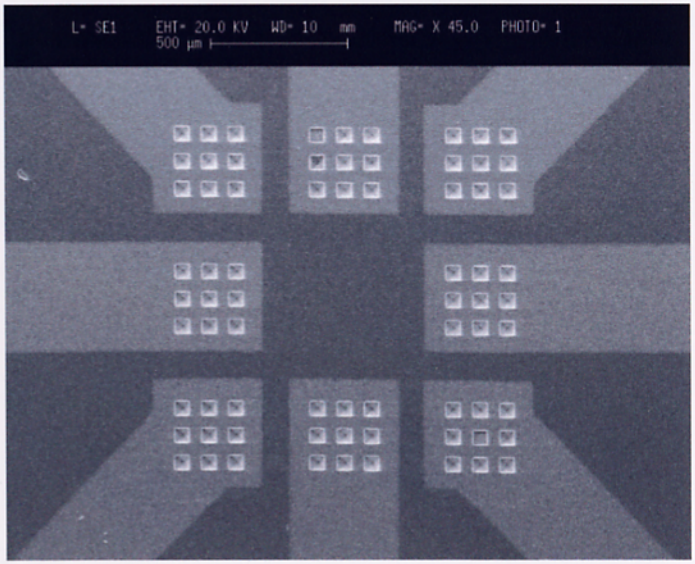

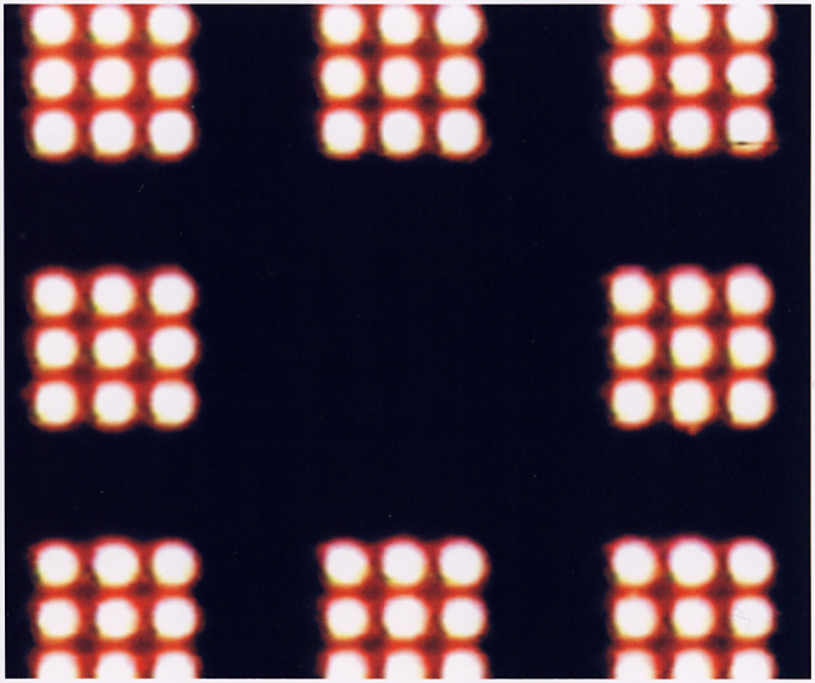

340 V, 0.492 mA, 500 Torr Neon

UIUC
Laboratory for Optical Physics and Engineering

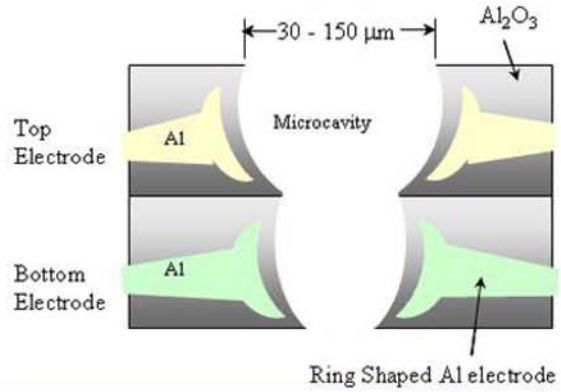

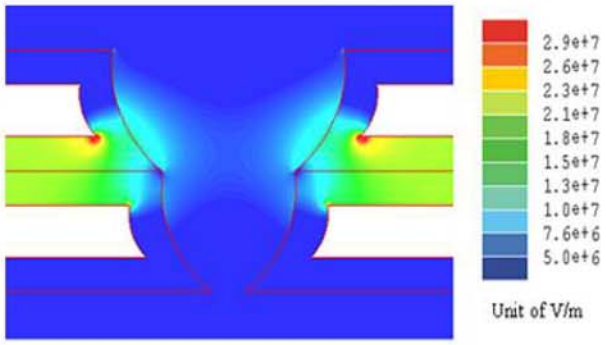

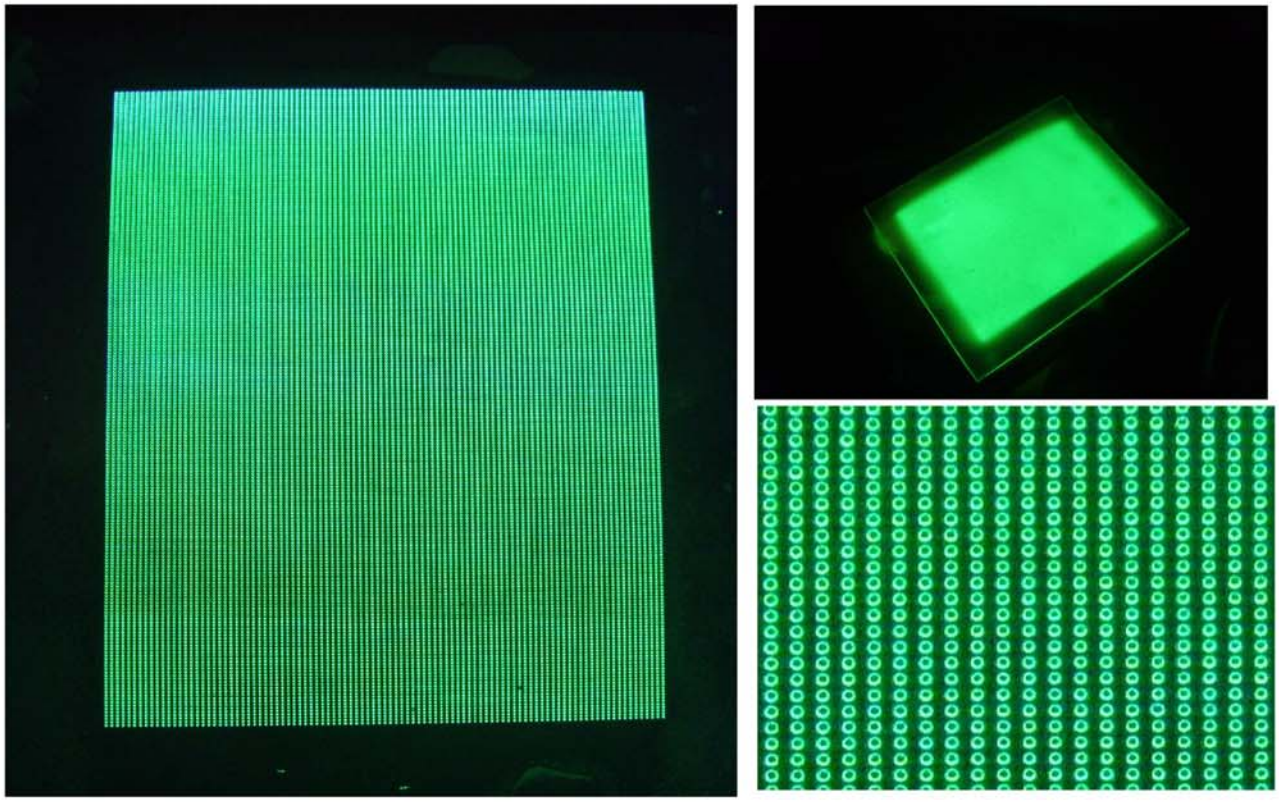

Microplasma (Ne/Xe = 70/30 500 Torr)
(top) Microcavity powered at 20 kHz, 170V
(bottom) 20,000 pixels

K. S. Kim, et al., Trans Plasma Sci. 36, 1288 (2008)

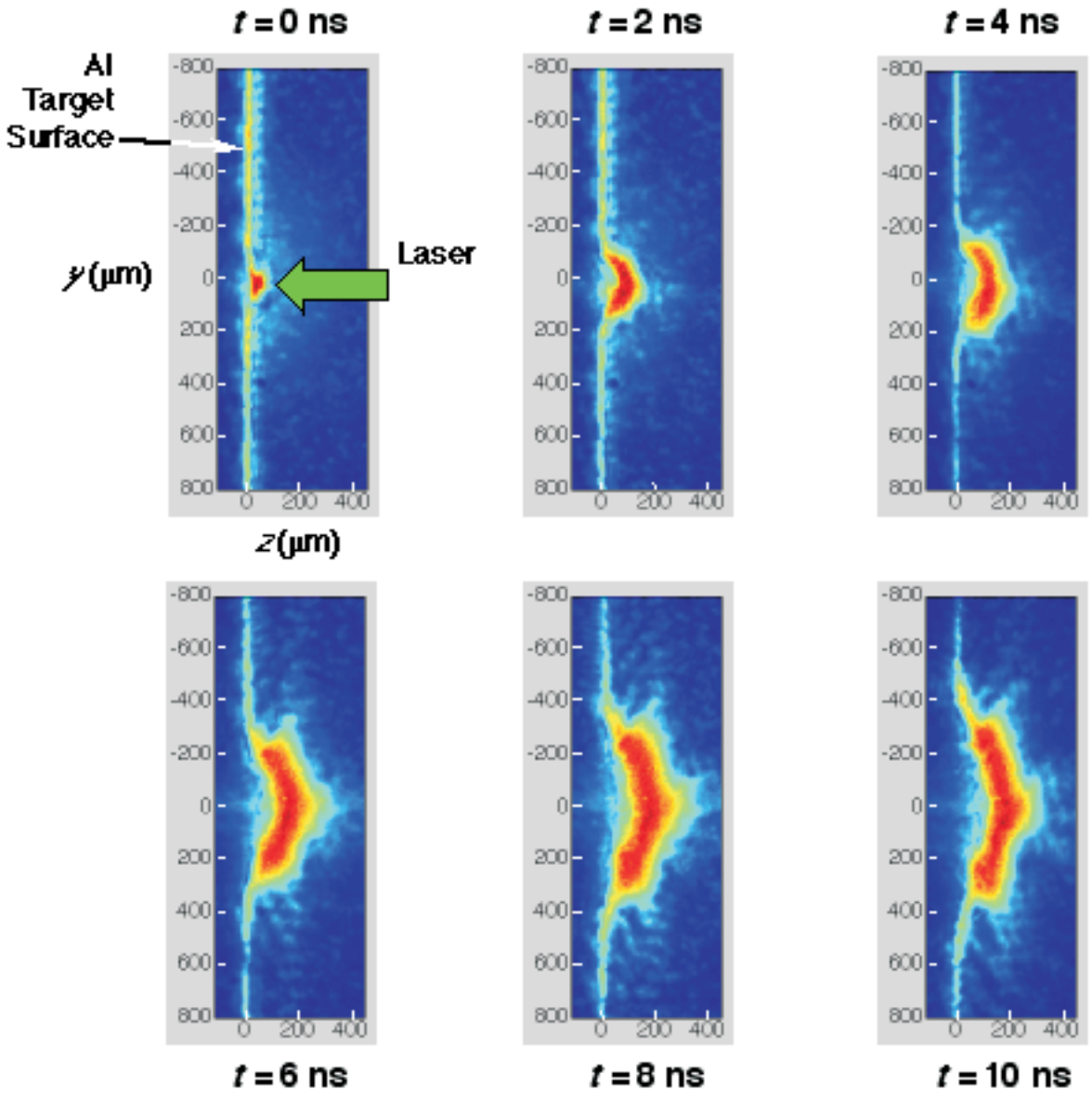

Laser Generated Plasma
(10^{19} < [e] < 10^{20} cm^{-3})

J. F. Camacho, D. E. Bliss and S. M. Cameron,
Trans. Plasma Sci. 30, 42 (2002)

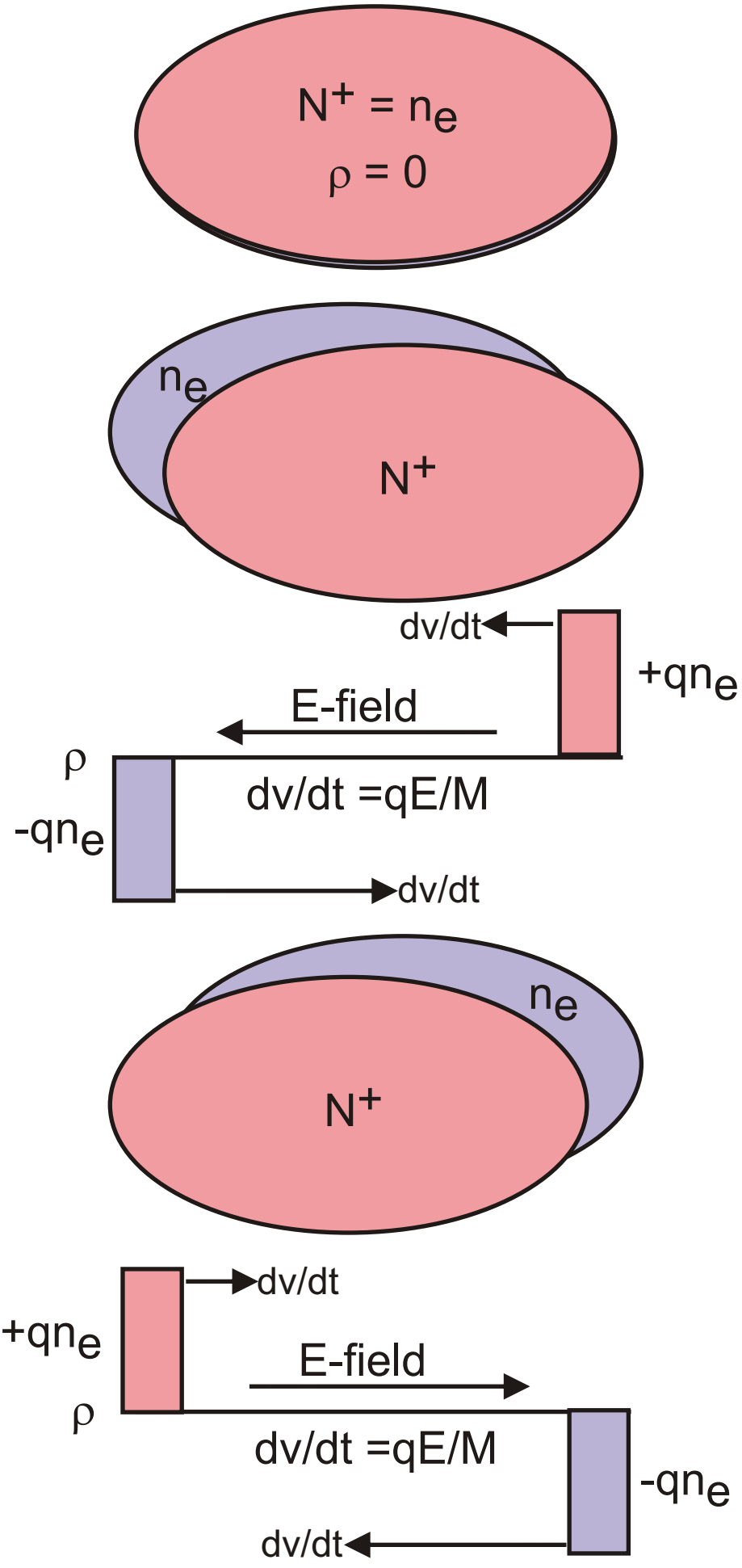
N+ = ne
ρ = 0
ne
N+
dv/dt
+qne
E-field
ρ
dv/dt =qE/M
-qne
dv/dt
ne
N+
dv/dt
+qne
E-field
ρ
dv/dt =qE/M
-qne
dv/dt

RELATION BETWEEN CROSS SECTION, FLUX, RATE OF COLLISION, AND RATE COEFFICIENT

Consider a single atom with cross sectional "area" of σ_o cm^2. If electrons with energy ε randomly pass through a plane of area A, then the probability of any one single electron passing through area A of hitting the atom is

$$P_1 = \frac{\sigma_o}{A}$$

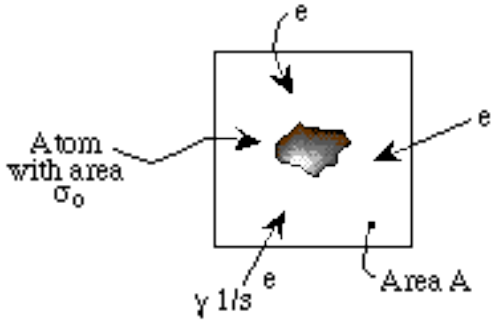

Now if the total number of electrons with energy ε passing through A per second is γ, then the rate of all electrons with energy ε hitting a single atom is

$$R_1 = \gamma P_1 \frac{1}{s} = \gamma \frac{\sigma_o}{A} = \left(\frac{\gamma}{A}\right) \sigma_o = \phi \sigma_o \frac{1}{s}$$

where the electron flux ϕ $\left[\frac{}{cm^2\text{-}s}\right]$ is the number of electrons passing through the plane per unit area.

Now if there are N_T total atoms in a volume V then the total rate of collisions of all electrons striking all atoms per unit volume is

$$R_2 = \left(R_1 \frac{N_T}{V}\right) \frac{1}{cm^3\text{-}s} = R_1 N \frac{1}{cm^3\text{-}s}, \quad N = \frac{N_T}{V} \frac{1}{cm^3}$$

$$= \phi \sigma_o N \frac{1}{cm^3\text{-}s}$$

where N is the number density of atoms.

So finally the rate at which a single electron with energy ε strikes a single atom per unit volume (n_T total electrons with energy ε in V) is

$$R_3 = R_2 \frac{1}{\left(\frac{n_T}{V}\right)\left(\frac{N_T}{V}\right)} \frac{cm^3}{s} = \frac{\phi \sigma_o N}{nN} = \frac{\phi \sigma_o}{n} \frac{cm^3}{s},$$

where n_T is the total number of electrons in volume V having energy ε, and where $n = \frac{n_T}{V}$ $\left(\frac{}{cm^3}\right)$ is the number density of electrons at energy ε.

The flux of electrons at energy ε is

$$\phi(\varepsilon) = n(\varepsilon)\left(\frac{2\varepsilon}{m_e}\right)^{1/2} = n(\varepsilon)v\,\frac{\#}{cm^2\text{-}s}$$

where $v = \left(\frac{2\varepsilon}{m_e}\right)^{1/2}$ is the electron velocity, so

$$R_3(\varepsilon) = \frac{\phi(\varepsilon)\,\sigma_o(\varepsilon)}{n(\varepsilon)} = \sigma_o(\varepsilon)v\,\frac{cm^3}{s}.$$

With these definitions, the average rate at which a <u>single</u> <u>electron</u> strikes a <u>single</u> <u>atom</u> per unit volume for an entire distribution of electron energies is

$$k = \int_0^\infty f(\varepsilon)R_3(\varepsilon)d\varepsilon = \int_0^\infty f(\varepsilon)\,\sigma_o(\varepsilon)\left(\frac{2\varepsilon}{m_e}\right)^{1/2} d\varepsilon\ \frac{cm^3}{s}$$
$$= <\sigma_o\, v>$$

where k = electron impact rate coefficient $\left(\frac{cm^3}{s}\right)$

$f(\varepsilon)$ = electron energy distribution function (eV^{-1}) normalized as

$$\int_0^\infty f(\varepsilon)d\varepsilon = 1$$

Example: The time rate of change of electron density due to electron impact ionization collisions is

$$\frac{dn_e}{dt}\left(\frac{1}{cm^3\text{-}s}\right) = \begin{bmatrix}\text{Rate of ionizing}\\ \text{collisions per unit}\\ \text{volume of a single}\\ \text{electron with a}\\ \text{single atom}\end{bmatrix} \times \begin{bmatrix}\text{Number of}\\ \text{electrons}\\ \text{per unit volume}\end{bmatrix} \times \begin{bmatrix}\text{Number of}\\ \text{atoms}\\ \text{per unit volume}\end{bmatrix}$$

$$k_I\left(\frac{cm^3}{s}\right) \qquad n_e\left(\frac{1}{cm^3}\right) \qquad N\left(\frac{1}{cm^3}\right)$$

$$= n_e\, k_I\, N\left(\frac{1}{cm^3\text{-}s}\right)$$

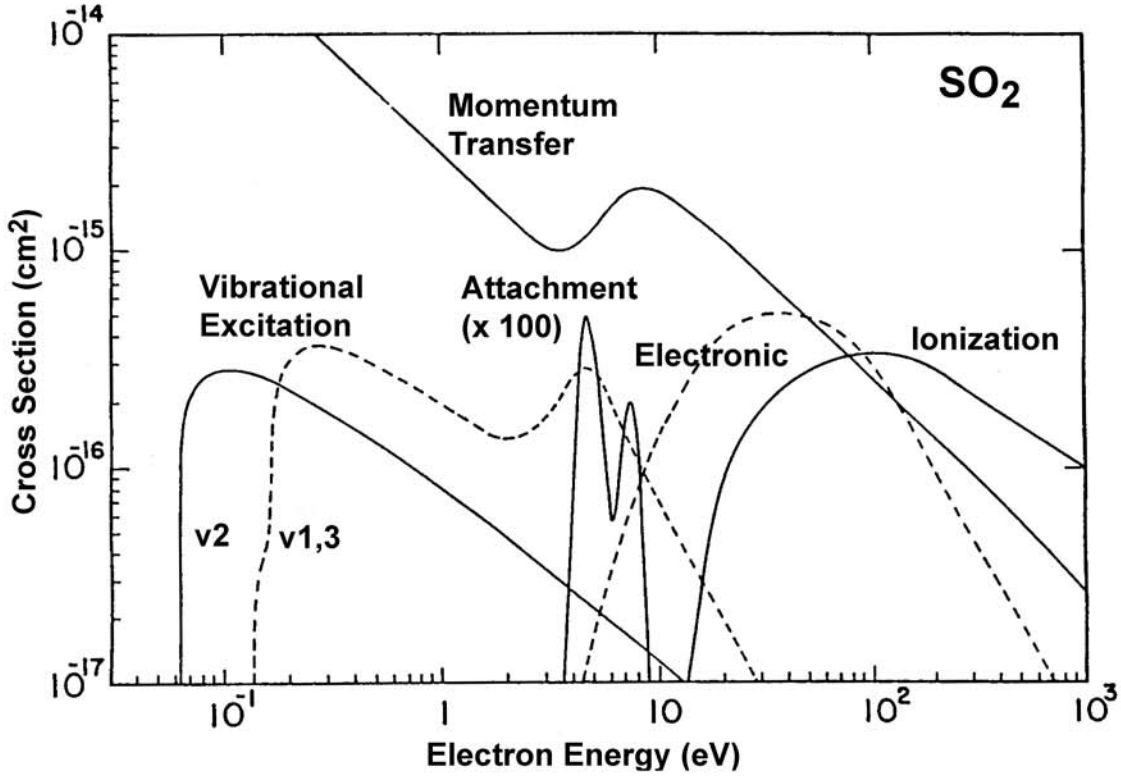

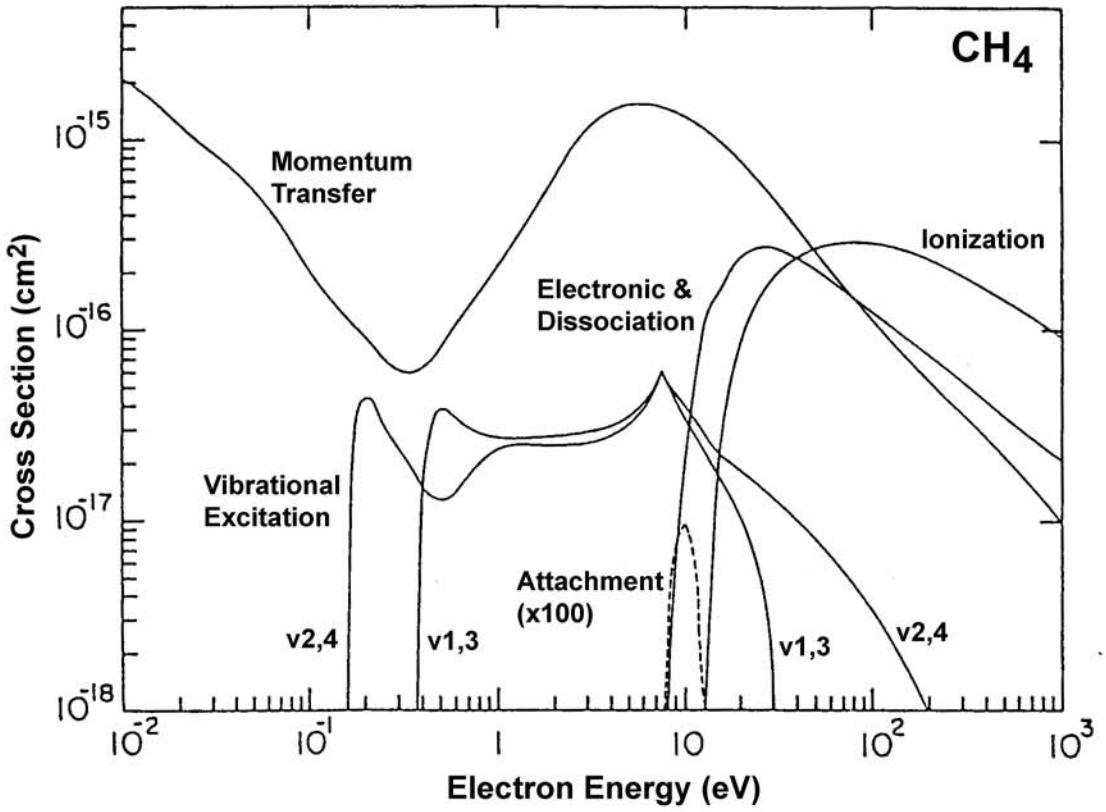

Ref: M. Hayashi in
"Swarm Studies and Inelastic Electron-Molecule Collisions)

IDEAL MOLECULE CROSS SECTIONS

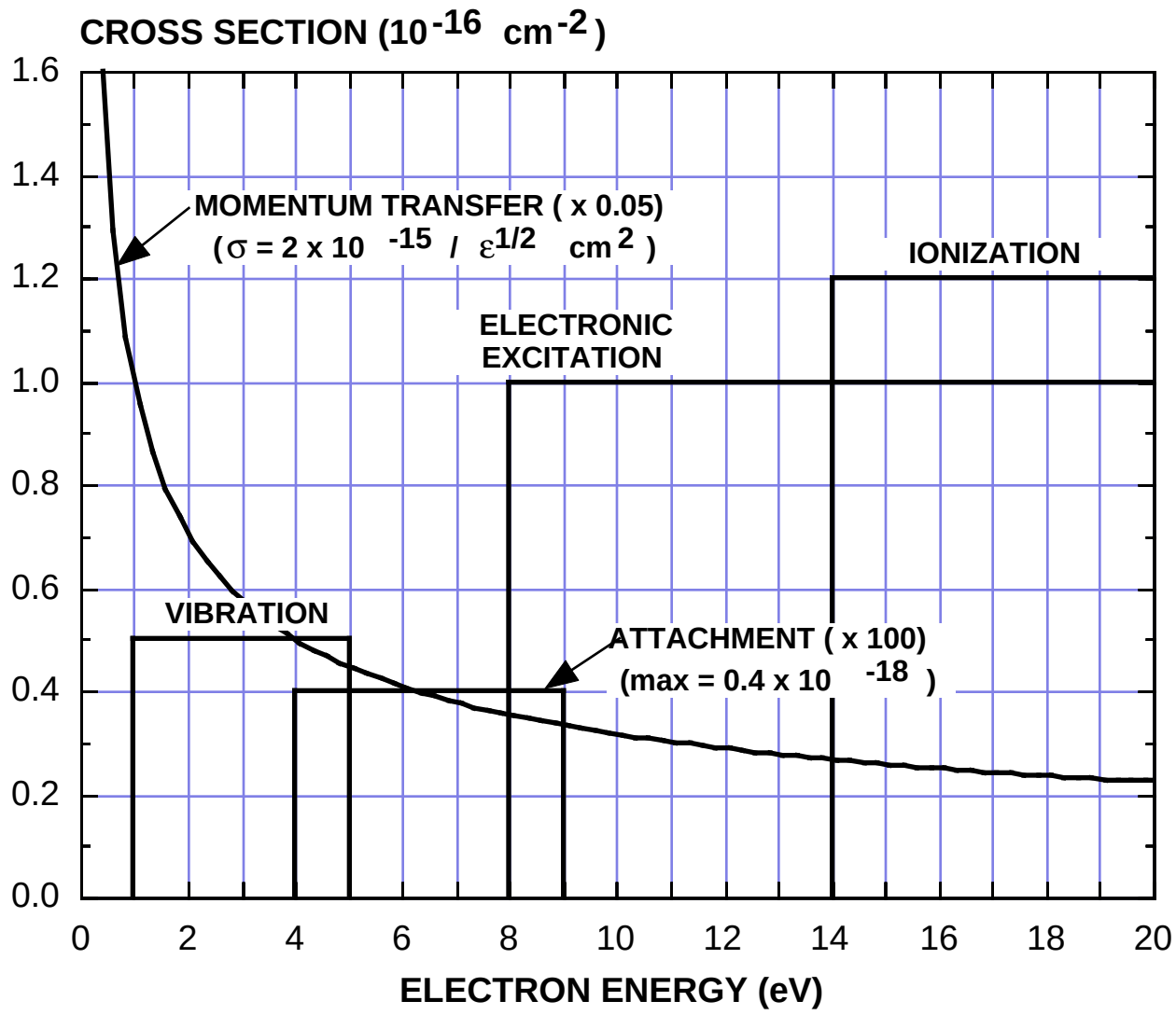

Elastic scattering of low-energy electrons by Ne, Ar, Kr, and Xe

R. Haberland, L. Fritsche, and J. Noffke
Institut für Theoretische Physik der Technischen Universität Clausthal, D-3392 Clausthal-Zellerfeld, Federal Republic of Germany
(Received 24 September 1985)

We treat low-energy electron scattering by atoms within a Kohn-Sham-type one-particle theory. In applying this theory, all many-body effects involved in the projectile-target interaction are absorbed into a one-particle potential. Hence, one merely has to solve an elementary potential-scattering problem. However, there are two crucial points to be observed in the construction of the scattering potential. (1) The Kohn-Sham-type exchange-correlation potential must be formed by using correlation factors which are required to have certain asymptotic and integral properties. (2) Since the scattering process is viewed as being quasistationary, the unbound projectile state must be modified by a bell-jar-type envelope function to account for the effect of a finite residence time in the target where the projectile causes a finite perturbation. During this time the entire system has to be treated as consisting of $N+1$ indistinguishable electrons which in a Kohn-Sham-type theory are described by only $N+1$ self-consistent one-particle states. Once the analytical forms of the correlation factors and the envelope function have been chosen, the calculational procedure is completely parameter-free. Although it is considerably simpler than well-established methods in this field, it provides comparably good results on differential cross sections and scattering-induced polarizations in a wide range of impact energies (5–100 eV).

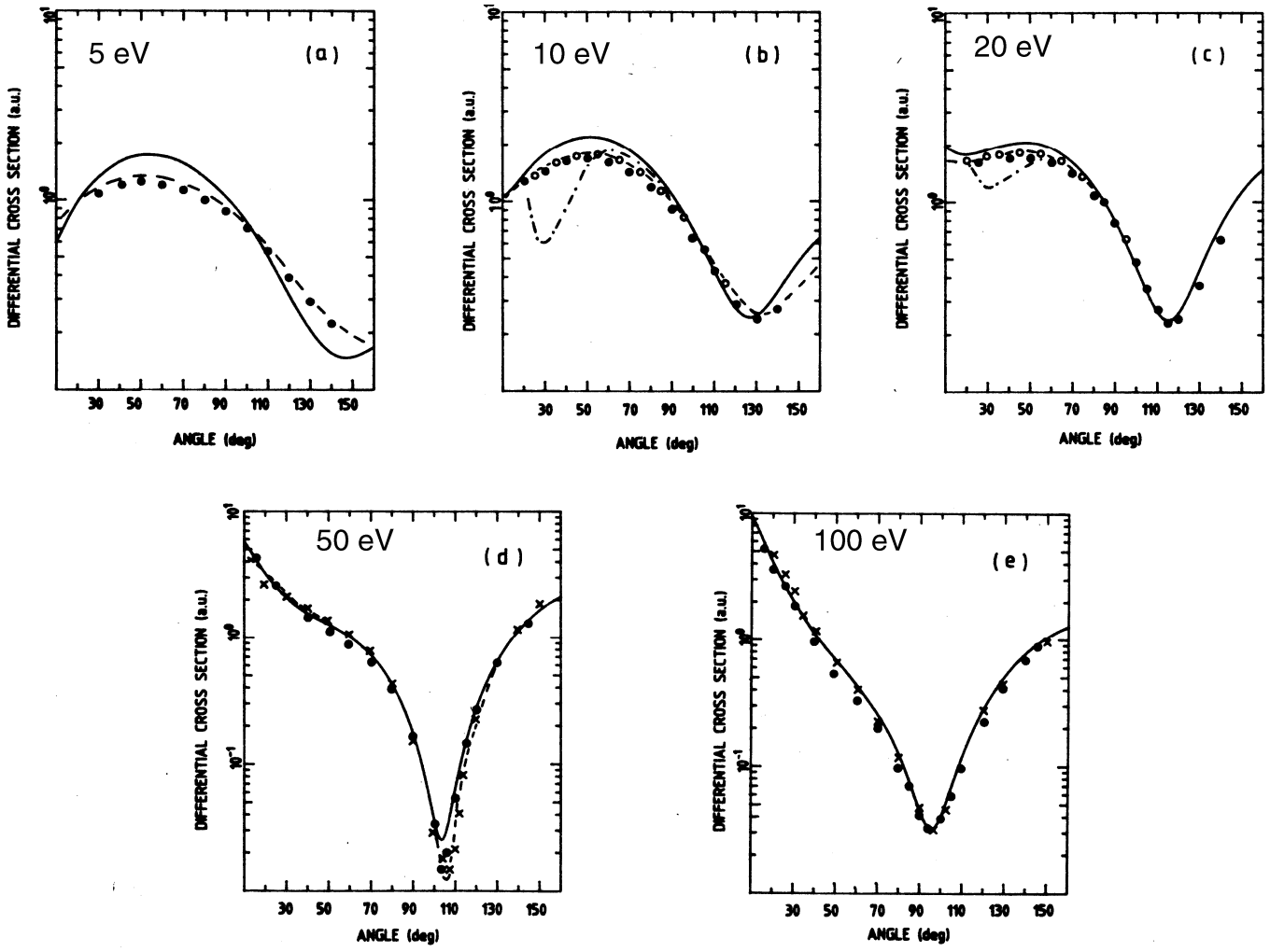

FIG. 2. Differential cross sections for elastic scattering of electrons by Ne atoms (in atomic units): (a) 5 eV, (b) 10 eV, (c) 20 eV, (d) 50 eV, (e) 100 eV. Experiment: ●, Ref. 14; ○, Ref. 15; ×, Ref. 16. Theory: ——, present work; — — —, McEachran and Stauffer (Ref. 13); —·—·—·, Fritsche *et al.* (Ref. 1).

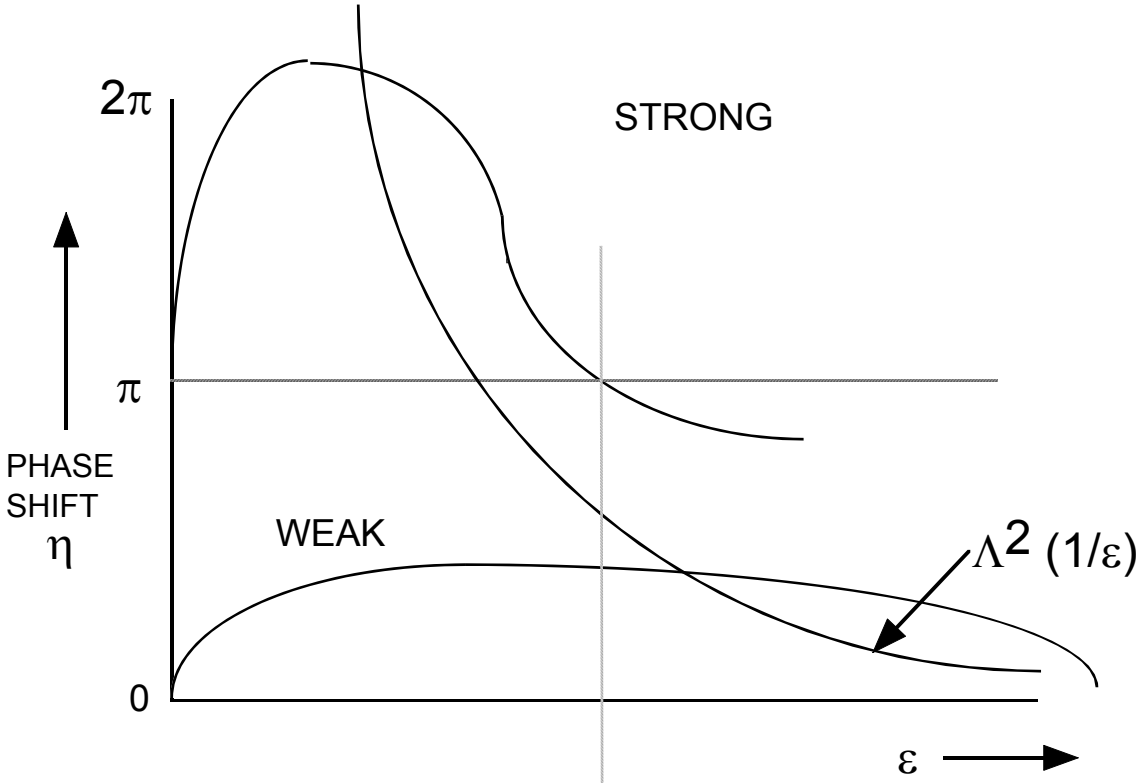

$$\sigma(\varepsilon) = (1/\pi)\Lambda^2 \sum (2l+1)\sin^2(\eta_l)$$

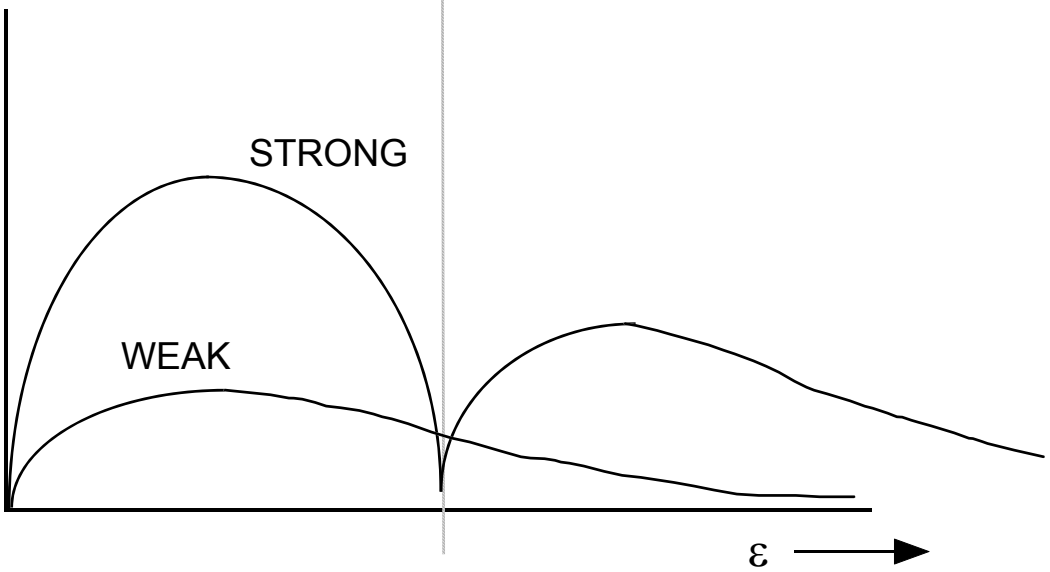

ramsauer_origin.cdd

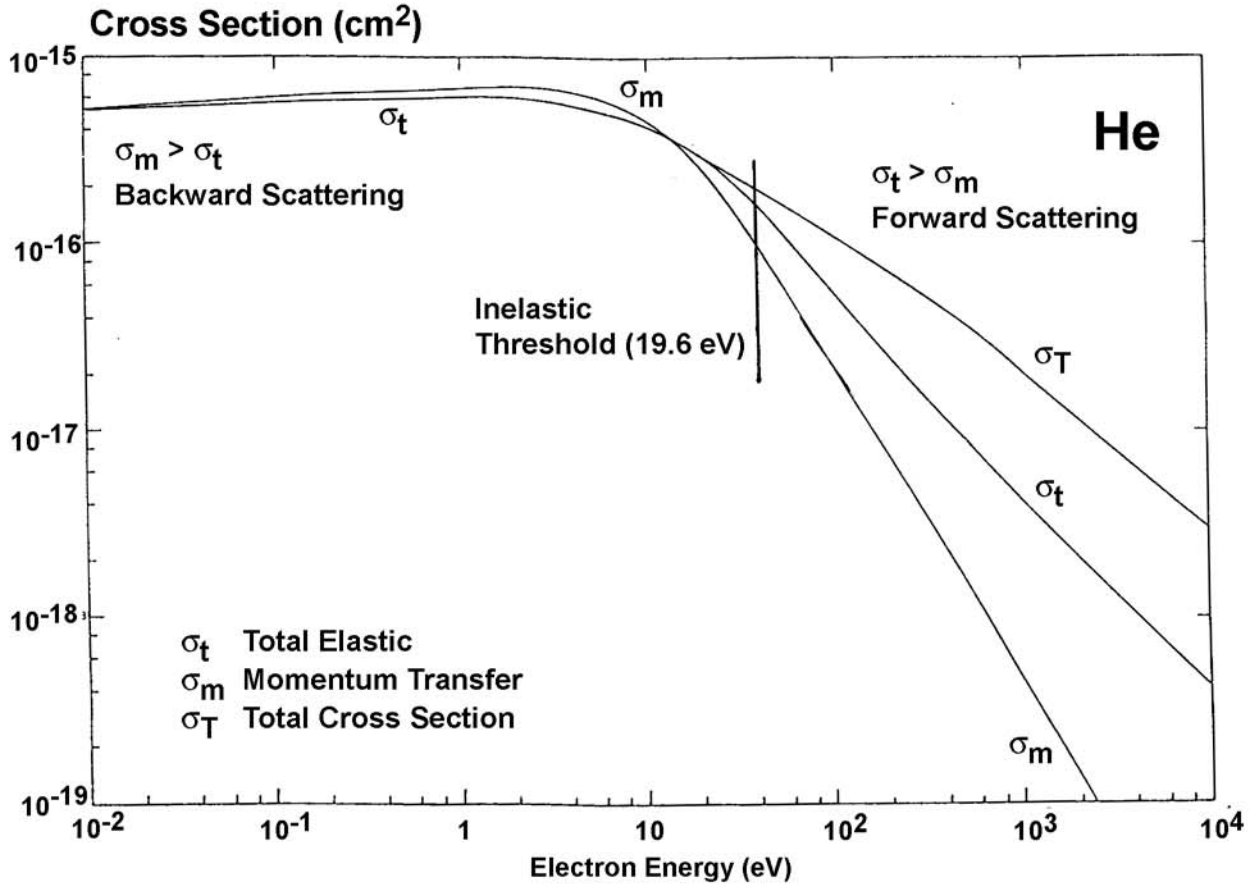

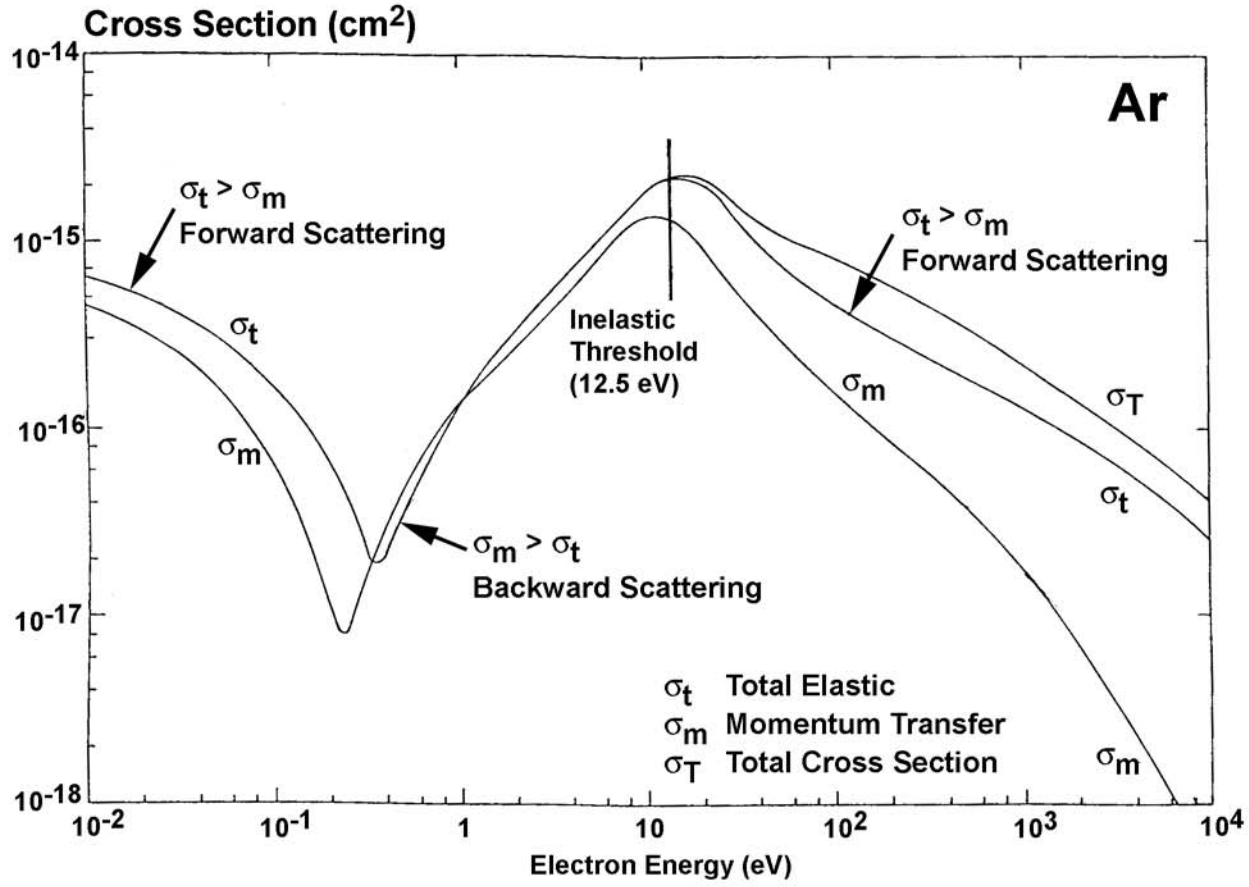

Ref: M. Hayashi, Nagoya University

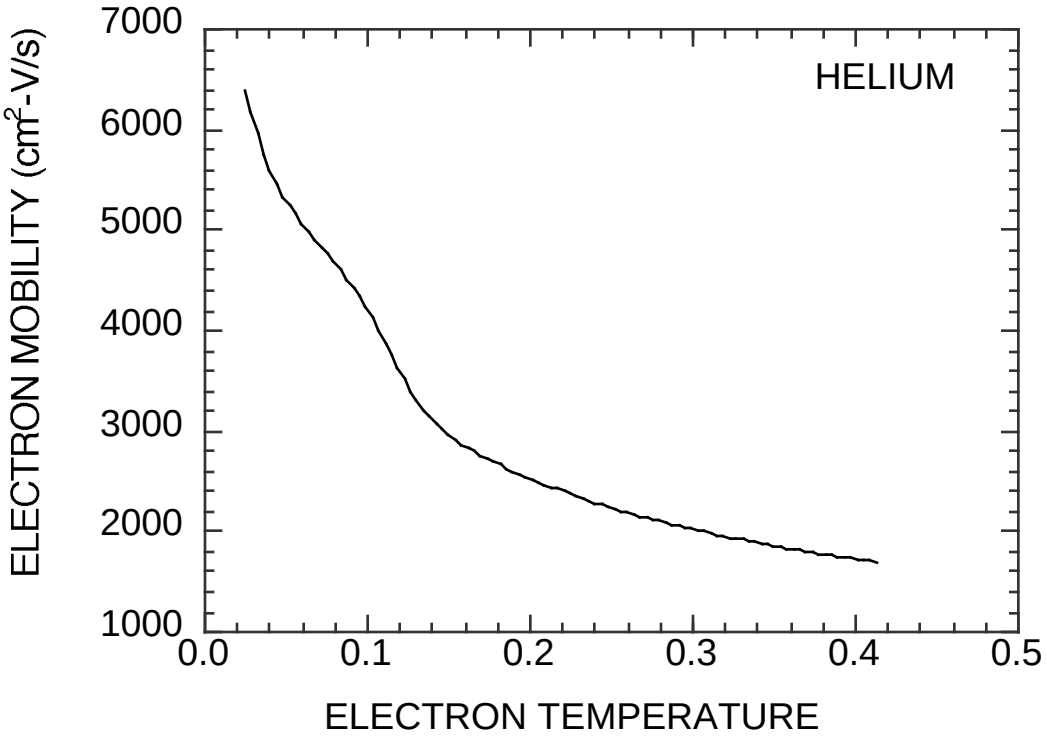
HELIUM
ELECTRON MOBILITY (cm^2-V/s)
7000
6000
5000
4000
3000
2000
1000
0.0
0.1
0.2
0.3
0.4
0.5
ELECTRON TEMPERATURE

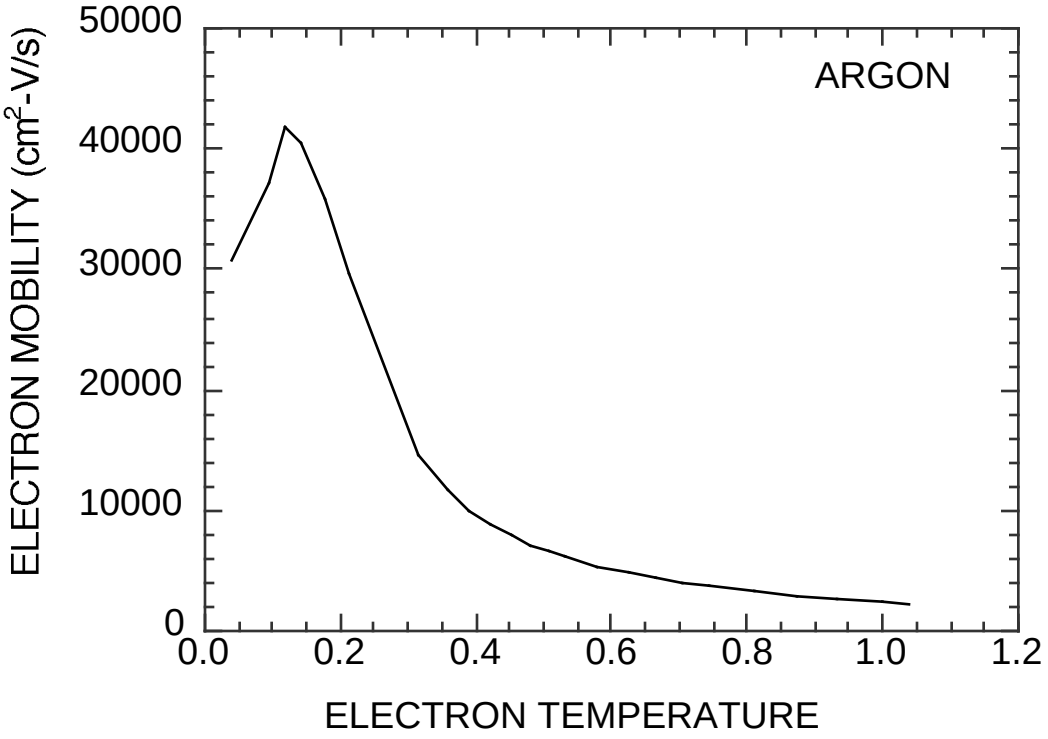
ARGON
ELECTRON MOBILITY (cm^2-V/s)
50000
40000
30000
20000
10000
0
0.0
0.2
0.4
0.6
0.8
1.0
1.2
ELECTRON TEMPERATURE

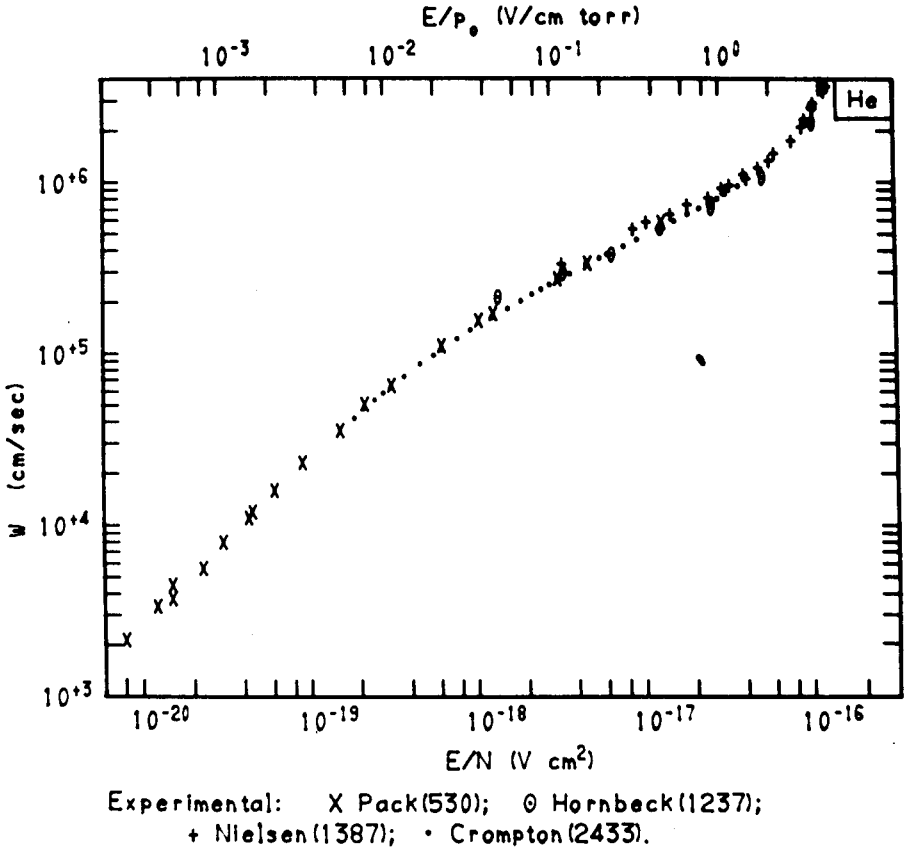

FIGURE 1.1. Experimental values of W as a function of E/N for values of $E/N < 1.3 \times 10^{-16}$ V cm² in helium.

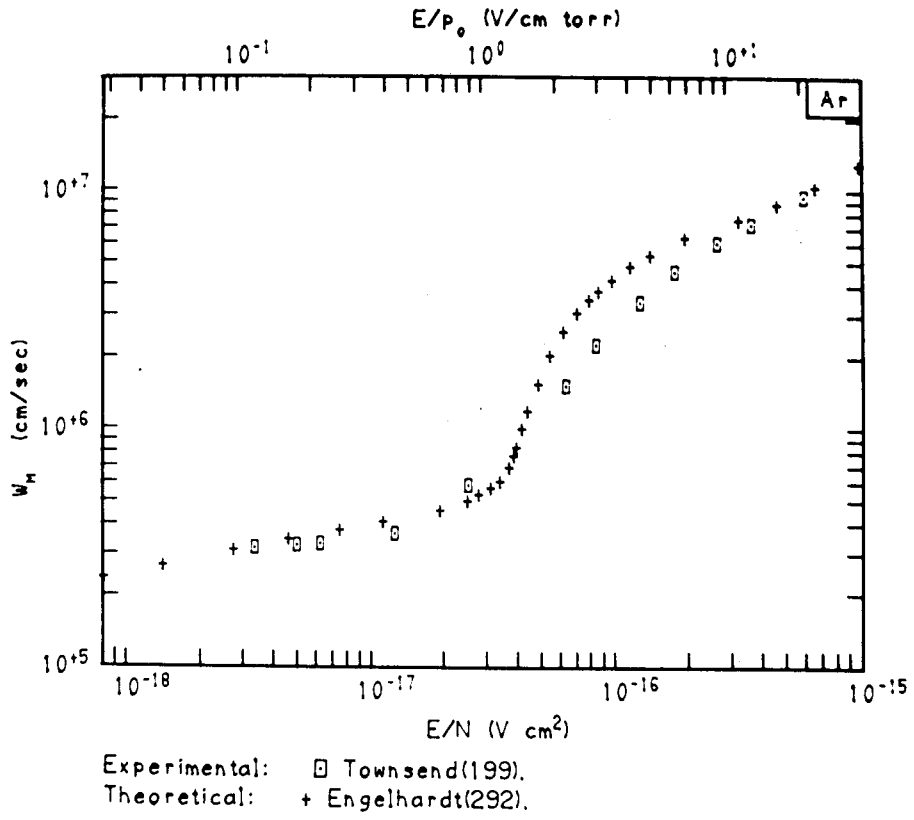

FIGURE 1.13. W_M, E/N for argon.

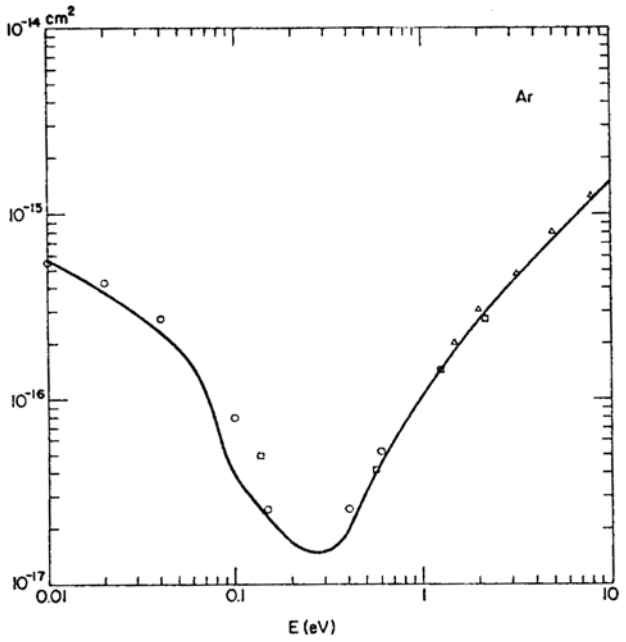

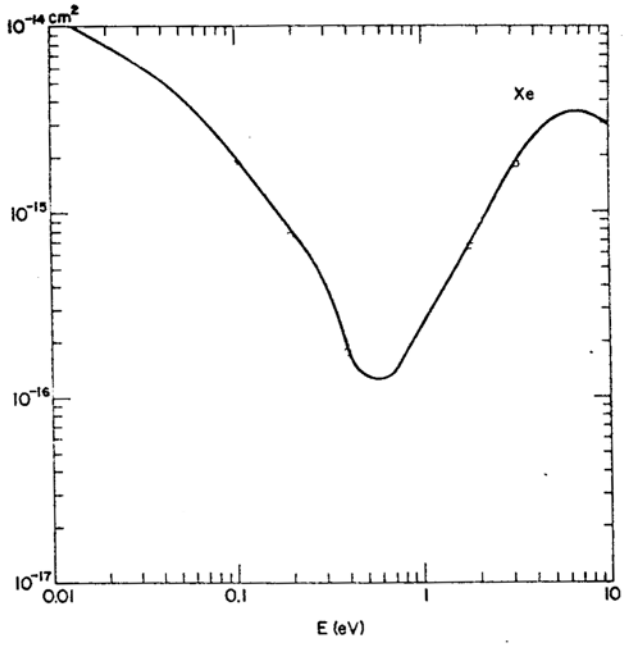

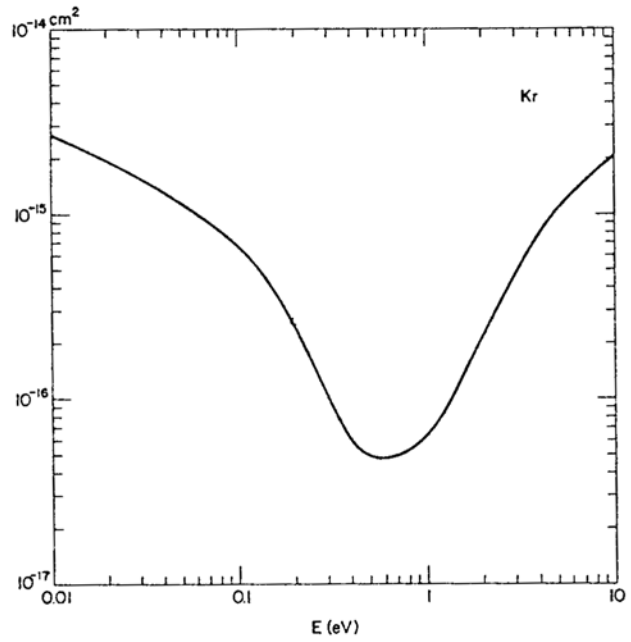

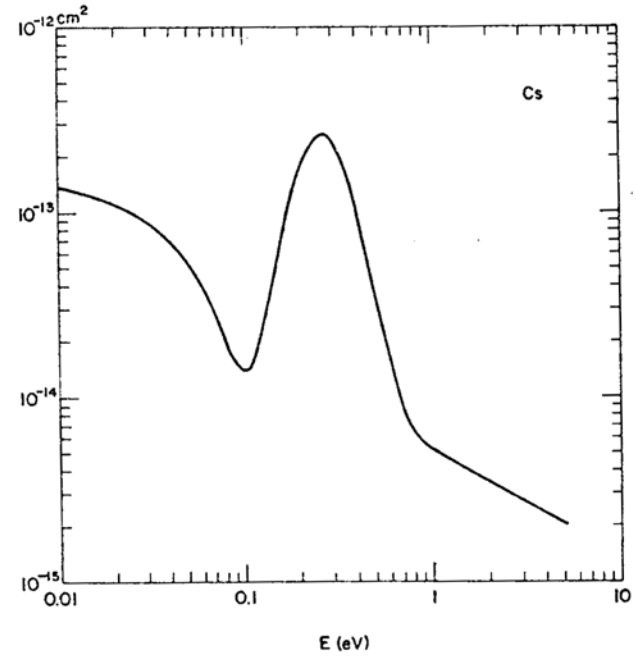

Momentum Transfer Cross Sections

Y. Itikawa
Atomic Data and Nuclear Data Tables
vol. 14, July 1974

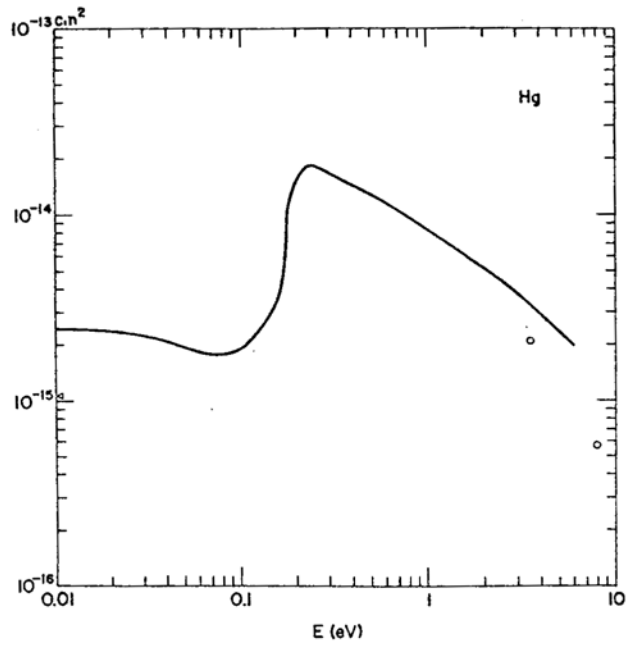

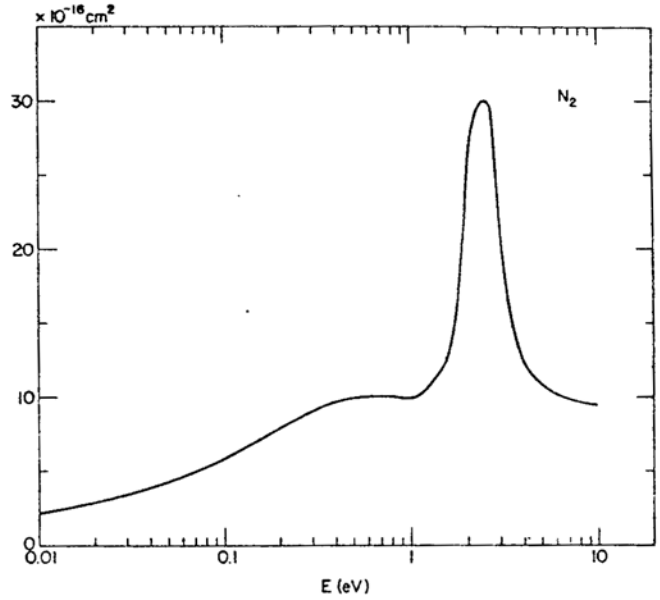

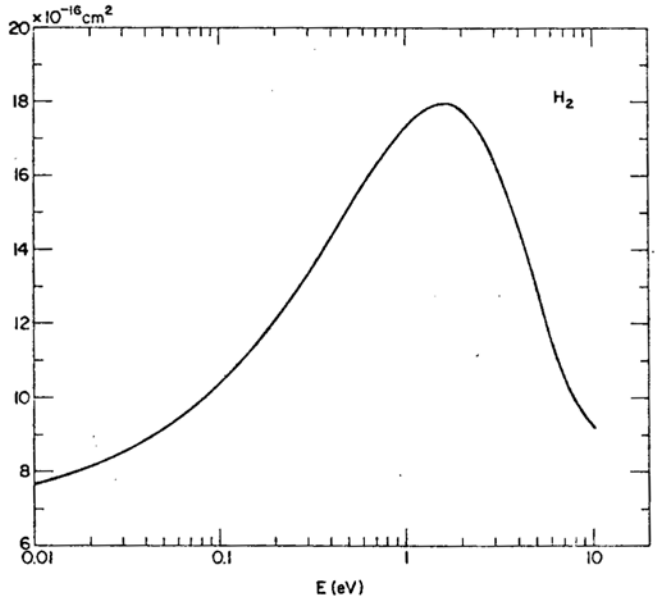

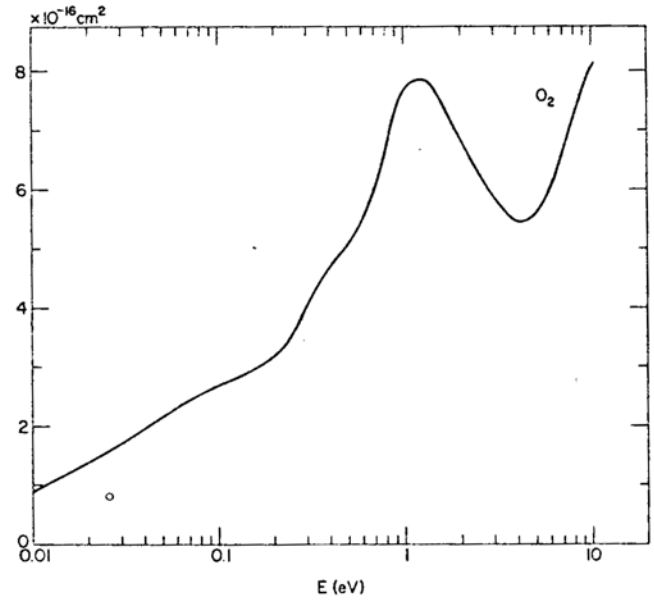

Momentum Transfer Cross Sections

Y. Itikawa
Atomic Data and Nuclear Data Tables
vol. 14, July 1974

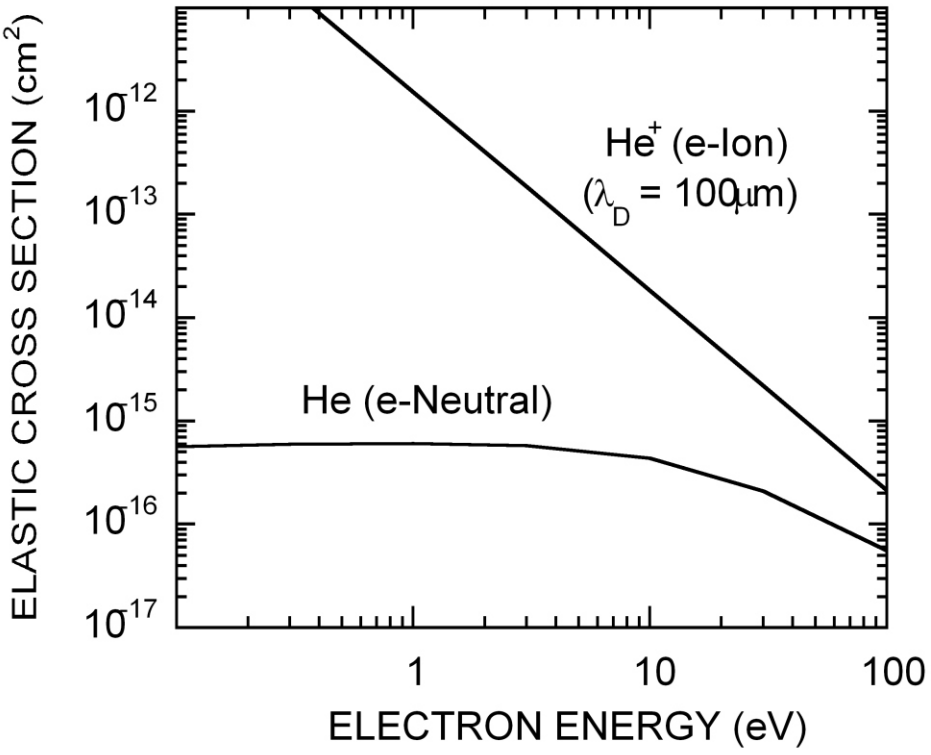

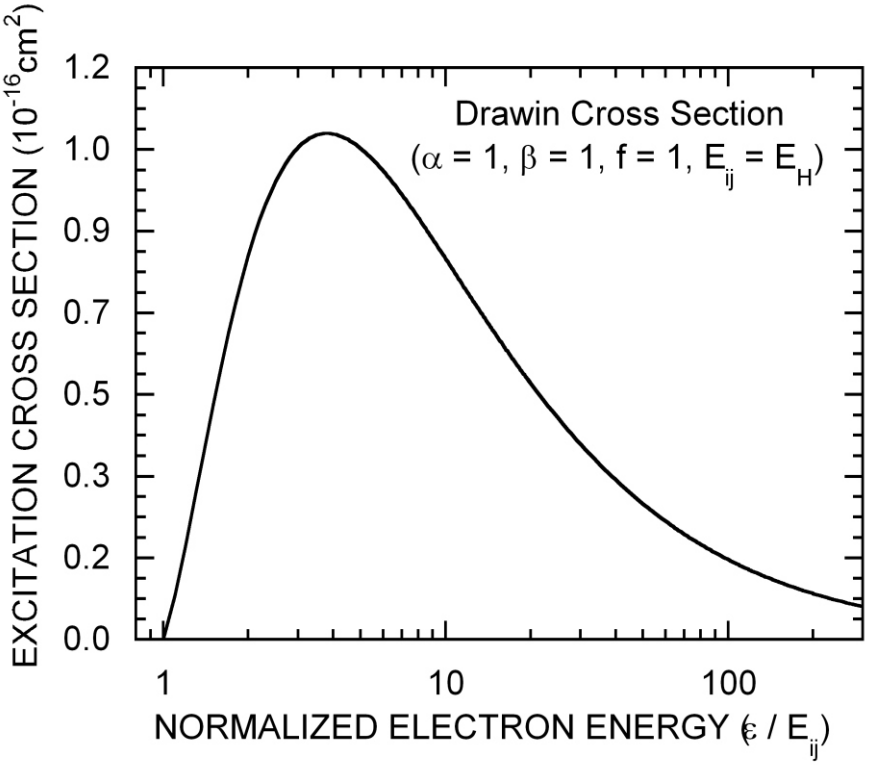

helium_xsections_v02

Values for transitions in atomic hydrogen (allowed transitions)

Transition	equ.(42)		equ.(43)	
	α_{ij}	$1.25\beta_{ij}$	$c_{ij}E_{ij}$	α_{ij}
1s → 2p	1.00	1.25	1.26	1
2s → 3p	0.81	1.25	0.51	1
2p → 3d	0.90	1.25	1.10	1
3s → 4p	0.75	1.25	0.33	1
3p → 4d	0.80	1.25	0.50	1
3d → 4f	0.85	1.25	0.92	1
4s → 5p	0.72	1.25	0.24	1
4p → 5d	0.77	1.25	0.33	1
4d → 5f	0.79	1.25	0.46	1
4f → 5g	0.83	1.25	0.79	1

Transition	equ.(42)		equ.(43)	
	α_{ij}	$1.25\beta_{ij}$	$c_{ij}E_{ij}$	α_{ij}
1s → 3p	1	1.77	2.33	1
1s → 4p	1	2.03	2.75	1
1s → 5p	1	2.15	2.94	1
1s → 6p	1	2.24	3.08	1
2s → 4p	0.83	1.25	0.83	1
2s → 5p	0.93	1.25	1.04	1
2s → 6p	0.95	1.25	1.18	1
2s → 7p	0.95	1.25	1.28	1
3s → 5p	0.82	1.25	0.51	1
3s → 5d	0.90	1.25	0.94	1
3d → 5f	1	1.93	2.59	1

Values for transitions in atomic helium (allowed transitions)

Transition	equ. (42)		
	f_{ij}	α_{ij}	$1.25\beta_{ij}$
$1^1S \rightarrow 2^1P$	0.276	1.1	1.25
$\rightarrow 3^1P$	0.073	1.2	1.25
$\rightarrow 4^1P$	0.030	1.4	1.25
$\rightarrow 5^1P$	0.015	1.3	1.25
$\rightarrow 6^1P$	0.009	1.1	1.25
$2^1S \rightarrow 2^1P$	0.376	0.9	1.25
$\rightarrow 3^1P$	0.151	1.2	1.25

Transition	equ. (42)		
	f_{ij}	α_{ij}	$1.25\beta_{ij}$
$2^1S \rightarrow 4^1P$	0.051	1.1	1.25
$\rightarrow 5^1P$	0.022	1.0	1.25
$\rightarrow 6^1P$	0.013	1.0	1.25
$2^3S \rightarrow 2^3P$	0.539	0.8	1.25
$\rightarrow 3^3P$	0.645	0.95	1.25
$\rightarrow 4^3P$	0.023	1.0	1.25
$\rightarrow 5^3P$	0.011	1.0	1.25
$\rightarrow 6^3P$	0.006	1.0	1.25

H. Drawin, EUR-CEA-FC-383, 1966

Sinfailam, A. L., Nesbet, R. K. Phys. Rev. A, 6, 2118 (1972)

Electronic Excitation

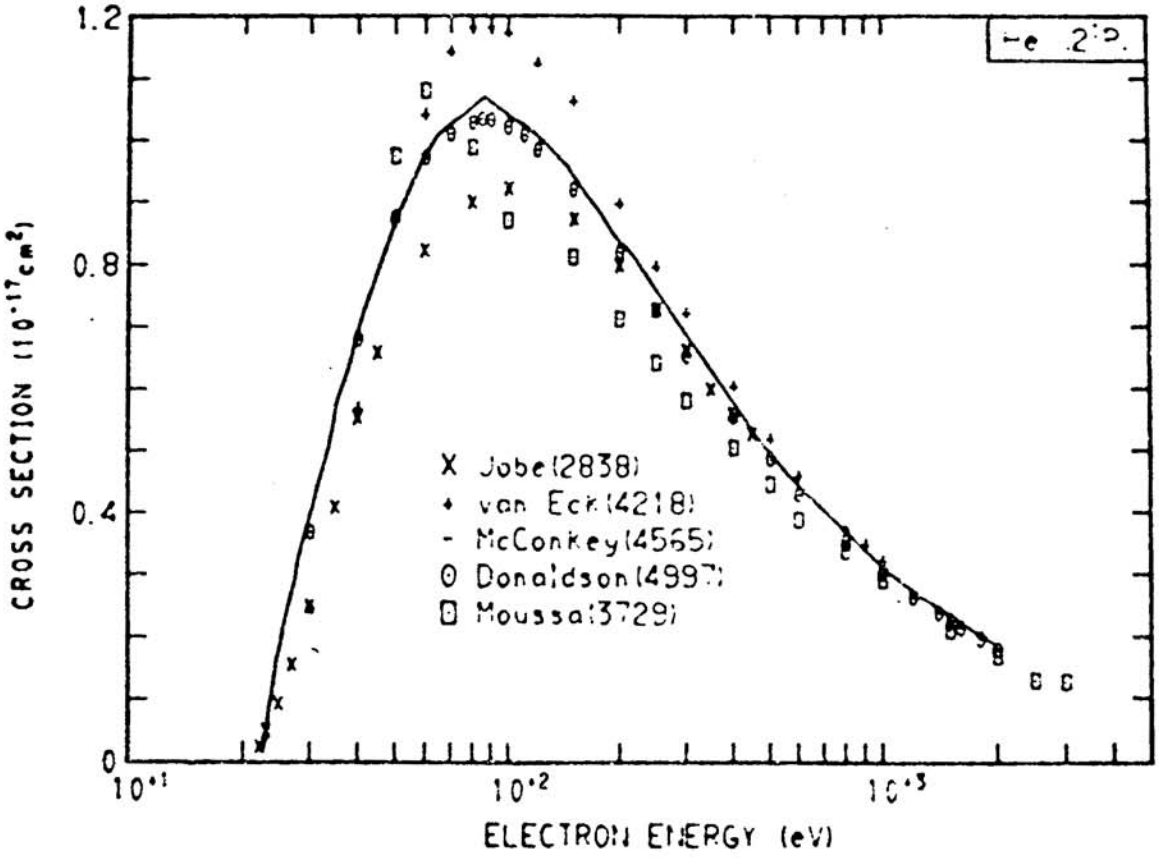

Experimental Measurement of
Electron impact cross section for He 2^1P **Ref: Kieffer, JILA**

Electron-impact excitation cross sections for Na II

P. S. Ganas, M. Aryafar, and L. P. Gately
Department of Physics and Astronomy, California State University at Los Angeles, Los Angeles, California 90032

J. Chem. Phys. **81** (4), 15 August 1984

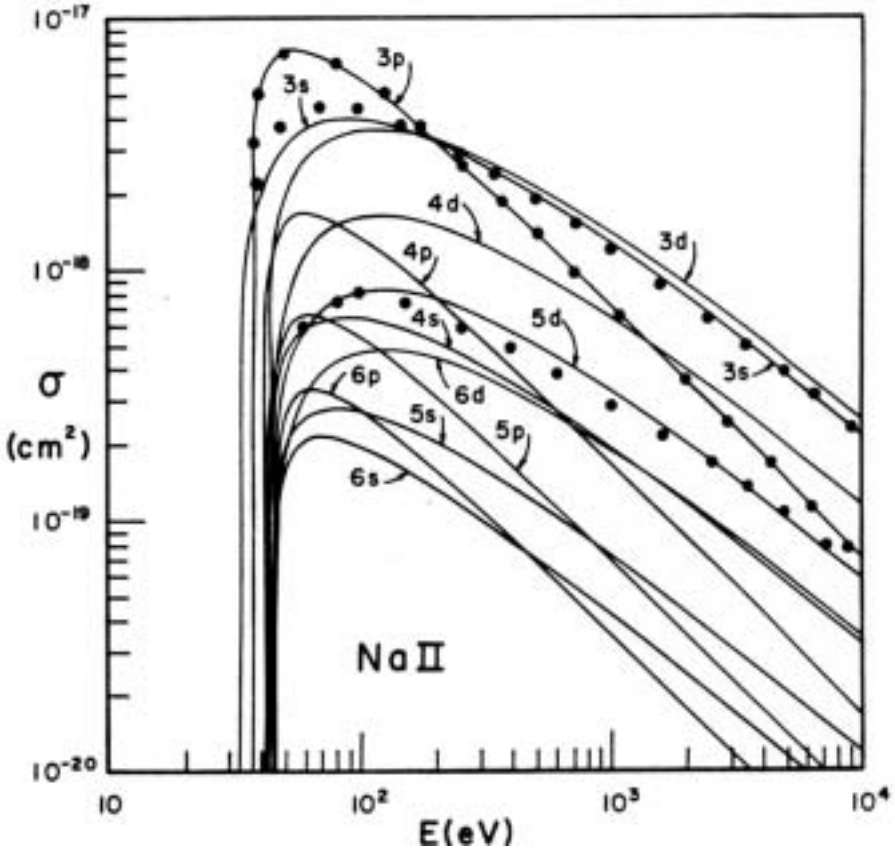

NA_XSECTION

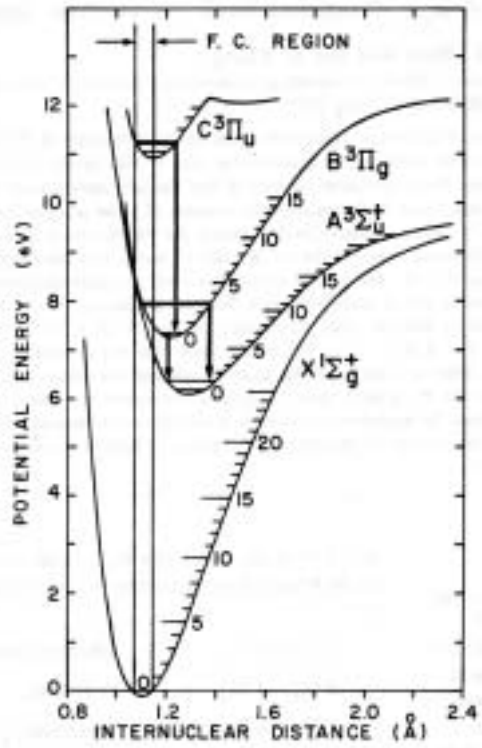

Excitation of Metastable $N_2(A)$ Vibrational Levels
by Electron Impact
W. L. Borst and S. L. Chang,
J. Chem. Phys. 59, 5830 (1973)

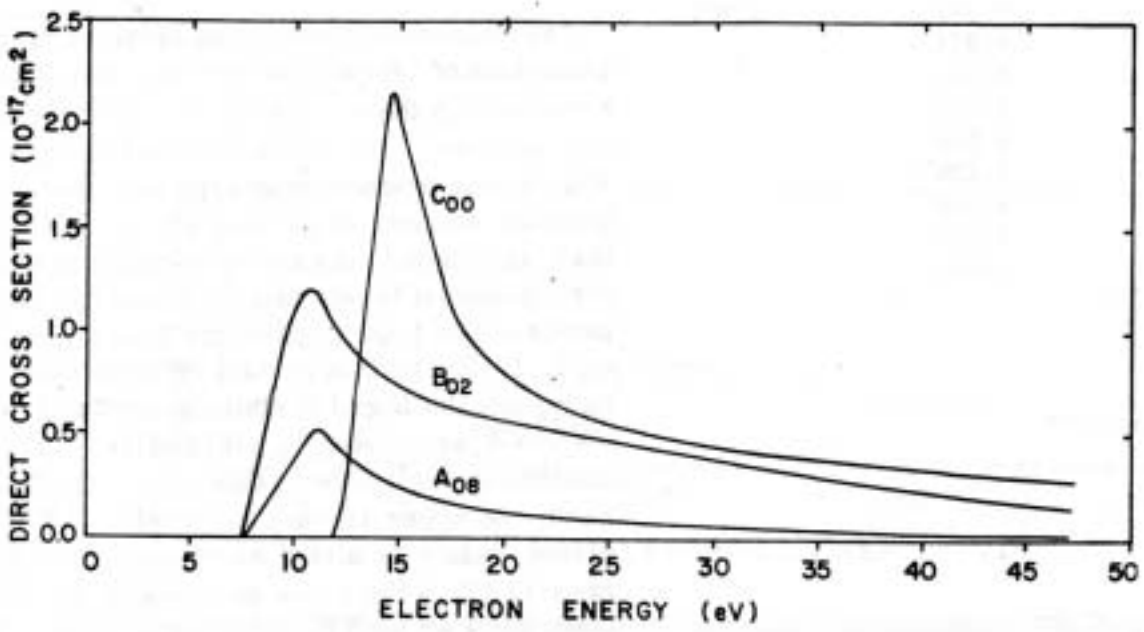

FIG. 3. Examples of direct excitation cross sections for individual vibrational levels of the *A*, *B*, and *C* states. The vibrational levels chosen are those with the largest cross section, *i.e.*, maximum Franck–Condon factor. The label A_{08} denotes the $v=8$ level of the *A* state as excited from the $v=0$ level of the N_2 ground state and similar labeling applies to the *B* and *C* states.

N2_XSECTION

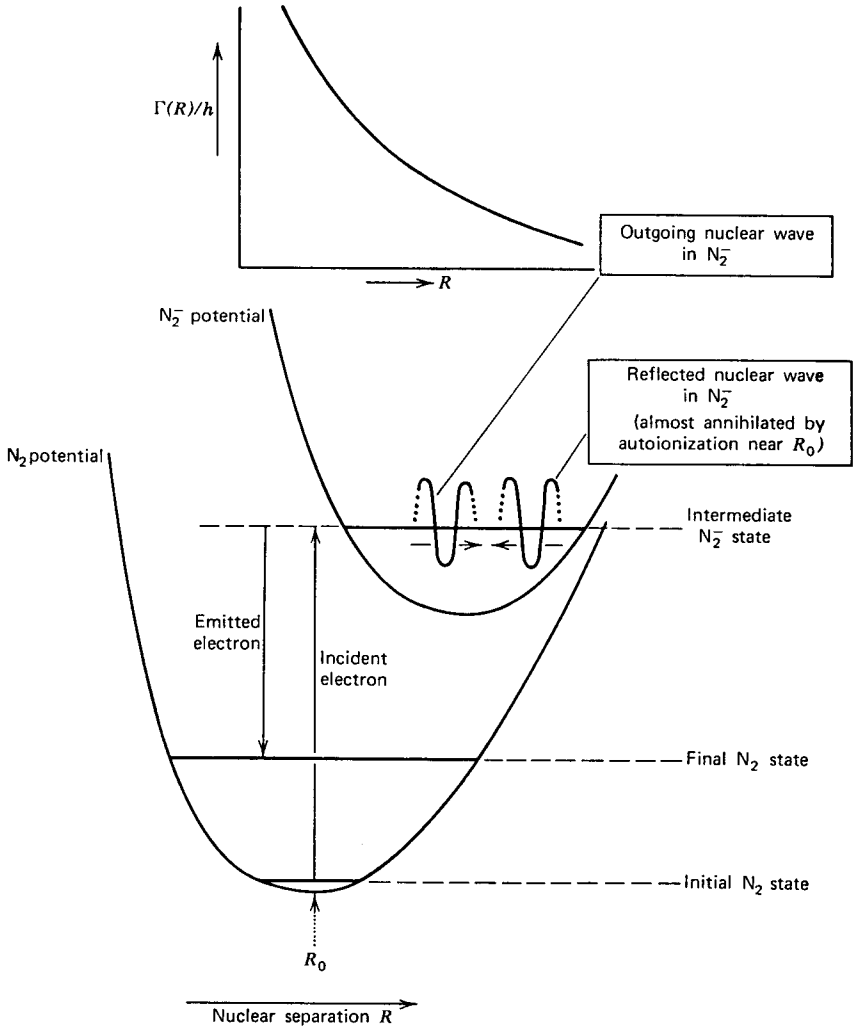

Fig. 2.1 The "boomerang" model of the nuclear wavefunction applied to the N_2^- ion. This model is discussed by Herzenberg (1968). It is based on the assumption that the magnitude and R-dependence of the width $\Gamma(R)$ are such that only a single outgoing and a single reflected wave are important. (From Birtwistle and Herzenberg, 1971.)

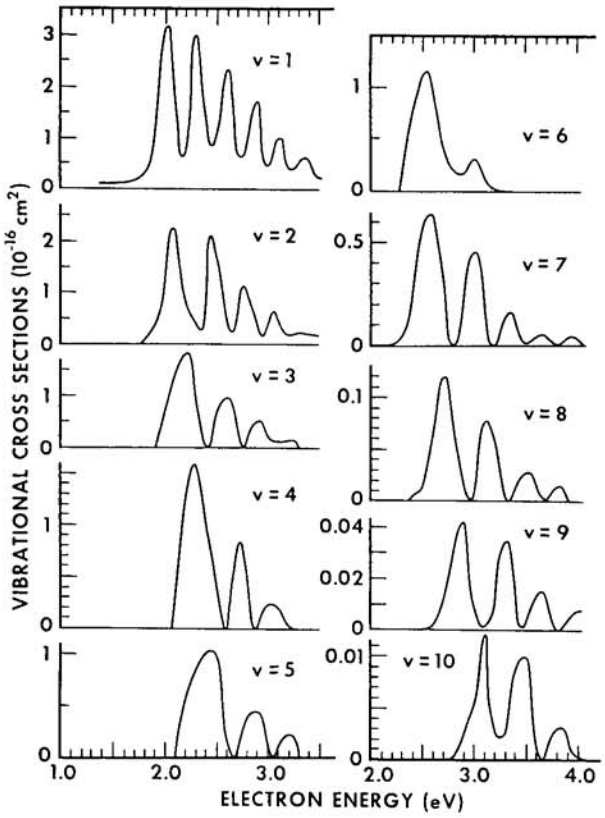

Fig. 2.6 Vibrational cross sections to $v = 1$ to 10 in N_2. The data plotted here are from Schulz (1964) for $v = 1$ to 6 and from Boness and Schulz (1973) for $v = 7$ to 10, normalized to the value given by Spence, Mauer and Schulz (1972). A digitized listing has been assembled by Kieffer (1973). The absolute values shown here may be too low by a factor of up to two (Wong, private communication).

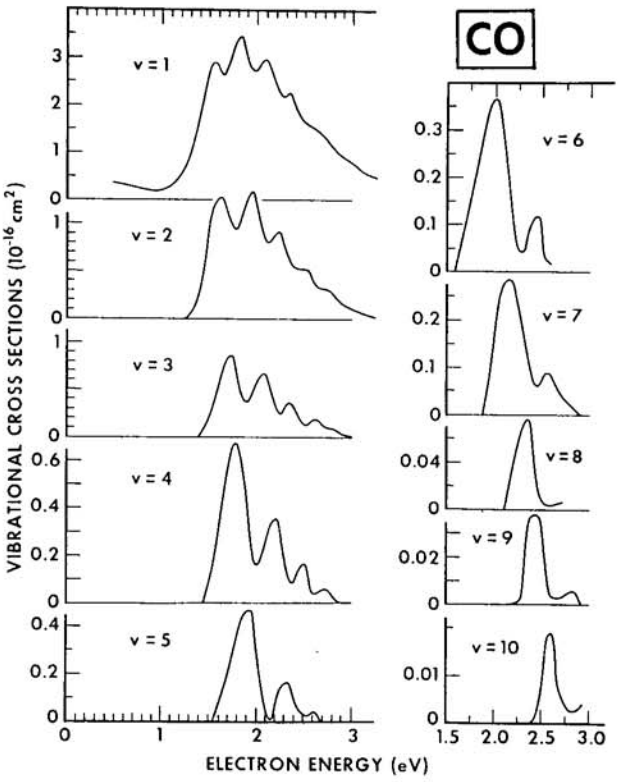

Fig. 2.7 Vibrational cross sections for $v = 1$ to 10 in CO. The data are taken from Ehrhardt et al. (1968) for $v = 1$ to 7 and from Boness and Schulz (1973) for $v = 8$ to 10. Absolute values are taken from Ehrhardt et al. (1968) as listed by Kieffer (1973).

Vibrationally inelastic and elastic cross sections for $e + NF_3$ collisions

L Boesten†, Y Tachibana†, Y Nakano†, T Shinohara§, H Tanaka† and M A Dillon‡

J. Phys. B: At. Mol. Opt. Phys. **29** (1996) 5475–5491.

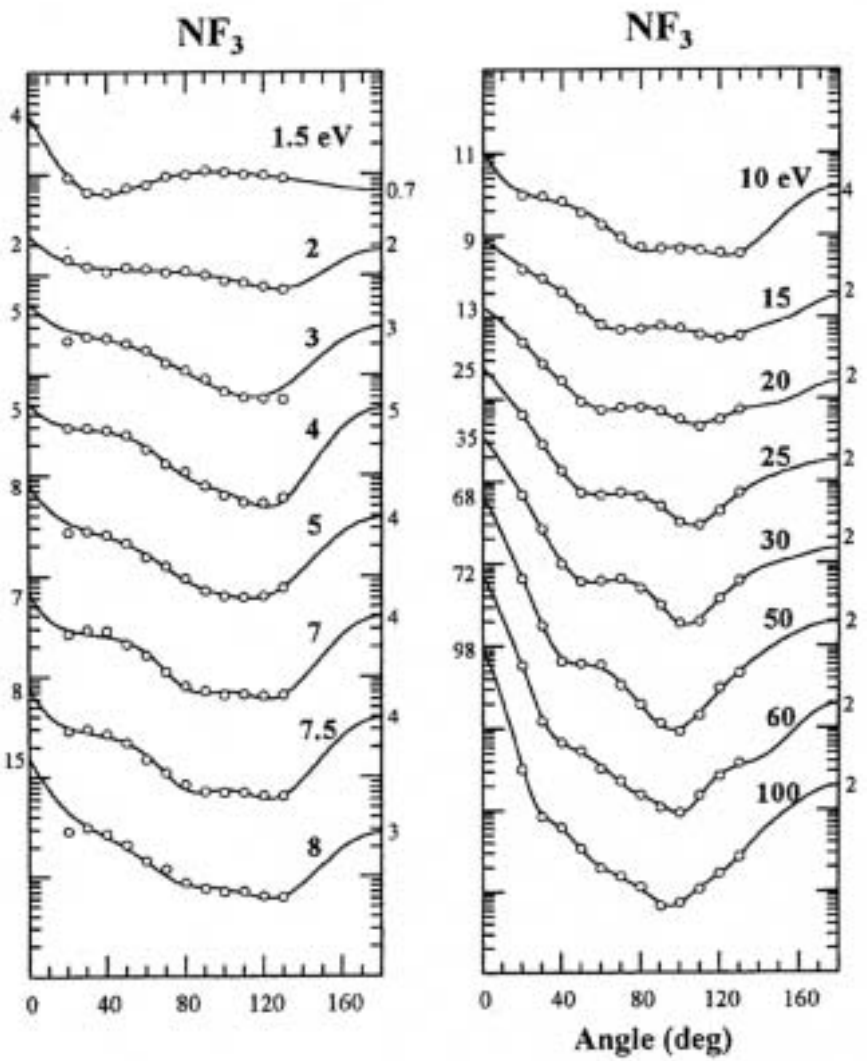

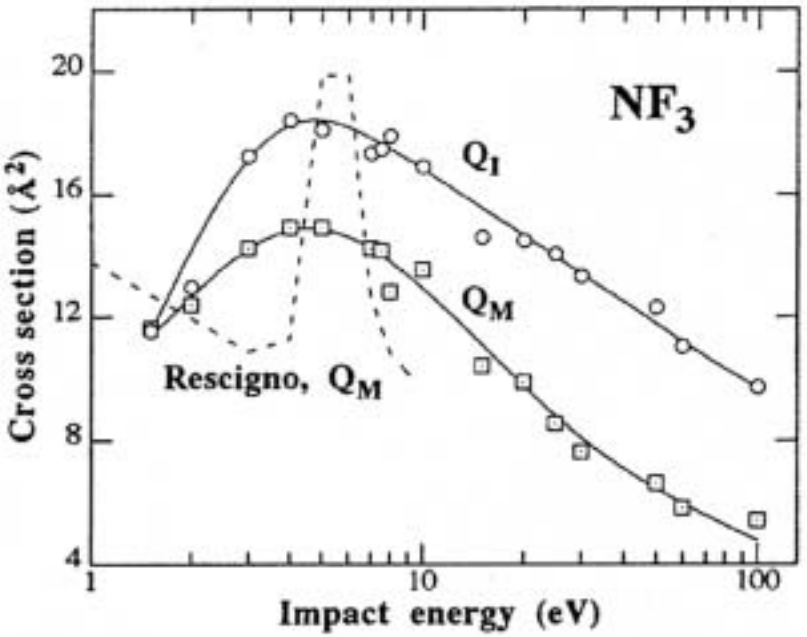

NF3_VIB_XSECTION

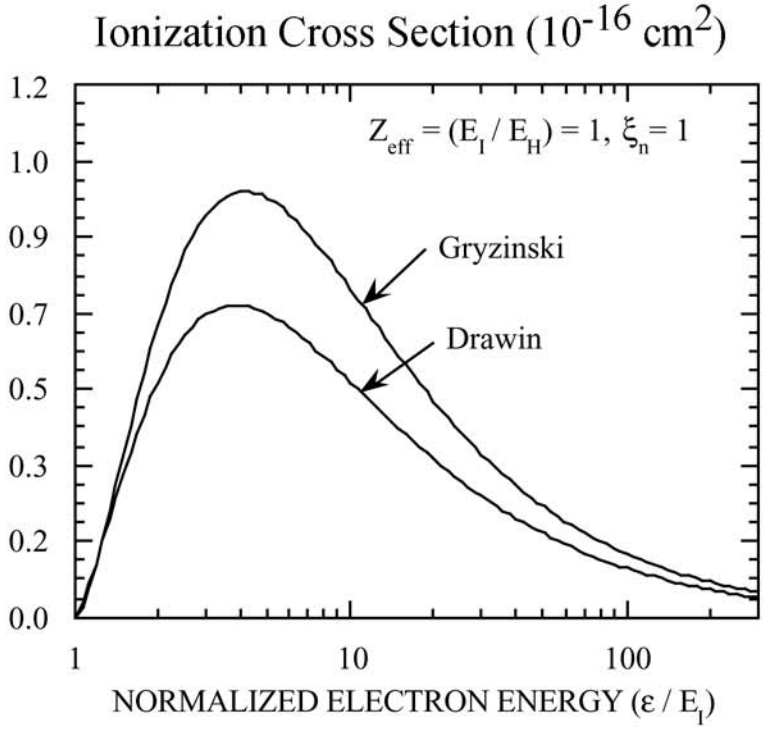
Ionization Cross Section (10^{-16} cm^2)
$Z_{eff} = (E_I / E_H) = 1$, $\xi_n = 1$
Gryzinski
Drawin
1.2
1.0
0.9
0.7
0.5
0.3
0.2
0.0
1
10
100
NORMALIZED ELECTRON ENERGY (ε / E_I)

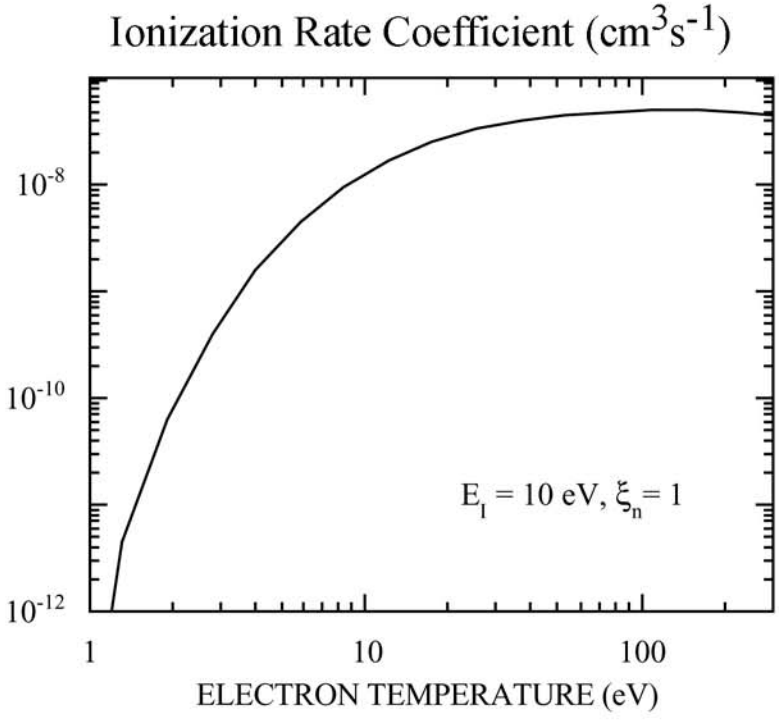
Ionization Rate Coefficient (cm^{3}s^{-1})
10^{-8}
10^{-10}
10^{-12}
E_I = 10 eV, ξ_n = 1
1
10
100
ELECTRON TEMPERATURE (eV)

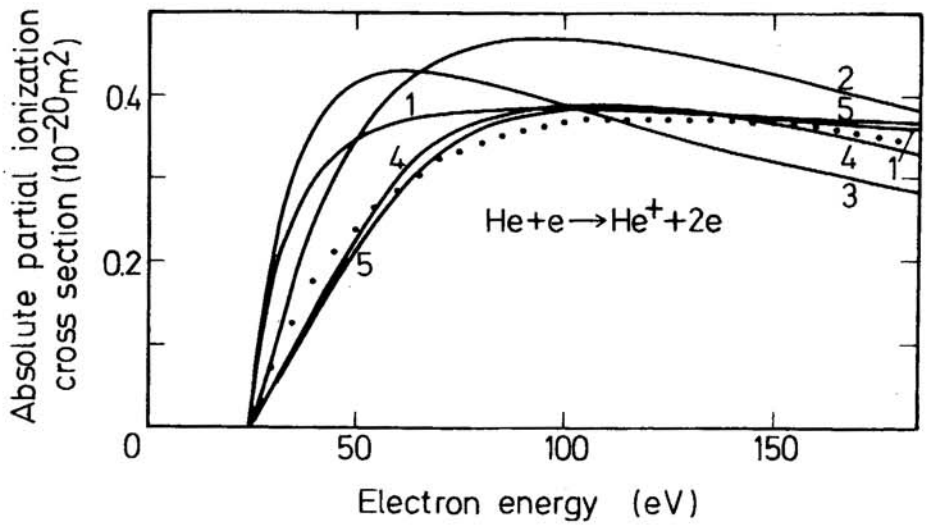

Fig. 2-1. Absolute partial ionization cross sections for $He+e \rightarrow He^+ + 2e$ after Märk (1982a). *Experimental*: Full dots: Stephan *et al.* (1980). *Theoretical*: Curve 1: Elwert 1952 (given by Pitchford *et al.* 1980), Curve 2: Gryzinski 1965 (Pitchford *et al.* 1980), Curve 3: Burgess 1964-Vriens 1966 a, b (Pitchford *et al.* 1980), Curve 4: Gryzinski 1959 (Ochkur and Petrunkin 1963), Curve 5: Ochkur 1964 (Peach 1966)

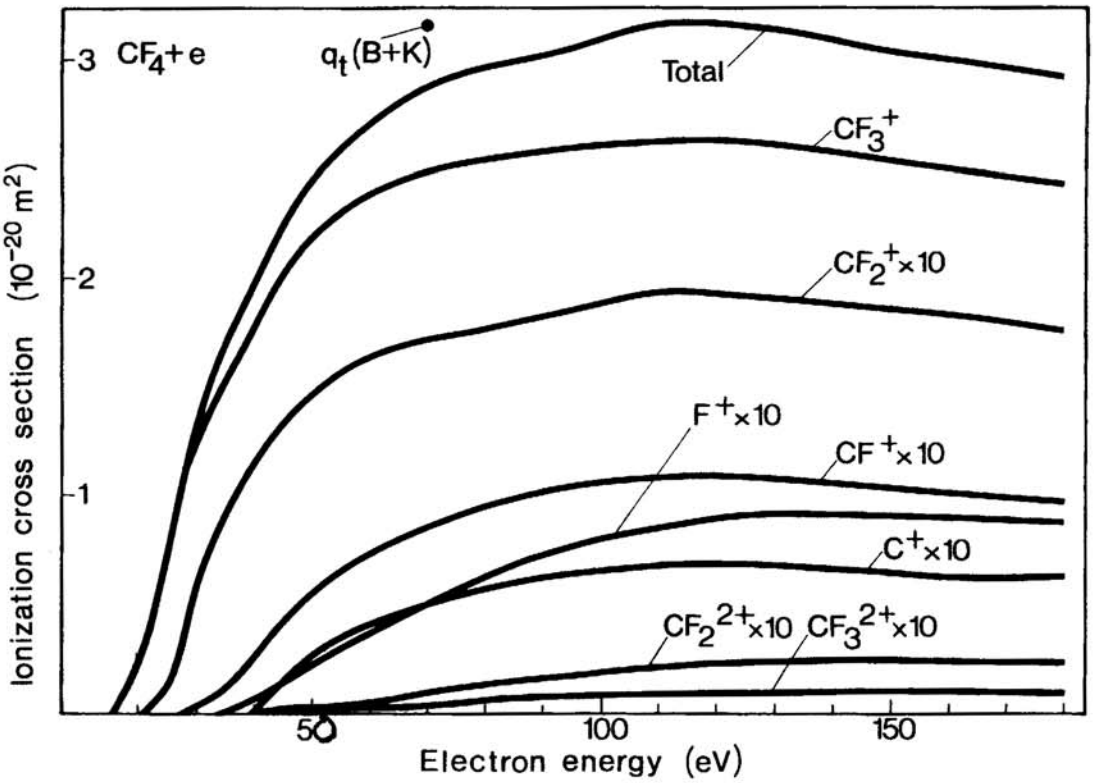

Fig. 5-34. Partial and total ionization cross section functions for fragment ions of CF_4 as measured by Stephan *et al.* (1983 d, e). Full dot: total cross section at 70 eV determined by Beran and Kevan (1969) recalibrated to the Ar value of Rapp and Englander-Golden (1965)

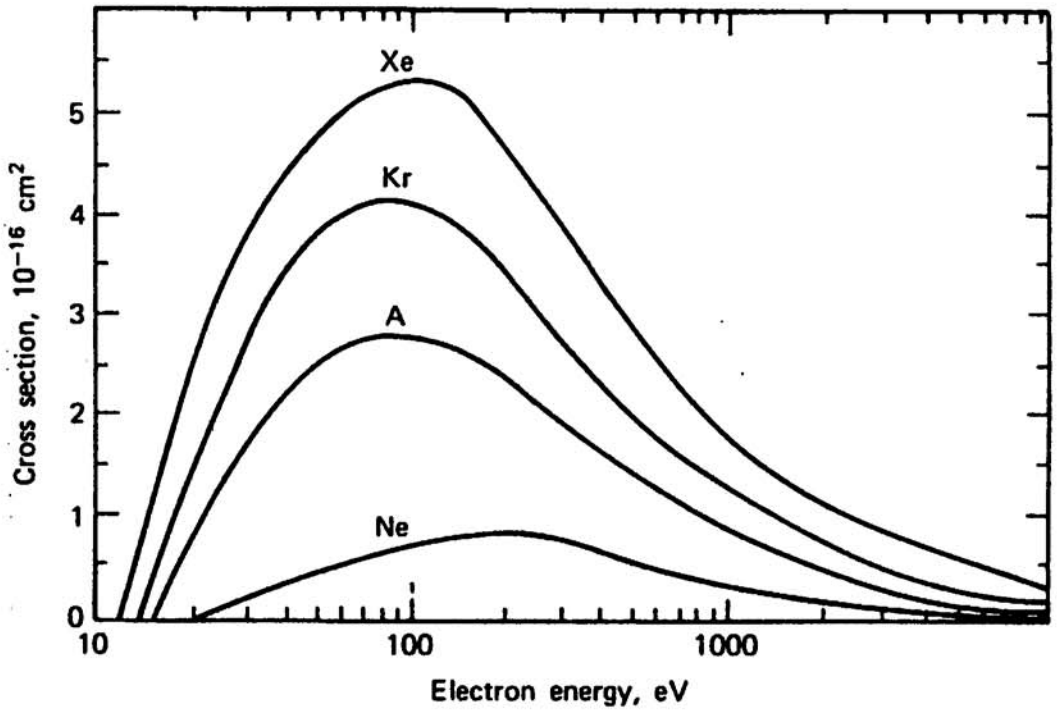

Total Ionization Cross Sections for Rare Gases

Derivation of
Superelastic Cross Section

A "superelastic" collision (or collision of the second kind) occurs when an electron de-excites a higher lying state. In doing so, the electron gains energy

Inelastic	Superelastic
$e + N \rightarrow N^* + (e - \Delta\varepsilon)$	$e + N^* \rightarrow N + (e + \Delta\varepsilon)$

where $\Delta\varepsilon$ is the energy loss (inelastic) or energy gain (superelastic) resulting from the collision. The superelastic cross section is obtained from the excitation cross section through the Klein-Rosseland formula.

Assume we have two atomic levels

n_i = density of level
g_i = degeneracy
E_i = energy of level
$\Delta\varepsilon = E_2 - E_1$
σ_{12} = excitation cross section
σ_{21} = superelastic cross section

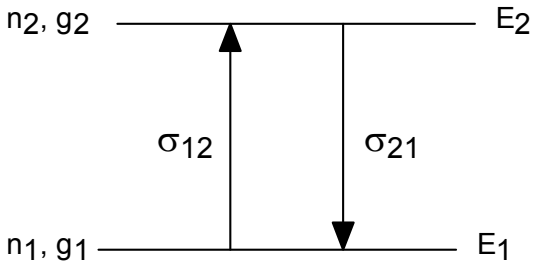

For a Maxwell Boltzmann electron energy distribution the number of electrons in $(\varepsilon, \varepsilon + d\varepsilon)$ is proportional to

$$f(\varepsilon)d\varepsilon = K\exp\left(\frac{-\varepsilon}{kT_e}\right)\varepsilon^{1/2}d\varepsilon$$

where K is a constant. The total rate of excitation of n_2 by these electrons is

$$R_{12}(\varepsilon)d\varepsilon = K\sigma_{12}(\varepsilon)n_1\left(\frac{2\varepsilon}{m_e}\right)^{1/2} f(\varepsilon)d\varepsilon \qquad \frac{\#}{cm^3 s}$$

The total rate of de-excitation is

$$R_{21}(\varepsilon)d\varepsilon = K\sigma_{21}(\varepsilon)n_2\left(\frac{2\varepsilon}{m_e}\right)^{1/2} f(\varepsilon)d\varepsilon \qquad \frac{\#}{cm^3 s}$$

If there is only one inelastic process, then electrons can only enter $(\varepsilon, \varepsilon + d\varepsilon)$ with $\varepsilon < \Delta\varepsilon$ by suffering inelastic collisions from higher energies, and can only leave $(\varepsilon, \varepsilon + d\varepsilon)$ by suffering superelastic collisions.

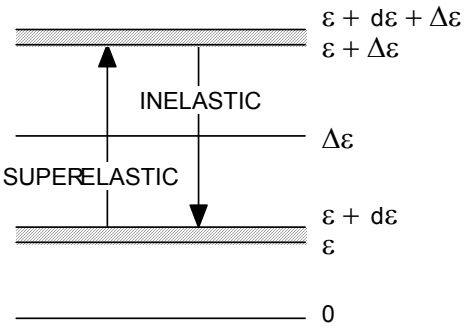

So in the steady state we must have the rate of population and depopulation of $(\varepsilon, \varepsilon + d\varepsilon)$ be equal.

$$\phi_{\text{INTO}(\varepsilon,\varepsilon+d\varepsilon)} = R_{12}(\varepsilon + \Delta\varepsilon) \qquad \begin{bmatrix} \text{Electrons at } \varepsilon + \Delta\varepsilon \\ \text{exciting } n_1 \text{ and} \\ \text{losing energy.} \end{bmatrix}$$

$$\phi_{\text{OUT OF}(\varepsilon,\varepsilon+d\varepsilon)} = R_{21}(\varepsilon) \qquad \begin{bmatrix} \text{Electrons at } \varepsilon \text{ de exciting } n_2 \\ \text{and gaining energy.} \end{bmatrix}$$

$$\sigma_{12}(\varepsilon + \Delta\varepsilon) n_1 \left(\frac{2(\varepsilon + \Delta\varepsilon)}{m_e}\right)^{1/2} \exp\left(\frac{-(\varepsilon + \Delta\varepsilon)}{kT_e}\right)(\varepsilon + \Delta\varepsilon)^{1/2} =$$

$$\sigma_{21}(\varepsilon) n_2 \left(\frac{2\varepsilon}{m_e}\right)^{1/2} \exp\left(\frac{-\varepsilon}{kT_e}\right)\varepsilon^{1/2}$$

$$\sigma_{21}(\varepsilon) = \sigma_{12}(\varepsilon + \Delta\varepsilon)\left(\frac{\varepsilon + \Delta\varepsilon}{\varepsilon}\right)\frac{n_1}{n_2}\exp\left(\frac{-\Delta\varepsilon}{kT_e}\right)$$

If we are in equilibrium then $\dfrac{n_2}{n_1} = \dfrac{g_2}{g_1}\exp\left(\dfrac{-\Delta\varepsilon}{kT_e}\right)$ so

$$\sigma_{21}(\varepsilon) = \frac{g_1}{g_2}\left(\frac{\varepsilon + \Delta\varepsilon}{\varepsilon}\right)\sigma_{12}(\varepsilon + \Delta\varepsilon)$$

$\sigma_{21}(\varepsilon)$ is always nonzero for $\varepsilon > 0$ since $\sigma_{12}(\varepsilon + \Delta\varepsilon)$ is nonzero.

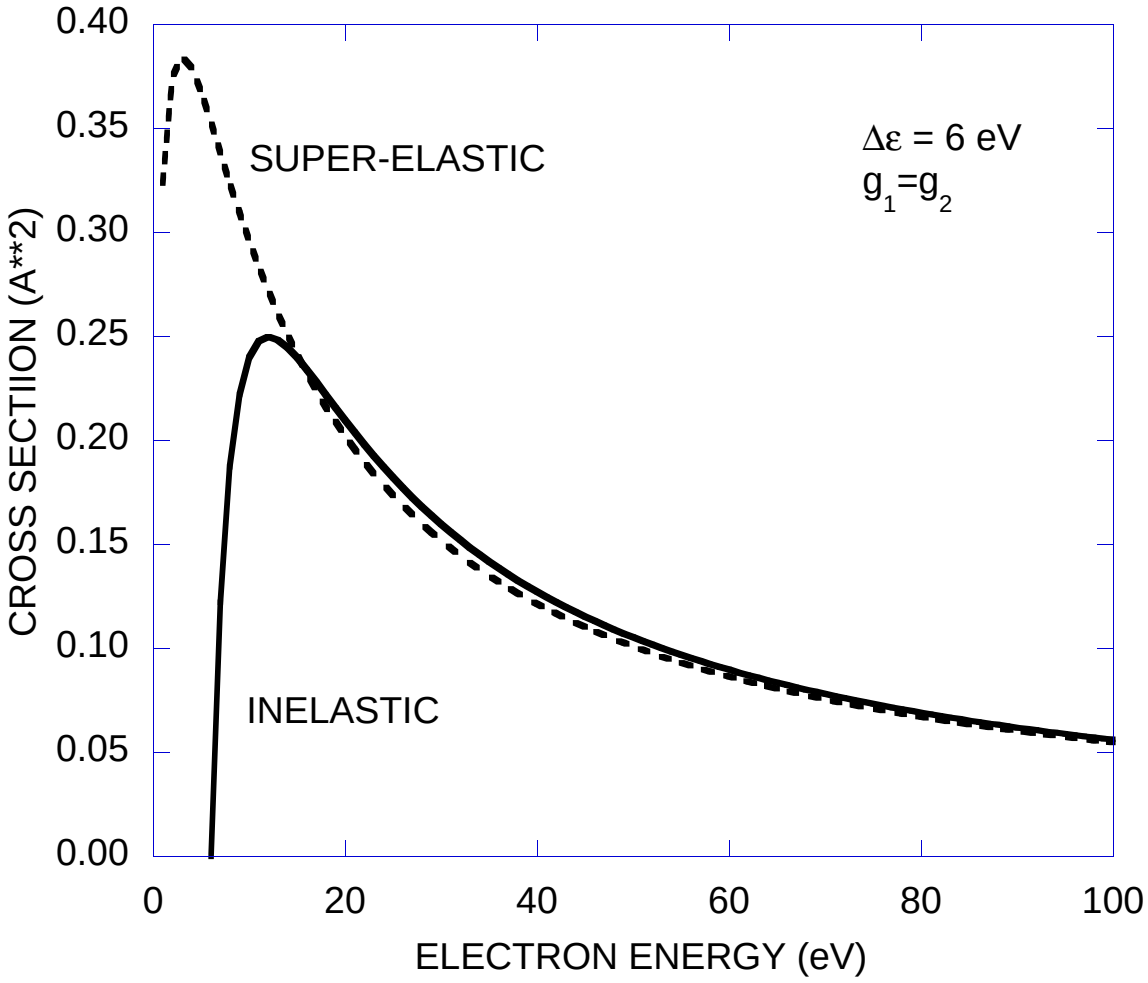
0.40
0.35
0.30
0.25
0.20
0.15
0.10
0.05
0.00
CROSS SECTIION (A**2)
SUPER-ELASTIC
Δε = 6 eV
g1=g2
INELASTIC
0
20
40
60
80
100
ELECTRON ENERGY (eV)

ANALYTIC EXPRESSIONS FOR ELECTRON IMPACT CROSS SECTIONS

$m_e = electron\ mass = 9.11\times10^{-28}\,g$, $M = atomic\ mass$, $q = elementary\ charge$,

$a = Bohr\ radius = \dfrac{\hbar^2}{m_e q^2} = 0.529\times10^{-8}\,cm$, $\hbar = \dfrac{Planck\ constant}{2\pi} = \dfrac{6.63\times10^{-34}\,J-s}{2\pi}$,

$\varepsilon = electron\ energy$, $\mu = reduced\ mass = \dfrac{m_e M}{(m_e + M)}$, $k = wave\ vector = \left(\dfrac{2\varepsilon m_e}{\hbar^2}\right)^{1/2}$,

$\lambda_D = Debye\ Length = \left(\dfrac{\varepsilon_o k_B T_e}{m_e n_e}\right)^{1/2}$, $k_B = Boltzmann's\ constant = 1.38\times10^{-23}\,J-K$,

$\varepsilon_o = permittivity\ free\ space = 8.85\times10^{-12}\,\dfrac{F}{m}$, $n_e = electron\ density$, $N_I = ion\ density$,

$T_e = electron\ temperature$, $Z = charge\ number\ of\ ion$, $f_{ij} = oscillator\ strength$,

$b_o = scattering\ parameter\ for\ 90^0\ collision = \dfrac{Zq^2}{8\pi\varepsilon_o}$, $E_H = Rydberg\ energy = 13.6\ eV$,

ξ_n = *number of orbital electrons in the outer shell of the atom*

Born cross section for elastic collisions:

$$\sigma(\varepsilon) = \frac{16\pi\mu^2 q^4 a^4}{\hbar^4\left(4k^2a^2+1\right)}$$

For electron scattering on helium, $\sigma(\varepsilon) = \dfrac{14\times10^{-16}}{0.3\cdot\varepsilon(eV)+1}\,cm^2$

Coulomb cross section for electron-ion collisions:

$$\sigma(\varepsilon) = 4\pi b_o^2\left[\ln\left(1+\left(\frac{\lambda_D}{b_o}\right)^2\right)\right]$$

Electron-ion collision frequency for a Maxwellian electron energy distribution

$$\nu_{eI} = \frac{4\sqrt{2\pi}}{3}\left(\frac{m_e}{k_B T_e}\right)^{3/2}\left(\frac{q^2}{4\pi\varepsilon_o m_e}\right)^{3/2}\ln\Lambda \approx N_I\left(cm^{-3}\right)\frac{2.9\times10^{-6}}{T_e(eV)}\ln\Lambda\ s^{-1}$$

$$\Lambda = \frac{\lambda_D}{\bar{b}_o},\ \bar{b}_o = \frac{Zq^2}{12\pi\varepsilon_o k_B T_e}$$

Drawin expression for Born-Bethe electron impact excitation cross section:

For excitation of state j (higher energy) from state i (lower energy) having energy separation E_{ij}

$$\sigma_{ij}(\varepsilon) = 4\pi a^2 \left(\frac{E_H}{E_{ij}}\right) f_{ij}\alpha_{ij}\frac{U_{ij}-1}{U_{ij}^2}\ln(1.25\beta_{ij}U_{ij}), \quad U_{ij} = \frac{\varepsilon}{E_{ij}}$$

α_{ij} and β_{ij} are atomic constants depending on the i,j with values of order 1.

Drawin expression for electron-impact ionization:

For ionization of atom or molecule with ionization potential E_I

$$\sigma_I(\varepsilon) = 2.66\pi a^2 \xi_n \frac{U-1}{U^2}\ln(1.25\beta U), \quad U = \frac{\varepsilon}{E_I}, \quad \beta = 1+\left(\frac{Z_e-1}{Z_e+2}\right), \quad Z_e = \left(\frac{E_I}{E_H}\right)^{1/2}$$

Gryzinski expression for electron-impact ionization:

For ionization of atom or molecule with ionization potential E_I

$$\sigma_I(\varepsilon) = 4\pi a^2 \xi_n \left(\frac{E_H}{E_I}\right)^2 g(U),$$

$$g(U) = \frac{1}{U}\left(\frac{U-1}{U+1}\right)^{3/2}\left(1+\frac{2}{3}\left(1-\frac{1}{2U}\right)\ln\left(2.7+(U-1)^{1/2}\right)\right), \quad U = \frac{\varepsilon}{E_I}, \quad \beta = 1+\left(\frac{Z_e-1}{Z_e+2}\right), \quad Z_e = \left(\frac{E_I}{E_H}\right)^{1/2}$$

Super-elastic collisions:

For de-excitation of state j (higher energy) to state i (lower energy) having energy separation E_{ij}

$$\sigma_{ji}(\varepsilon) = \frac{g_i}{g_j}\left(\frac{\varepsilon+E_{ij}}{\varepsilon}\right)\sigma_{ji}(\varepsilon+E_{ij})$$

$\sigma_{ij}(\varepsilon)$ is the excitation cross section of state j (higher energy) from state i (lower energy)
g_j is the degeneracy of state j.

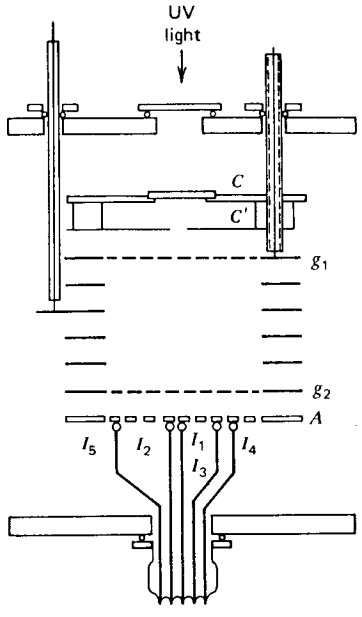

FIG. 11.20. Schematic diagram of Naidu's and Prasad's apparatus.[51] Electrons were produced by photoelectric emission from the back-illuminated gold-coated surface of C. The grids g_1 and g_2, used for measurements of W with the same apparatus, were removed during the measurements of D/μ. The distribution of current over the anode A was determined by measuring the currents $I_1, I_2, \ldots, I_5$.

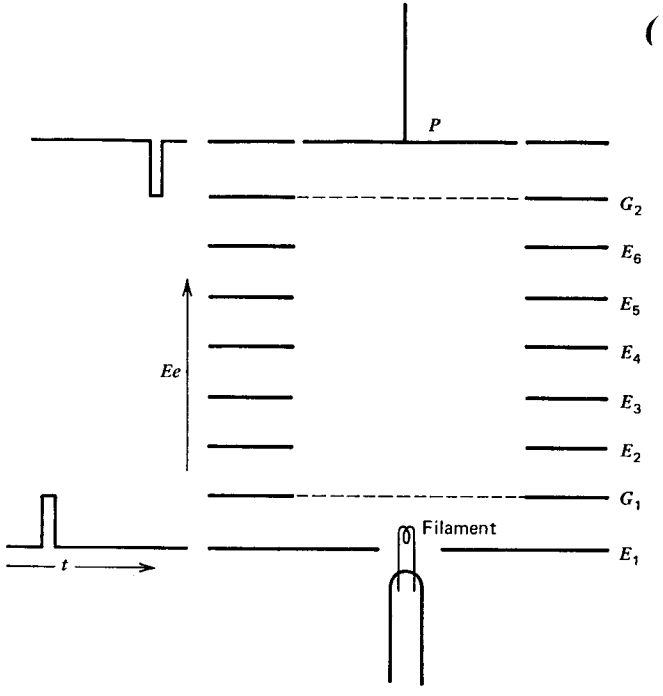

FIG. 12.7. Schematic diagram showing the principle of the method introduced by Doehring. The electric field in the regions E_1G_1 and G_2P is reversed except during the times at which the rectangular pulses are applied.

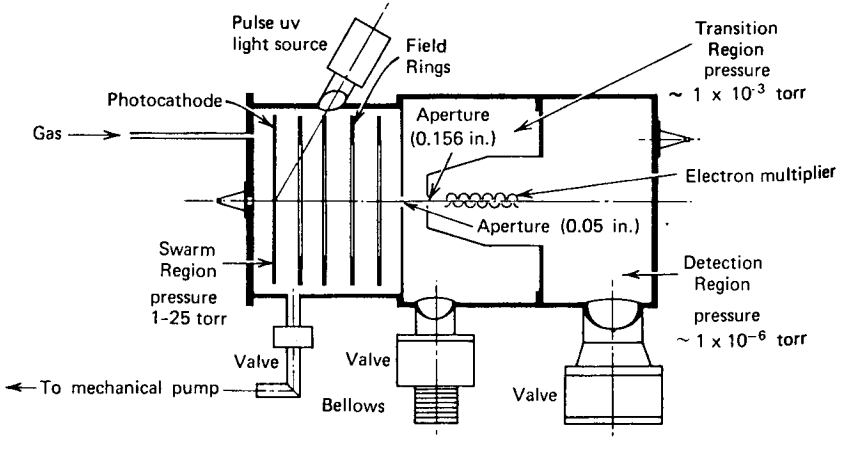

FIG. 10.12. Time-of-flight apparatus developed by Wagner et al.[24] The vacuum chamber is divided into three regions, operating in the pressure ranges shown.

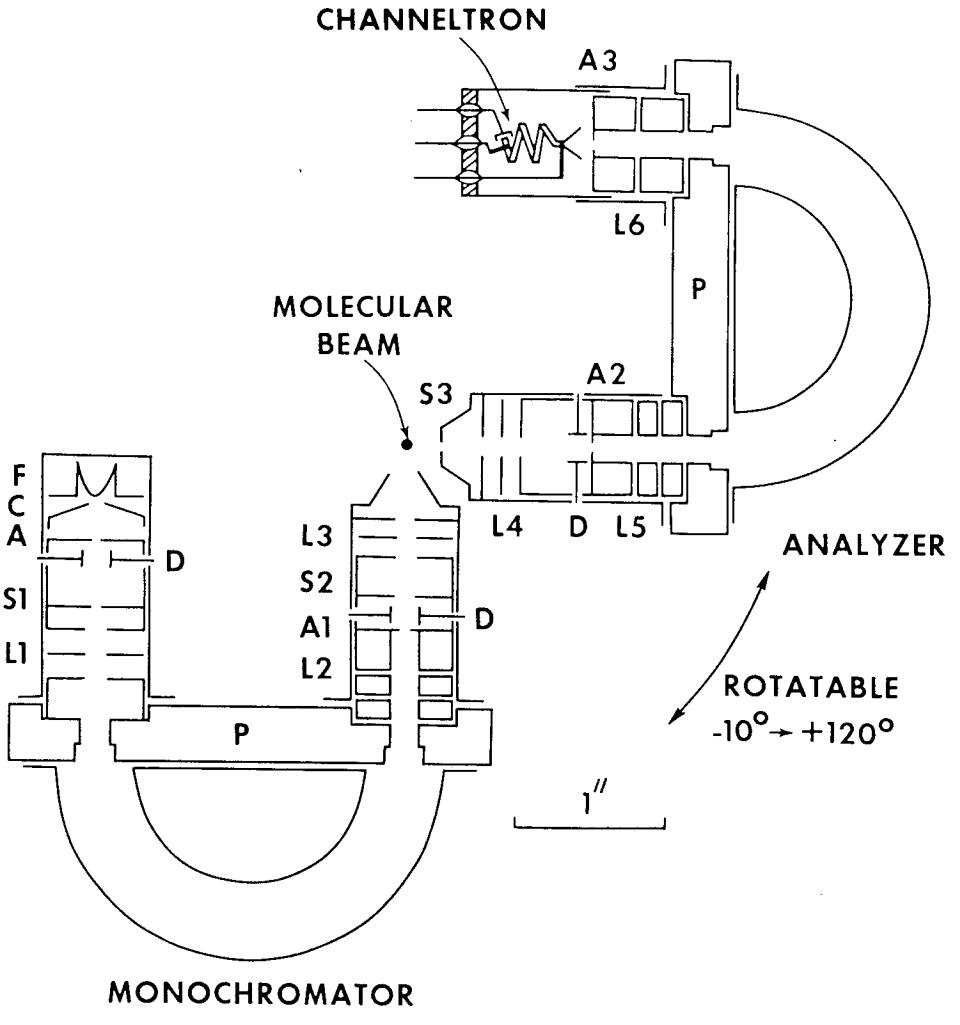

Fig. 2.5 Schematic diagram of the double hemispherical electron spectrometer. Lenses are designated by *L*, angular stops by *S*, imaging apertures by *A*, deflector plates by *D*, and mounting plates by *P*. The filament is designated by *F*, the cathode by *C*. This type of apparatus is most useful for a study of vibrational cross sections. (From Boness and Schulz, 1974.)

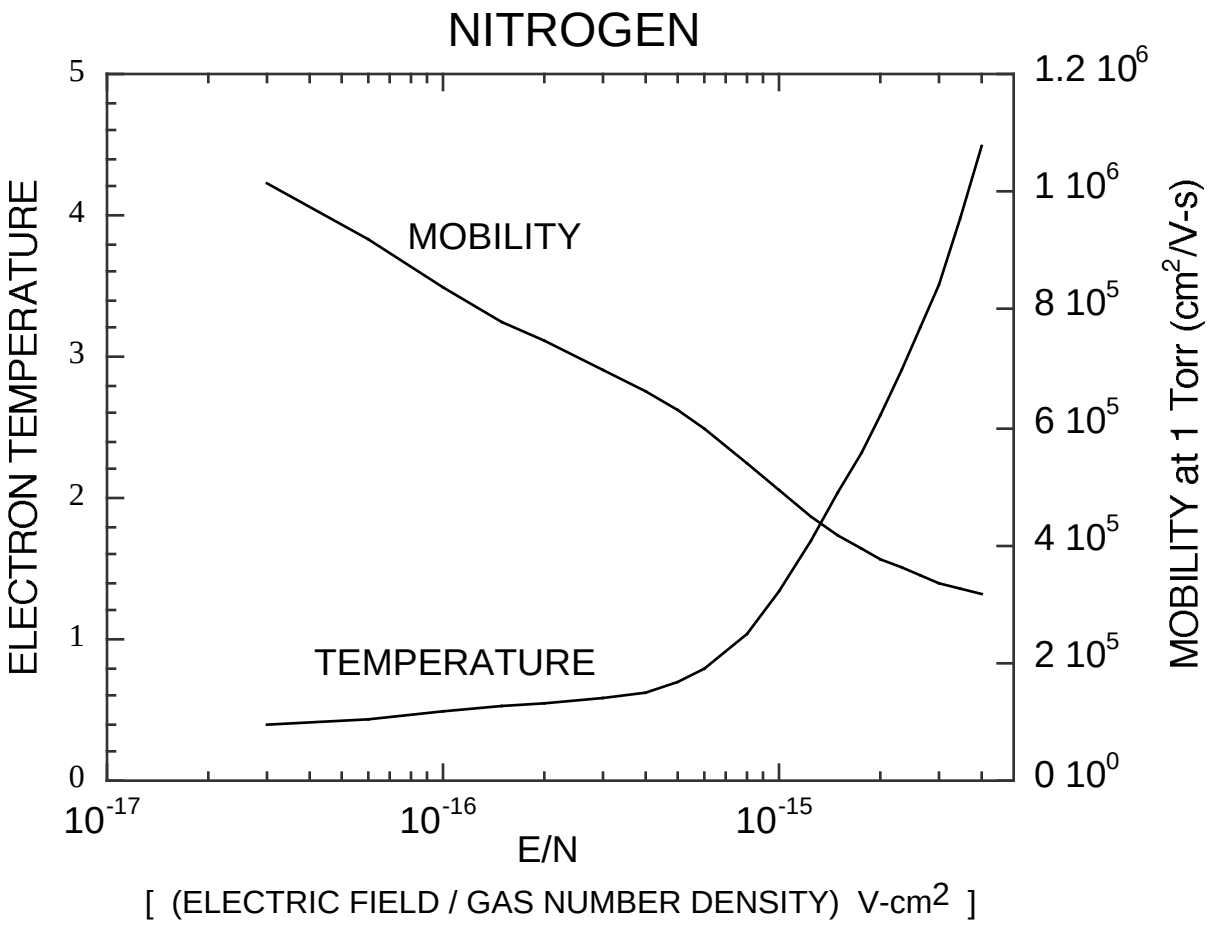
NITROGEN
ELECTRON TEMPERATURE
MOBILITY at 1 Torr (cm²/V-s)
MOBILITY
TEMPERATURE
E/N
[(ELECTRIC FIELD / GAS NUMBER DENSITY) V-cm²]
0
1
2
3
4
5
10⁻¹⁷
10⁻¹⁶
10⁻¹⁵
0 10⁰
2 10⁵
4 10⁵
6 10⁵
8 10⁵
1 10⁶
1.2 10⁶

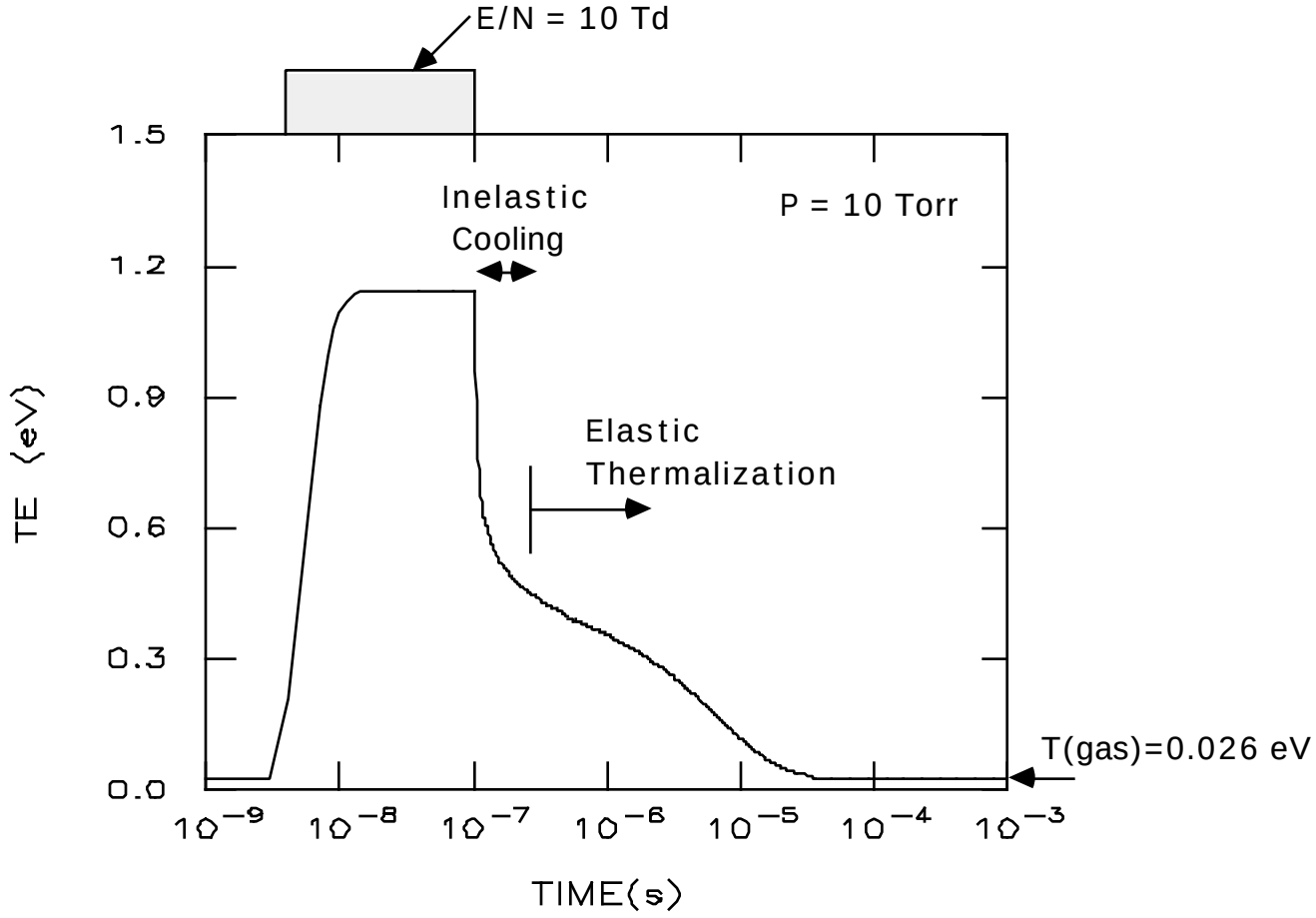
E/N = 10 Td
1.5
1.2
0.9
0.6
0.3
0.0
TE (eV)
Inelastic
Cooling
P = 10 Torr
Elastic
Thermalization
T(gas)=0.026 eV
10^-9
10^-8
10^-7
10^-6
10^-5
10^-4
10^-3
TIME(s)

REVIEW: OBTAINING THE ELECTRON TEMPERATURE

1. **ELECTRON TEMPERATURE** is obtained from a power balance

$$\frac{d}{dt}\left(\frac{3}{2}\,k_{BOLTZ}T_e n_e\right) = \frac{n_e\,q^2E^2}{m\,k_m N} - n_e\left(\frac{2m_e}{M}\right)k_m\,N\,\frac{3}{2}\,k_B\,(T_e - T_g)$$

$$\begin{bmatrix}\text{Total energy}\\ \text{density of electrons}\end{bmatrix}\begin{bmatrix}j \bullet E\\ \text{power deposition}\end{bmatrix}\begin{bmatrix}\text{power loss due}\\ \text{to elastic collisions}\end{bmatrix}$$

$$- n_e\,N\sum_i\,k_i\,\Delta\varepsilon_i$$

$$\begin{bmatrix}\text{power loss due to}\\ \text{inelastic collisions}\end{bmatrix}$$

In principle, you can solve for T_e if you know the value of E/N.

$$T_e = T_g + \frac{2}{3k_{BOLTZ}}\,\frac{1}{\left(\frac{2m_e}{M}\right)}\left[\frac{q^2}{m_e k_m^2}\left(\frac{E}{N}\right)^2 - \frac{\sum_i k_i\Delta\varepsilon_i}{k_m}\right]$$

The electron temperature is elevated above the gas temperature due to heating by the electric field. Inelastic collisions reduce temperature.

2. **DOMINANT LOSSES** of electrons and ions in many low pressure glow discharges is by diffusion

$$\frac{\partial n_e}{\partial t} = \underbrace{n_e\,k_{ION}\,N}_{\text{Ionization}} - \underbrace{n_e\,k_{att}\,N}_{\text{Attachment}} + \underbrace{\nabla \bullet D\nabla n_e}_{\text{Diffusion}}$$

If the diffusion coefficient is independent of position then

$$\frac{\partial n_e}{\partial t} = \ldots + \nabla \bullet D\nabla n_e = D\nabla^2 n_e \approx \frac{-D}{\Lambda^2}\,n_e$$

where Λ = diffusion length of container

$= \frac{L}{\pi}$ (L = spacingbetweenparallelplates)

$= \frac{R}{2.405}$ (R = radius of discharge tube)

3. **IF DIFFUSION DOMINATES** then the continuity equation is homogenous; and you cannot solve for n_e in the steady state. The electron density must be obtained from another relationship, such as that for the current density.

$$\frac{\partial n_e}{\partial t} = n_e k_{ION}(T_e)N - n_e \frac{D(T_e)}{\Lambda^2} = 0$$

$$k_{ION}(T_e)N - \frac{D(T_e)}{\Lambda^2} = 0$$

Since, however, k_{ION} and D are functions of T_e, then you can solve for T_e from the continuity equation by requiring that the source of electrons by ionization be balanced by the loss of electrons by diffusion.

$$k_{ION}(T_e)N = \frac{D(T_e)}{\Lambda^2}$$

Once you solve for T_e from this equation, you can solve for E/N from the energy balance equation.

DERIVATION OF EINSTEIN RELATION

In equilibrium, the density of particles having temperature T in an electric potential U is

$$N = N_o \exp\left(\frac{qU}{kT}\right), \quad q = \pm e$$

where k = Boltzmann's constant. The gradient of particles due to a gradient in potential is

$$\nabla N = \frac{q}{kT}\nabla U \bullet \left(N_o \exp\left(\frac{qU}{kT}\right)\right) = \frac{q}{kT}\nabla U \bullet N$$

where the Electric field is $-\nabla U$. The total flux of particles at equilibrium is zero, and is

$$j = \pm \mu \nabla U \bullet N - D \nabla N = 0$$

$$= \mu \nabla U \bullet N - D\frac{q}{kT}\nabla U N$$

$$= \pm \nabla U \bullet N\left(\mu - \frac{De}{kT}\right) = 0$$

$$D = \frac{kT\mu}{e}$$

where μ is the mobility $\left(\frac{cm^2}{V-s}\right)$ and D is the diffusion coefficient $\frac{cm^2}{s}$.

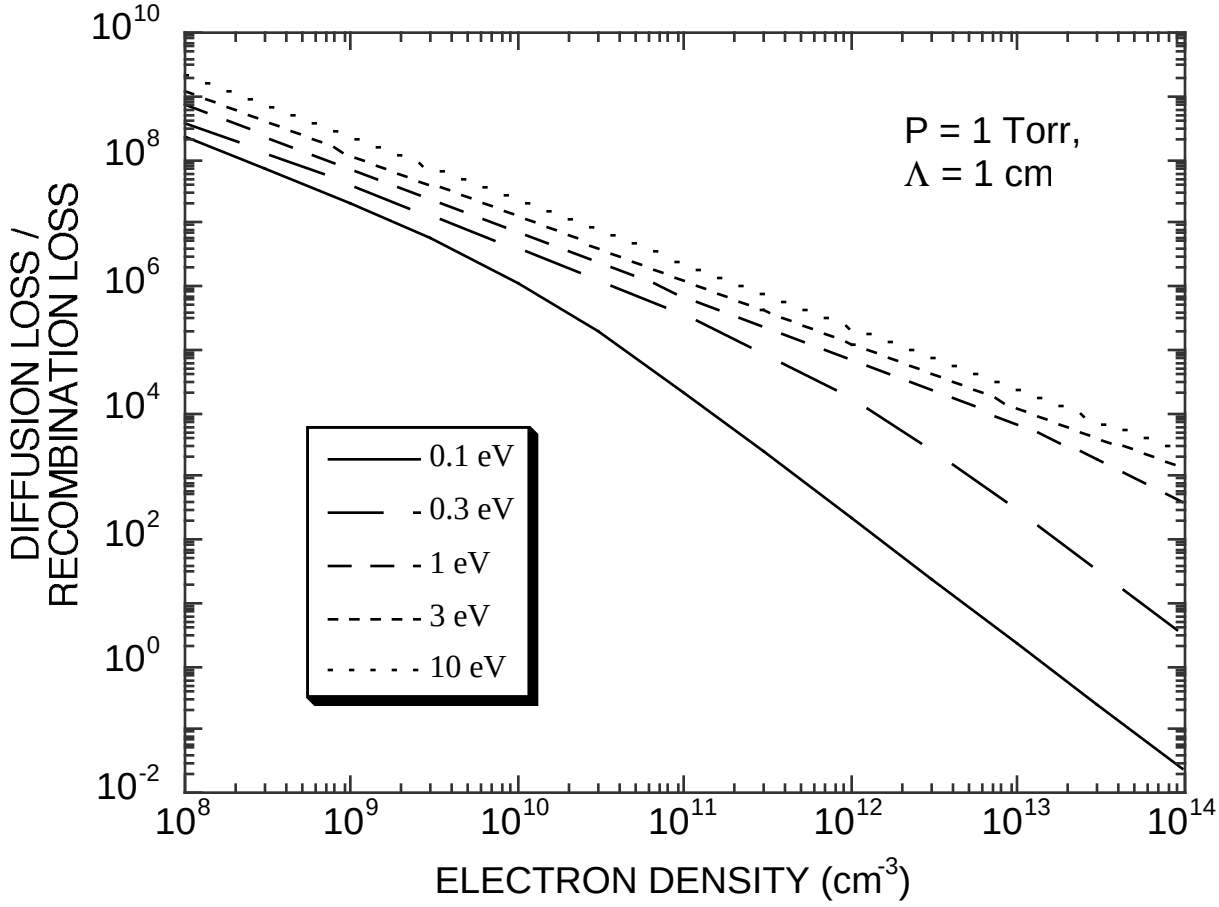
DIFFUSION LOSS / RECOMBINATION LOSS
ELECTRON DENSITY (cm-3)
P = 1 Torr,
Λ = 1 cm
0.1 eV
0.3 eV
1 eV
3 eV
10 eV
10^10
10^8
10^6
10^4
10^2
10^0
10^-2
10^8
10^9
10^10
10^11
10^12
10^13
10^14

Diffusion Coefficients (cm^2/s) for Drift in Helium at 1 Torr

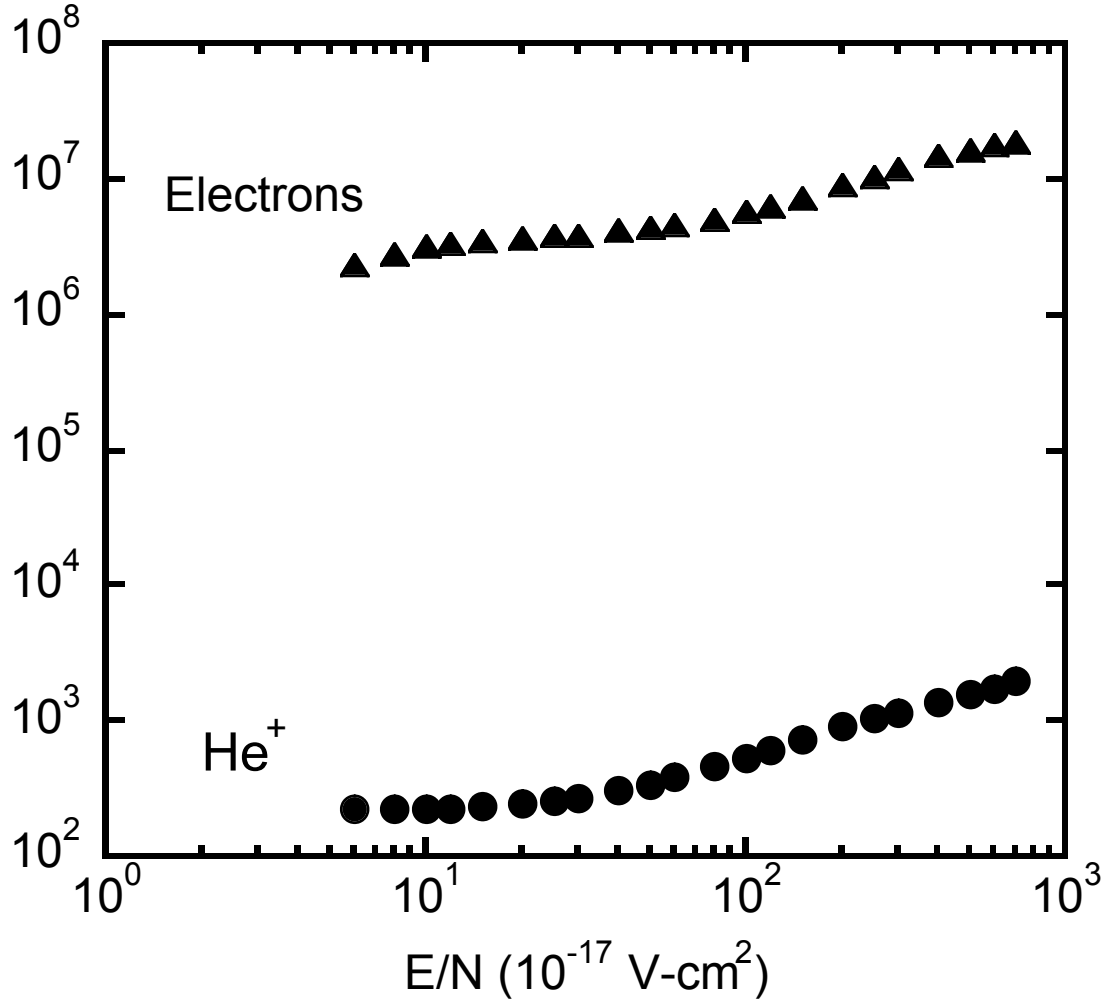

- Ion data adapted from At. Data Nucl. Data Tables, v 31, 1984
- Electron data from ODP Boltzmann

diff_coef_e_ion_helium

DERIVATION OF AMBIPOLAR DIFFUSION COEFFICIENT AND AMBIPOLAR ELECTRIC FIELD

Start with continuity equations for electrons and ions. This accounts for transport due only to diffusion processes. This would be, for example, for transport of electrons and ions to the walls in a narrow plasma tube whose length is much greater than the radius. The transport of electrons and ions along the axis of the plasma tube due to an externally applied electric field is not accounted for here. The ambipolar electric field included here is a self generated electric field to keep the flux of electrons and ions to the walls equal – it is not the applied electric field along the axis.

$$\frac{\partial n_e}{\partial t} = -\nabla \bullet \Gamma_e = -\nabla \bullet (-D_e \nabla n_e - \mu_e E_A n_e) = D_e \nabla^2 n_e + \mu_e E_A \nabla n_e + \mu_e n_e \nabla \cdot E_A$$

$$\frac{\partial N_I}{\partial t} = -\nabla \bullet \Gamma_I = -\nabla \bullet (-D_I \nabla N_I + \mu_I E_A N_I) = D_I \nabla^2 N_I - \mu_I E_A \nabla N_I - \mu_I N_I \nabla \cdot E_A$$

Where

E_A	Ambipolar electric field (V/cm)
n_e, N_I	Electron, ion density ($1/cm^3$)
Γ_e , Γ_I	Electron, ion flux ($1/cm^2$-s)
μ_e , μ_I	Electron, ion mobility (cm^2/V-s)
D_e , D_I	Electron, ion free diffusion coefficient (cm^2/s)

Assuming that $\nabla \bullet E_A = 0$ then

$$\frac{\partial n_e}{\partial t} = D_e \nabla^2 n_e + \mu_e E_A \nabla n_e \qquad \text{(a)}$$

$$\frac{\partial N_I}{\partial t} = D_I \nabla^2 N_I - \mu_I E_A \nabla N_I \qquad \text{(b)}$$

Multiply (a) by μ_I, multiply (b) by μ_e, and add them together while assuming that $n_e = N_I$, $\frac{\partial n_e}{\partial t} = \frac{\partial N_I}{\partial t}$, $\nabla n_e = \nabla N_I$ and $\nabla^2 n_e = \nabla^2 N_I$ then

$$\mu_I \frac{\partial n_e}{\partial t} = \mu_I D_e \nabla^2 n_e + \mu_I \mu_e E_A \nabla n_e$$

$$\mu_e \frac{\partial N_I}{\partial t} = \mu_e D_I \nabla^2 N_I - \mu_e \mu_I E_A \nabla N_I$$

One then obtains

$$\frac{\partial n_e}{\partial t} = \left[\frac{D_e \mu_I + D_I \mu_e}{\mu_e + \mu_I} \right] \nabla^2 n_e = D_A \nabla^2 n_e$$

where the ambipolar diffusion coefficient is:

$$D_A = D_I \frac{\left(1 + \frac{D_e}{D_I} \frac{\mu_I}{\mu_e}\right)}{\left(1 + \frac{\mu_I}{\mu_e}\right)}.$$

Using the Einstein relation $D = \frac{kT}{q} \mu$ and assuming that $\mu_e >> \mu_I$, then

$$D_A = D_I \frac{\left(1 + \frac{T_e}{T_I}\right)}{\left(1 + \frac{\mu_I}{\mu_I}\right)} \approx D_I \left(1 + \frac{T_e}{T_I}\right)$$

Both electrons and ions appear to diffusion with the same coefficient, D_A, which includes the effects of both their own free diffusion and the acceleration by the ambipolar electric field, E_A.

We can now solve for E_A. Starting with the expressions for fluxes, subtract Γ_e from Γ_I (noting that $\Gamma_e = \Gamma_I$), and solve for E_A.

$$\Gamma_e = -D_e \nabla n_e - \mu_e n_e E_A$$
$$\Gamma_I = -D_I \nabla N_I + \mu_I N_I E_A$$

$$E_A = -\frac{D_e \nabla n_e - D_I \nabla N_I}{\mu_e n_e + \mu_I N_I} \approx -\frac{\nabla n_e}{n_e} \frac{D_e - D_I}{\mu_e + \mu_I}$$

For $D_e >> D_I$, $\mu_e >> \mu_I$, $E_A \approx -\frac{\nabla n_e}{n_e} \frac{D_e}{\mu_e} = -\frac{\nabla n_e}{n_e} \frac{k_B T_e}{q}$

For $\nabla \sim \frac{1}{\Lambda}$ (Λ is the diffusion length), then $E_A \approx \frac{1}{\Lambda} \frac{k_B T_e}{q}$.

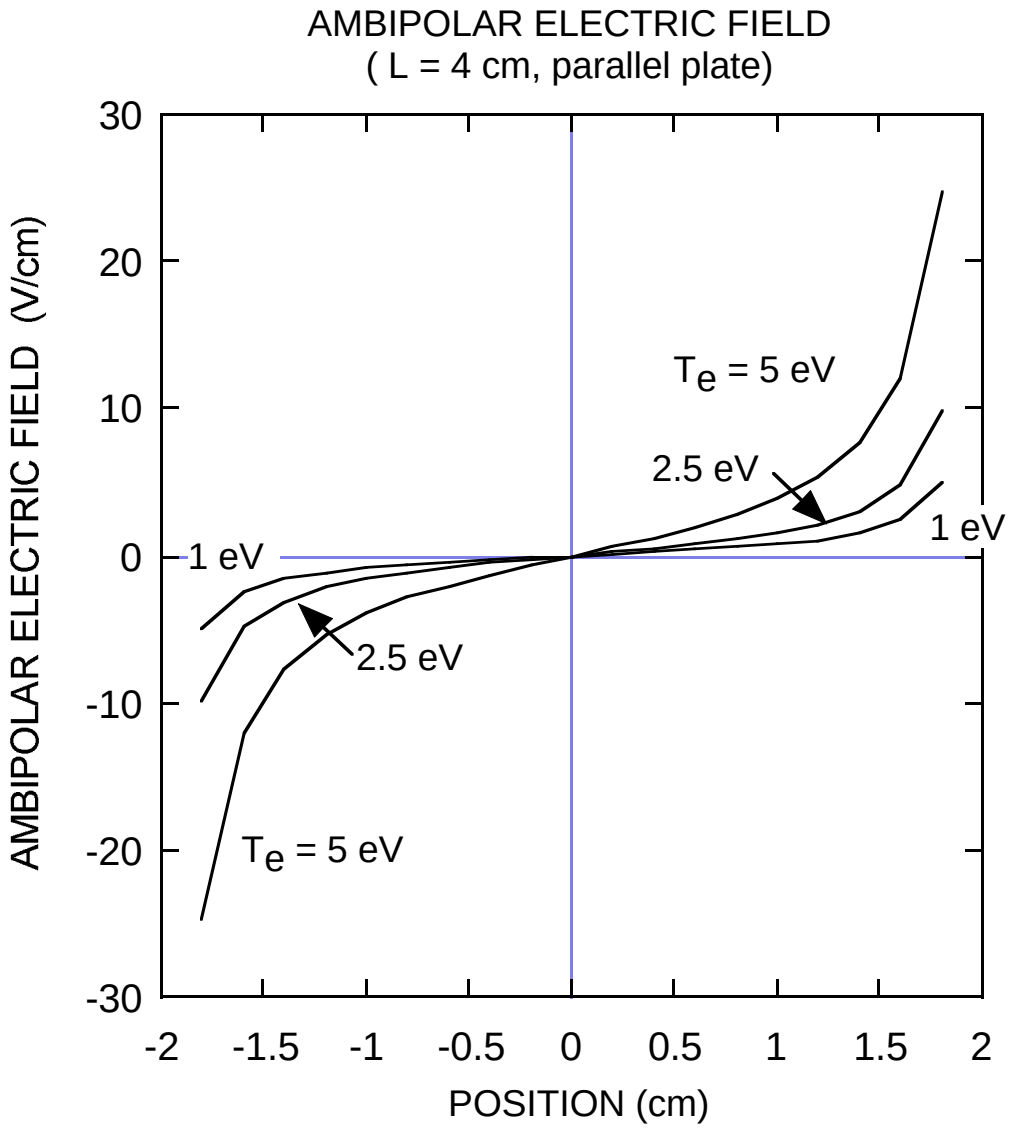
AMBIPOLAR ELECTRIC FIELD
(L = 4 cm, parallel plate)
AMBIPOLAR ELECTRIC FIELD (V/cm)
POSITION (cm)
30
20
10
0
-10
-20
-30
-2
-1.5
-1
-0.5
0
0.5
1
1.5
2
Te = 5 eV
2.5 eV
1 eV
1 eV
2.5 eV
Te = 5 eV

Phys. Rev A v39, 4117 (1989)

Radial distributions of charged-particle densities and electric field strength in the positive column

A. Metze,* D. W. Ernie, and H. J. Oskam
Department of Electrical Engineering, University of Minnesota, Minneapolis, Minnesota 55455
(Received 28 October 1988)

A model is presented for the radial distribution of ion and electron densities and electric field strength in the positive column of a dc discharge for a plasma consisting of a singly charged positive-ion species, electrons, and neutral species. The set of equations involved consists of the particle- and momentum-conservation equations for the ions and electrons and Poisson's equation. Utilizing this single set of equations and appropriate assumptions, the model has been solved, through suitable numerical techniques, for various gas pressures p_0 and tube radii R. These calculations show the development of both the electric field in the "bulk" of the positive column and the sheath field "near" the discharge wall. The results also demonstrate the existence of a nonzero difference between the ion and electron densities at the discharge axis, with an increase in this difference for decreasing p_0R. The importance of including the various terms in the momentum-conservation equations of both the ions and electrons when solving the model has been investigated. The model can be used to calculate the radial properties of positive-column discharges for conditions ranging from the ambipolar diffusion limit to the free-diffusion limit.

$$\frac{1}{r}\frac{d}{dr}[r\Gamma_r(r)]=\nu_i n_e(r) ,$$

$$\frac{m_i}{r}\frac{d}{dr}\left[\frac{r\Gamma_r^2(r)}{n_i(r)}\right]+kT_i\frac{d}{dr}n_i(r)-en_i(r)E_r(r) = -m_i\Gamma_r(r)\nu_{mi} ,$$

$$\frac{m_e}{r}\frac{d}{dr}\left[\frac{r\Gamma_r^2(r)}{n_e(r)}\right]+kT_e\frac{d}{dr}n_e(r)+en_e(r)E_r(r) = -m_e\Gamma_r(r)\nu_{me} ,$$

$$\frac{1}{r}\frac{d}{dr}[rE_r(r)]=\frac{e}{\epsilon_0}[n_i(r)-n_e(r)] .$$

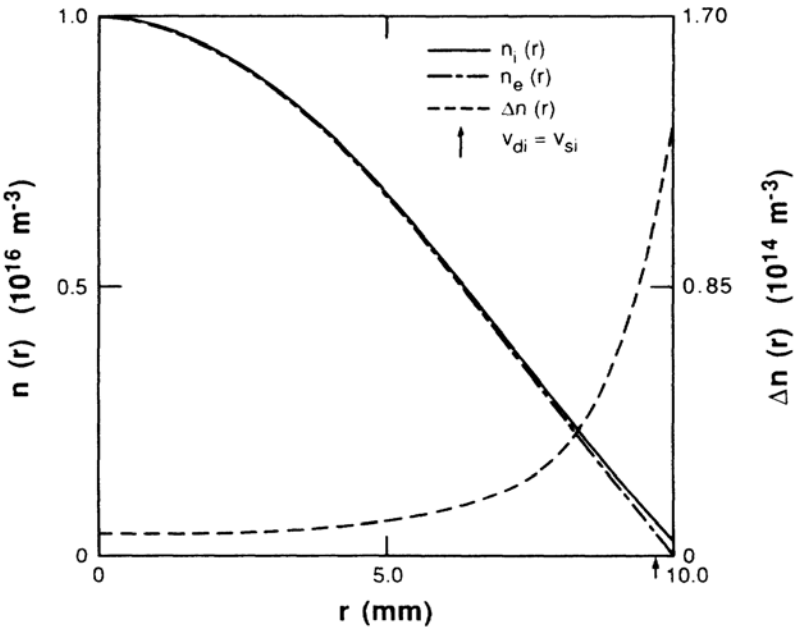

FIG. 1. Numerical calculations of the radial distributions for the ion density $n_i(r)$, the electron density $n_e(r)$, and the net charged-particle density $\Delta n(r)$ in a helium discharge with $p_0 = 5.0$ Torr and $R = 1.0$ cm ($p_0 R = 5.0$ Torr cm), implying $T_e = 26\,000$ K, and yielding $\nu_i = 1.95 \times 10^4\ \mathrm{s}^{-1}$.

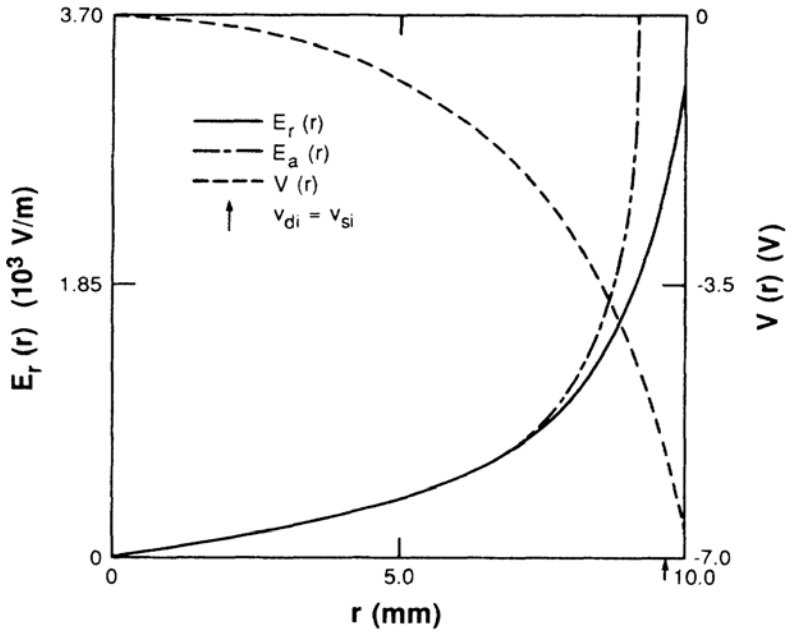

FIG. 2. Numerical calculations of the radial distributions for the electric field strength $E_r(r)$ and the resulting electric potential $V(r)$ for the parameters given in Fig. 1 (i.e., $p_0 R = 5.0$ Torr cm). The ambipolar radial electric field $E_a(r)$ is also shown for comparison.

DOES AMBIPOLAR DIFFUSION VIOLATE THE DEBYE SHIELDING REQUIREMENTS?

Debye shielding states that the distance over which a charge separation Δn can be sustained is

$$\lambda_D = \left(\frac{\varepsilon_o kT_e}{q^2 \Delta n}\right)^{1/2} \approx 750\left(\frac{T_e}{\Delta n}\right)^{1/2} \text{cm}$$

where T_e (electron temperature) is in eV and Δn is in units of cm^{-3}. According to ambipolar diffusion theory, plasmas in containers actually are slightly electropositive. The slight positive space charge generates an electric field which accelerates ions out of the plasma and "holds back" electrons. This field (in plane parallel geometries) is

$$E_A = \frac{\pi}{L}\frac{kT_e}{q}\tan\left(\frac{\pi x}{L}\right)$$

where the separation between the plates is L. The implied charge separation can be obtained from applying Poisson's Equation $\nabla \bullet E = \frac{\rho}{\varepsilon_o}$.

$$\frac{dE_A}{dx} = \frac{q\Delta n}{\varepsilon_o} = \frac{d}{dx}\left(\frac{\pi}{L}\frac{kT_e}{q}\tan\left(\frac{\pi x}{L}\right)\right) = \left(\frac{\pi}{L}\right)^2 \frac{kT_e}{q}\frac{1}{\cos^2\left(\frac{\pi x}{L}\right)}$$

Solving for Δn we have

$$\Delta n(x) = \frac{\varepsilon_o kT_e}{q^2}\left(\frac{\pi}{L}\right)^2 \frac{1}{\cos^2\left(\frac{\pi x}{L}\right)}$$

Using typical values (L = 2 cm, kT_e = 1 eV) we have

$$\Delta n(x) = \frac{10^6 \text{cm}^{-3}}{\cos^2\left(\frac{\pi x}{L}\right)} = \frac{\Delta n_o}{\cos^2\left(\frac{\pi x}{L}\right)}$$

The charge separation (or depletion of negative charge) is small and increases towards the wall where the E-field also increases. If we solve for $\frac{L}{\pi}$, the diffusion length, we get

$$\frac{L}{\pi} = \left(\frac{1}{\cos\left(\frac{\pi x}{L}\right)}\right) \bullet \left(\frac{\varepsilon_o kT_e}{q^2 \Delta n(x)}\right)^{1/2} = \left(\frac{\varepsilon_o kT_e}{q^2 \Delta n_o}\right)^{1/2} = \lambda_o$$

where λ_o is the Debye length based on Δn_o. So we see that the charge separation dictated by ambipolar diffusion over the diffusion length of the container is consistent with a Debye length of the same distance. (Remember that λ_D is really based on maximum charge separation and not maximum or total density.)

EXAMPLE: **CYLINDRICAL GLOW DISCHARGE PARAMETERS**

What are the electron density, electron temperature and self-sustaining electric field in a low temperature plasma having the following properties?

$j = 10\ \frac{mA}{cm^2}$, cylindrical tube 1.5 cm diameter

$P = 3$ Torr, $T_g = 400$ K, $M_g = 40$ AMU, $D_{ION} = 100\ \frac{cm^2}{s}$

$k_m = 3 \times 10^{-7}\ \frac{cm^3}{s}$, $k_{ion} = 3 \times 10^{-11} \exp\left(\frac{-\Delta\varepsilon}{T_e}\right)\frac{cm^3}{s}$, $\Delta\varepsilon = 9$ eV

ELECTRON TEMPERATURE (assume diffusion losses dominate):

$$\frac{\partial n_e}{\partial t} = 0 = n_e \cdot k_{ION} \cdot N_G - \frac{D_A N^+}{\Lambda^2} = 0$$

$$n_e \approx N^+, \quad \Lambda = \frac{R}{2.405}, \quad D_A = D_I\left(1 + \frac{T_e}{T_I}\right), \quad T_I \approx T_g$$

$$N_G = \frac{9.654 \times 10^{18} \times 3\,\text{Torr}}{400\,\text{K}} = 7.24 \times 10^{16}\,\text{cm}^{-3}$$

$$3 \times 10^{-11} \exp\left(\frac{-9\ \text{eV}}{T_e}\right)\frac{\text{cm}^3}{\text{s}} \cdot 7.24 \times 10^{16}\,\text{cm}^{-3}$$

$$= 100\ \frac{\text{cm}^2}{\text{s}} \times \frac{(2.405)^2}{(1.5/2)^2\,\text{cm}^2}\left(1 + \frac{T_e}{(400/11594.2)\ \text{eV}}\right)$$

Solve for T_e and find $T_e = 2.76$ eV.

AXIAL ELECTRIC FIELD:

$$T_e = T_g + \frac{2}{3k_B}\frac{1}{\left(\frac{2m_e}{M}\right)}\left(\frac{q^2}{m_e k_m^2}\left(\frac{E}{N}\right)^2 - \frac{k_I \Delta\varepsilon}{k_m}\right)$$

$$\left(\frac{E}{N}\right) = \left[\left(\left(\frac{2m_e}{M}\right)\frac{3}{2}k_B\left(T_e - T_g\right) + \frac{k_I \Delta\varepsilon}{k_m}\right)\frac{m_e k_m^2}{q^2}\right]^{1/2}$$

$$= \left[\left(\left(\frac{2 \times 0.911 \times 10^{-27}\,\text{g}}{40 \times 1.67 \times 10^{-24}\,\text{g}} \right) \times \frac{3}{2} \left(2.76 - \frac{400}{11594.2} \right) \text{eV} + \frac{3 \times 10^{-11} \exp\left(\frac{-9}{2.76} \right) \cdot 9\,\text{eV}}{3 \times 10^{-7}} \right) \right.$$

$$\left. \cdot 1.6 \times 10^{-19}\,\frac{\text{J}}{\text{eV}} \cdot \frac{0.911 \times 10^{-30}\,\text{kg}}{(1.6 \times 10^{-19}\,\text{c})^2} \times \left(3 \times 10^{-7}\,\frac{\text{cm}^3}{\text{s}} \times 10^{-6}\,\frac{\text{m}^3}{\text{cm}^3} \right)^2 \right]^{1/2}$$

$$= 8.65 \times 10^{-21}\,\frac{\text{J}}{\text{c}} \cdot \text{m}^2 = 8.65 \times 10^{-21}\,\text{V} \cdot \text{m}^2 \times \left(\frac{10^4\,\text{cm}^2}{\text{m}^2} \right)$$

$$\left(\frac{\text{E}}{\text{N}} \right) = 8.65 \times 10^{-17}\,\text{V - cm}^2 = 8.65\,\text{Td}$$

$$\text{E} = \left(\frac{\text{E}}{\text{N}} \right) \cdot \text{N} = 8.65 \times 10^{-17} \cdot 7.2 \times 10^{16}\,\text{V - cm}^2 \times \frac{1}{\text{cm}^3} = 6.2\,\frac{\text{V}}{\text{cm}}$$

ELECTRON DENSITY:

$$\text{j} = \sigma \cdot \text{E} = \text{q} \cdot \text{n}_\text{e} \cdot \mu \cdot \text{E} = \frac{\text{q}^2 \cdot \text{n}_\text{e} \cdot \text{q}}{\text{m}_\text{e} \nu_\text{m}} \cdot \text{E} = \frac{\text{q}^2 \cdot \text{n}_\text{e}}{\text{m}_\text{e} \cdot \text{k}_\text{m}} \cdot \left(\frac{\text{E}}{\text{N}} \right)$$

$$\text{n}_\text{e} = \frac{\text{j} \cdot \text{m}_\text{e} \cdot \text{k}_\text{m}}{\text{q}^2 \cdot \left(\frac{\text{E}}{\text{N}} \right)}$$

$$= \frac{10 \times 10^{-3}\,\text{c} / \left(\text{cm}^2 \text{ - s} \right) \cdot 0.911 \times 10^{-30}\,\text{kg} \times 3 \times 10^{-7}\,\frac{\text{cm}^3}{\text{s}}}{(1.6 \times 10^{-19}\,\text{c})^2 \times 8.65 \times 10^{-17}\,\frac{\text{kg - m}^2 \cdot \text{cm}^2}{\text{s}^2 \text{ - cm c}} \times 10^4\,\frac{\text{cm}^2}{\text{m}^2}}$$

$$= 1.23 \times 10^{11}\,\text{cm}^{-3}$$

Space-Charge-Controlled Diffusion in an Afterglow*

M. A. Gusinow and R. A. Gerber
Sandia Laboratories, Albuquerque, New Mexico 87115
(Received 15 October 1971)

Calculations of space-charge-controlled diffusion of electrons and positive ions in an isothermal afterglow are presented. In particular, the transition from electron-ion ambipolar diffusion to free diffusion of the electrons and ions is investigated. The results are in qualitative agreement with the experiment of Gerber, Gusinow, and Gerardo insofar as predicting the general features of the transition from electron-ion ambipolar diffusion to free diffusion. In addition, the results substantiate the general behavior implicitly predicted by the more elaborate steady-state calculations of Allis and Rose.

For an isothermal afterglow confined within an infinite parallel plane geometry, the equations that are to be solved in one dimension are the continuity equations for the electrons and ions and the Poisson equation for the self-consistent electric field:

$$\frac{\partial P}{\partial t} = D_+ \frac{\partial^2 P}{\partial x^2} - \mu_+ \frac{\partial}{\partial x}(PE), \tag{1}$$

$$\frac{\partial N}{\partial t} = D_- \frac{\partial^2 N}{\partial x^2} + \mu_- \frac{\partial}{\partial x}(NE), \tag{2}$$

$$\frac{\partial E}{\partial x} = \frac{e}{\epsilon_0}(P - N), \tag{3}$$

where P and N are the ion and electron densities in particles/m^3, E is the magnitude of the space-charge electric field in V/m, μ and D are the relevant species mobilities and diffusion coefficients, and $e/\epsilon_0 = 1.809\times10^{-8}$ Vm. It is pertinent to normalize the above equations as follows:

$$\frac{\partial p}{\partial \tau} = \frac{\partial^2 p}{\partial \rho^2} - \frac{\partial}{\partial \rho}(p\mathcal{E}), \tag{1'}$$

$$\frac{\partial n}{\partial \tau} = s\frac{\partial^2 n}{\partial \rho^2} + s\frac{\partial}{\partial \rho}(n\mathcal{E}), \tag{2'}$$

$$\mathcal{E} = \frac{e}{\epsilon_0}\frac{\pi^2}{4}\int_0^\rho (p - n)\, d\rho'. \tag{3'}$$

Here $p = (\mu\Lambda^2/D)P$, $n = (\mu\Lambda^2/D)N$, $s = D_-/D_+$, $\tau = t/(L^2/D_+)$, $\rho = x/L$, and $\Lambda = (2/\pi)L$, where $2L$ is the spacing of the parallel plate container. The quantity D/μ is the ratio of the diffusion and mobility coefficients for the electrons or ions and by the Einstein relation is equal to kT/e for an isothermal plasma. The results presented in this work are to be compared with those of Ref. 1. The quantities to be compared are the effective diffusion coefficients of the central electron and ion densities. In Ref. 1 these diffusion coefficients are presented as a function of $N_0\Lambda^2\mu/D$, while the calculations utilize a normalized (and dimensionless) density of $N_0\Lambda^2\mu e/D\epsilon_0$. Since Refs. 1 and 4 present the pertinent calculations as a function of the former normalized density, we have chosen to compute densities using the normalization factor $D/\Lambda^2\mu$ even though this gives our densities the units of (Vm)$^{-1}$. All currents will be normalized to $(D_+/\Lambda^2 L)(kT/e)$. The electric field will be measured in units of $(kT/e)/L$. Notice that $N\mu\Lambda^2/D = (\epsilon_0/\epsilon)(\Lambda/\Lambda_D)^2$, where Λ_D is the electron shielding distance.

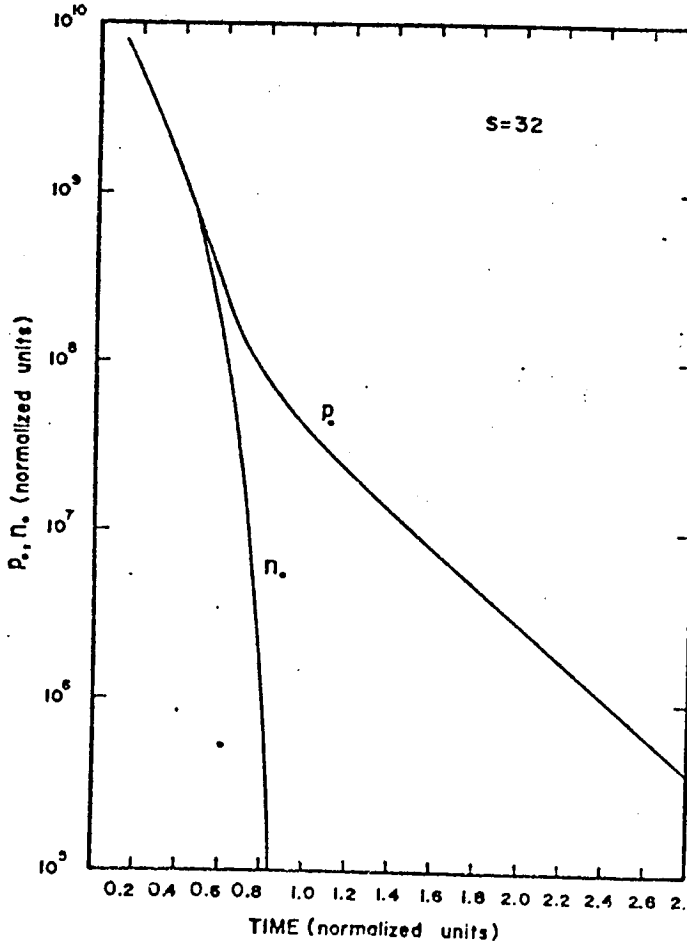

FIG. 1. The normalized central ($\rho = 0$) electron and ion densities n_0 and p_0 as a function of normalized time for $s = 32$.

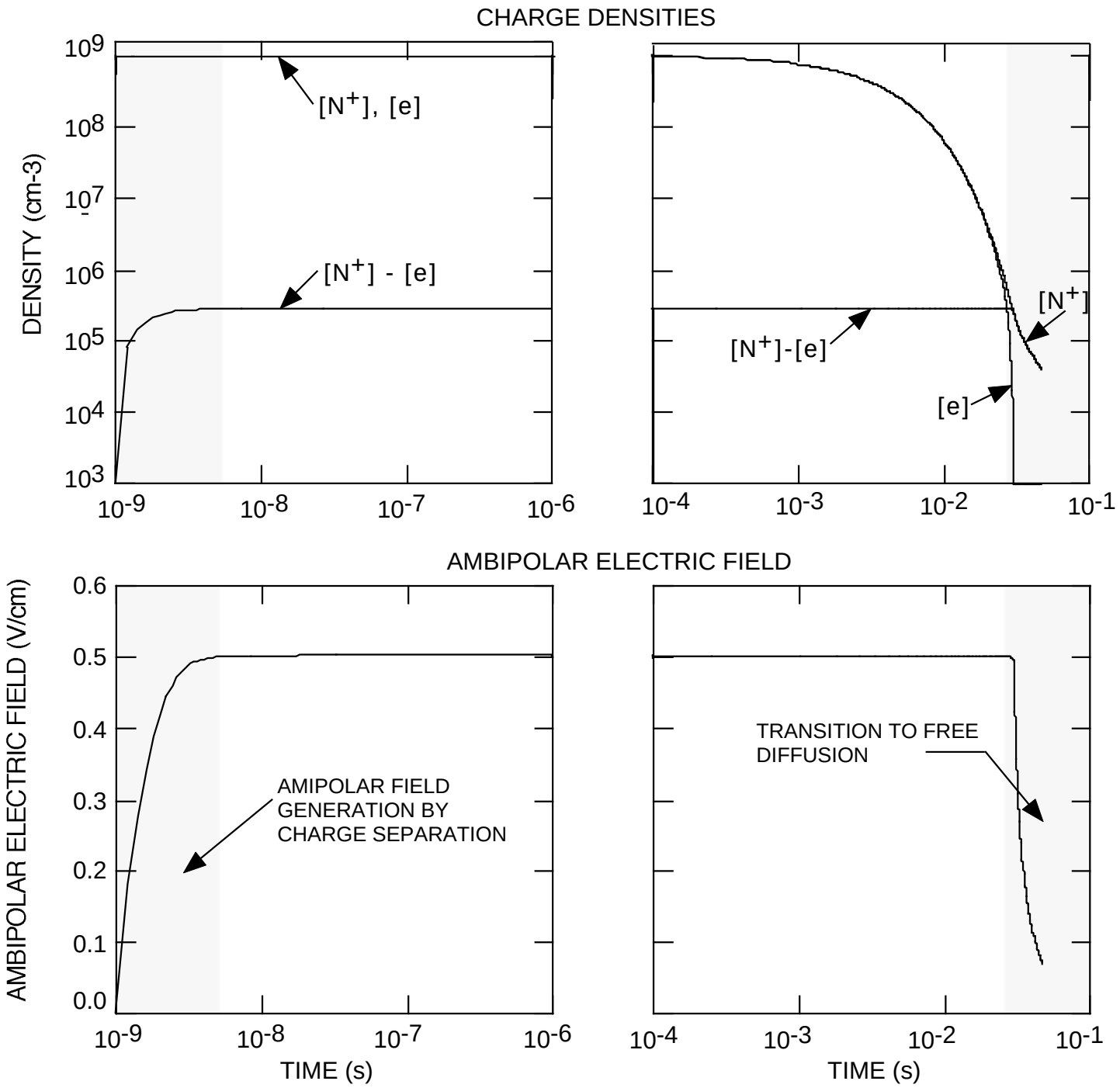
CHARGE DENSITIES
DENSITY (cm-3)
10^9
10^8
10^7
10^6
10^5
10^4
10^3
[N+], [e]
[N+] - [e]
10^{-9}
10^{-8}
10^{-7}
10^{-6}
[N+]
[N+]-[e]
[e]
10^{-4}
10^{-3}
10^{-2}
10^{-1}
AMBIPOLAR ELECTRIC FIELD
AMBIPOLAR ELECTRIC FIELD (V/cm)
0.6
0.5
0.4
0.3
0.2
0.1
0.0
AMIPOLAR FIELD
GENERATION BY
CHARGE SEPARATION
TRANSITION TO FREE
DIFFUSION
TIME (s)
TIME (s)

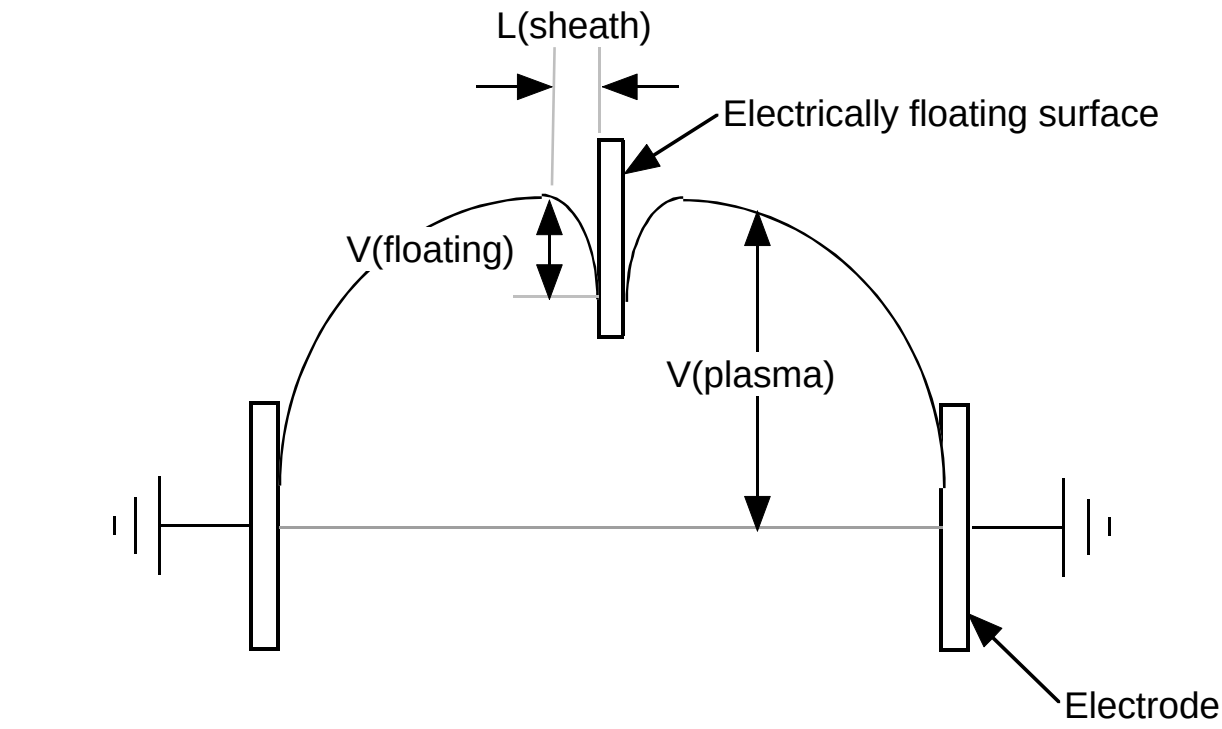
L(sheath)
Electrically floating surface
V(floating)
V(plasma)
Electrode

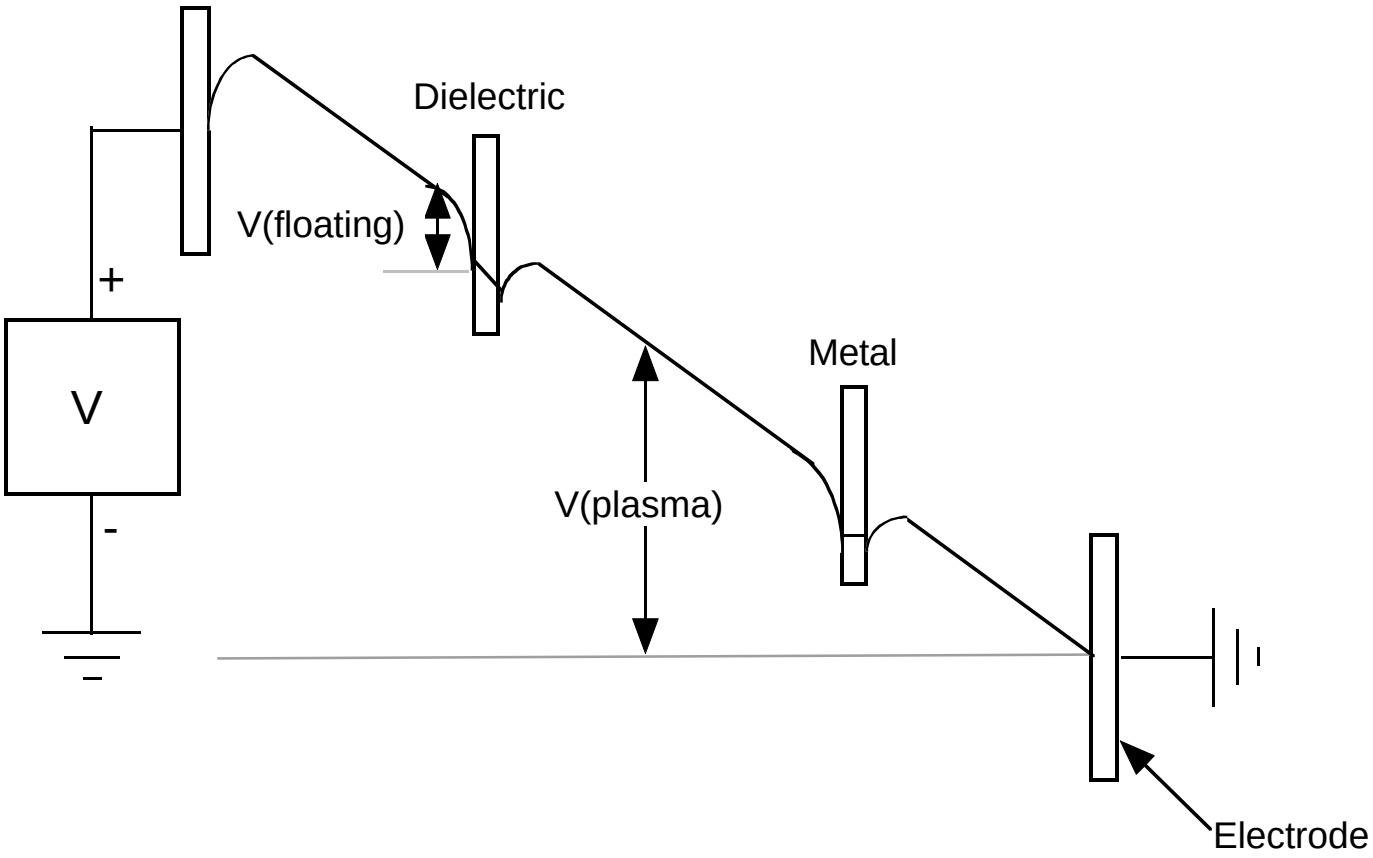
Dielectric
V(floating)
+
V
-
Metal
V(plasma)
Electrode

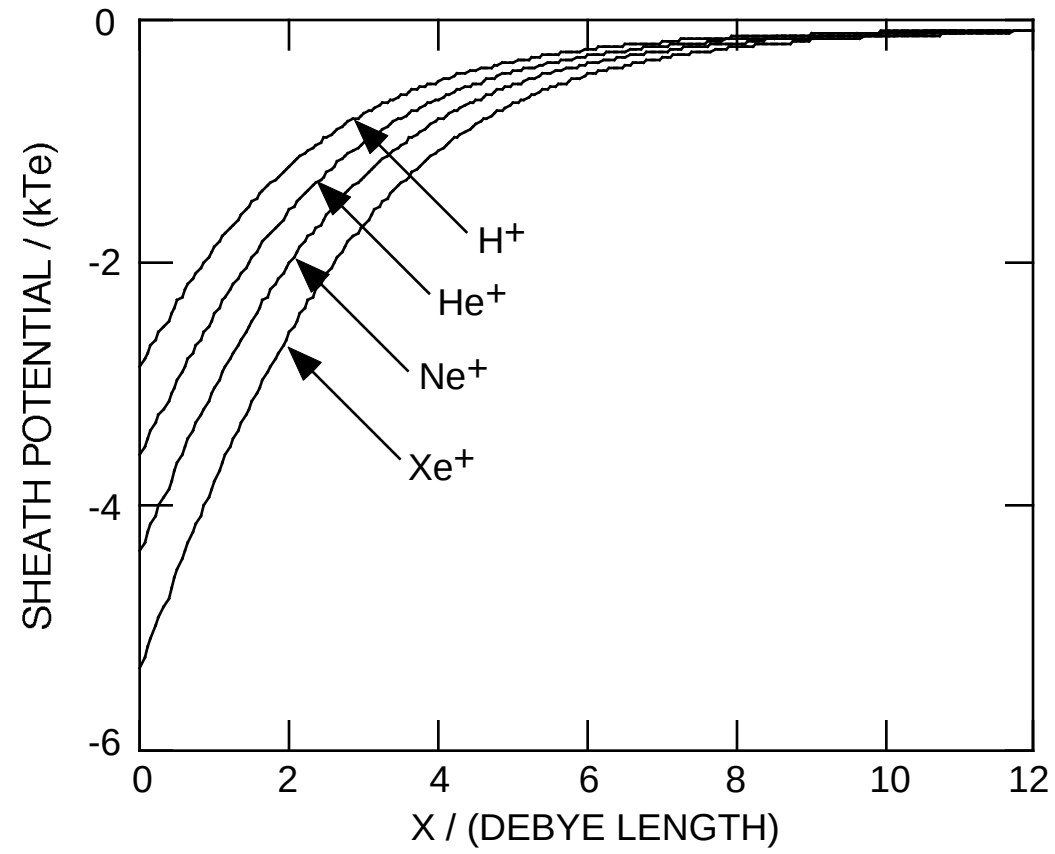
0
-2
-4
-6
SHEATH POTENTIAL / (kTe)
H+
He+
Ne+
Xe+
0
2
4
6
8
10
12
X / (DEBYE LENGTH)

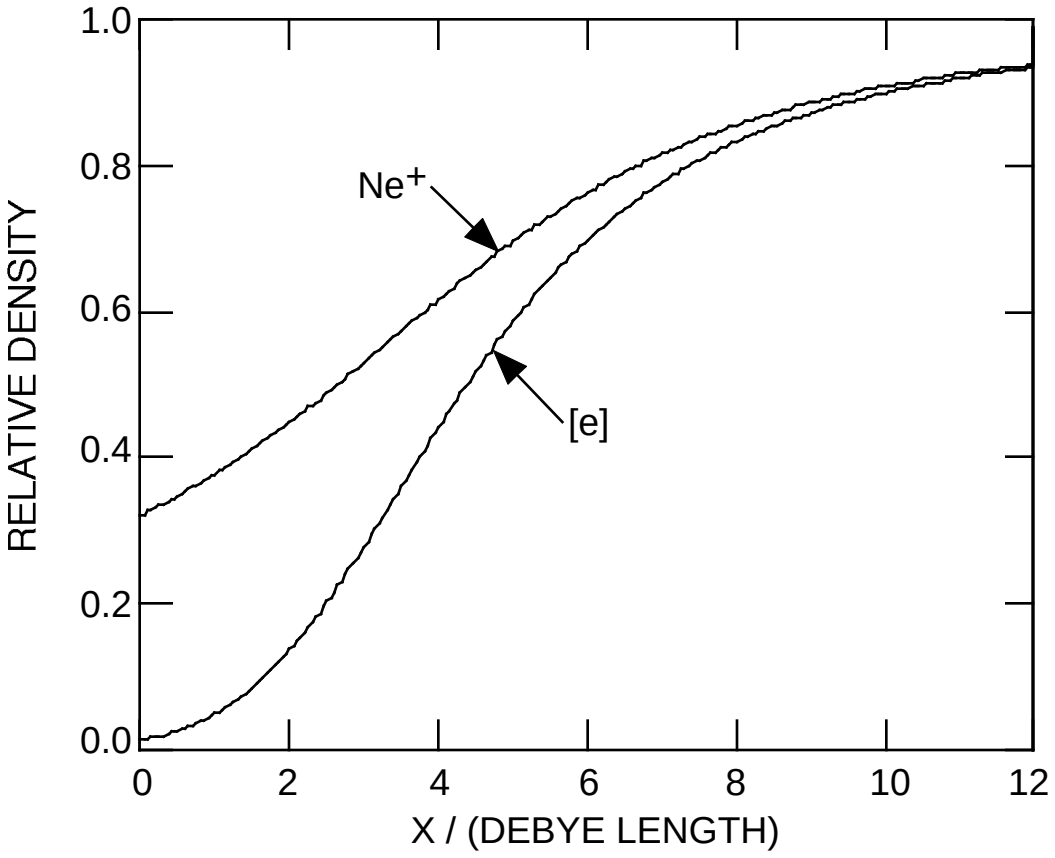
1.0
0.8
0.6
0.4
0.2
0.0
RELATIVE DENSITY
Ne+
[e]
0
2
4
6
8
10
12
X / (DEBYE LENGTH)

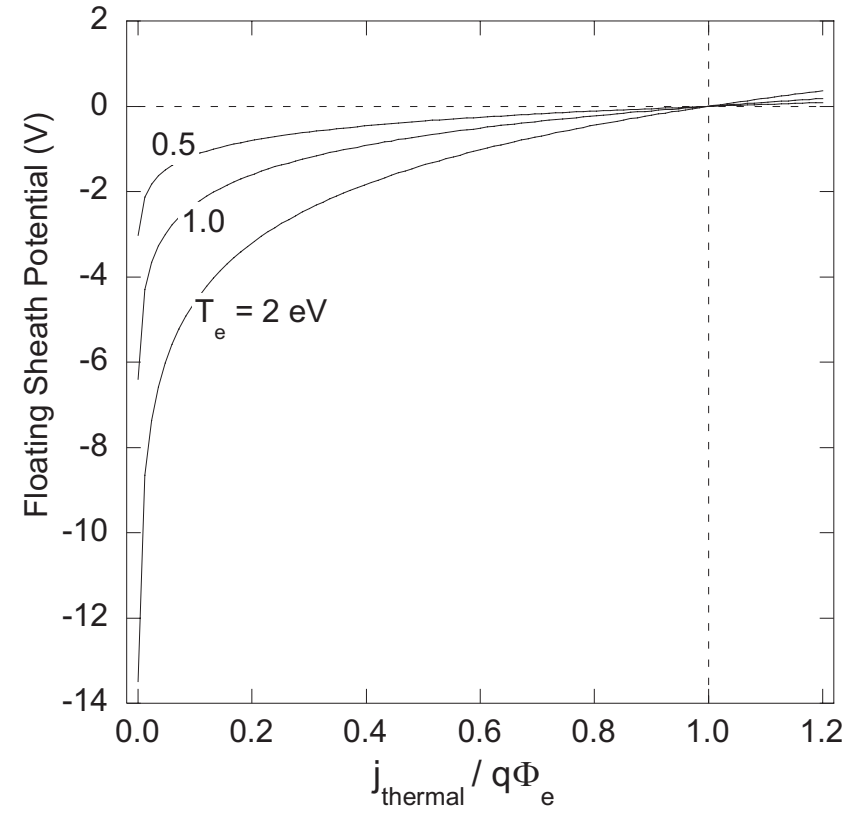

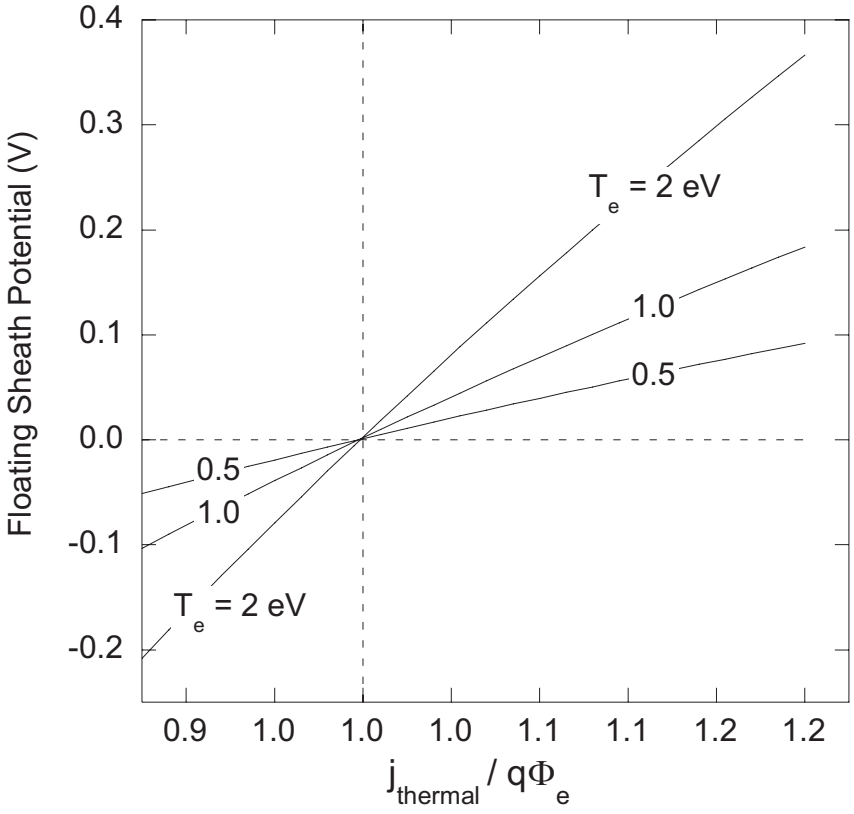

T_{ion} = 0.1 eV, M_{ion} = 20 AMU

floating_sheath_potential_jthermal.qpc
floating_sheath_potential_jthermal_closeup.qpc
floating_sheath_potential_jthermal.cdr

NOTE ON NOTATION

The electron distribution function technically has units of (VELOCITY)$^{-3}$ or (eV)$^{-3/2}$. This results from the normalization

$$\int f(\vec{v})\, d^3V = 1$$

When this is translated to an energy representation, then we have

$$\int f(\varepsilon)\ \underbrace{\varepsilon^{1/2} d\varepsilon}_{\substack{\text{Differential} \\ \text{corresponding to } d^3V}} = 1$$

where f(ε) retains the normalization of (eV)$^{-3/2}$. Now people will very often lump the $\varepsilon^{1/2}$ into the distribution function

$$\int \bar{f}(\varepsilon)\, d\varepsilon = 1$$

so that $\bar{f}(\varepsilon) = f(\varepsilon)\,\varepsilon^{1/2}$ which has units of (eV)$^{-1}$. The units of f(ε) tell you which normalization is used. Also $\bar{f}(\varepsilon)$ (eV^{-1}) is always zero at ε = 0 whereas f(ε) eV$^{-3/2}$ is not (it is finite at zero)

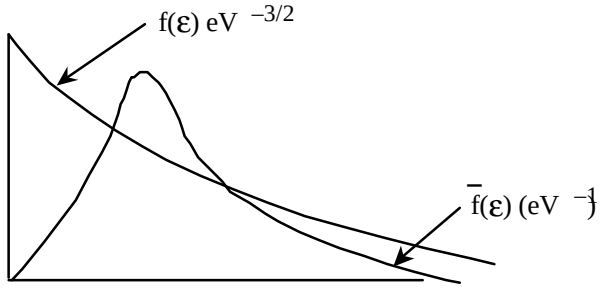

$\underline{f(\vec{v})\ \text{vs}\ f(v)\ \text{vs}\ f(\varepsilon)}$

$f(\vec{v})$ has normalization

$$\int f_o(\vec{v})\, d^3v = 1, \qquad f_o(\vec{v}) \equiv eV^{-3/2}$$

When using the Spherical Harmonic Expansion, $f_o(\vec{v}) \rightarrow f_o(v)$ (function of speed v instead of velocity $\vec{v}$). The normalization is then

$$\int f_o(v)\, 4\pi v^2 dv, \qquad f_o(v) \equiv eV^{-3/2}$$

where $4\pi v^2 dv$ is the volume element (a spherical shell in velocity space). Once we have f(v) we can equivalently express the distribution as f(ε), where

$$\frac{1}{2}\, m_e v^2 = \varepsilon$$

$$m_e v\, dv = d\varepsilon, \qquad dv = \frac{d\varepsilon}{m_e v} = \frac{d\varepsilon}{(2 m_e \varepsilon)^{1/2}}, \qquad v = \left(\frac{2\varepsilon}{m_e}\right)^{1/2}$$

Therefore

$$f_o(\varepsilon)\, d\varepsilon = f_o(v)\, d^3v$$

Normalization eV^{-1}: $\quad f_o(\varepsilon)\, eV^{-1} = f_o(v)\, \dfrac{4\pi v^2 dv}{d\varepsilon} = \dfrac{4\pi\sqrt{2}}{m_e^{3/2}}\, \varepsilon^{1/2}\, f_o(v)$

or

Normalization $eV^{-3/2}$: $\quad f_o(\varepsilon)\, eV^{-3/2} = \dfrac{4\pi\sqrt{2}}{m_e^{3/2}}\, f_o(v)$

Boltzmann's equation $\left(\dfrac{\partial}{\partial z} = \dfrac{\partial}{\partial t} = 0,\ \text{elastic collisions only}\right)$ in an energy representation is then

$$\frac{\partial}{\partial\varepsilon}\left(\frac{q^2E^2\varepsilon}{3N\sigma_m(\varepsilon)}\left(\frac{\partial f_o(\varepsilon)}{\partial\varepsilon}\right)\right) +$$

$$\frac{2m_e}{M}\frac{\partial}{\partial\varepsilon}\left[\varepsilon^2 N\sigma_m(\varepsilon)\left[f_o(\varepsilon) + kT_g\left(\frac{\partial f_o}{\partial\varepsilon}\right)\right]\right] = 0$$

where $f_o(\varepsilon) = eV^{-1}$.

SPHERICAL HARMONIC EXPANSION

1. Expand the electron velocity distribution in a series of Legendre polynomials. Each term in the series brings in more anisotropy

$$f(\vec{v}, \vec{r}, t) = \sum_{k=0}^{\infty} P_k(\cos\theta)\, f_k(v, \vec{r}, t)$$

where $\vec{v}$ is the vector velocity and v is the speed.

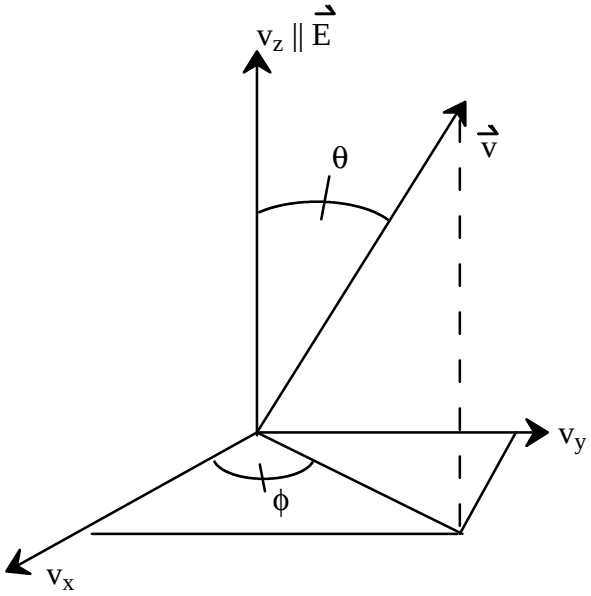

a. θ is measured from the direction of $\vec{E}$, usually aligned along $\vec{v}_z$.

b. f_k is a function only of $|\vec{v}_k| = v$.

$$f_{k+n} << f_k$$

c. $P_k(\cos\theta)$ is the k^{th} Legendre polynomial

k	
0	$P_0(\cos\theta) = 1$ -Isotropic component
1	$P_1(\cos\theta) = \cos\theta$ -Drift in direction of field
2	$P_2(\cos\theta) = \frac{1}{4}(1 + 3\cos 2\theta)$ -Higher order transport $= \frac{1}{2}(3\cos^2\theta - 1)$

2. Keep only the first two terms

$$f(\vec{v}, \vec{r}, t) = f_0(v, \vec{r}, t) + f_1(v, \vec{r}, t)\cos\theta, \int_0^{\infty} f_0(v) 4\pi v^2 dv = 1$$

where f_0 is the isotropic component. Substitute into Boltzman's equation with $\vec{E} = E_z\hat{z}, \quad \vec{a} = \frac{-q\vec{E}}{m_e}$. (See Appendix A of Cherrington.)

a. $\frac{\partial f_0}{\partial t} + \frac{v}{3}\frac{\partial f_1}{\partial z} - \frac{qE_z}{m_e}\frac{1}{3}\frac{1}{v^2}\frac{2}{2v}\left(v^2 f_1\right) = S_0$

b. $\frac{\partial f_1}{\partial t} + v\frac{\partial f_0}{\partial z} - \frac{qE_z}{m_e}\frac{\partial f_0}{\partial v} = S_1$

$$S_k = \frac{2k+1}{4\pi}\int P_k \left(\frac{\partial f}{\partial t}\right)_c d\Omega$$

3. Elastic collisions only:

For $\frac{\partial f}{\partial t} = 0$, $\frac{\partial}{\partial z} = 0$, and elastic collisions only.

$$\text{So} = \frac{1}{2v^2}\frac{\partial}{\partial v}\left(v^2 \delta \nu_m(v)\left(\frac{kT_g}{m_e}\frac{\partial f_0}{\partial v} + v f_0\right)\right)$$

$$\delta = \frac{2m_e}{M}, \quad \nu_m = v \cdot N \cdot \sigma_m(v)$$

Solve for S_1 from **b.** and substitute into **a.**

$$f_1 = \frac{qE_z}{m_e \nu_m}\frac{\partial f_0}{\partial v}$$

Note that f_1 is finite (e.g., anisotropic) only for $E \neq 0$.

$$\frac{-qE_z}{m_e}\frac{1}{3}\frac{1}{v^2}\frac{\partial}{\partial v}\left(v^2 \frac{qE}{m_e \nu_m}\frac{\partial f_0}{\partial v}\right) = \frac{1}{2v^2}\frac{\partial}{\partial v}\left(v^2 \delta \nu_m\left(\frac{kT_g}{m_e}\frac{\partial f_0}{\partial v} + v f_0\right)\right)$$

Note: $f_0(\varepsilon) = 4\pi\sqrt{2}\, f_0(v)\varepsilon^{1/2}/m_e^{3/2}$, $\quad v = \left(\frac{2\varepsilon}{m_e}\right)^{1/2}$

$$dv = \frac{d\varepsilon}{m_e v} = \frac{d\varepsilon}{(2m_e\varepsilon)^{1/2}}$$

In energy representation

$$\frac{\partial}{\partial \varepsilon}\left(\frac{q^2E_z^2\varepsilon}{3N\sigma_m(\varepsilon)}\left(\frac{\partial f_0}{\partial \varepsilon}\right)\right) + \frac{2m_e}{M}\frac{\partial}{\partial \varepsilon}\left(\varepsilon^2 N\sigma_m(\varepsilon)\left(f_0 + kT_g\left(\frac{\partial f_0}{\partial \varepsilon}\right)\right)\right) = 0$$

In velocity representation, solve for $\frac{\partial f_0}{\partial v}$.

$$\frac{\partial f_0}{\partial v} = \left(\frac{m_e}{kT_g} v f_0\right) \Big/ \left(1 + \frac{2}{3}\frac{1}{\delta kT_g \nu_m^2}\cdot\frac{q^2E^2}{m_e}\right)$$

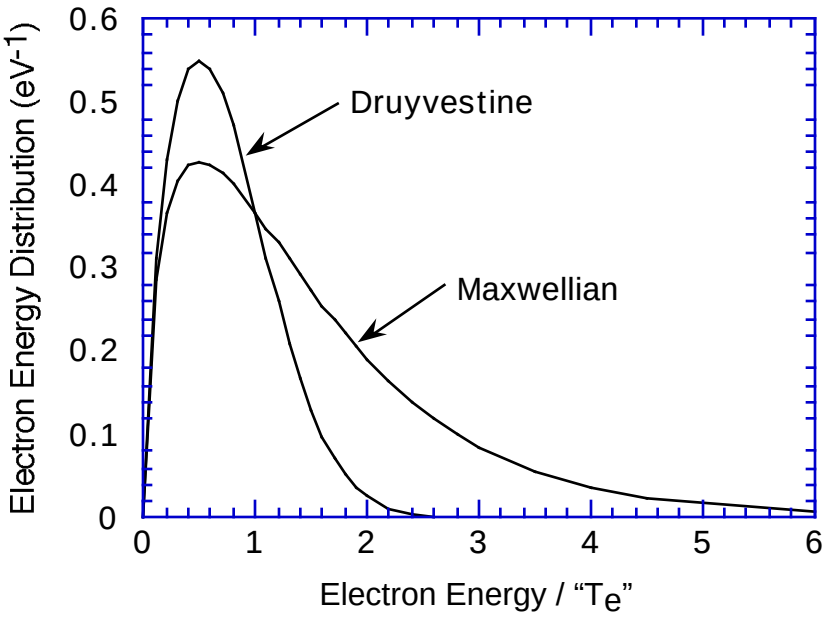
Electron Energy Distribution (eV-1)
0.6
0.5
0.4
0.3
0.2
0.1
0
0
1
2
3
4
5
6
Druyvestine
Maxwellian
Electron Energy / "Te"

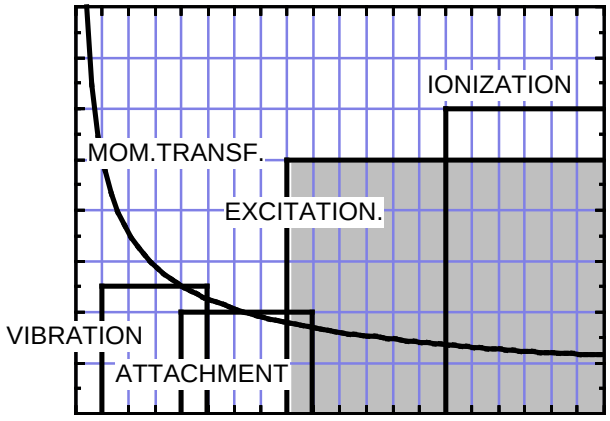

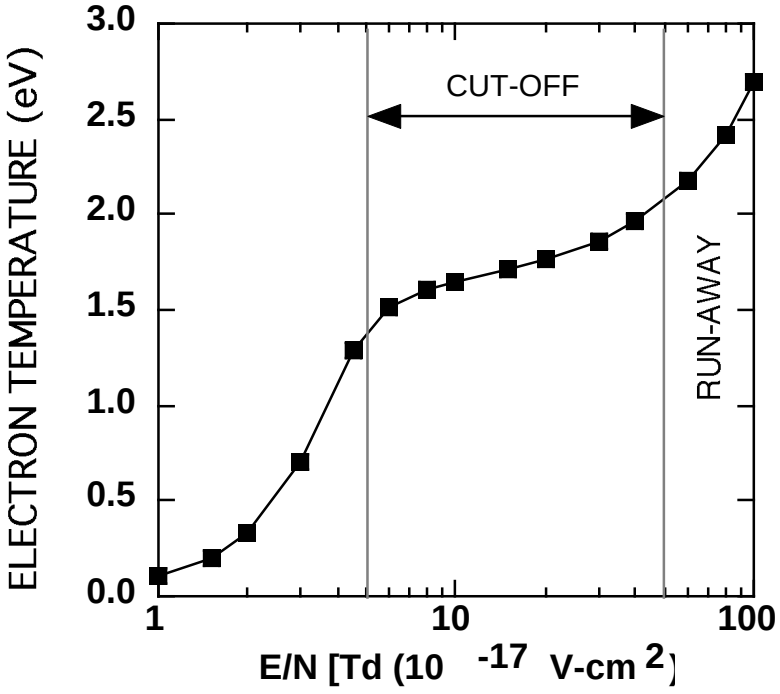

MOMENTUM TRANSFER AND ELECTRONIC EXCITATION

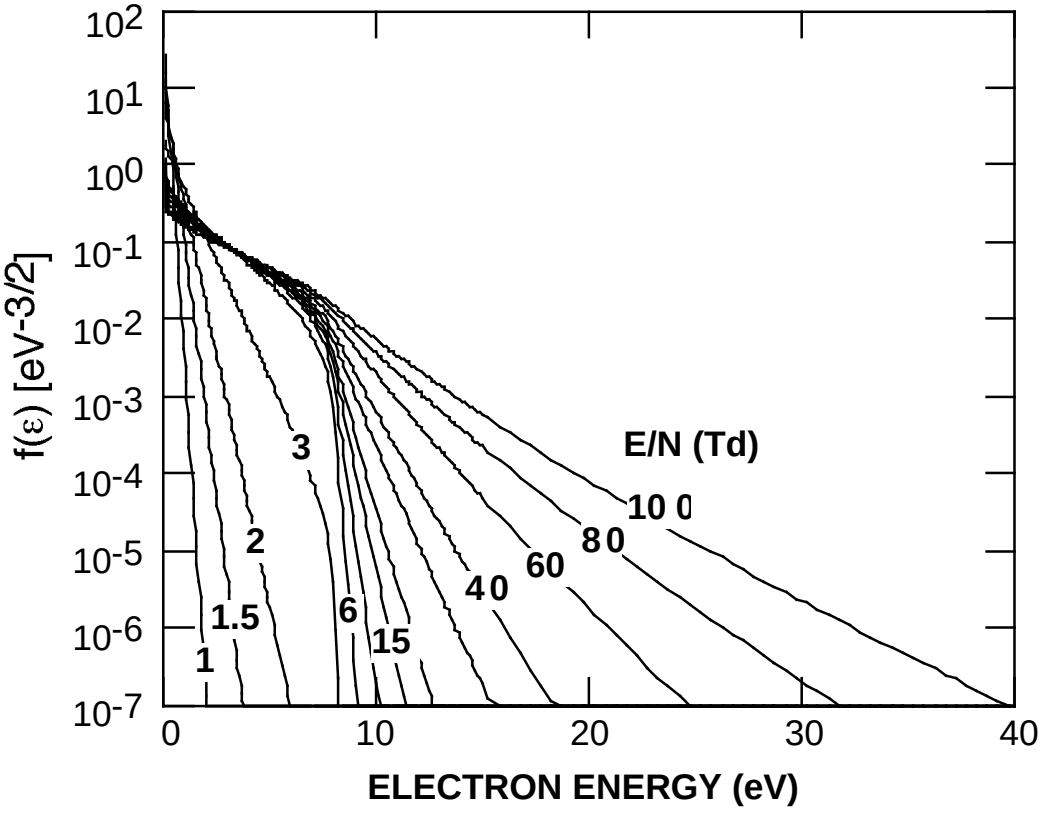

F(E) EXCITATION ONLY

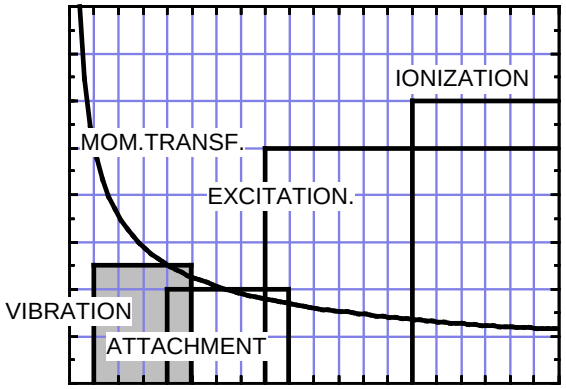

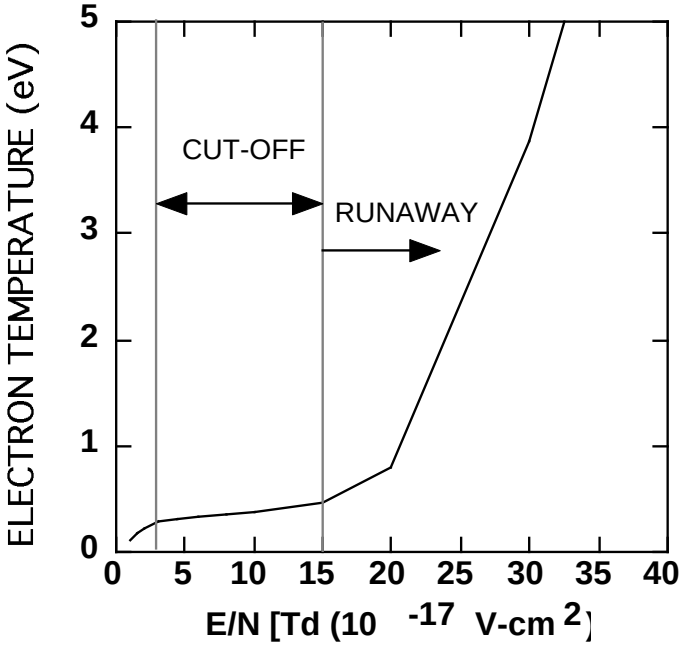

MOMENTUM TRANSFER and VIBRATIONAL EXCITATION

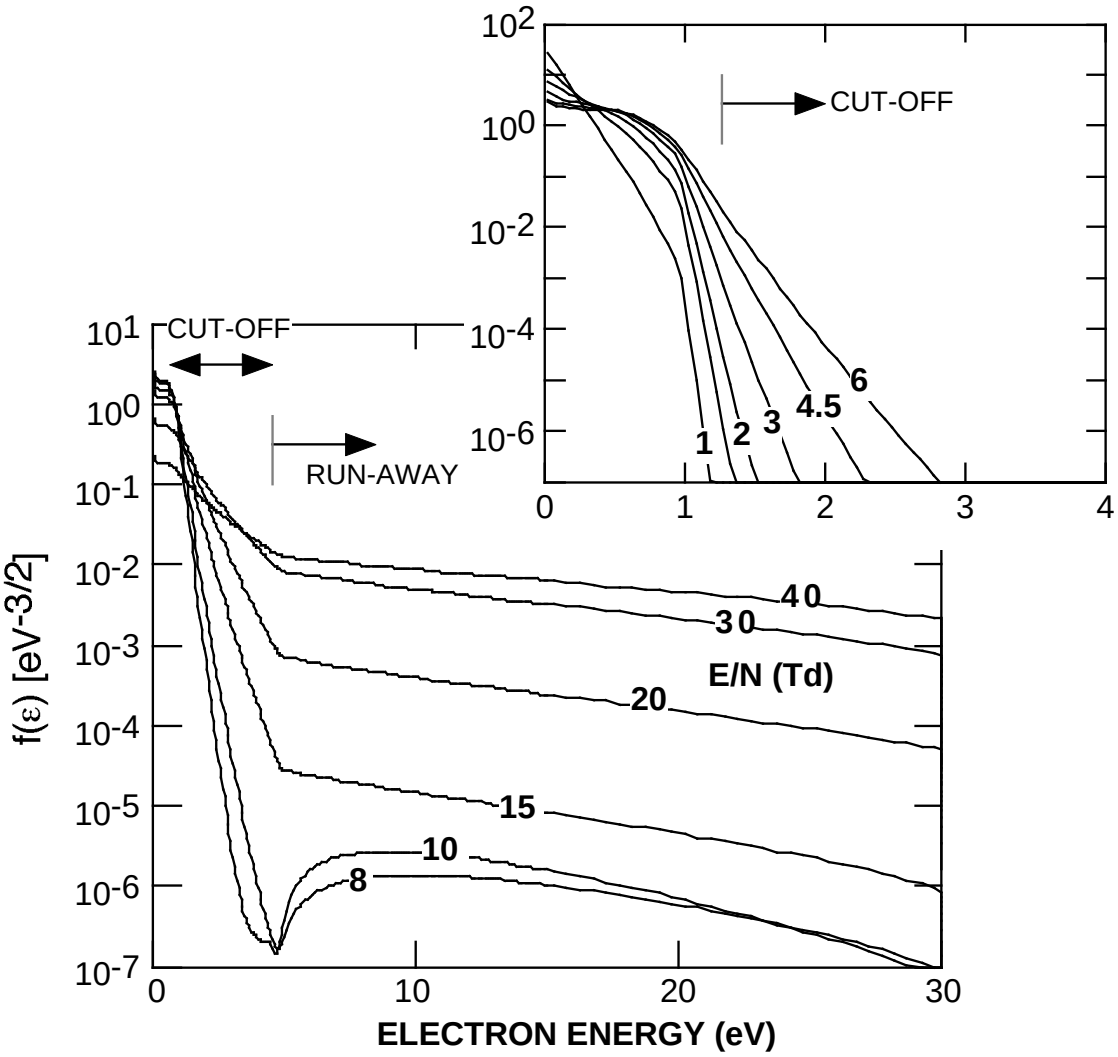

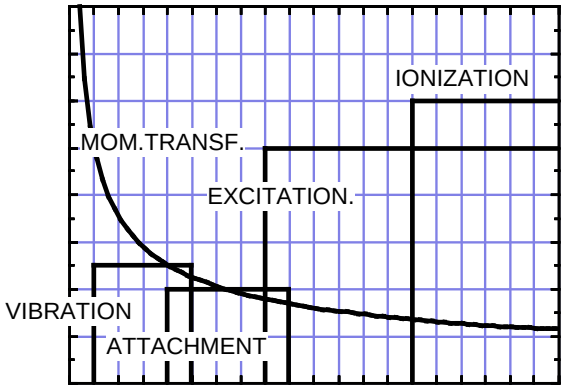

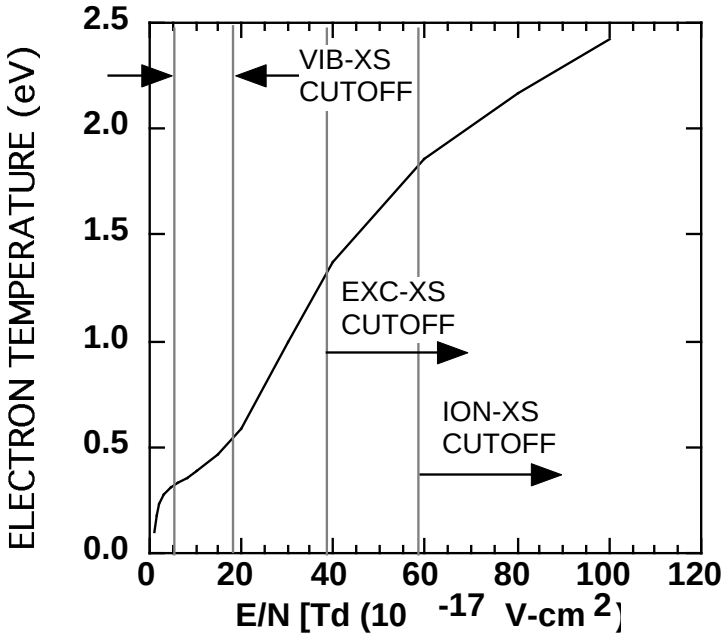

ALL COLLISIONS

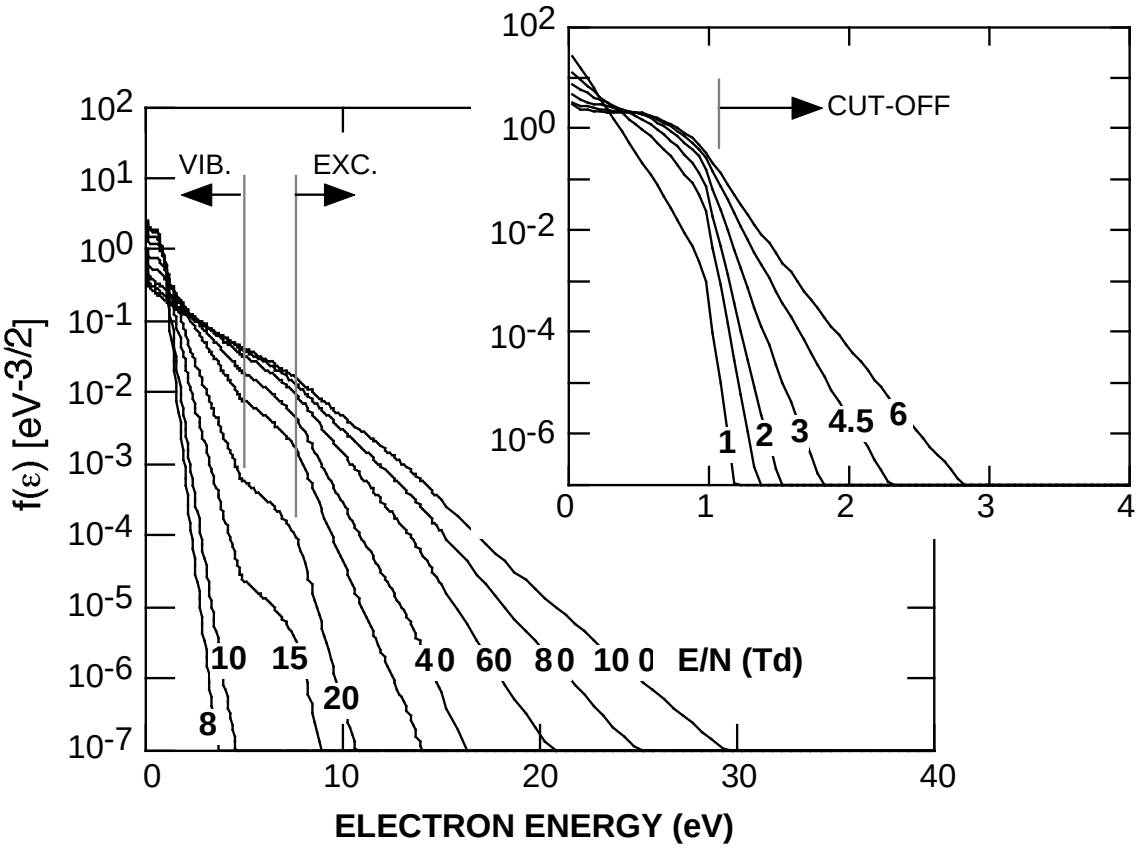

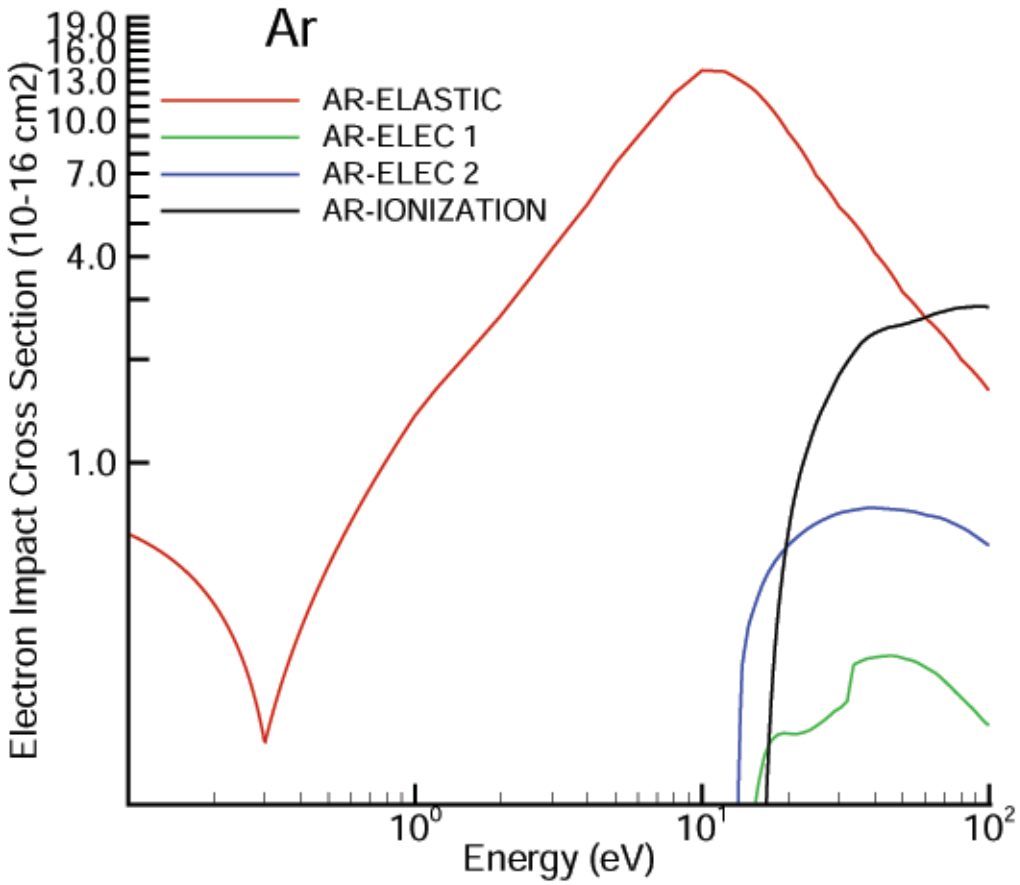
Ar
AR-ELASTIC
AR-ELEC 1
AR-ELEC 2
AR-IONIZATION
Electron Impact Cross Section (10-16 cm2)
19.0
16.0
13.0
10.0
7.0
4.0
1.0
10^0
10^1
10^2
Energy (eV)

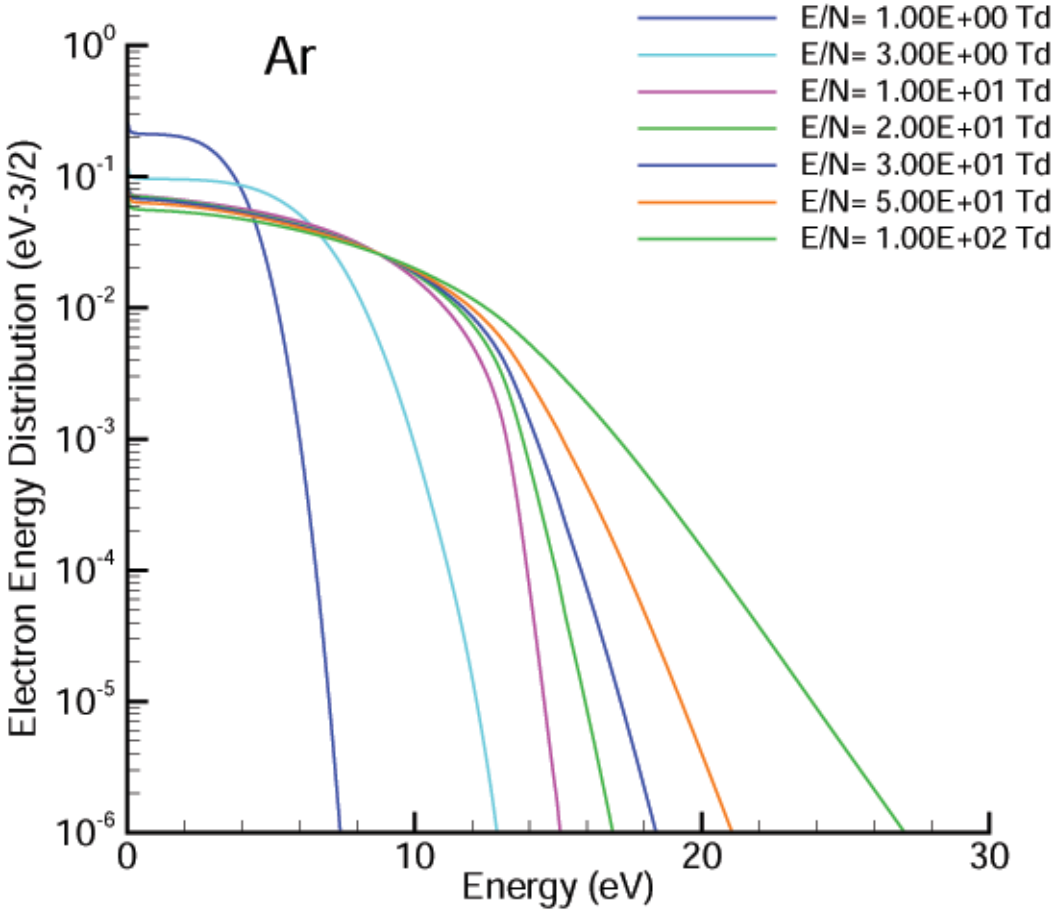
Ar
E/N= 1.00E+00 Td
E/N= 3.00E+00 Td
E/N= 1.00E+01 Td
E/N= 2.00E+01 Td
E/N= 3.00E+01 Td
E/N= 5.00E+01 Td
E/N= 1.00E+02 Td
Electron Energy Distribution (eV-3/2)
10^0
10^{-1}
10^{-2}
10^{-3}
10^{-4}
10^{-5}
10^{-6}
0
10
20
30
Energy (eV)

AR_XS_EED.CDD

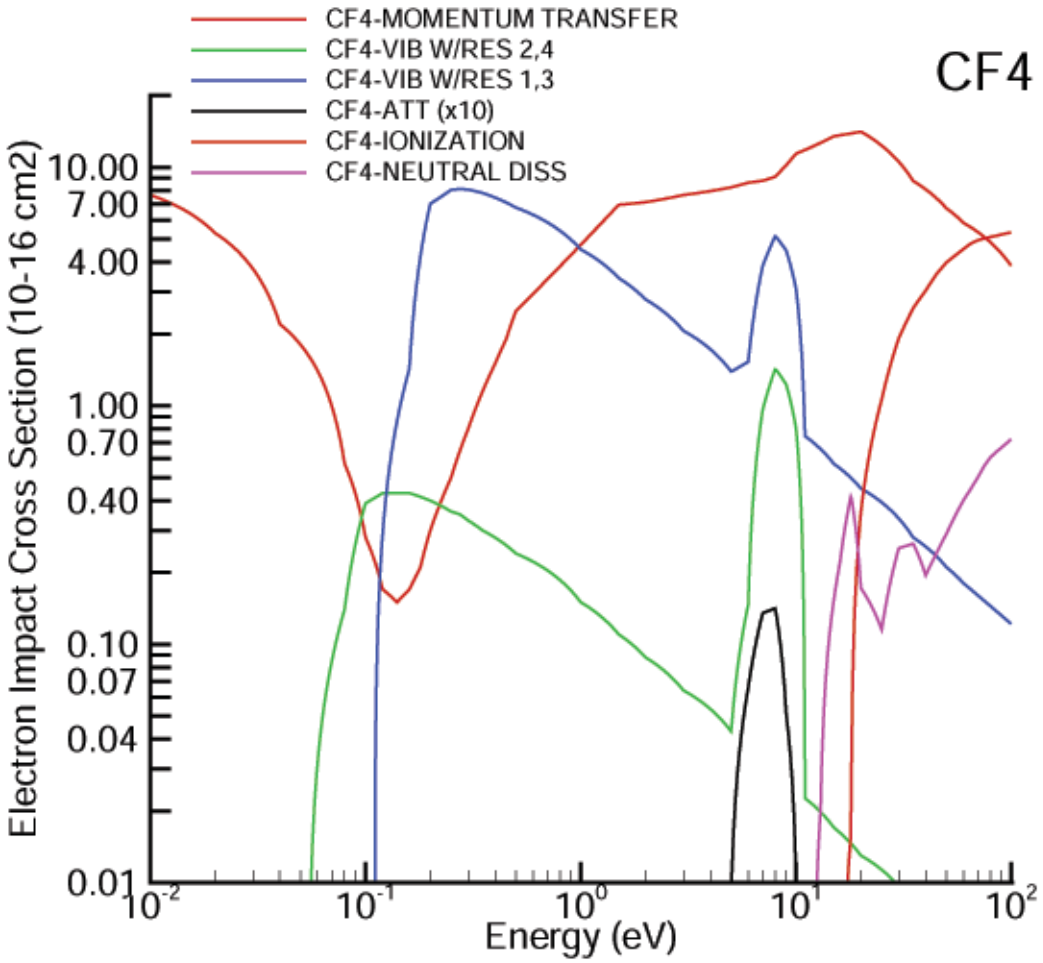

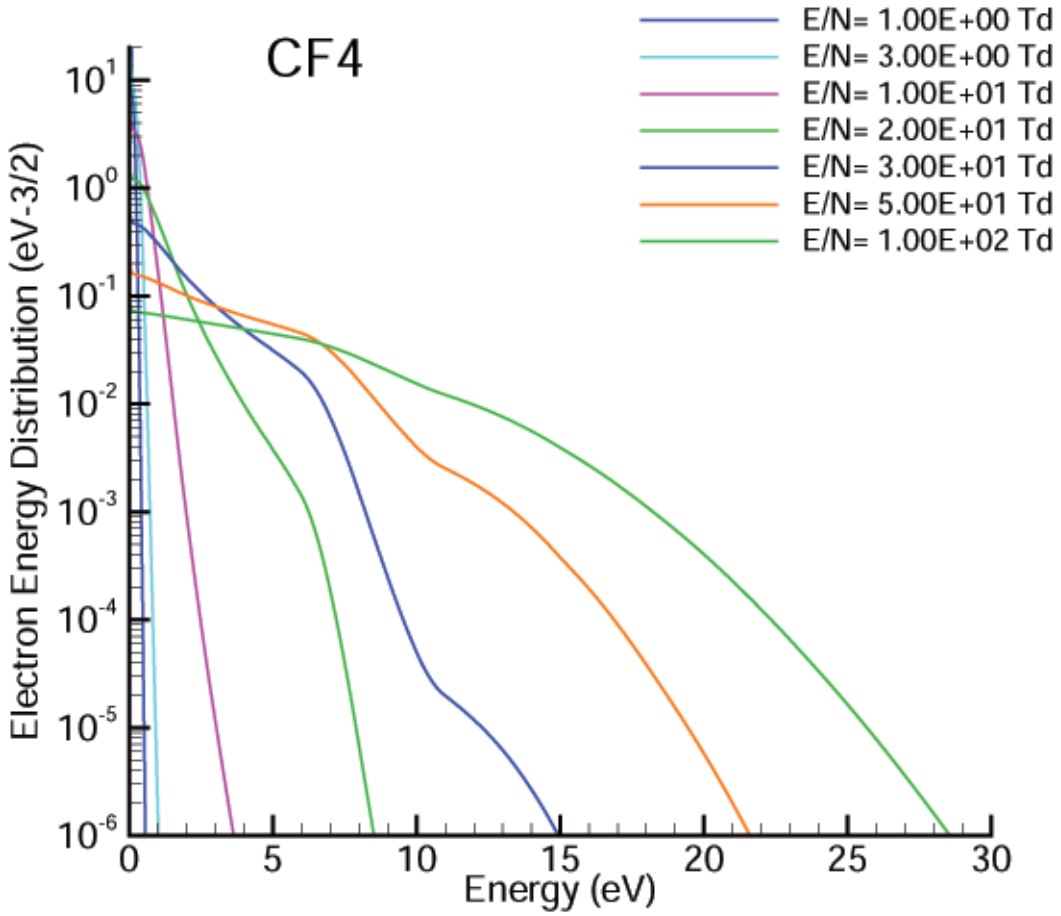

CF4_XS_EED.CDD

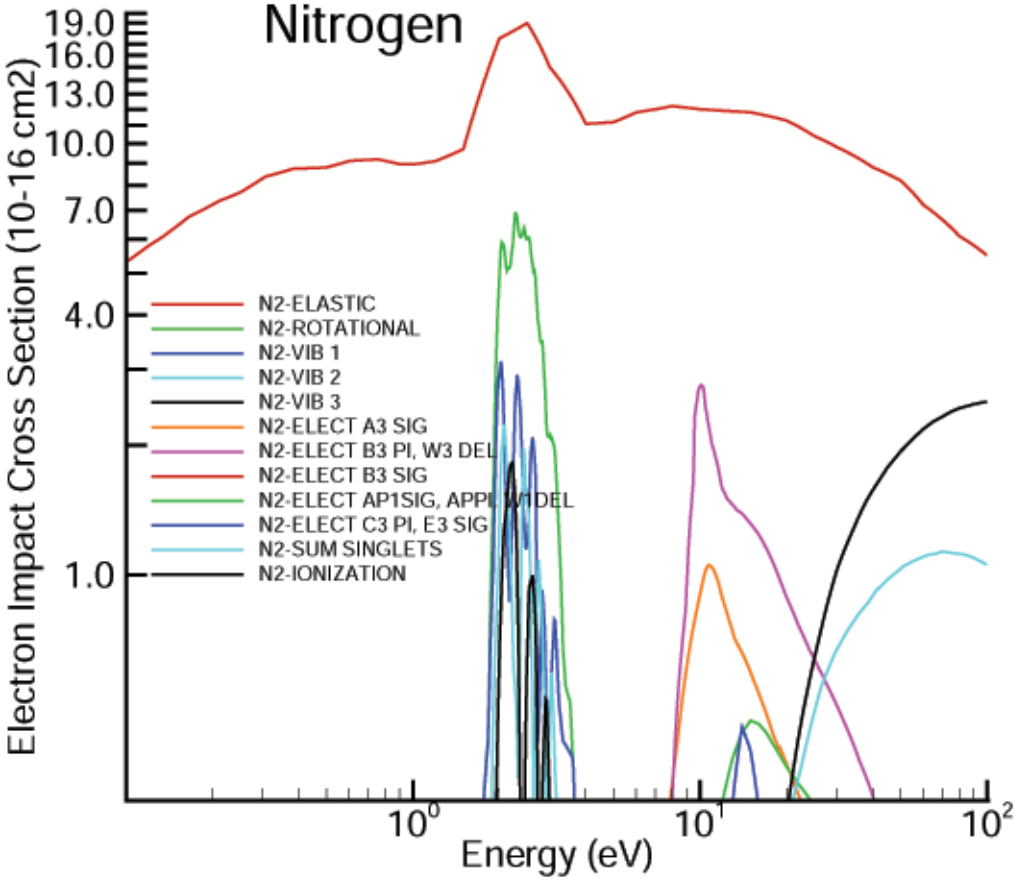
Nitrogen
Electron Impact Cross Section (10-16 cm2)
19.0
16.0
13.0
10.0
7.0
4.0
1.0
N2-ELASTIC
N2-ROTATIONAL
N2-VIB 1
N2-VIB 2
N2-VIB 3
N2-ELECT A3 SIG
N2-ELECT B3 PI, W3 DEL
N2-ELECT B3 SIG
N2-ELECT AP1SIG, APPL W1DEL
N2-ELECT C3 PI, E3 SIG
N2-SUM SINGLETS
N2-IONIZATION
10^0
10^1
10^2
Energy (eV)

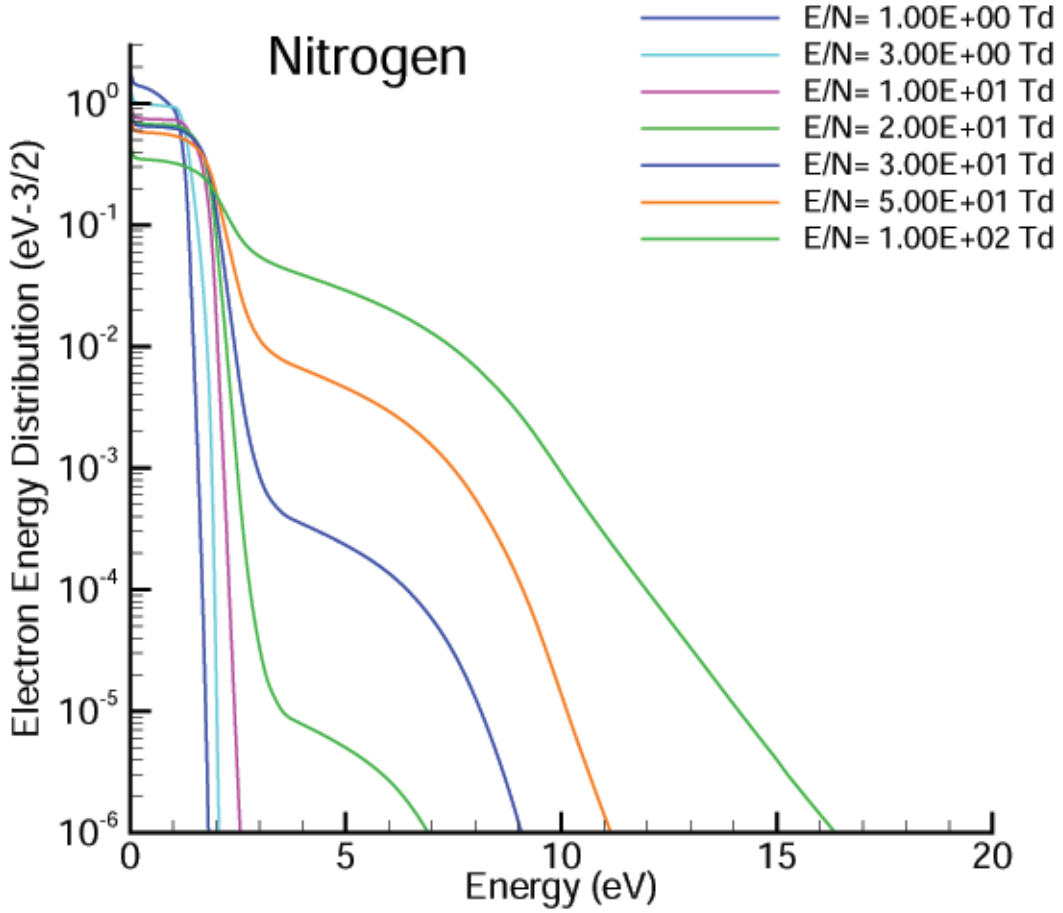
Nitrogen
E/N= 1.00E+00 Td
E/N= 3.00E+00 Td
E/N= 1.00E+01 Td
E/N= 2.00E+01 Td
E/N= 3.00E+01 Td
E/N= 5.00E+01 Td
E/N= 1.00E+02 Td
Electron Energy Distribution (eV-3/2)
10^0
10^-1
10^-2
10^-3
10^-4
10^-5
10^-6
0
5
10
15
20
Energy (eV)

N2_XS_EED.CDD

DRIFT VELOCITY FROM BOLTZMANN'S EQUATION

From the two-term spherical harmonic expansion

$$f(\vec{v}) = f_0(v) + f_1(v)\cos\theta$$

$$\int_0^\infty \int_0^\pi f_0(v) 2\pi v^2 \sin\theta \, d\theta \, dv = 1$$

$$f_1(v) = \frac{qE}{m_e \nu_m(v)} \frac{\partial f_0(v)}{\partial v}$$

Drift velocity for $\vec{E} = E\hat{z}$ is v_z.

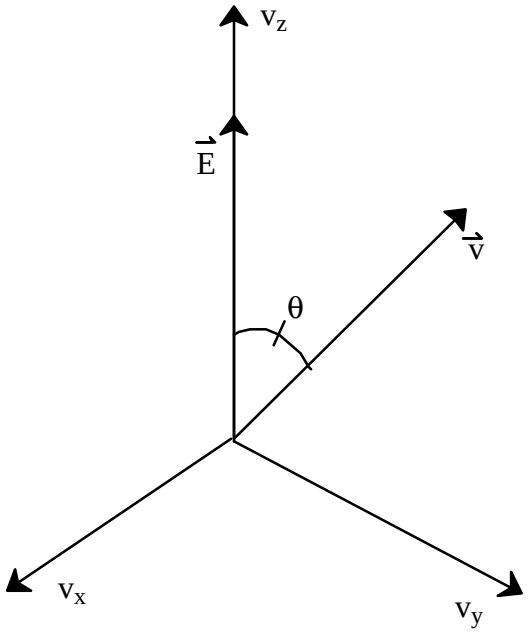

$$v_d = \langle v_z \rangle = \langle v\cos\theta \rangle = \int_0^\infty \int_0^\pi \left(f_0(v) + f_1(v)\cos\theta\right) v\cos\theta \, 2\pi v^2 \sin\theta \, d\theta \, dv$$

Since f_0 is isotropic, $\int f_0 \cos\theta \, d\Omega$ integrates to zero.

$$v_d = \int_0^\infty \int_0^\pi \frac{qE}{m\nu_m} \frac{\partial f_0}{\partial v} 2\pi v^3 \cos^2\theta \sin\theta \, d\theta \, dv$$

$$v_d = \left[-\frac{4\pi}{3m_e} \int_0^\infty \frac{\partial f_0}{\partial v} \frac{1}{\nu_m(v)} v^3 dv \right] E = \mu E$$

where the mobility $\mu = \left[-\frac{4\pi}{3m_e} \int_0^\infty \frac{\partial f_0}{\partial v} \frac{1}{\nu_m(v)} v^3 dv \right]$

If $\nu_m(v)$ = constant, then

$$\mu = \frac{q}{m_e \nu_m} \left[\int_0^\infty -\frac{4}{3}\pi \frac{\partial f_0}{\partial v} v^3 dv \right] = \frac{q}{m_e \nu_m}$$

where the brackets integrate to 1.

DIFFUSION FLUX AND COEFFICIENT FROM BOLTZMANN'S EQUATION

From the two-term spherical harmonic expansion,

$$\frac{\partial f_1}{\partial t} + v\frac{\partial f_0}{\partial z} - \frac{qE_z}{m_e}\frac{\partial f_0}{\partial v} = -\nu_m f_1$$

where $\int f_0 \, 2\pi v^2 \sin\theta \, d\theta = n_0$, the average electron density.

Set $\frac{\partial}{\partial t} = 0$ and E = 0 (only "thermal motion")

$$v\frac{\partial f_0}{\partial z} = -\nu_m f_1, \qquad f_1 = \frac{-v}{\nu_m}\frac{\partial f_0}{\partial z}$$

The diffusion flux in the z direction is $\Gamma_z = n_0 v_z = n_0 < v \cos\theta > = \int_0^\infty \int_0^\pi v_z (f_0 + f_1 \cos\theta) \, d^3v$.

Since $\int f_0 \cos\theta \, d\Omega$ integrates to zero, then

$$\Gamma_z = \int_0^\infty \int_0^\pi v_z f_1 \cos\theta d^3v$$

$$= \int_0^\infty \int_0^\pi v\cos\theta \left[\frac{-v}{\nu_m}\frac{\partial f_0}{\partial z}\right] \cos\theta \, 2\pi v^2 \sin\theta \, d\theta \, dv$$

$$= -\int_0^\infty \int_0^\pi \frac{2\pi v^2}{\nu_m}\frac{\partial f_0}{\partial z} v^2 \cos^2\sin\theta \, d\theta \, dv$$

$$= -\int_0^\infty \frac{4\pi v^2}{3}\frac{v^2}{\nu_m}\frac{\partial f_0}{\partial z} dv = -n$$

$$\Gamma_z = -\frac{\partial}{\partial z}\left[\int_0^\infty \frac{4}{3}\pi v^2 \frac{v^2}{\nu_m} f_0 dv\right]$$

Now returning to the momentum conservation equation we have

$$\frac{\partial(nv)}{\partial t} = -\frac{\nabla P}{m} - nv\nu_m = 0$$

$$-\frac{\nabla nkT}{m} = nv\nu_m$$

$$\Gamma_z = nv_z = -\frac{\nabla nkT}{m\nu_m} = -\frac{kT}{m\nu_m}\nabla n = -D\nabla n$$

where we assume T = constant and the diffusion coefficient D = $\frac{kT}{m\nu_m}$ (also called the Einstein relation).

So we see that obtaining the conventional expression for diffusion flux as described by Ficks Law requires as a minimum that temperature T not be a function of position. However to go from our expression for Γ_z to Ficks Law we must also assume the $\nu_m(v)$ = constant and the $f_0(v)$ is a Maxwellian. We then have

$$\Gamma_z = -\frac{1}{\nu_m}\frac{\partial}{\partial z}\left[\int_0^\infty \frac{4}{3}\pi v^2 f_0 v^2 dv\right] = -\frac{1}{\nu_m}\frac{\partial}{\partial z}\left[\frac{nkT}{m}\right]$$

$$= -\frac{kT}{m\nu_m}\frac{\partial n}{\partial z} = -D\frac{\partial n}{\partial z}$$

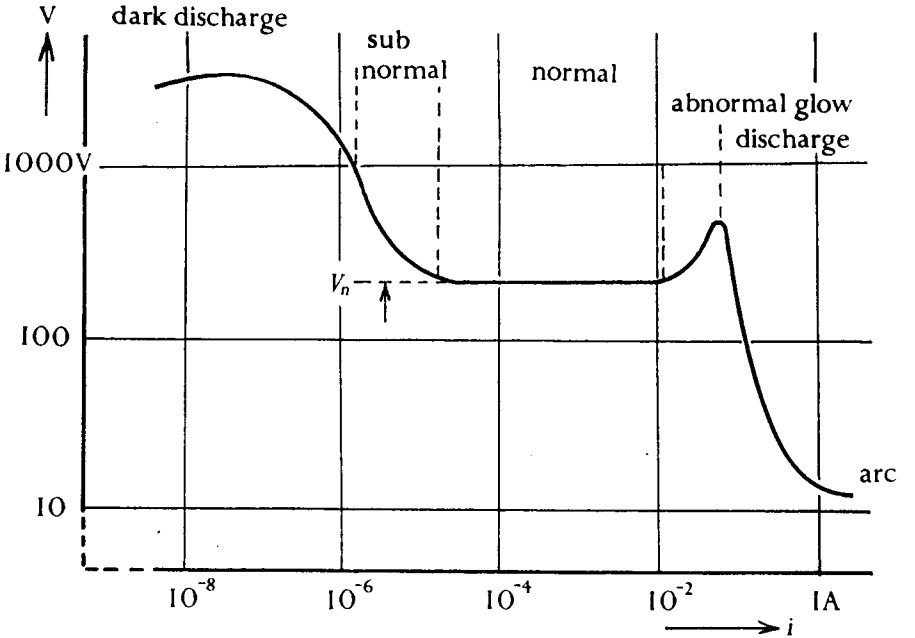

FIG. 115. Lowest maintenance potentials of the three main types of self-sustained discharges. V_n is the normal cathode fall in potential.

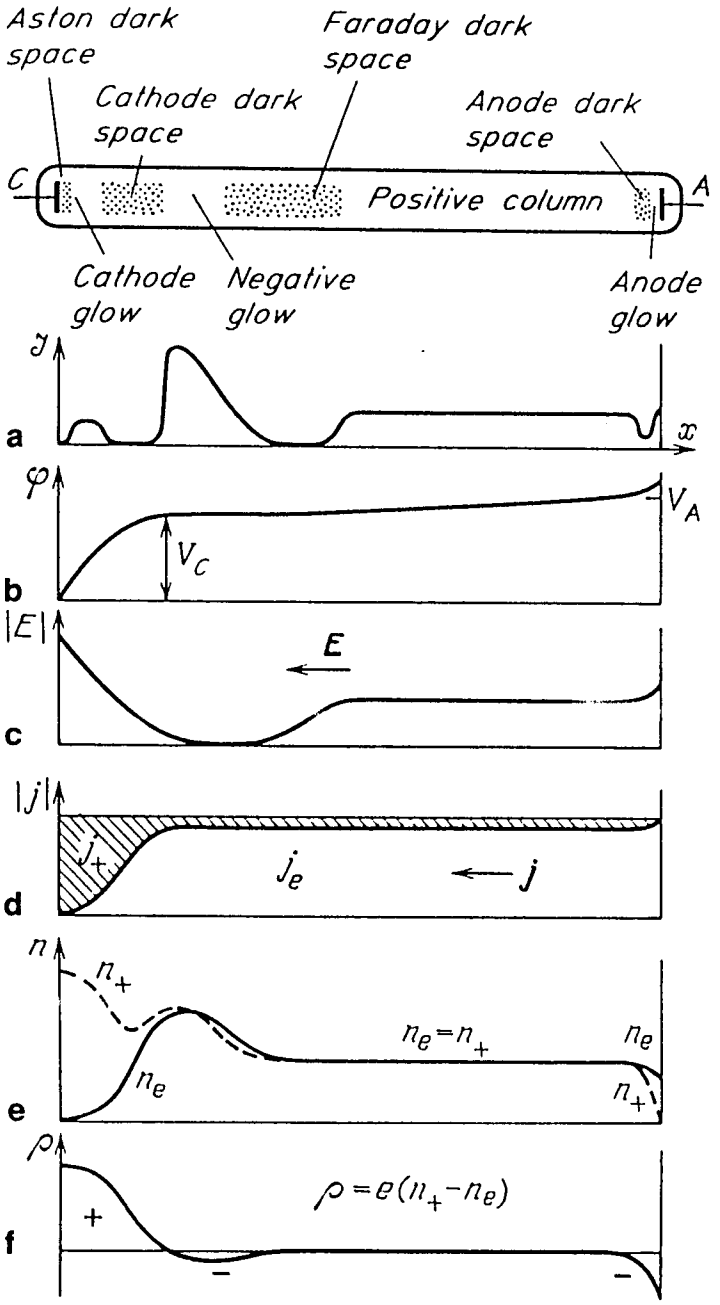

Fig. 8.2. Glow discharge in a tube and the distribution of: **(a)** glow intensity, **(b)** potential φ, **(c)** longitudinal field E, **(d)** electronic and ionic current densities j_e and j_+, **(e)** charge densities n_e and n_+, and **(f)** space charge $\varrho = e(n_+ - n_e)$

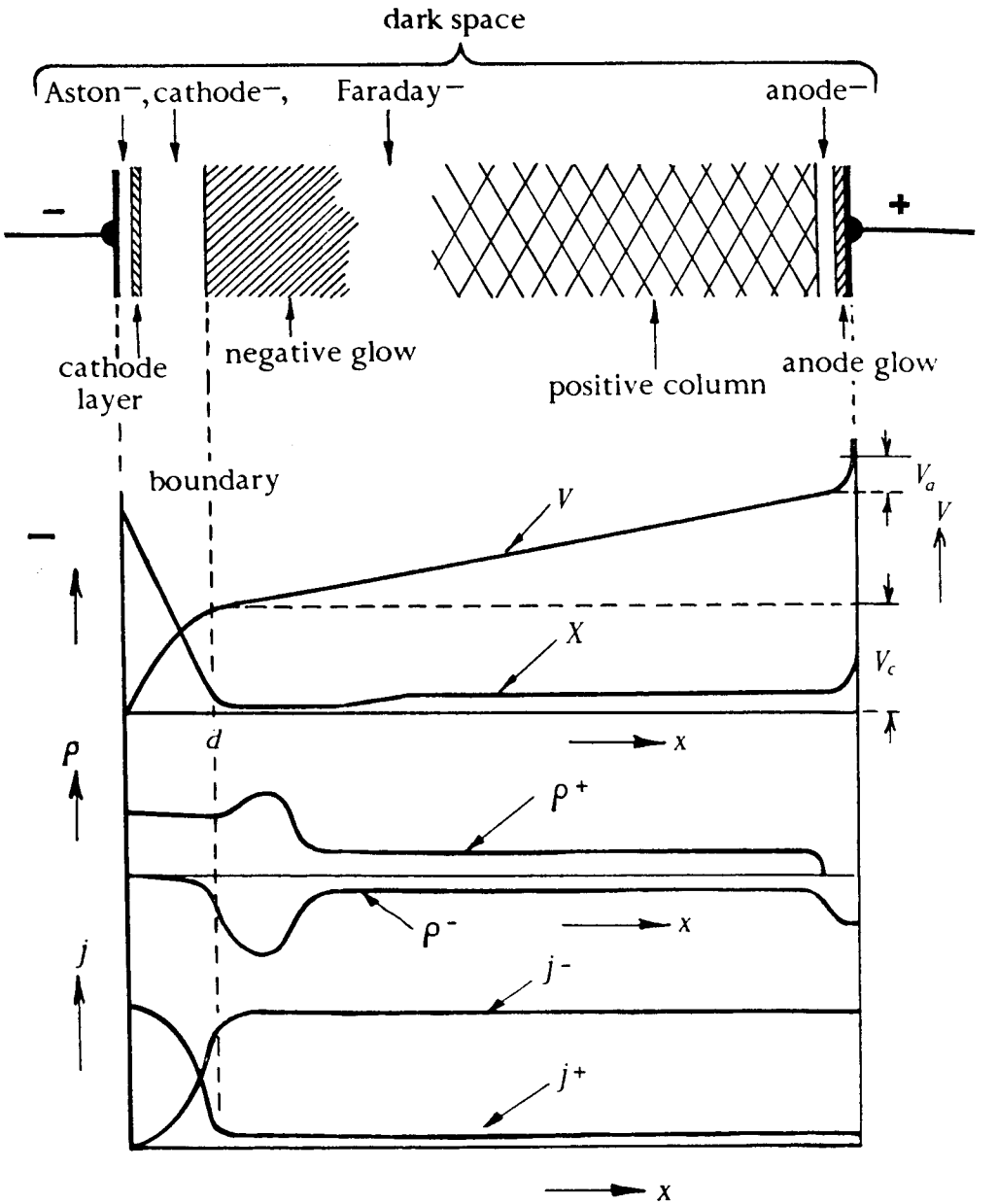

FIG. 113. Spatial distribution of dark and luminous zones, electric field X, space-charge densities ρ^+ and ρ^-, and current densities j^+ and j^- in a glow discharge (schematically).

A. von Engle

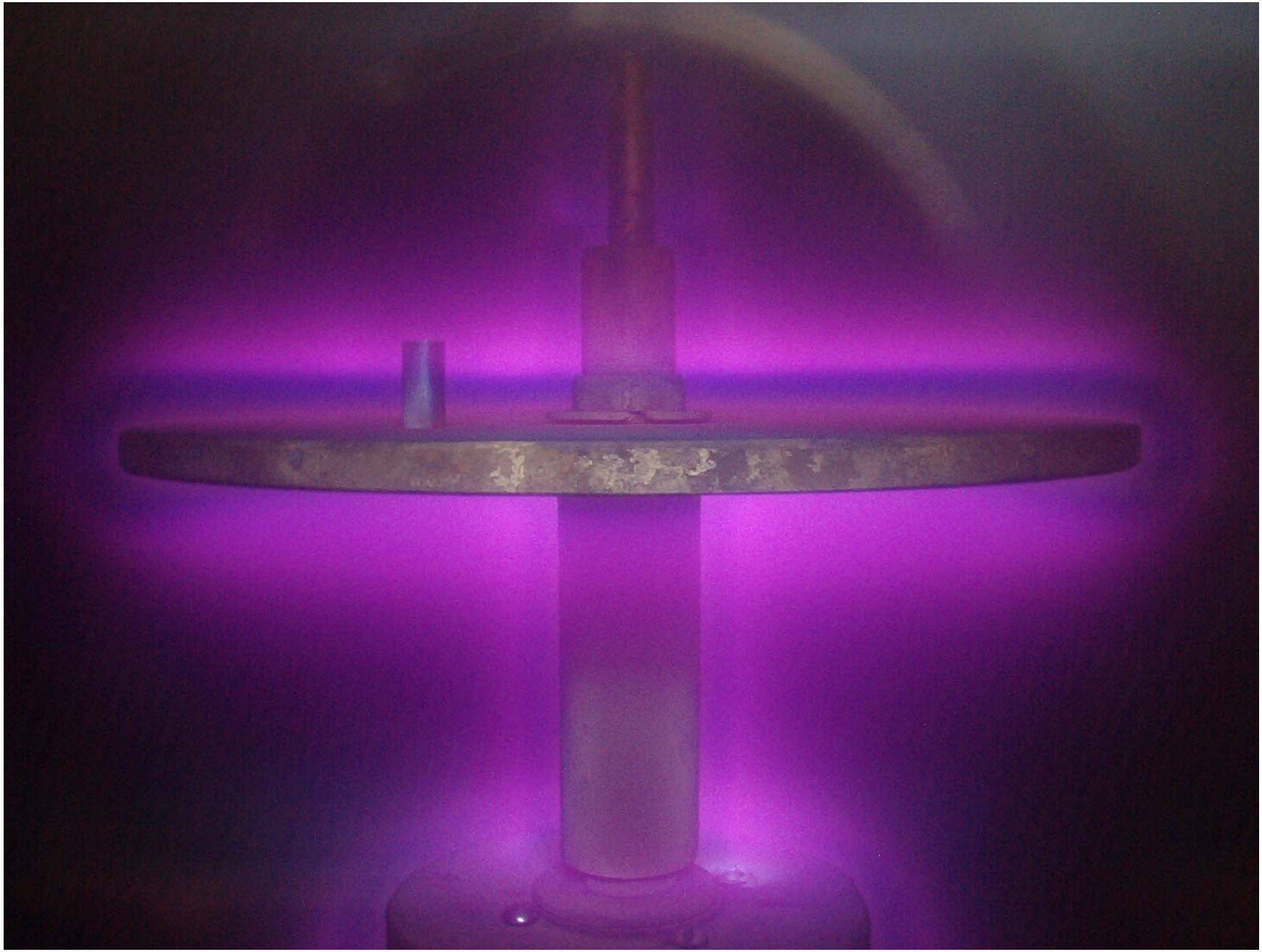

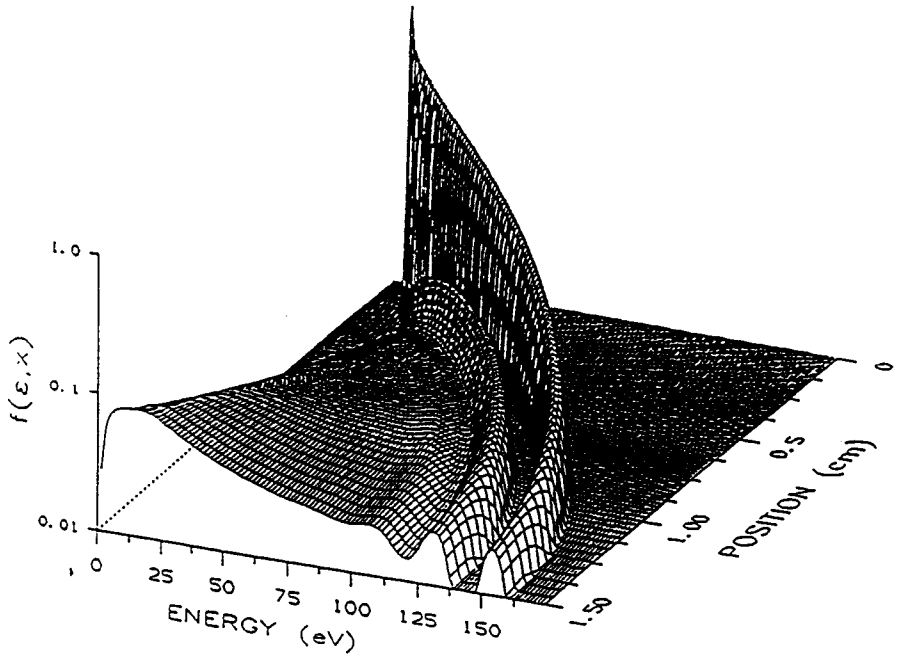

Fig. 2 Electron energy and spatial distribution function in the cathode fall obtained using the monomodal approximation with a gas pressure of 1 Torr. (V_c= 150 V, d_c= 1.3 cm)

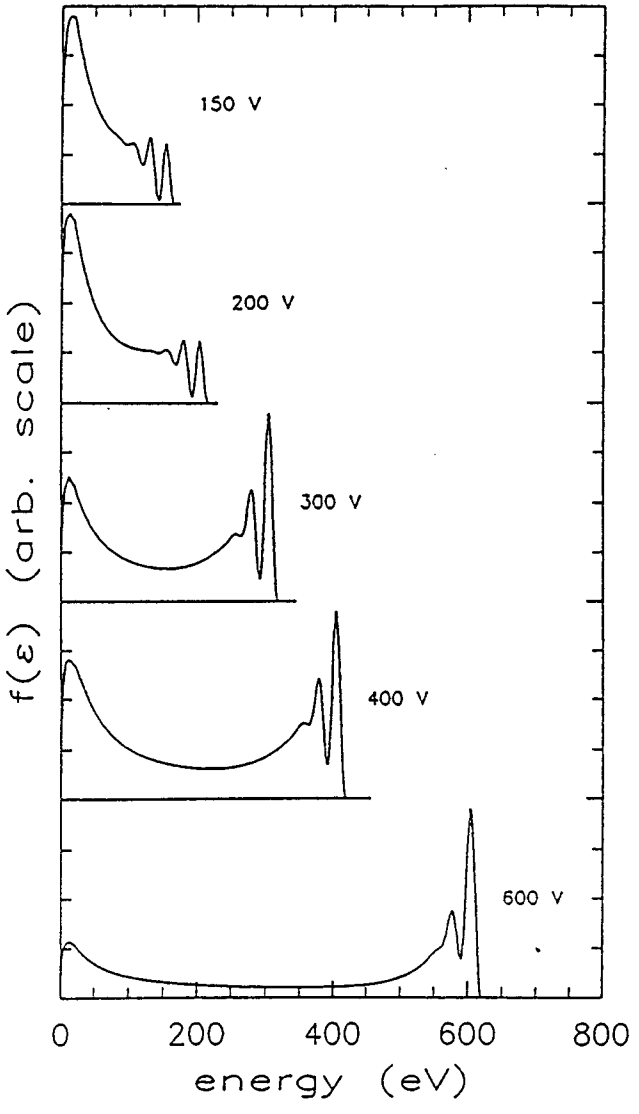

Fig. 6 Electron energy distribution function at the boundary between the cathode fall and the negative glow for various cathode fall voltages, obtained with the monomodal FCT model.

ANALYSIS OF THE CATHODE FALL OF A NORMAL GLOW

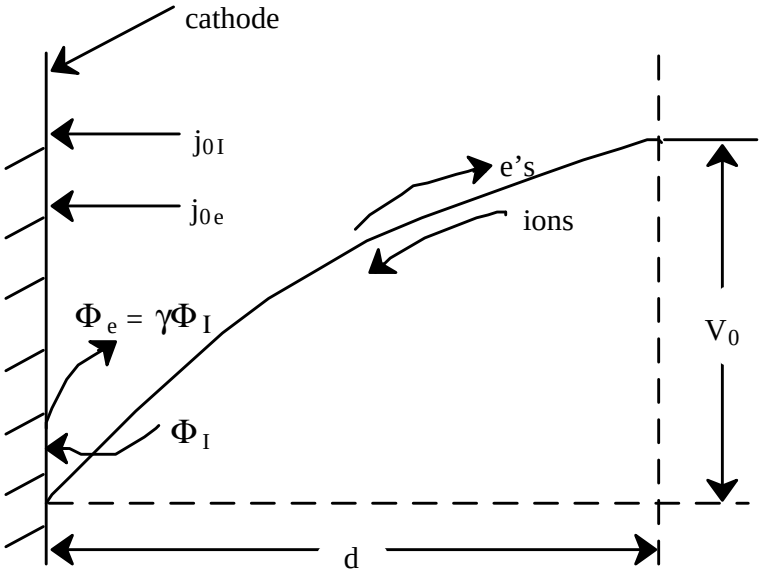

j_{0I} = current density of ions at cathode (A/cm^2)

j_{0e} = current density of e's at cathode (A/cm^2)

V_0 = voltage drop across cathode fall

d = thickness of cathode fall (cm)

Assume $n_e << N_I$ and the $N_I \cong$ constant in the cathode fall. Poisson's equation becomes

$$\frac{\partial E}{\partial x} = \frac{\rho}{\varepsilon_0} = \frac{q(N_I - n_e)}{\varepsilon_0} \approx \frac{qN_I}{\varepsilon_0} \approx \frac{j_I}{\varepsilon_0 v_I} \approx \text{constant}$$

$$j_I = q \cdot v_{drift} \cdot N_I \qquad \text{so that} \qquad N_I = \frac{j_I}{qv_I}$$

Integrating, $E(x) = E_0\left(1 - \frac{x}{d}\right)$ E_0 is electric field at the cathode where E_0 >> E in positive column. The cathode fall voltage drop is $v_0 = \int_0^d -E_0\left(1 - \frac{x}{d}\right)$.

$$V(x) = -E_0\left(x - \frac{x^2}{2d}\right), \quad V_0 = \frac{-E_0 d}{2}, \quad E_0 = \frac{-2V_0}{d}$$

Ions striking the cathode produce electrons by secondary emission with probability γ. The secondary electrons are accelerated back into the plasma producing ionizations in the dark space with Townsend coefficient α.

$$j_0 = j_{0I} + j_{0e} = j_{0I} + \gamma j_{0I} = (1 + \gamma) j_{0I}$$

With $j_{0I} = qN_I v_I$, $v_I = \mu_I E_0$,

$$\left.\frac{\partial E}{\partial x}\right|_{x=0} = \frac{E_0}{d} = \frac{qN_I}{\varepsilon_0}, \qquad N_I = \frac{\varepsilon_0 E_0}{dq} \qquad \text{so} \qquad j_{0I} = q \cdot \left(\frac{\varepsilon_0 E_0}{dq}\right) \cdot \mu_I E_0 = \frac{\varepsilon_0 \mu_I E_0^2}{d}$$

The total current density is then

$$j_0 = (1+\gamma) j_{0I} = (1+\gamma)\frac{\varepsilon_0 \mu_I E_0^2}{d} = \frac{(1+\gamma) 4 \varepsilon_0 \mu_I V_0^2}{d^3}$$

Define j_e = electron current at edge of dark space

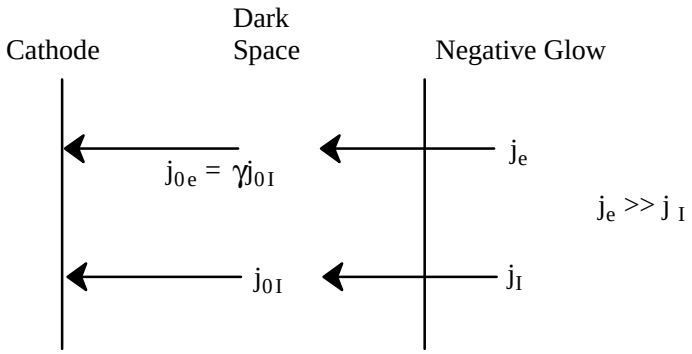

Since $j_e >> j_I$ then

$$j_0 = j_{0e} + j_{0I} = j_e + j_I \approx j_e, \qquad j_{0I} = j_0 - j_{0e} \approx j_e - j_{0e}$$

But $j_{0e} = \gamma j_{0I} = \gamma(j_0 - j_{0e}) \approx \gamma(j_e - j_{0e})$

$$j_{0e} \approx \left(\frac{\gamma}{\gamma+1}\right) j_e$$

The electron current from the cathode through the dark space is amplified by electron impact ionization

$$\frac{dj}{dx} = j \cdot \alpha(x), \qquad \alpha = \text{First Townsend Coefficient}$$

$$j_e = j_{0e} \exp\left(\int_0^d \alpha(x) dx\right)$$

$$= j_{0e} \exp\left(\int_0^d \alpha\left(\frac{E}{N}(x)\right) dx\right)$$

With $j_{0e} \approx \left(\frac{\gamma}{\gamma+1}\right) j_e \approx \left(\frac{\gamma}{\gamma+1}\right) j_{0e} \exp\left(\int_0^d \alpha(x)dx\right)$

$$\ln\left(1+\frac{1}{\gamma}\right) = \int_0^d \alpha\left(\frac{E}{N}(x)\right)dx$$

where $E(x) = E_0\left(1-\frac{x}{d}\right)$, $\quad E_0 = \frac{-2V_0}{d}$

From empirical data,

$$\alpha = A \cdot p \cdot \exp\left(\frac{-Bp}{E}\right)$$

p = pressure (Torr), $\quad A = \frac{1}{\text{cm - Torr}}$, $\quad B = \frac{V}{\text{cm - Torr}}$

So, $$\ln\left(1+\frac{1}{\gamma}\right) = \int_0^d Ap \exp\left(\frac{-Bp}{E_0\left(1-\frac{x}{d}\right)}\right)dx$$

The integral can be solved analytically

$$\ln\left(1+\frac{1}{\gamma}\right) = \left[\frac{A(pd)^2 B}{2V_0}\right] S\left(\frac{2V_0}{(pd)B}\right)$$

where $S(x) = \int_0^x e^{-\frac{1}{y}}dy = xe^{-\frac{1}{x}} - E_1\left(\frac{1}{x}\right)$ $\quad E_1 =$ Exponential Integral.

We can now solve for V_0 in terms of d. A second relationship between v_0 and d is

$$j_0 = \frac{4\varepsilon_0 V_0^2 \mu_I (1+\gamma)}{d^3}$$

We could in principle solve for two of j_0, V_0 and d as a function of the third. Up to now, there is nothing unique to the normal glow.

Define two functions

$$C_1 = \frac{2A}{B \ln\left(1+\frac{1}{\gamma}\right)}, \qquad C_2 = \frac{\ln\left(1+\frac{1}{\gamma}\right)}{\varepsilon_0 A B^2 p^2 (p \cdot \mu_1)(1+\gamma)}$$

where $$1 = \frac{(C_1 V_0)^{1/3}}{(C_2 j_0)^{2/3}} \cdot S\left[\left(\frac{C_1 V_0}{C_2 j_0}\right)^{1/3}\right]$$

Note: Since $\mu_I \sim \frac{1}{\nu_I} \sim \frac{1}{p}$, then $p\mu_I$ is a constant.

If μ_0 is the mobility at pressure p_0, $\mu_I = \mu_0 \frac{p_0}{p}$.

Plot all points satisfying relationship

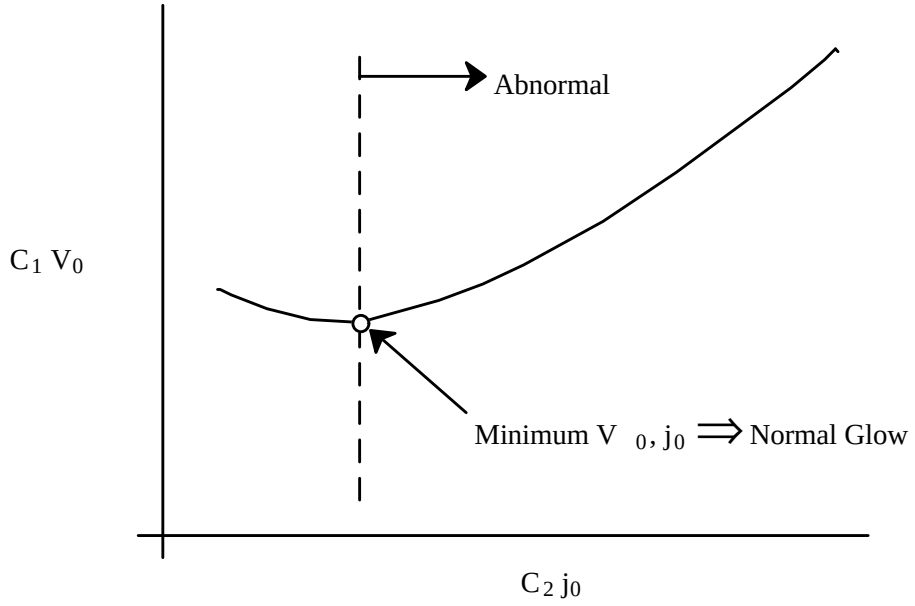

Minimum occurs at: $C_1 V_{NORMAL} = 6.0$

$C_2 j_n = 0.67$

which yields

$$V_{normal} = \frac{3B}{A}\ln\left(1+\frac{1}{\gamma}\right) \equiv \text{ function of gas, metal but not pressure}$$

$$j_n = \left[5.92 \times 10^{-14}\right] \cdot \frac{AB^2(\mu_0 p_0)(1+\gamma)}{\ln\left(1+\frac{1}{\gamma}\right)} \cdot p^2$$

where $A \equiv \frac{1}{cm - Torr}, B \equiv \frac{V}{cm - Torr}, j_n \equiv \frac{A}{cm^2}$

$p \equiv Torr$, $\mu_0 \equiv \frac{cm^2}{v - s}$ is the mobility at p_0

Note that $j_n \sim$ [function of gas type, metal] $\cdot p^2 \sim p^2$

Combine to find $d_n p = \frac{0.82}{A} \ln\left(1 + \frac{1}{\gamma}\right) \equiv$ function gas type and metal

Typical values are $V_n \approx 100\text{-}300$ V, $d_n p \approx 0.25\text{-}2.5$ Torr-cm

$$\frac{j_n}{p^2} \approx 0.005 - 0.5 \frac{mA}{cm^2 \, Torr^2}$$

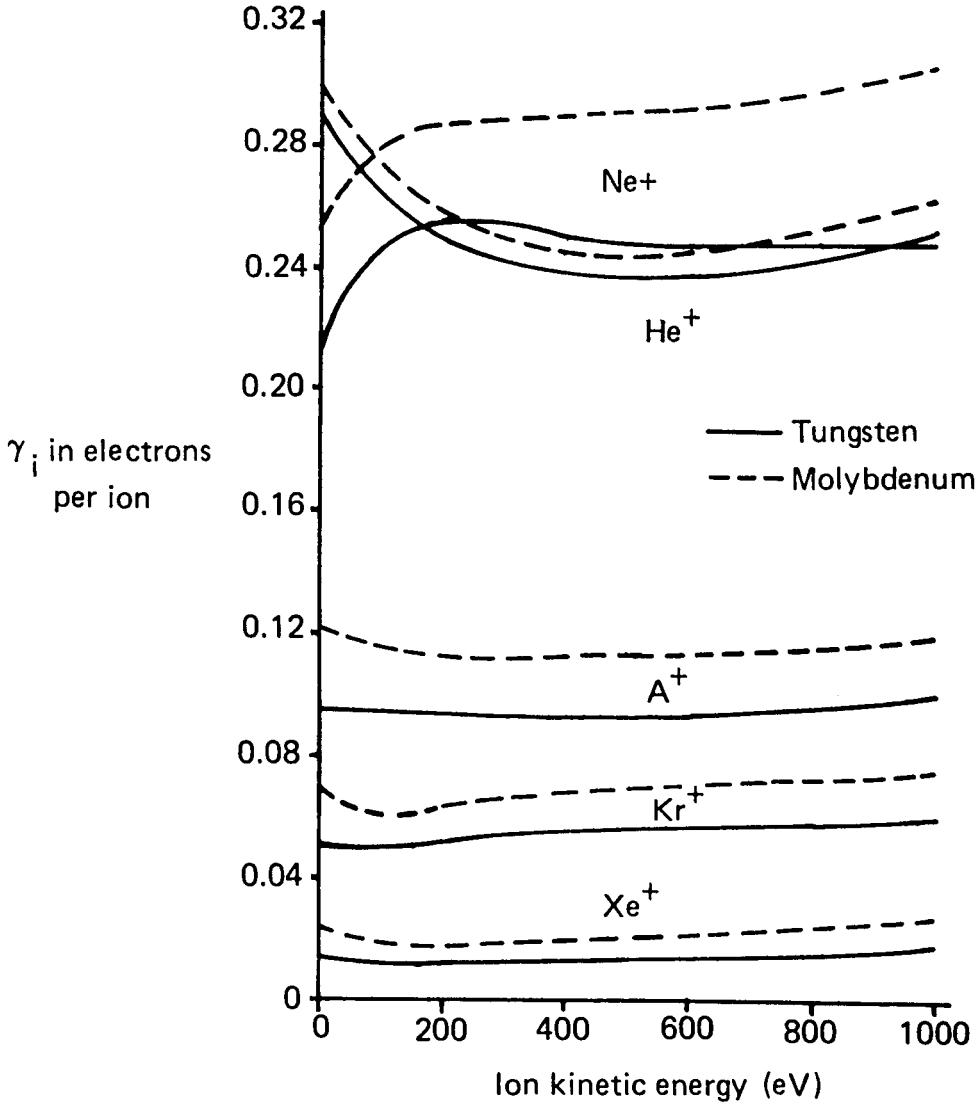

Secondary electron yields γ_i for noble gas ions on atomically clean tungsten and molybdenum (Hagstrum 1956b)

Values of the coefficients A and B in (7.11) for various gases

Gas	$A \frac{1}{cm\ mm\ \mathrm{Hg}}$	$B \frac{V}{cm\ mm\ \mathrm{Hg}}$	*Range of validity X/p*
N_2	12	342	100–600
H_2	5·4	139	20–1000
Air	15	365	100–800
CO_2	20	466	500–1000
H_2O	13	290	150–1000
A	12	180	100–600
He	3	34 (25)	20–150 (3–10)
Hg	20	370	200–600

1 mm Hg = 1 Torr, X/p = E/p = V/cm-Torr

A. von Engle

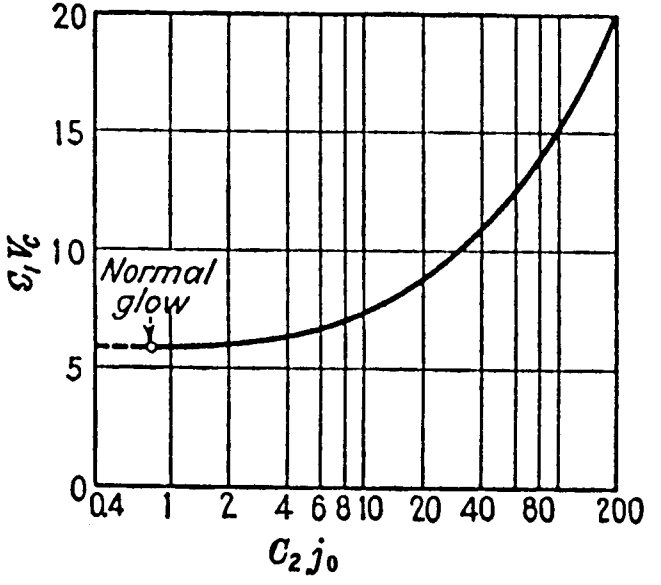

J. Cobine

Cathode fall of potential V_n in volts (17, 28*a*, 162)

Cathode:	*Gas:*	He	Ne	A	H_2	N_2	*Air*	Hg	*Gas*
Cu		177	220	130	214	208	375	450	CO: 484, CO_2: 460
Zn		143	..	119	184	216	280	..	O_2: 354, CO: 480
Hg		143	..	..	337	226	..	340	..
Al		140	120	100	170	180	230	245	Cl_2: 280, O_2: 310
C		..	..	..	280	..	424	475	CO: 525
Mo		109	107	103	..	..	..	..	..
W		..	125	..	..	..	..	305	..
Fe		150	150	165	250	215	270	300	O_2: 290, Xe: 306, K: 80, Cs: 340
Ni		160	140	130	271	200	226	275	..
Pt		165	152	130	276	216	277	..	O_2: 364, Cl_2: 275
K		60	68	64	94	170	180	..	K: 80
Glass		..	..	..	260	..	310	..	..

Reduced thickness of cathode dark space $d_n p$ in cm mm Hg (17, 162)

Cathode:	*Gas:*	He	Ne	A	H_2	N_2	*Air*	Hg	*Gas*
Cu		..	..	..	0·8	..	0·23	0·6	..
Mg		1·45	0·85	..	0·61	0·35	..	..	O_2: 0·25
Hg		..	..	..	0·9	..	..	..	..
Al		1·32	0·64	0·29	0·72	0·31	0·25	0·33	O_2: 0·24
C		..	..	..	0·9	..	..	0·69	..
Fe		1·3	0·72	0·33	0·9	0·42	0·52	0·34	O_2: 0·31, Xe: 0·23
Glass		..	..	..	0·8	..	0·3	..	..

Reduced normal current density j_n/p^2 in 10^{-6} A/cm^2 (mm Hg)^2 (17, 162)

Cathode:	*Gas:*	He	Ne	A	H_2	N_2	*Air*	Hg	*Gas*
Cu		..	..	..	64	..	240	15	..
Au		..	..	..	110	..	570	..	..
Mg		3	5	20	..	..	..	..	..
Al		..	..	..	90	..	330	4	..
Fe, Ni		2	6	160	72	400	..	8	Kr: 43, Xe: 16
Pt		5	18	150	90	380	550	..	..
Glass		..	..	..	~ 80	..	~ 40	..	..

Laser optogalvanic and fluorescence studies of the cathode region of a glow discharge

E. A. Den Hartog, D. A. Doughty, and J. E. Lawler
Department of Physics, University of Wisconsin, Madison, Wisconsin 53706
(Received 15 December 1987; revised manuscript received 4 April 1988)

Various laser diagnostics are used to study the cathode-fall and negative-glow regions of a He glow discharge with a cold Al cathode. The electric field and absolute metastable densities are mapped and the gas temperature is measured over a range of current densities from a near-normal (173 V) to a highly abnormal (600 V) cathode fall. These measurements are analyzed to yield the current balance at the cathode surface, the ionization rate in the cathode-fall region, and the metastable production rate in the cathode-fall and negative-glow regions. The experimental results compare favorably with the results of Monte Carlo simulations. The density and temperature of the low-energy electron gas in the negative glow is determined by combining information from the experiments and Monte Carlo simulations.

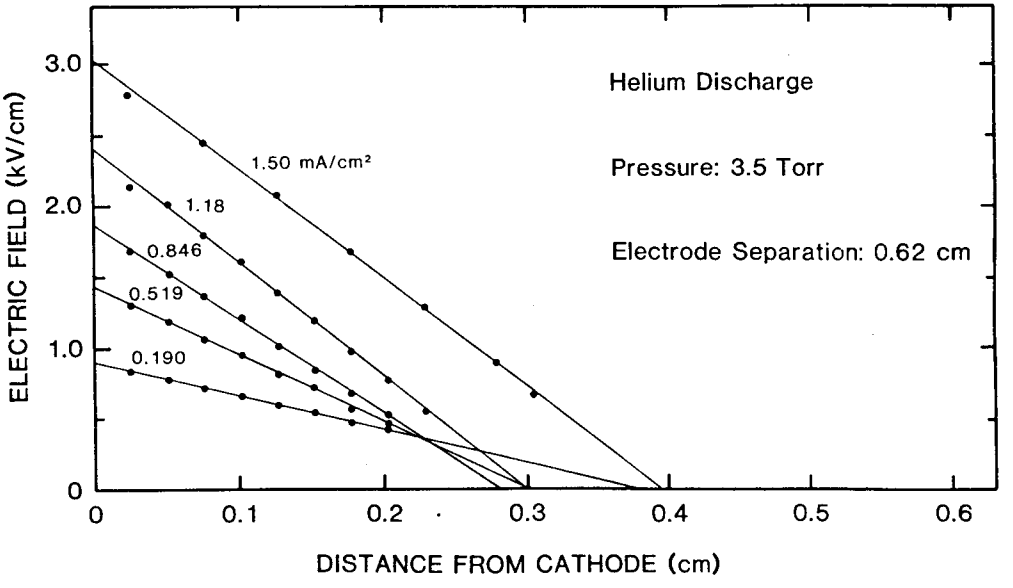

FIG. 4. Electric field as a function of distance from the cathode for five current densities, all at 3.50 Torr. The lines are linear-least-squares fits to the data. The anode corresponds to the right-hand side of the figure.

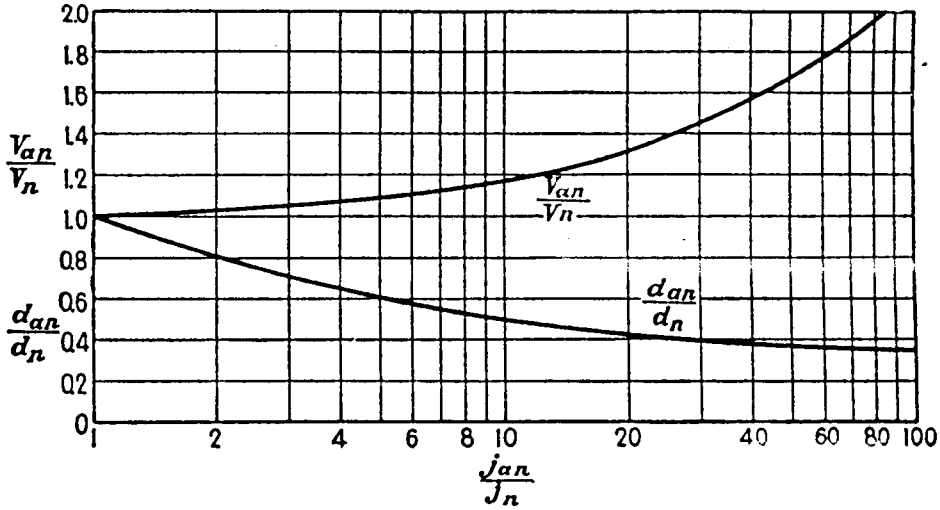

TABLE 8.6.—CONSTANTS FOR THE ASTON ABNORMAL-GLOW EQUATIONS FOR ALUMINUM CATHODE*

Gas	A	B	E	$F \times 10^{-2}$
Air	6.5	0.42	255	23.0
Argon	5.4	0.34	240	29.4
Carbon monoxide	10.0	0.42	255	41.5
Helium	36.0	0.49	255	100.0
Hydrogen	26.5	0.43	144	57.3
Nitrogen	6.8	0.40	230	23.6
Oxygen	5.7	0.49	290	17.6

Current density in 10^{-1} ma./sq. cm. Dark space in centimeters. Gas pressure in 10^{-1} mm. Hg.

*J. J. THOMSON and G. P. THOMSON, "Conduction of Electricity through Gases," Vol. 2, p. 424.

$$d_{an} = \frac{A}{p} + \frac{B}{\sqrt{j}} \qquad V_{an} = E + \frac{F\sqrt{j}}{p} \qquad pd_{an} = A + \frac{BF}{V_{an} - E}$$

J. Cobine

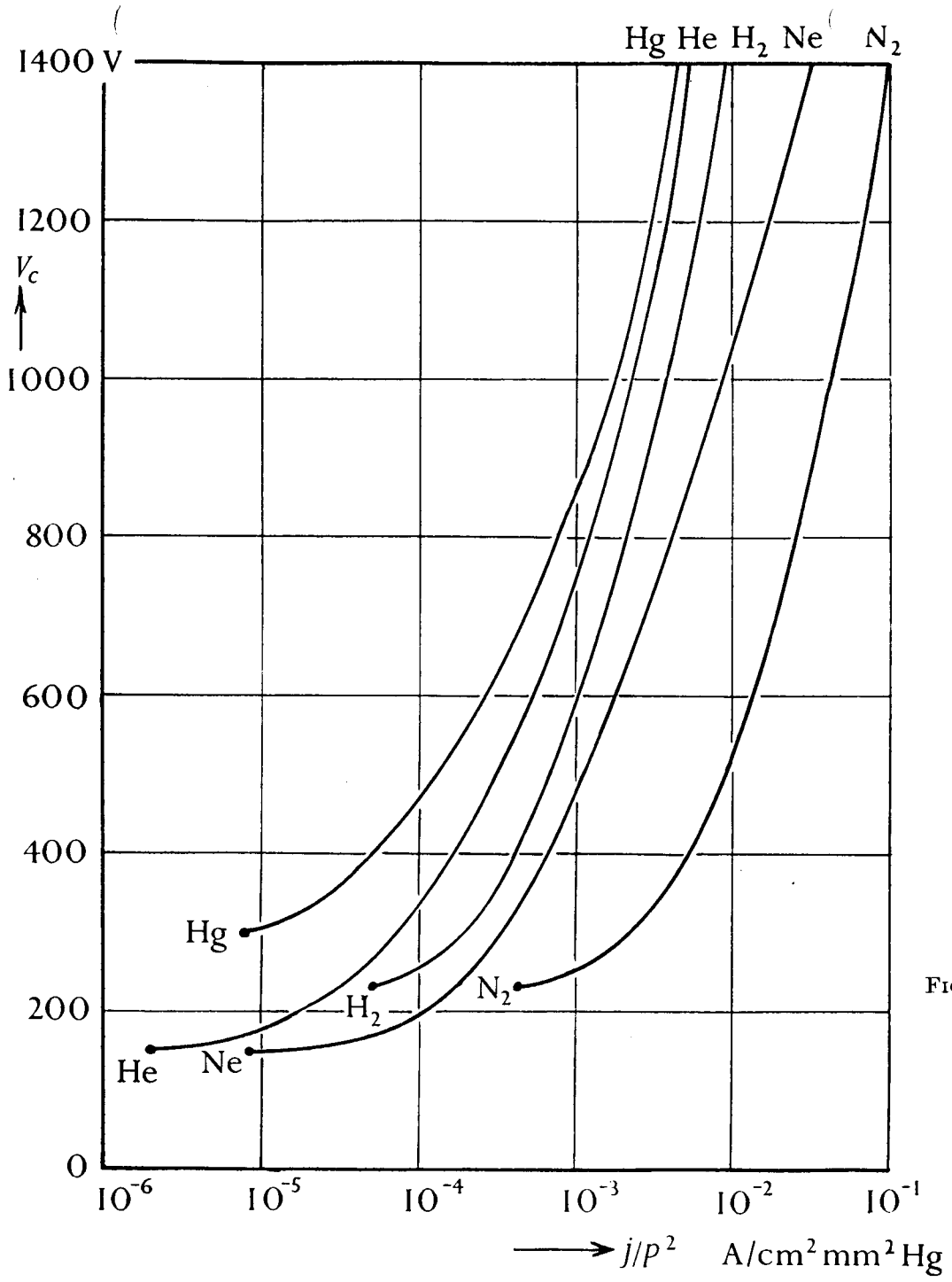

FIG. 118. Abnormal cathode fall V_c dependent on the reduced current density j/p^2 for an Fe cathode in various gases (165).

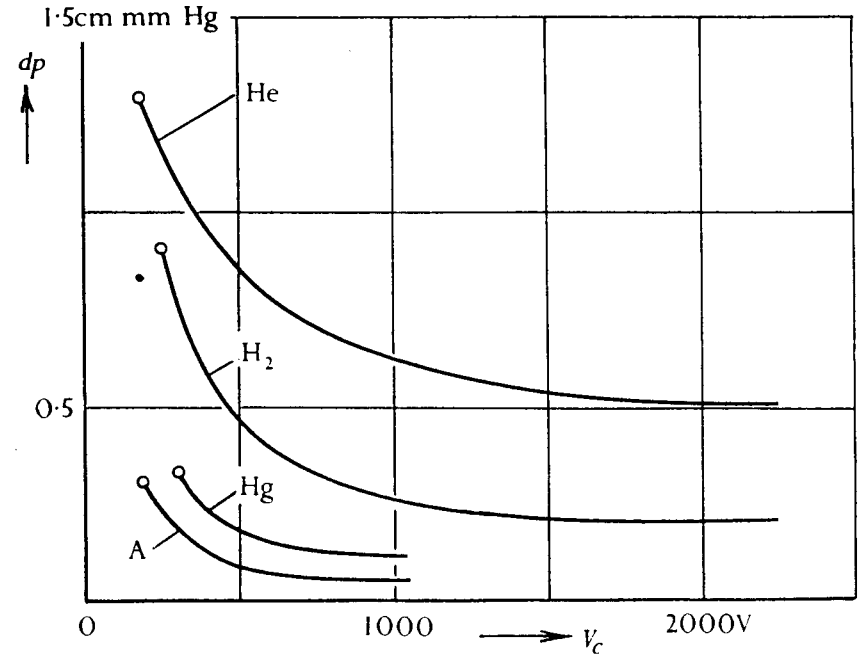

FIG. 117. Reduced thickness of dark space dp as a function of the cathode fall V_c for an Fe cathode in various gases (165).

A. von Engle

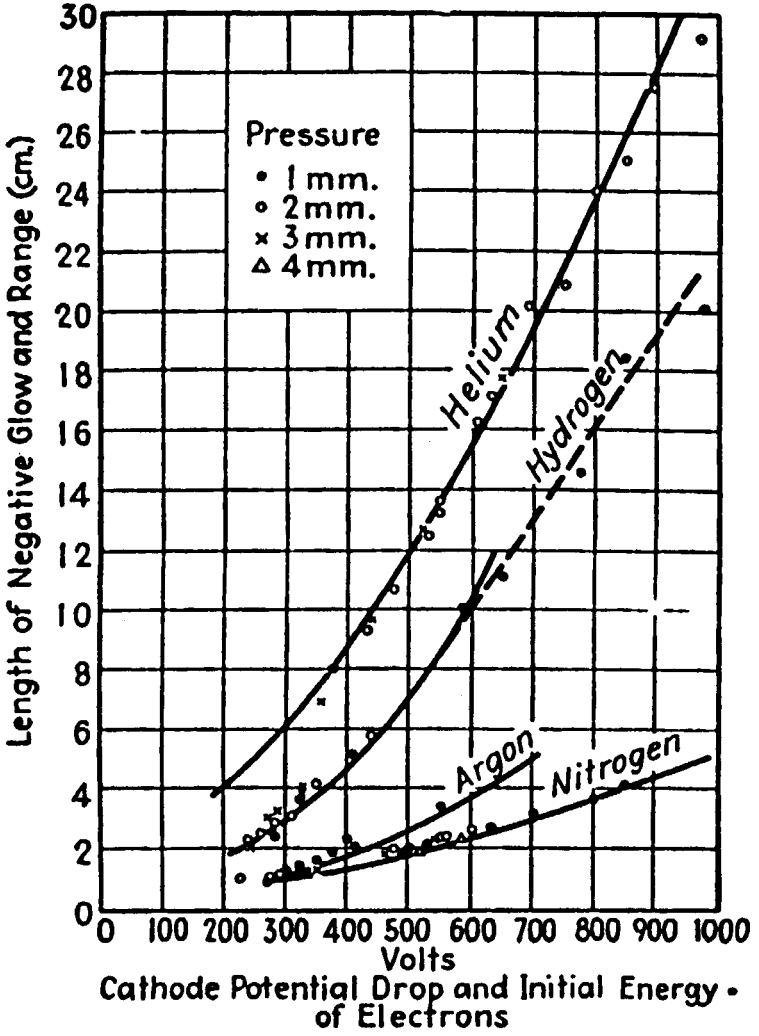

Cobine, "Gaseous Conductors", p. 220

1 W Operation of Singly Ionized Silver and Copper Lasers

B. E. WARNER, D. C. GERSTENBERGER, R. D. REID, J. R. McNEIL, R. SOLANKI, K. B. PERSSON, AND G. J. COLLINS

IEEE JOURNAL OF QUANTUM ELECTRONICS, VOL. QE-14, NO. 8, AUGUST 1978

Abstract—We report a multiline output power of 1 W from the 800.4, 825.5, and 840.4 nm Ag II transitions and 350 mW from the 408.6 nm Ag II transition resulting from pulsed operation of a silver hollow cathode laser. Continuous output of 1 W was obtained in a copper hollow cathode from the 780.8 nm Cu II transition. Design considerations for continuous high-power operation of the hollow cathode discharge are also discussed.

CONTINUOUS wave laser oscillation has been obtained in several nonvolatile metal vapors at numerous wavelengths between 224.3 and 840.4 nm, utilizing the hollow cathode discharge as the laser medium [1]–[8]. The laser tube employed in most of these investigations has been a Schuebel type slotted hollow cathode [9]. This design is simple to construct and reliable in pulsed operation. A cross section of the slotted hollow cathode laser employed in the metal vapor studies is seen in Fig. 1(a). The cathode consists of a 50 cm, 99.99 per-

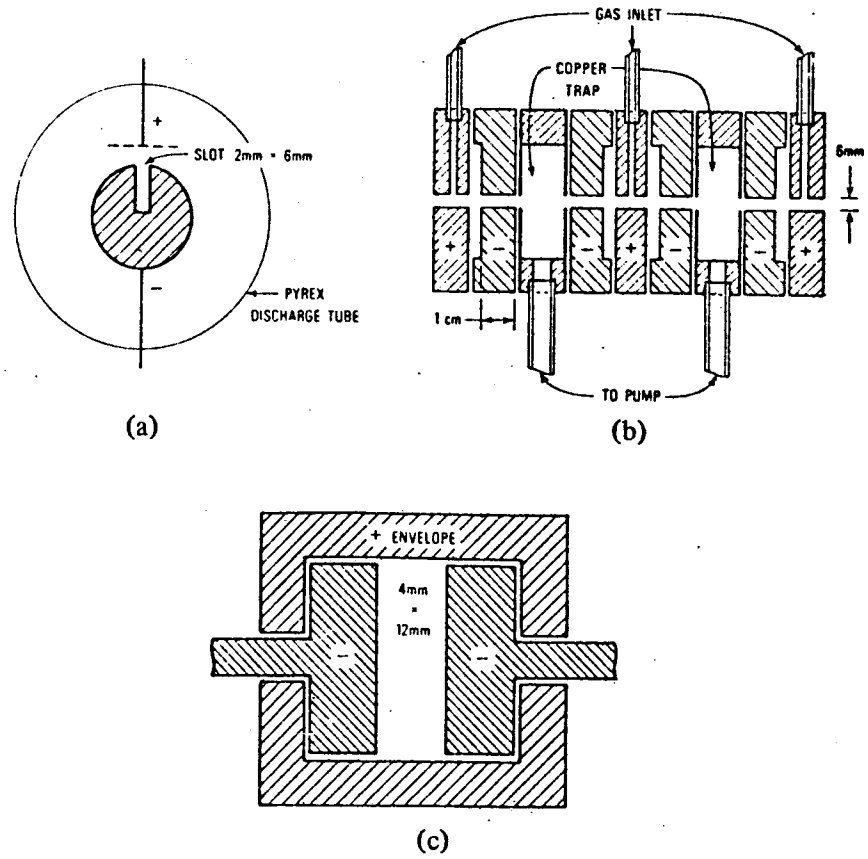

Fig. 1. High power hollow cathode laser designs. (a) Slotted hollow cathode, cross-sectional view; (b) coaxial hollow cathode, longitudinal section view; (c) rectangular hollow cathode, cross-sectional view.

Operating Conditions of the Slotted Hollow Cathode UV Cu^+ Laser

BODO AUSCHWITZ, HANS J. EICHLER, AND WOLFRAM WITTWER

Abstract—The performance of the UV Cu^+ laser in a slotted hollow cathode has been investigated experimentally. The laser power dependent on discharge current, neon pressure, cathode length, and laser mirror transmission has been measured. The optimum neon pressure was found to be 13 mbar. Single-pass gains about 8 percent · m^{-1} have been evaluated. The observed changes in the slot shape by sputtering during 100 h of operation are briefly discussed. The experimental results are compared to a recent sputtering theory and reasonable agreement is found. The sputtering theory, the spontaneous intensity measurements, and the evaluated gains are used to calculate the number densities of the 5*s* Cu^+ levels. Laser power is calculated from single-pass gains and agreement with experimental results is obtained.

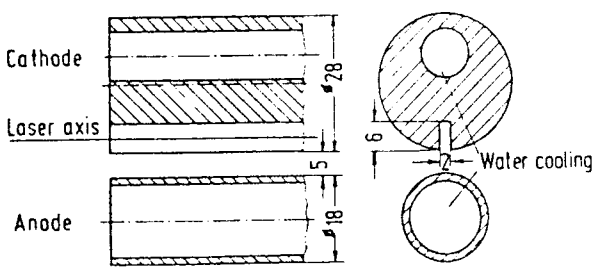

Fig. 1. Discharge arrangement.

Operating Characteristics of UV and IR Hollow-Cathode Silver, Gold and Copper Ion Lasers*

K. Jain

IBM Research Laboratory, San Jose, CA 95193, USA

S. A. Newton**

Edward L. Ginzton Laboratory, Stanford University, Stanford, CA 94305, USA

Received 2 March 1981/Accepted 10 April 1981

Abstract. Operating characteristics of silver, gold and copper vapor hollow-cathode lasers are presented. Dependence of the output power, gain and threshold current on the cathode length, composition of the buffer gas, and mirror transmission is described. Studies of multicomponent hollow cathodes which produce laser lines of several elements simultaneously are also presented.

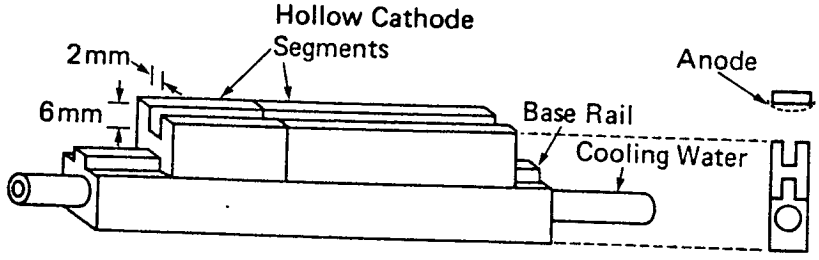

Fig. 3. Segmented slot hollow cathode. The total hollow cathode length is varied by placing segments of various lengths on the base rail

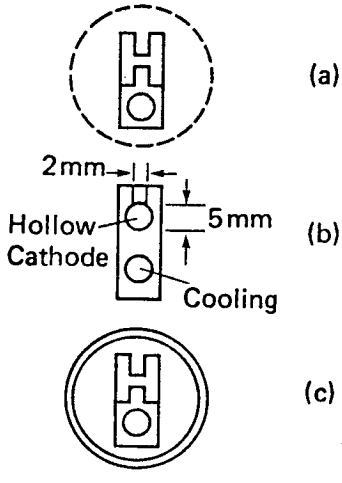

Fig. 6a–c. Various anode-cathode structures: (a) slotted and segmented hollow cathode with a circular mesh anode; (b) a flute cathode; (c) same as (a), except with a solid tubular anode

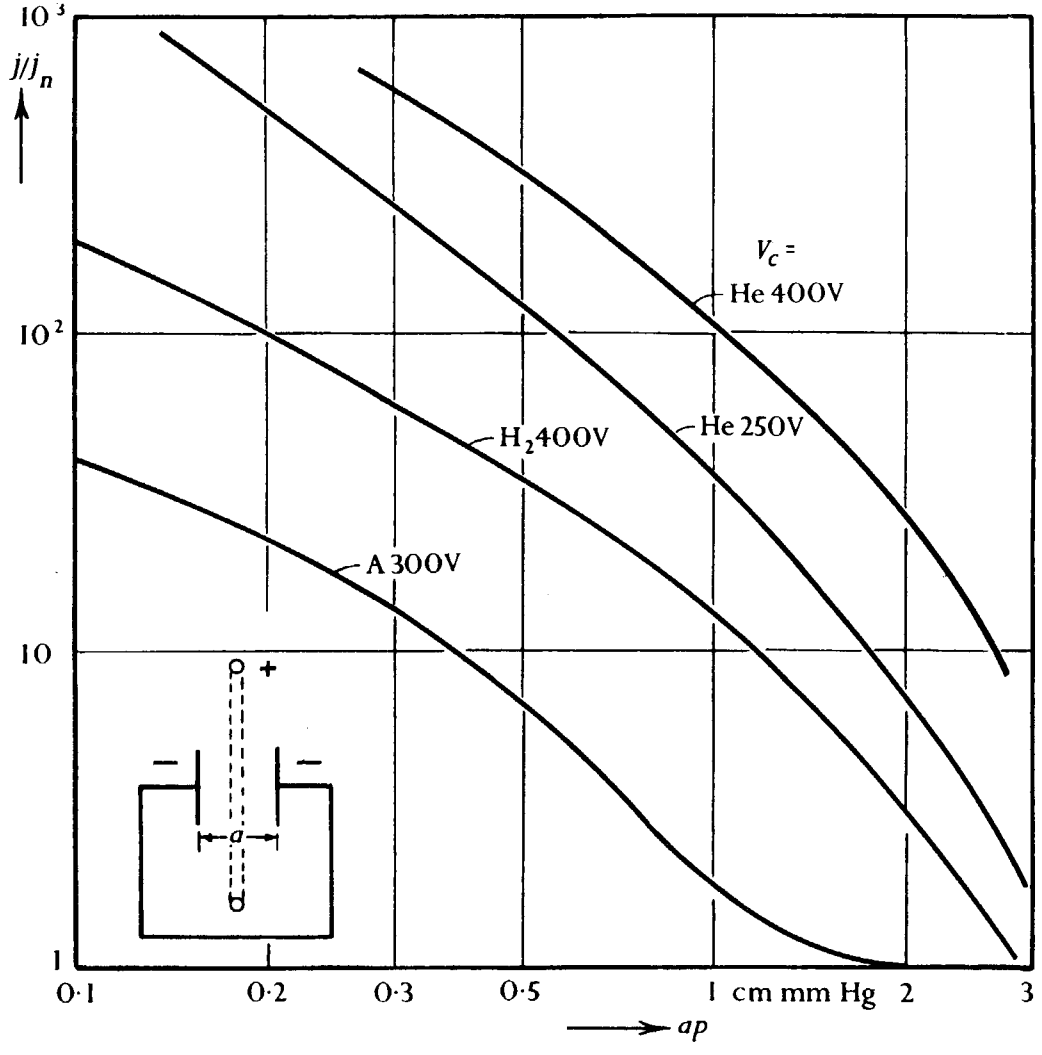

FIG. 121. Hollow cathode glow discharge. Reduced current density j/j_n as a function of the reduced inter-cathode distance ap for various gases and cathode falls V_c using plane Fe cathodes (167).

A. von Engel, "Ionized Gases", p. 237

Analysis of a Cu–Ne hollow cathode glow discharge at intermediate currents

J. Phys. D: Appl. Phys., 17 (1984) 953–968.

E M van Veldhuizen and F J de Hoog

Physics Department, University of Technology, P.O. Box 513, 5600 MB Eindhoven, The Netherlands

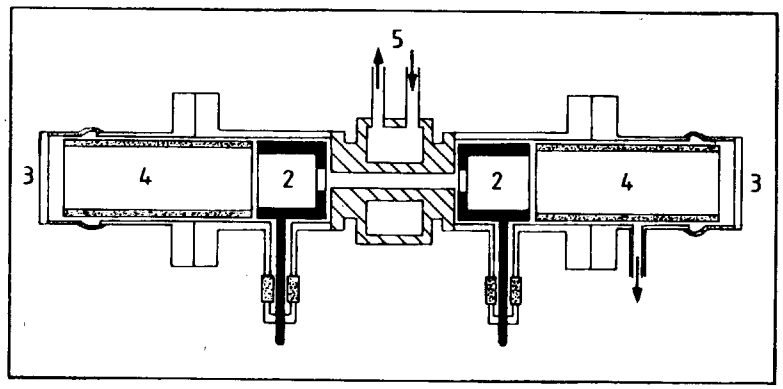

Figure 1. Sketch of the hollow cathode: 1, cathode made out of OHFC-copper; 2, anodes; 3, quartz viewing ports; 4, quartz insulating tubes; 5, cooling water.

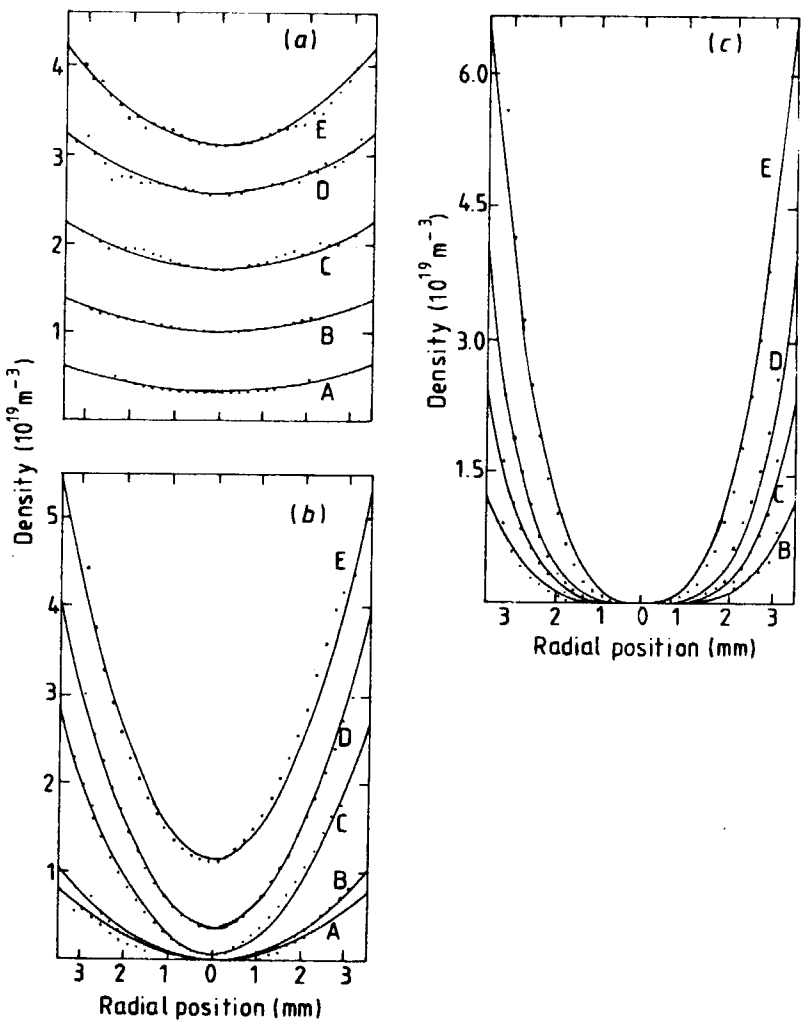

Figure 6. Measured copper ground state densities obtained with self-absorption at different pressures: (*a*) 260 Pa; (*b*) 650 Pa; (*c*) 1040 Pa; and currents: A 0.1 A; B 0.2 A; C 0.4 A; D 0.6 A; E 1.0 A.

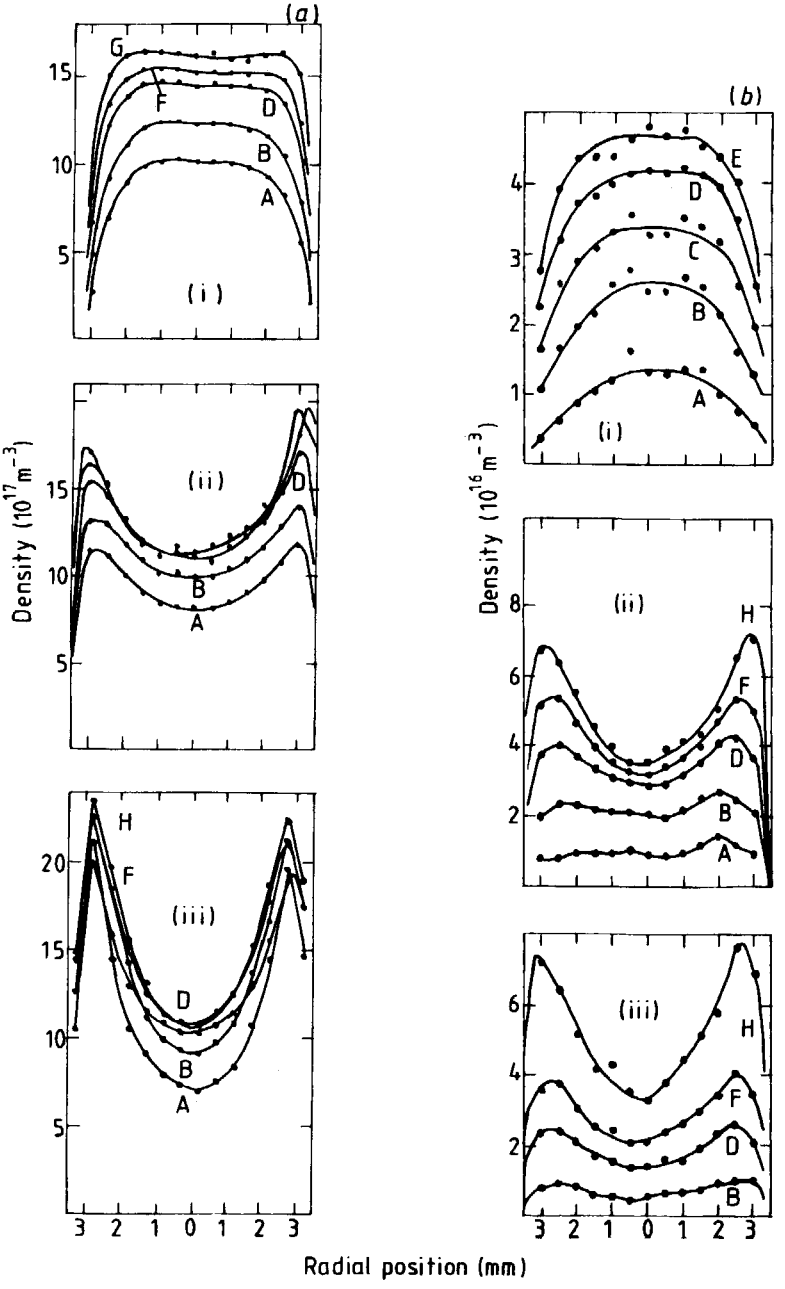

Figure 7. Densities of excited states obtained with laser light absorption, (*a*) 3s $[3/2]_2$ (metastable) and (*b*): 3p $[5/2]_3$ at different pressures: (i) 260 Pa; (ii) 650 Pa; (iii) 1040 Pa; and currents: A 0.1 A; B 0.2 A; C 0.3 A; D 0.4 A; E 0.5 A; F 0.6 A; G 0.8 A; and H 1.0 A.

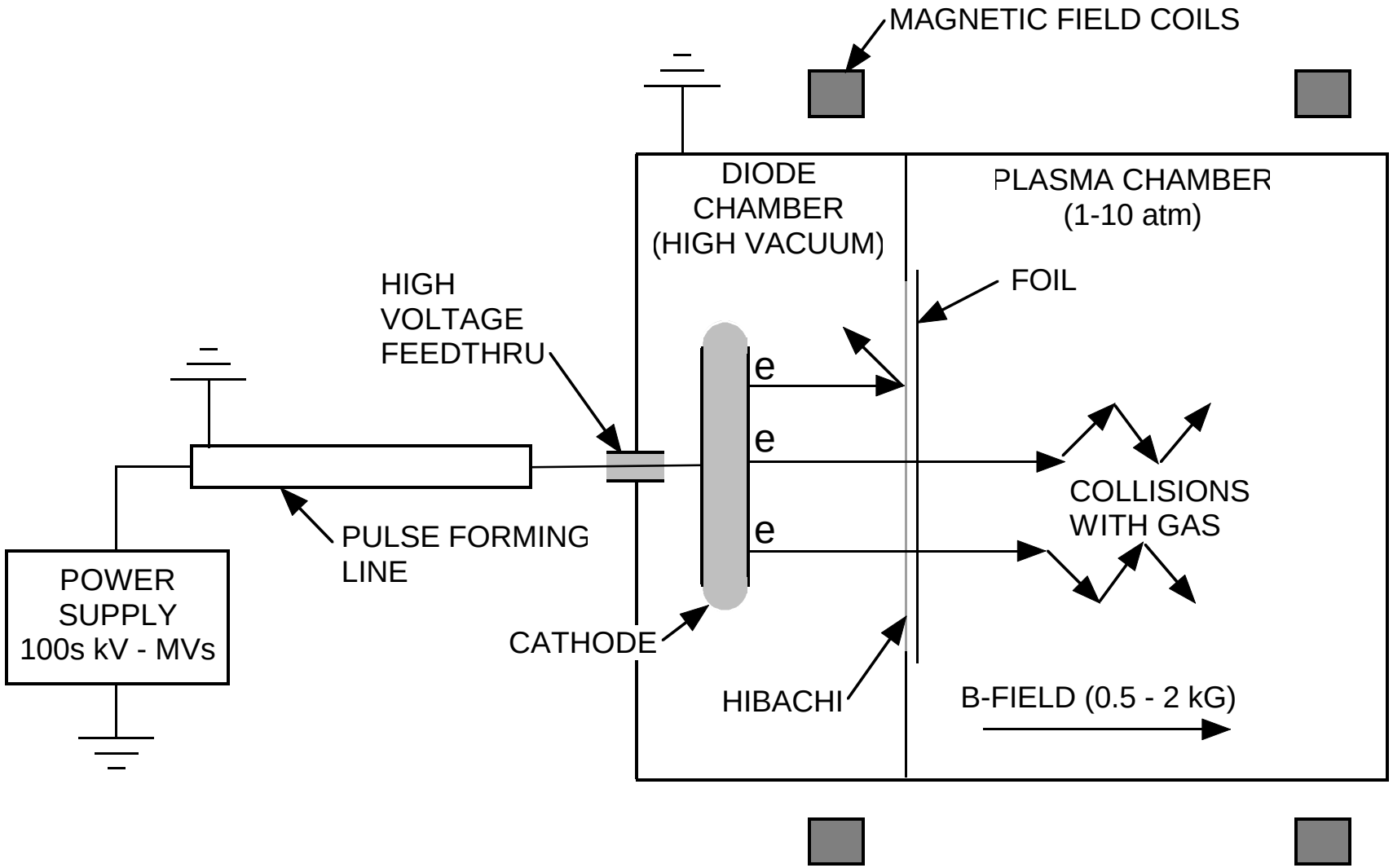

E-BEAM SCHEMATIC

The key issues for KrF are being addressed with the Electra and Nike Lasers at NRL

Electra:

> 400 J laser light
500 keV/100 kA/100 nsec
5 Hz; 100,000 shots (5 Hrs)

Develop technologies for:
- *Rep-Rate,*
- *Durability,*
- *Efficiency,*
- *Cost*

Nike:

3-5 kJ laser light
750 keV, 500 kA, 240 nsec
single shot

E-beam physics on full scale diode
Laser-target physics

http://wwwppd.nrl.navy.mil/branches/6730/6730.html
http://other.nrl.navy.mil/Electra/Global/Sethian.KrFTutorial.APS.DPP.2002/Sethian.KrFTutorial.APS.DPP.2002001.html

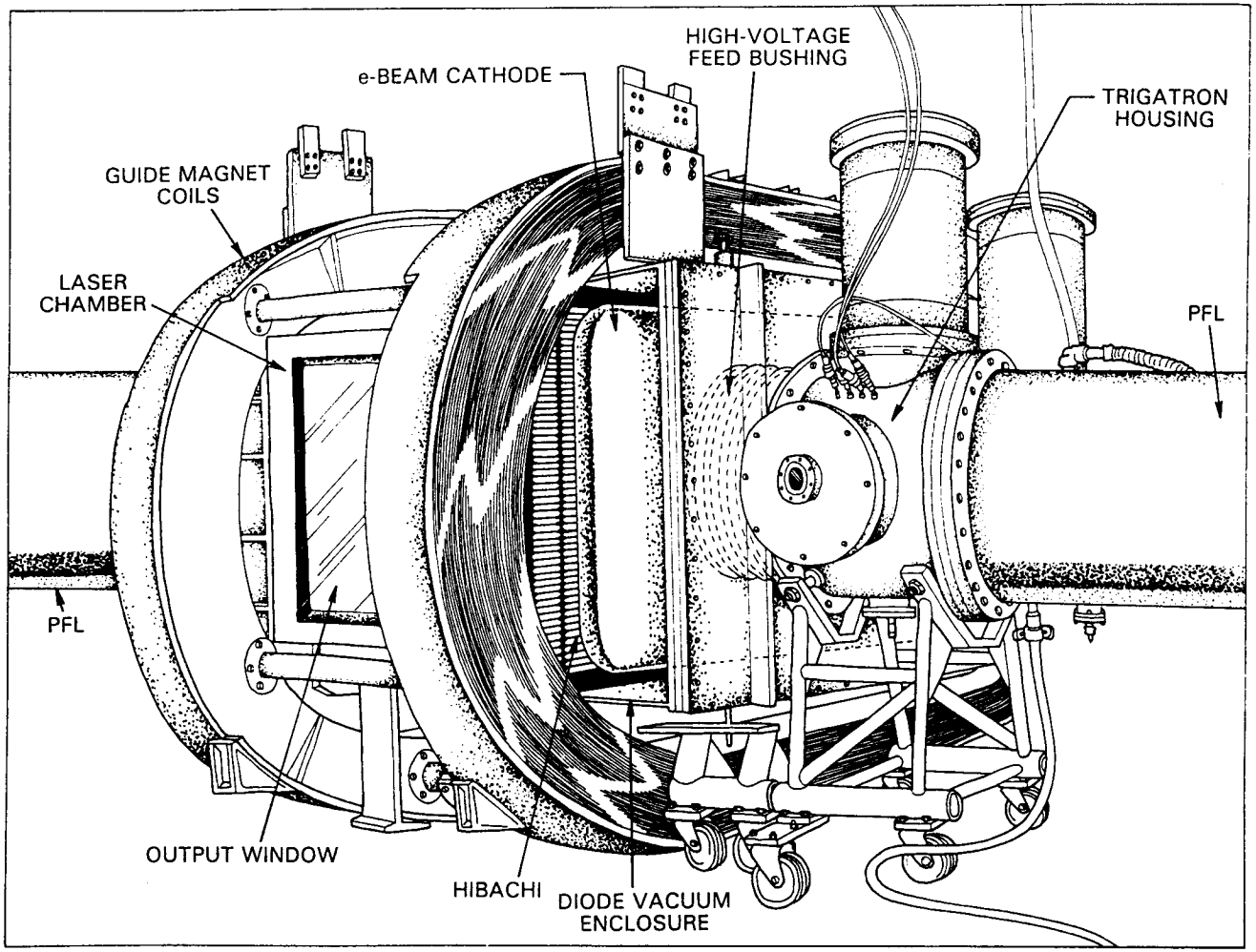

Fig. 8. Assembly drawing of the LAM. Shown are the laser chamber, the output window, the guide magnets, the water dielectric PFLs, and the *e*-gun assembly. This amplifier is representative of the amplifiers used in the Aurora chain. It is symmetrical in that it uses two sets of PFLs and two *e* guns in a double-sided pumping arrangement.

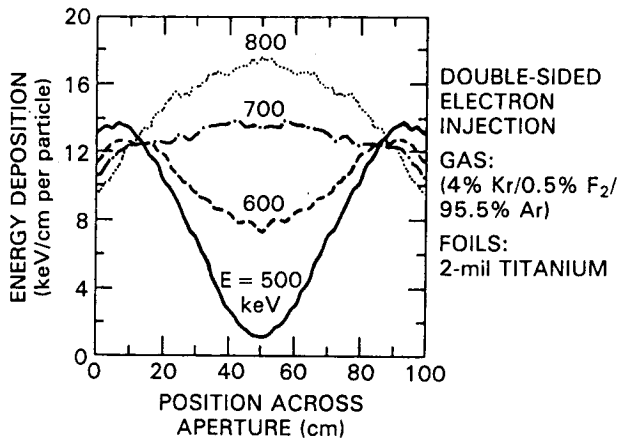

Fig. 10. Sample Monte Carlo method calculations[36] for the *e*-beam-energy deposition profile in the LAM laser gas plotted as a function of horizontal distance along the *e*-beam centerline with electron energy as a parameter. Electron beams are injected from both the right and left, resulting in a uniform energy deposition profile across the laser aperture for an optimum electron energy of ~675 keV. Similar calculations done with an imposed magnetic guide field show improvements in the deposition at the vertical edges of the *e* beam. The gas mixture is 4% krypton, 95.5% argon, and 0.5% F_2 at a total pressure of 1.75 atm, and the foils are 50-μm (2-mil)-thick titanium.

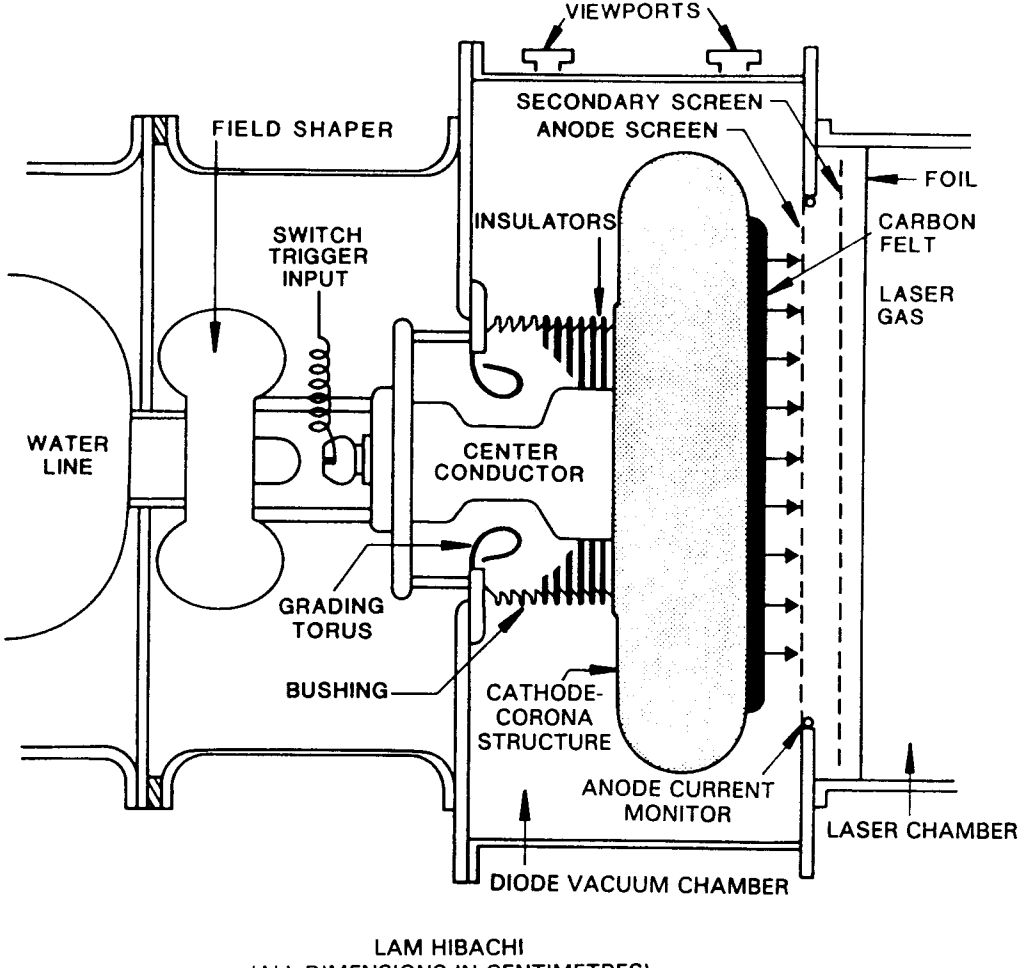

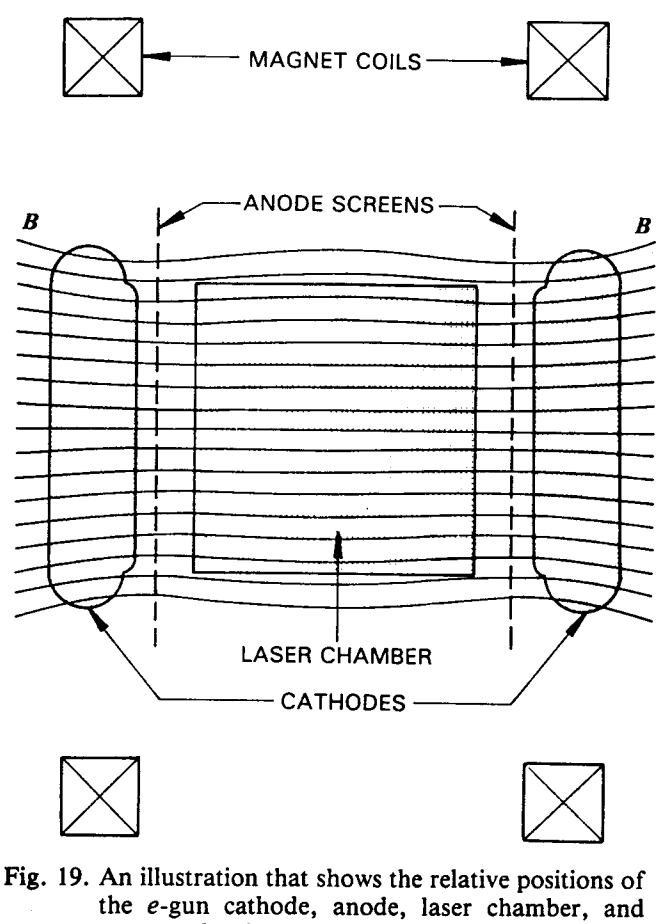

Fig. 19. An illustration that shows the relative positions of the *e*-gun cathode, anode, laser chamber, and magnets for the Aurora LAM. The magnetic field lines are tilted slightly at the cathode faces.

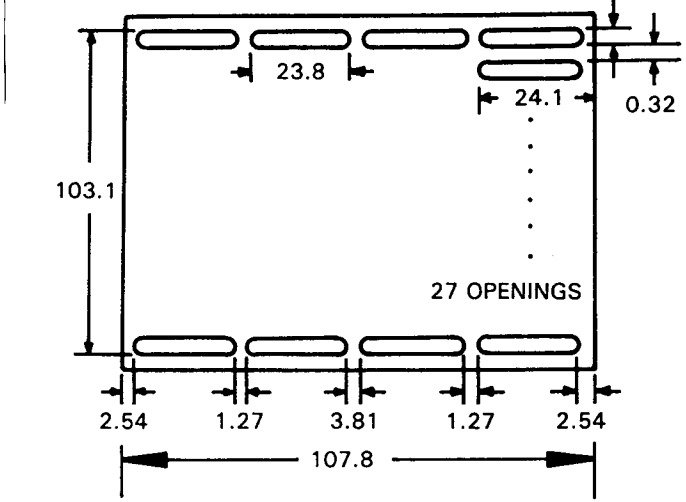

Fig. 21. The slot pattern for the LAM hibachis. Each LAM *e* gun uses two of these foil support structures placed side by side. The long dimension of the hibachi slots is oriented along the optical axis (horizontal slots).

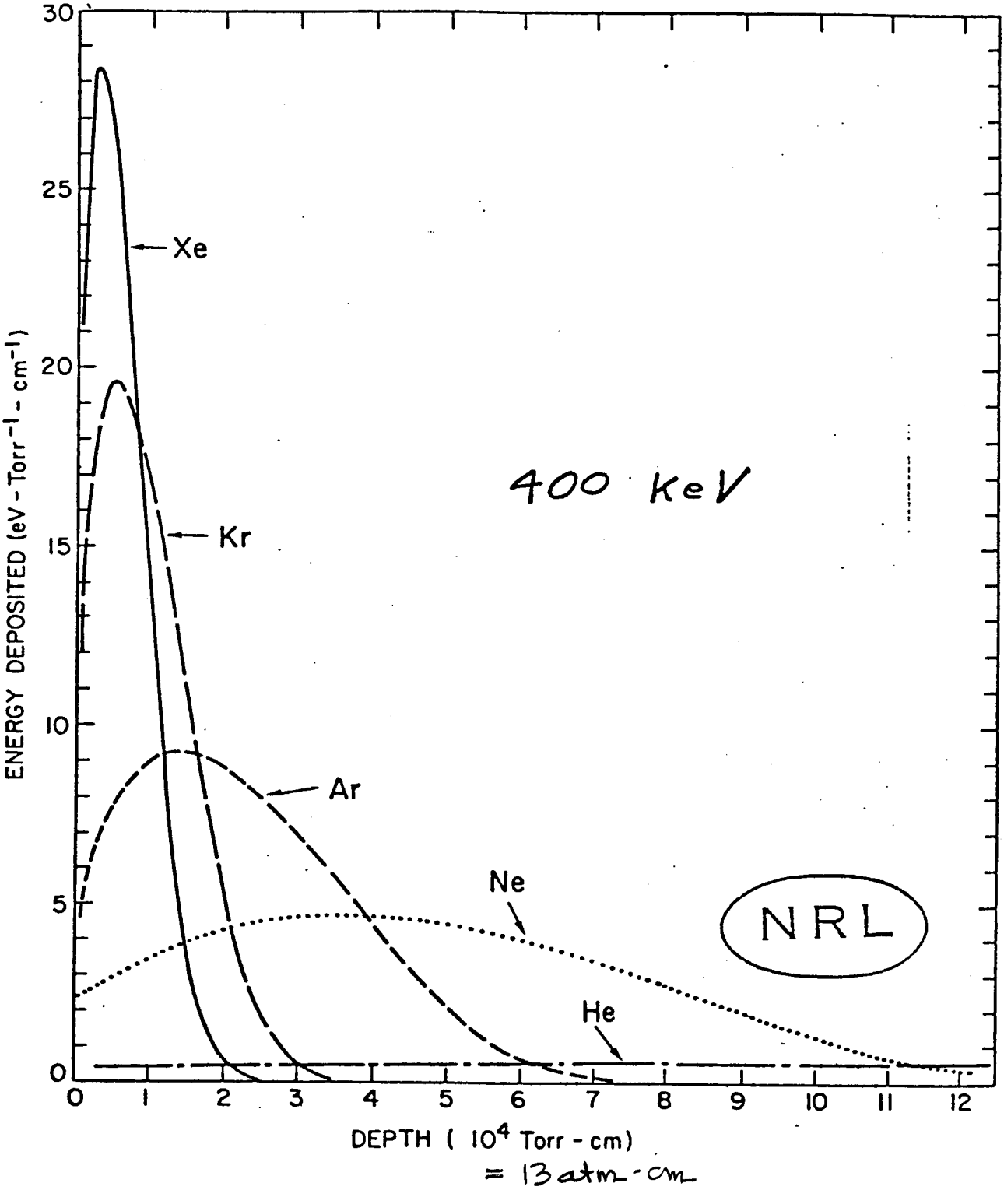
30
25
20
15
10
5
0
ENERGY DEPOSITED (eV - Torr^{-1} - cm^{-1})
Xe
Kr
Ar
Ne
He
400 KeV
NRL
0
1
2
3
4
5
6
7
8
9
10
11
12
DEPTH (10^4 Torr - cm)
= 13 atm - cm

Table 1. $A(E)$, $\Gamma(E)$ and $T_0(E)$ for He, N_2 and O_2*†

E	A	Γ	T_0
	He (I = 24·5 eV)		
50	0·0331	14·5	−10·9
100	0·0787	10·1	−13·8
200	0·0275	13·2	− 4·30
300	0·0175	14·3	− 2·19
500	0·0141	14·2	− 3·85
1000	0·00530	16·3	− 2·57
2000	0·00355	16·2	− 5·11
	N_2 (I = 15·6 eV)		
50	0·148	20·6	−10·7
100	0·177	12·8	−0·517
200	0·116	11·9	2·54
300	0·0867	12·5	2·40
500	0·0636	12·6	2·28
1000	0·0312	14·1	3·35
2000	0·0180	13·8	3·03
	O_2 (I = 12·1 eV)		
50	0·581	11·9	−20·7
100	0·411	13·9	−16·3
200	0·126	16·7	− 2·19
300	0·0836	16·9	− 0·519
500	0·0698	17·3	− 0·295
1000	0·0289	19·2	0·938
2000	0·0196	19·2	0·460

* $A(E)$ is in units of 10^{-16} cm²/eV, $\Gamma(E)$ and $T_0(E)$ are in eV.

† These values are obtained by fitting OPAL *et al.* (1971) data using equation (4) with $\kappa = 1$.

A. E. S. GREEN and T. SAWADA

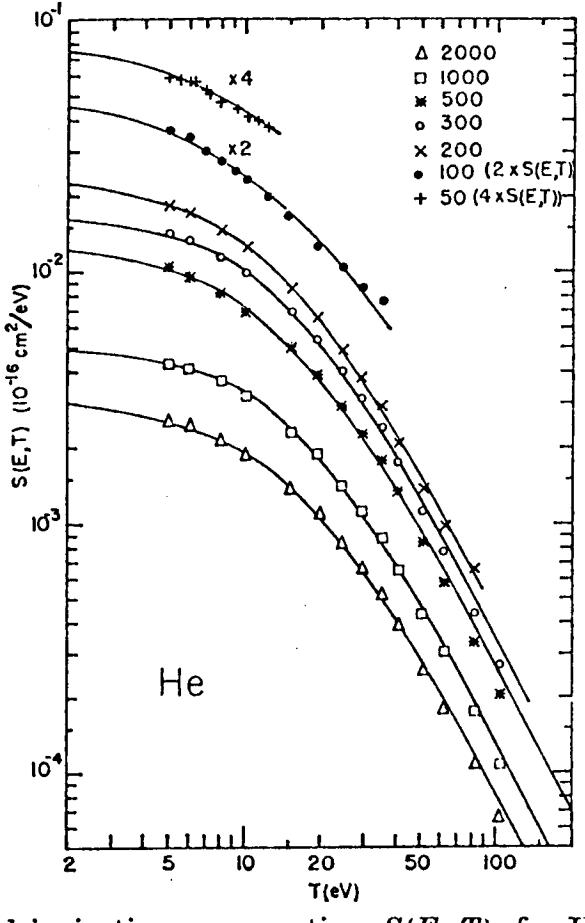

Fig. 1. Differential ionization cross section, $S(E, T)$, for He at various energies as indicated. Data points are selected from the data of OPAL *et al.* (1971), and the fits using equation (4) with $\kappa = 1$ are shown by the curves.

W Values

A "W" value is the energy deposition in a gas required to produce "an event" such as ionization or excitation. A large W-value implies that the process is less efficient than one with a small W-value because more energy is required to produce the event. The W-value is used to denote, for example, the rate of ionization or excitation in electron beam pumped plasmas. The rate of ionization is

$$\frac{d[e]}{dt} = \frac{P\left(\frac{W}{cm^3}\right)}{W\left(J\left[or\ eV\right]\right)} \frac{ionizations}{cm^3 - s}$$

where P is the power deposition in the plasma.

In general, for power deposition by high energy electron beams [V(e-beam) > 5-10 kV] the W-value is fairly constant and scales as

$$W_{ionization} \approx 1.8 - 2\ x\ ionization\ potential$$
$$W_{excitation} \approx 2x\ W_{ionization}$$

Since $W_{ionization} < W_{excitation}$ one gets more ionizations in the slowing of a high energy electron beam than excitations. This results from the energy degradation being monotonically from higher energies to lower energies where ionization cross sections are larger. For high energy beams slowing in rare gases,

	Ionization Potential (eV)	$W_{ionization}$ (eV)	$W_{excitation}$ (eV)	Ionization / Excitation	"G-value" (Ionizations for 100 eV of deposited energy)
He	24.6	46.8	72.0	1.54	3.53
Ne	20.1	36.5	81.8	2.24	3.96
Ar	15.8	27.3	53.8	1.97	5.52
Kr	14.0	23.6	44.5	1.89	6.48
Xe	12.1	20.9	34.8	1.67	7.66

In a gas discharges, electrons are being accelerated from lower energies to higher energies, and so encounter excitation cross sections before ionization cross sections. The rates of excitation are therefore larger than for ionization. For example, for a gas discharge in xenon,

E/N (Td)	Ionization / Excitation
50	0.014
100	0.08
150	0.16
200	0.22

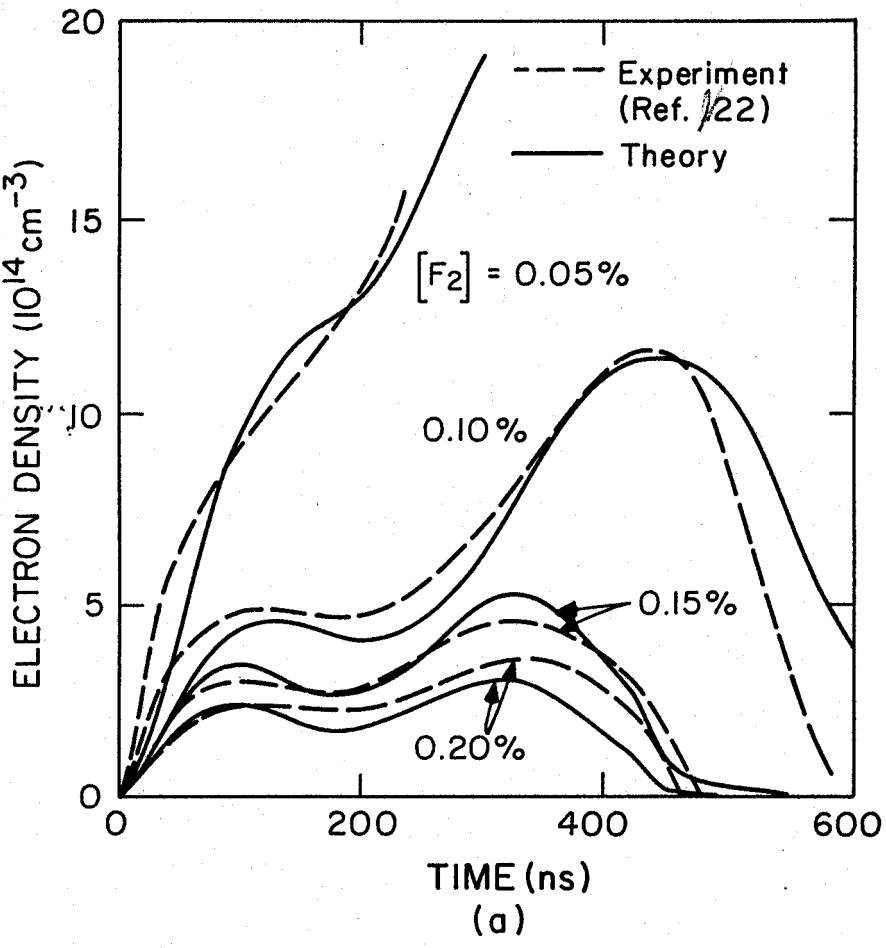
Experiment (Ref. 22)
Theory
[F2] = 0.05%
0.10%
0.15%
0.20%
ELECTRON DENSITY (10^14 cm^-3)
TIME (ns)
0
5
10
15
20
0
200
400
600

(a)

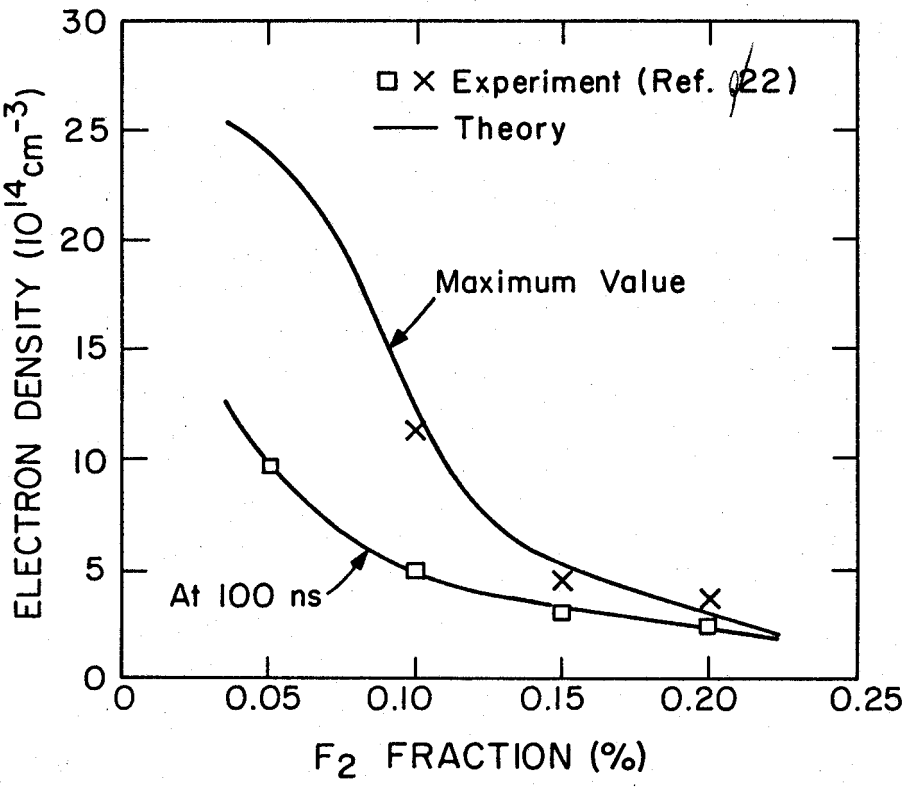
□ × Experiment (Ref. 22)
Theory
Maximum Value
At 100 ns
ELECTRON DENSITY (10^14 cm^-3)
F2 FRACTION (%)
0
5
10
15
20
25
30
0
0.05
0.10
0.15
0.20
0.25

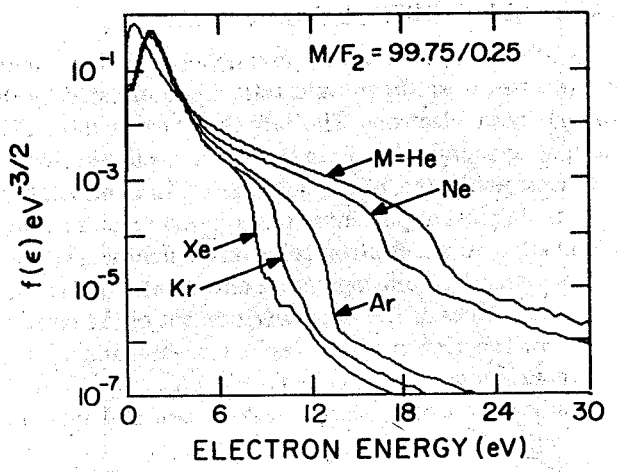

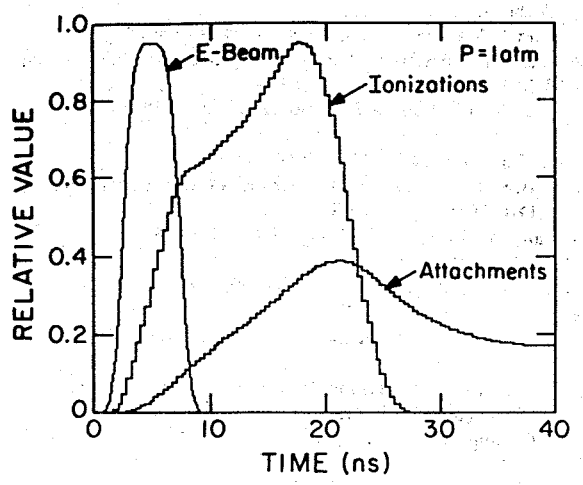

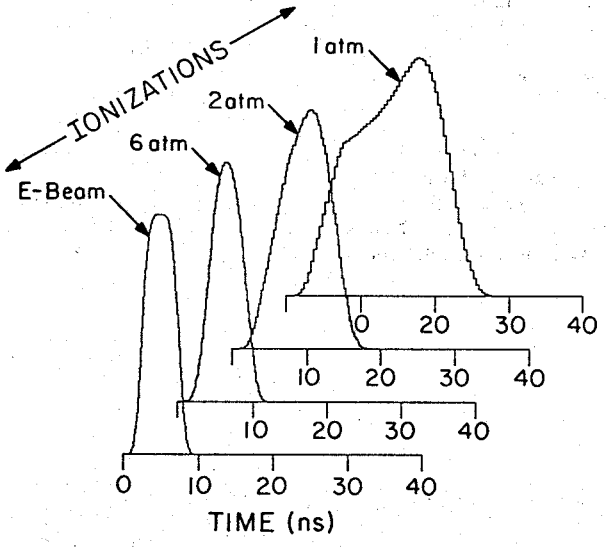

FIG. 9. The time dependence of electron collisions following a 500 keV electron beam pulse (5-ns FWHM) in an $Ar/Kr/F_2 = 90/10/0.25$ mixture. (top) Ionization and attachment events in a 1-atm mixture. Attachment cross sections are important only for $\epsilon < 2$ eV. Since thermalization is slow once electrons fall below the electronic thresholds of the buffer gas, there is a disparity in time between when ionizations and attachments occur. (bottom) Ionization events at pressures of 1, 2, and 6 atm. The *e*-beam response time at 6 atm is sufficiently small that ionizations track the *e*-beam current.

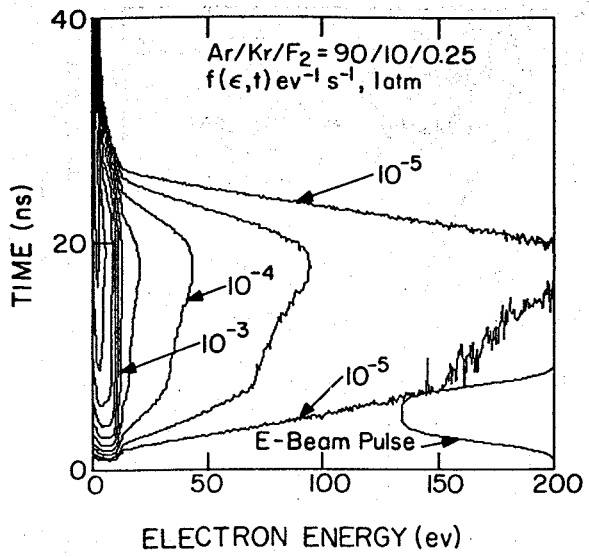

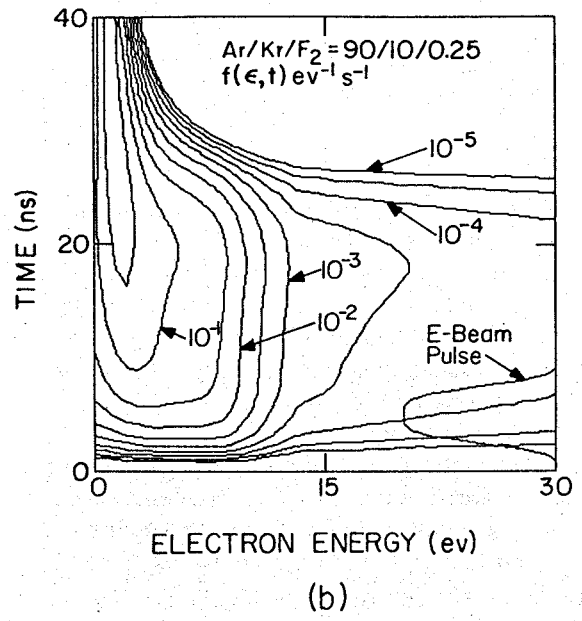

FIG. 6. The electron spectrum as a function of energy and time ($eV^{-1}s^{-1}$) for a 500-keV *e*-beam pulse (5-ns FWHM) slowing in a 1-atm $Ar/Kr/F_2 = 90/10/0.25$ mixture; (a) $0 \leqslant \epsilon \leqslant 200$ eV, and (b) $0 \leqslant \epsilon \leqslant 30$ eV. The time dependence of the *e*-beam pulse is at the bottom right in each figure. The *e*-beam response time for these conditions is $\simeq 20$ ns. Note the transition to thermalization at 20–30 ns.

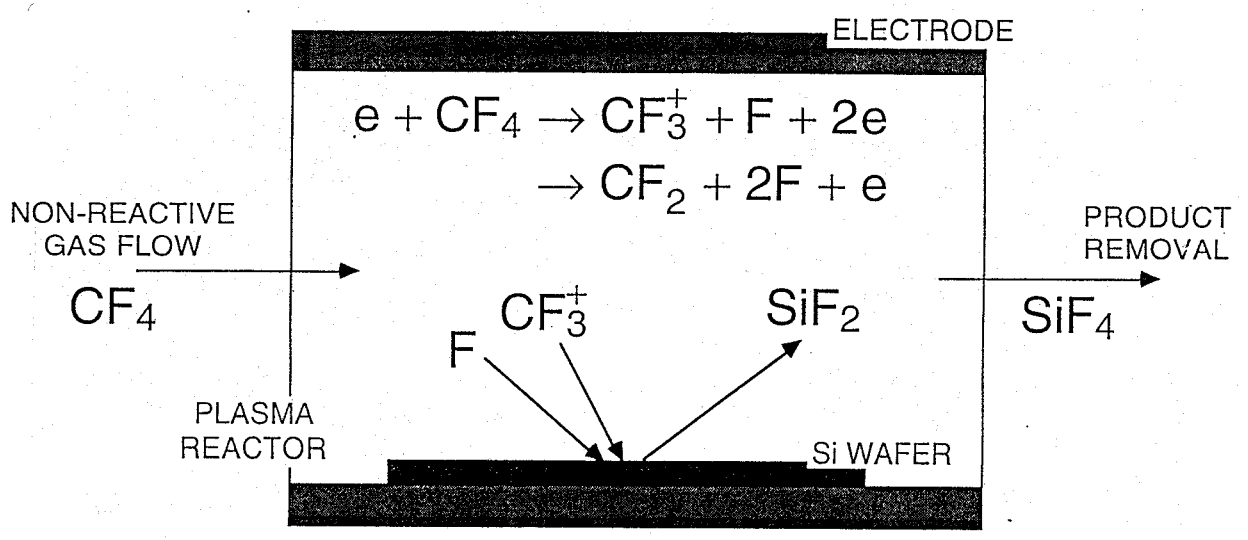

e

ELECTRON HEATING

$e + Cl_2 \rightarrow Cl_2^+ + e + e$

$e + Cl_2 \rightarrow Cl + Cl + e$

RADICAL / ION GENERATION

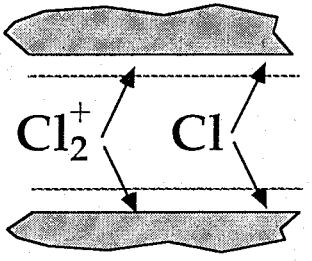

RADICAL / ION TRANSPORT TO WAFER

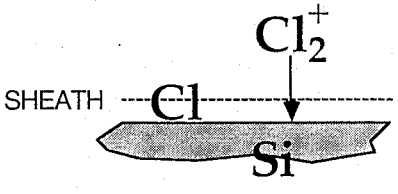

ION ACCELERATION INTO WAFER

RADICAL ADSORPTION

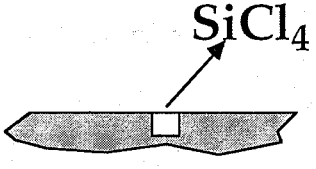

ETCHING

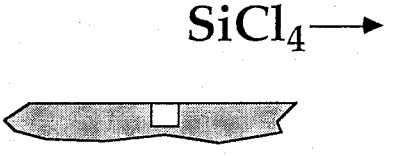

PRODUCT PUMPOUT

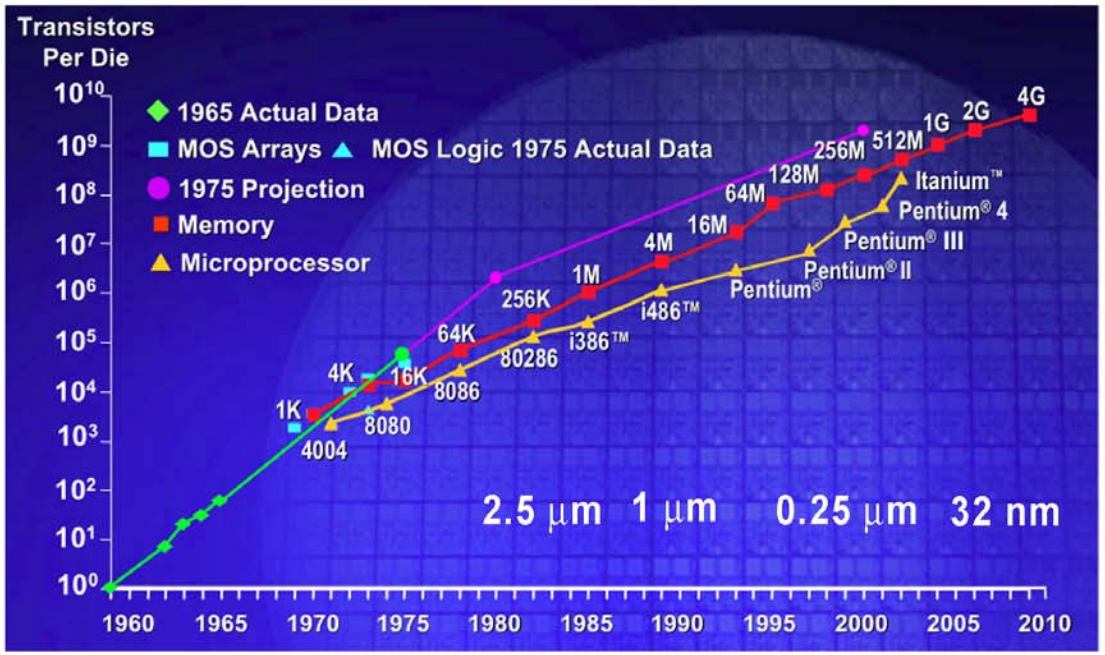

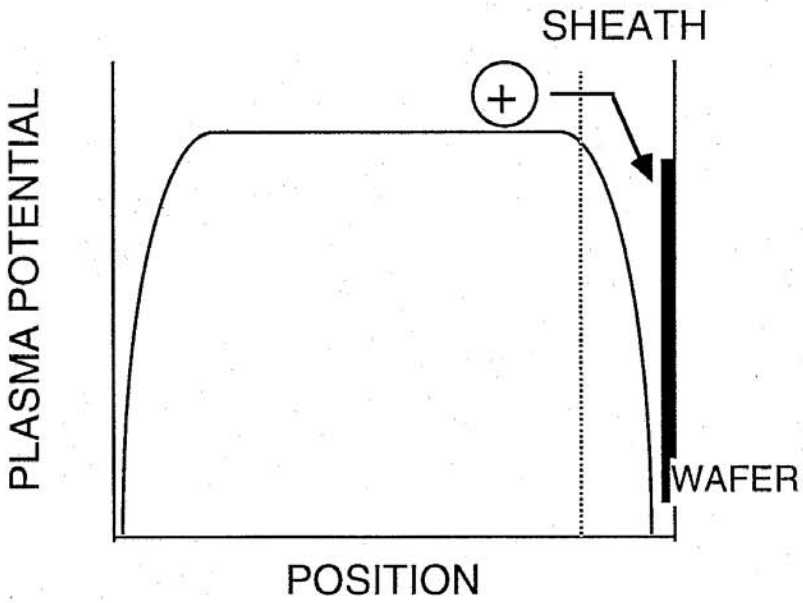

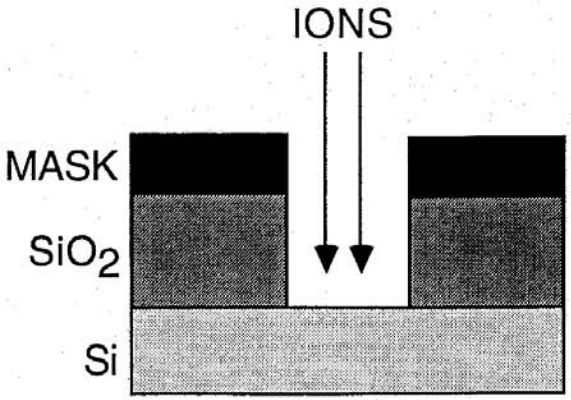

ION ASSISTED ETCHING

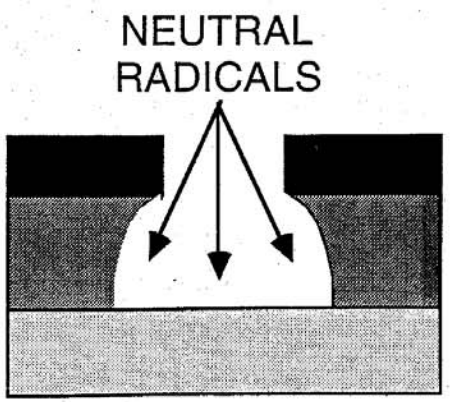

NEUTRAL DRIVEN ETCHING

ETCHING SPECIES	SOURCE GAS	ADDITIVE	MATERIALS	MECHANISM	SELECTIVE OVER
F	CF_4 C_2F_6 SF_6 NF_3 ClF_3 F_2	O_2 O_2 O_2 None None None	Si	Chemical	SiO_2 Resist
CF_x-film	CF_4 C_2F_6 CHF_3	H_2 H_2 None or O_2	SiO_2/Si_3N_4	Ion-energetic	Si
Cl	Cl_2	None	undoped Si	Ion-energetic	SiO_2
	Cl_2 CF_3Cl	C_2F_6 None	n-type Si	Ion-Inhibitor	
Cl	Cl_2	BCl_3 CCl_4 $CHCl_3$	Al	Ion-inhibitor	Resist SiO_2

Ref.: D. Flamm, "Plasma Etching: An Introduction"

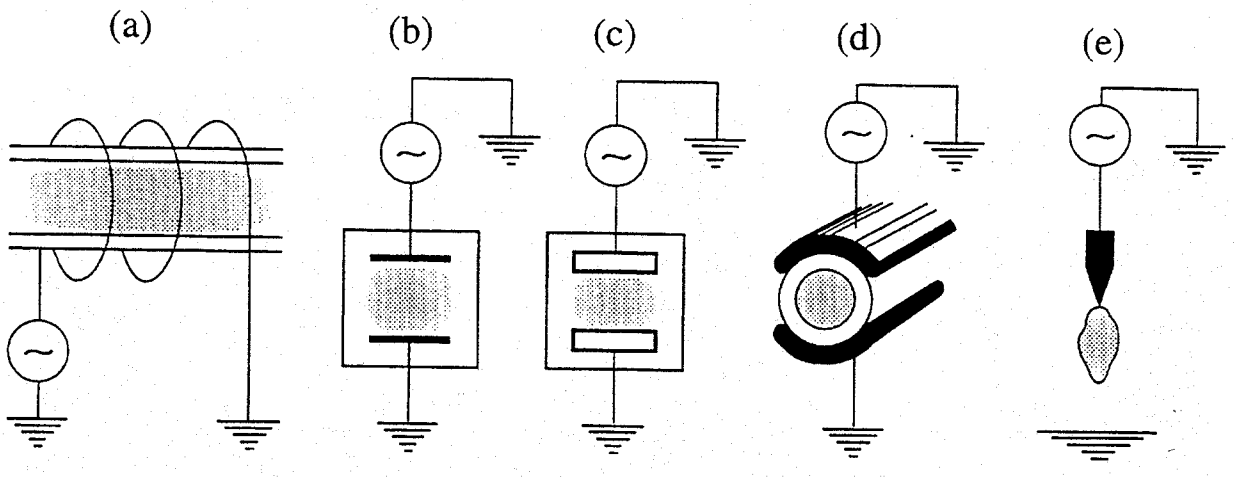

FIGURE 1.1
Basic ways of exciting RF discharges: (a) inductive discharge; (b)–(e) capacitive discharges with (b) plane naked electrodes, (c) coated electrodes, (d) external electrodes, and (e) with the earth as the other 'electrode' (torch single-electrode discharge).

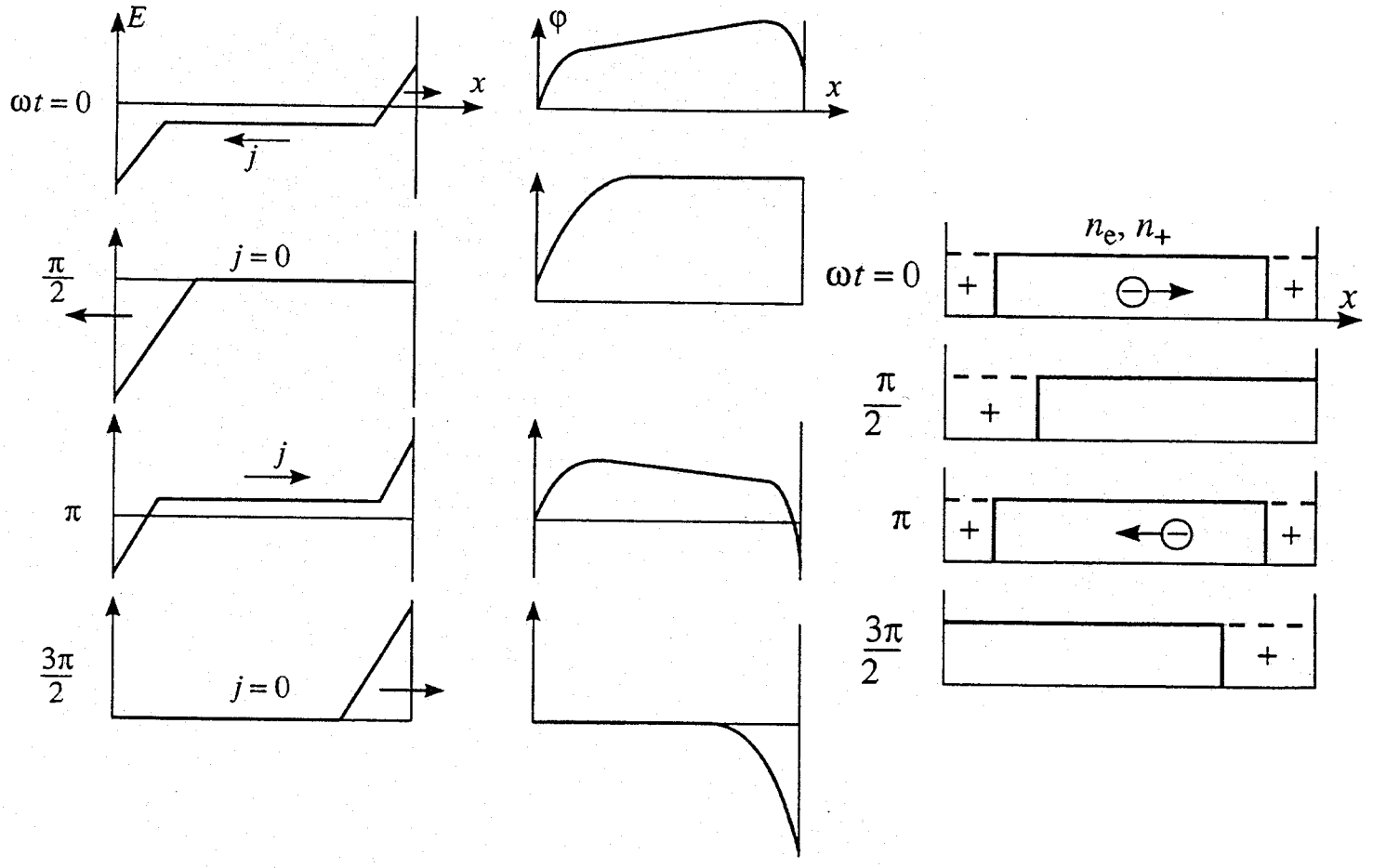

FIGURE 1.5
Field and potential distributions in the gap between plane electrodes for the n_+ and n_e distributions of Figure 1.4. Arrows indicate the direction of current j and field E. The left-hand electrode is grounded.

Electron Heating Mechanisms in Helium rf Glow Discharges: A Self-Consistent Kinetic Calculation

T. J. Sommerer,[a] W. N. G. Hitchon,[b] and J. E. Lawler[a]
University of Wisconsin, Madison, Wisconsin 53706
(Received 22 August 1989)

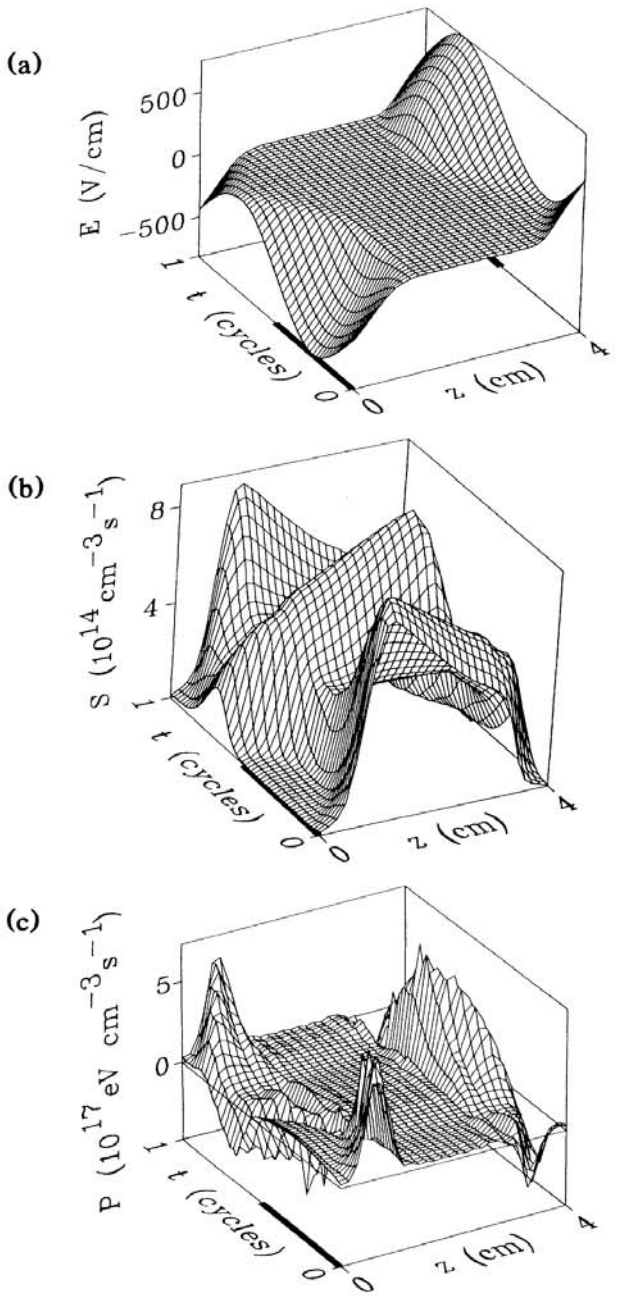

FIG. 1. Benchmark run: (a) electric field $E(z,t)$, (b) primary ionization rate per unit volume $S(z,t)$, and (c) power deposition into the electrons $P(z,t) = -n_e |e| E_z \langle v_z \rangle$, over one rf cycle $T = 7.375 \times 10^{-8}$ s. The heavy portions of the $z = 0$ and $z = 4$ cm lines indicate parts of the rf cycle where the corresponding electrode is cathodic.

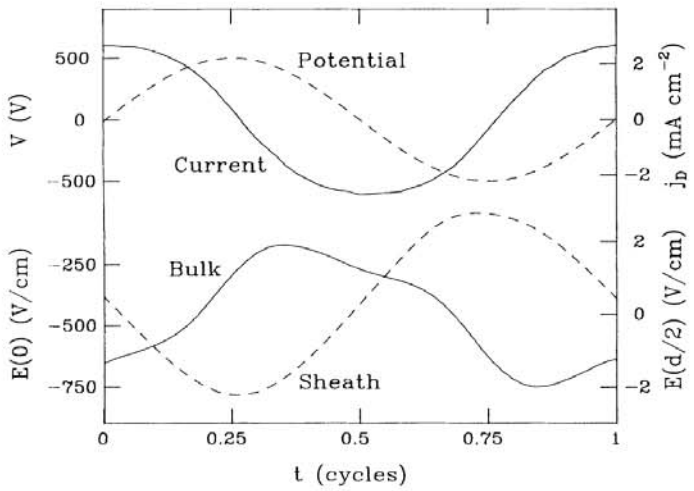

FIG. 2. The applied potential, discharge current, electric field at the $z = 0$ electrode, and bulk electric field ($z = d/2$) of the benchmark discharge over one rf cycle T.

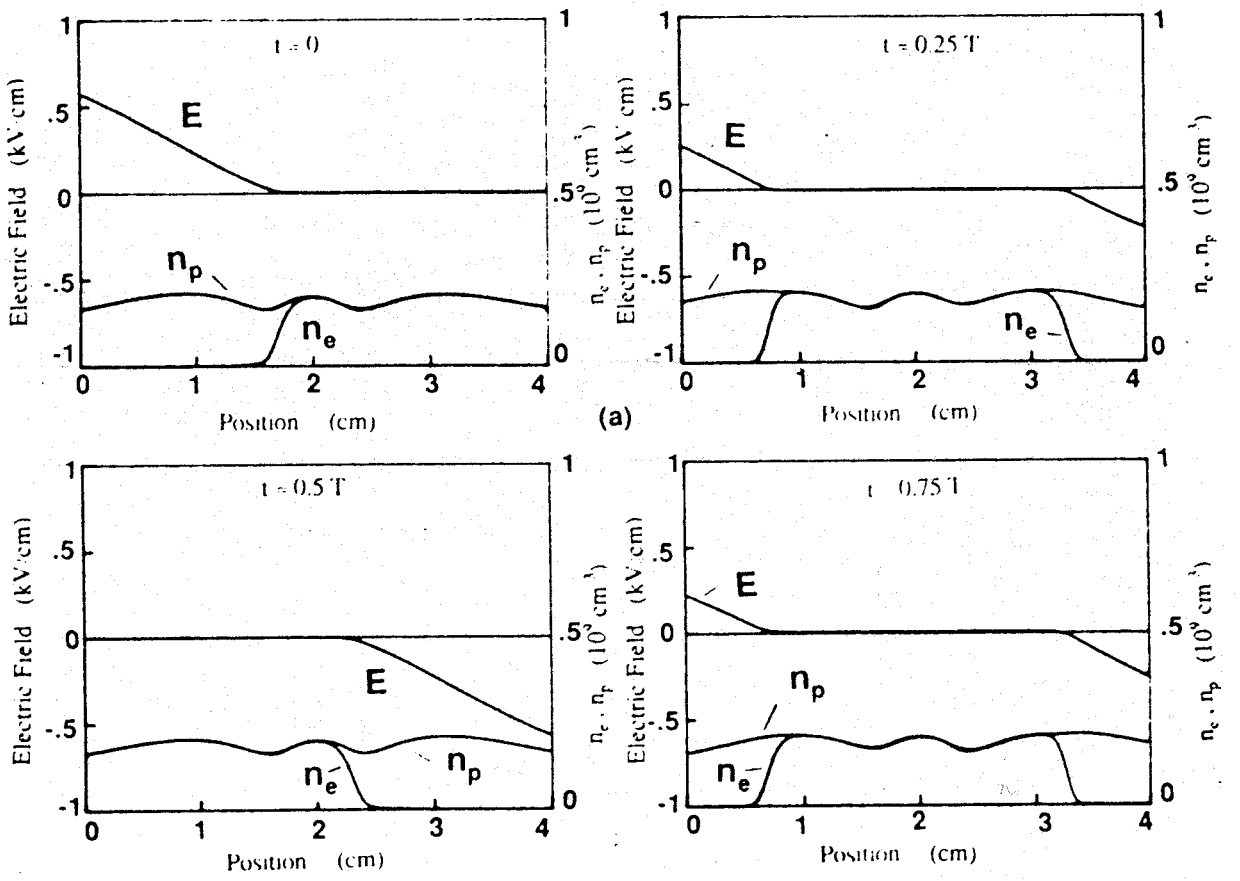

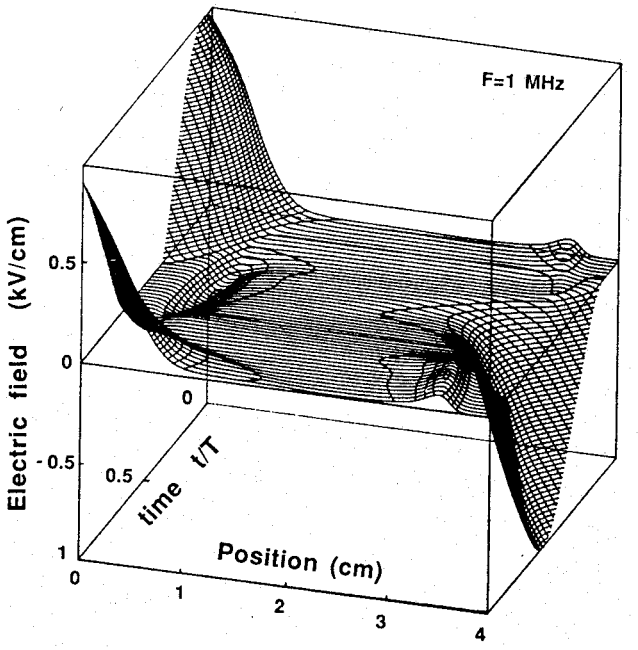

FIG. 10. Spatio-temporal variations of the electric field ($F=1$ MHz, $V_{rf}=500$ V, electronegative gas).

• J-P Boeuf (PRA, 1987)

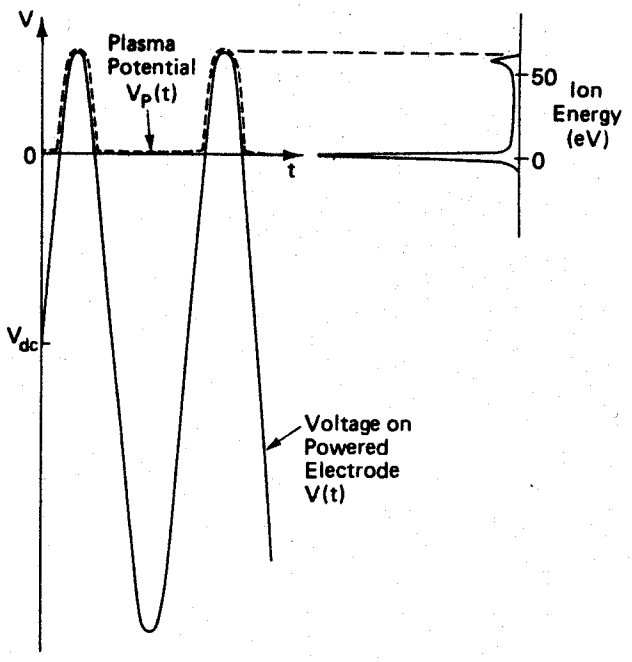

FIG. 2. Illustrative figure to show the relationship between the 100-kHz energy distribution in Fig. 1 and the plasma potential $V_p(t)$.

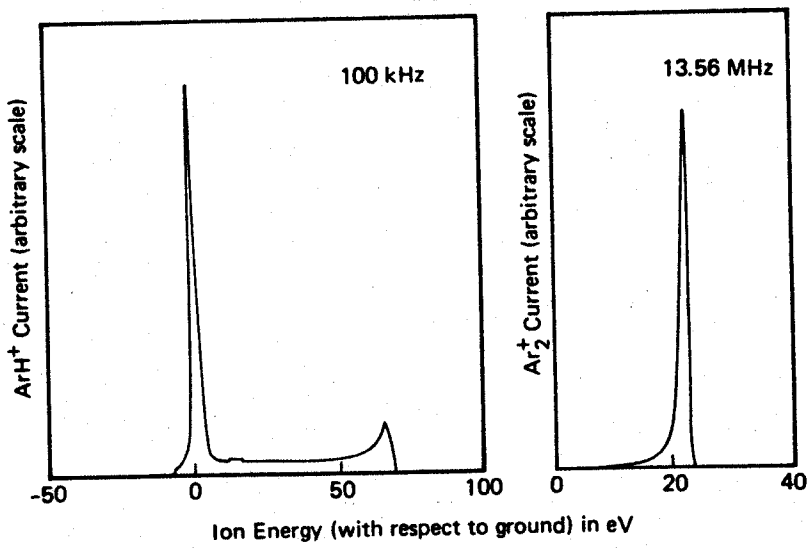

FIG. 1. Energy distributions of ions extracted through the ground plane of a planar diode rf glow discharge system with 100-kHz and 13.56-MHz excitation frequencies. Argon pressure = 50 mTorr.

K. Kohler, J. Appl. Phys. 58, 3350 (1985)

RF V-I SYMMETRIC

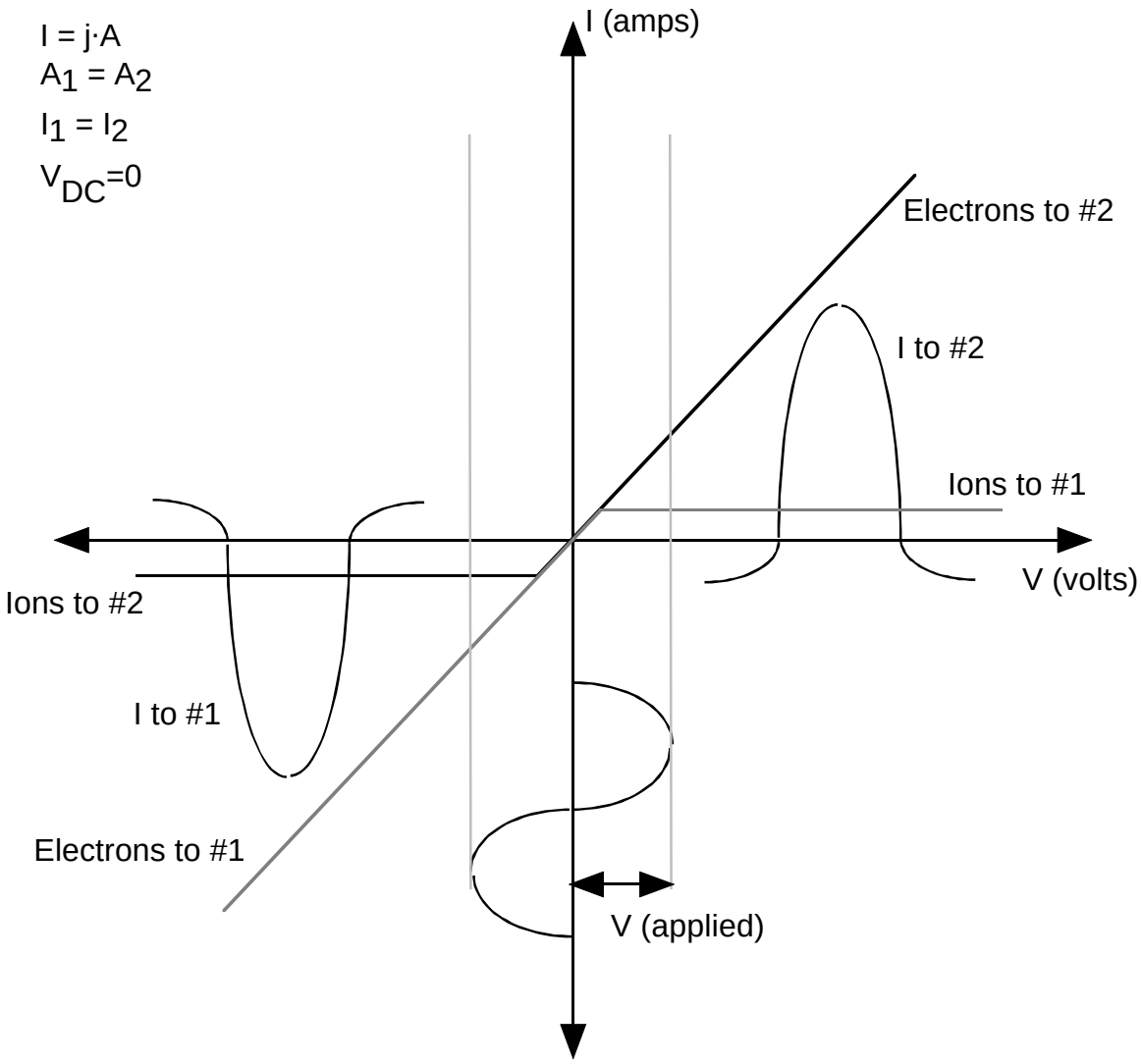

RF V-I ASSYMMETRIC-NO DC BIAS

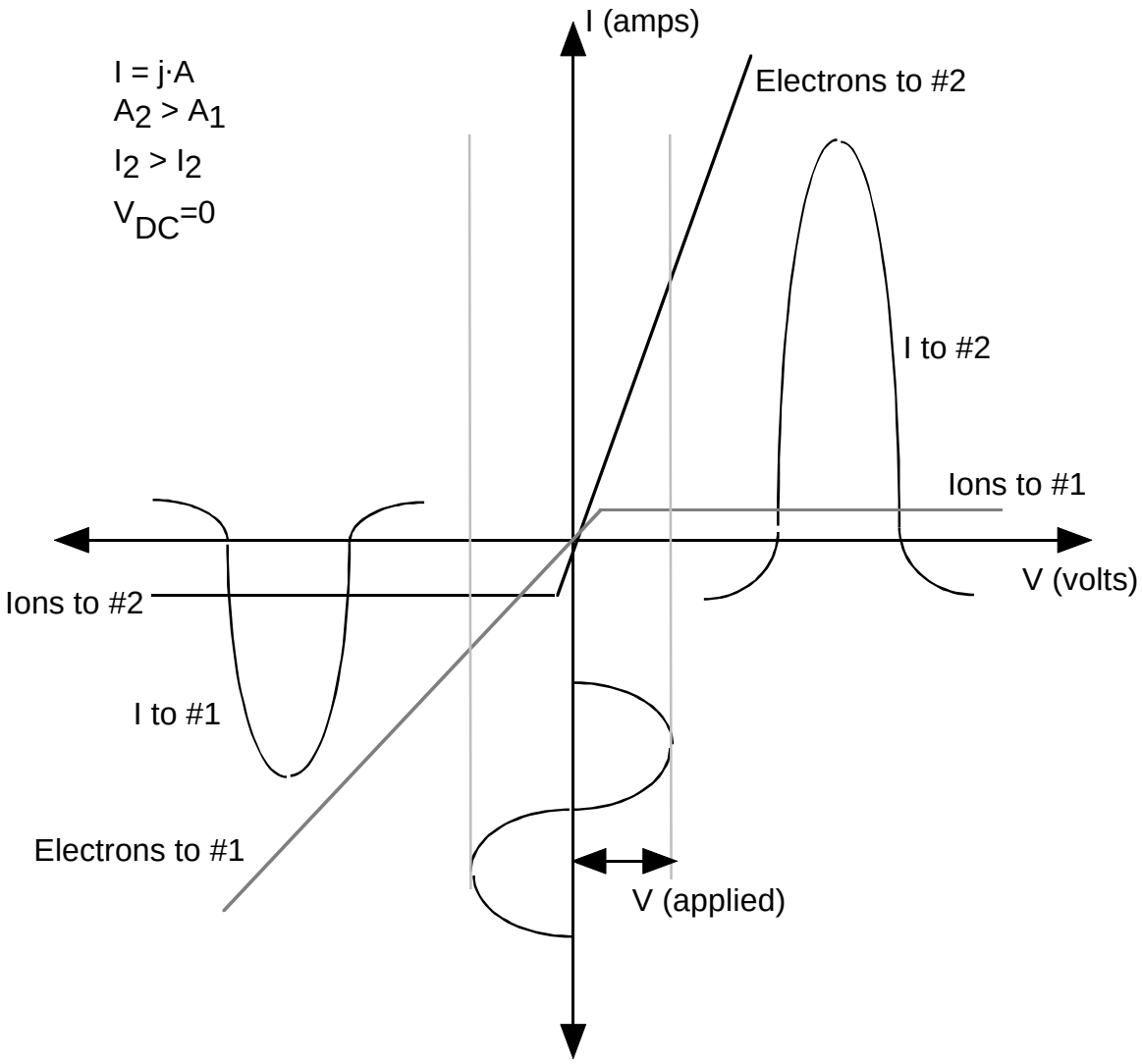

RF V-I ASSYMMETRIC-WITH DC BIAS

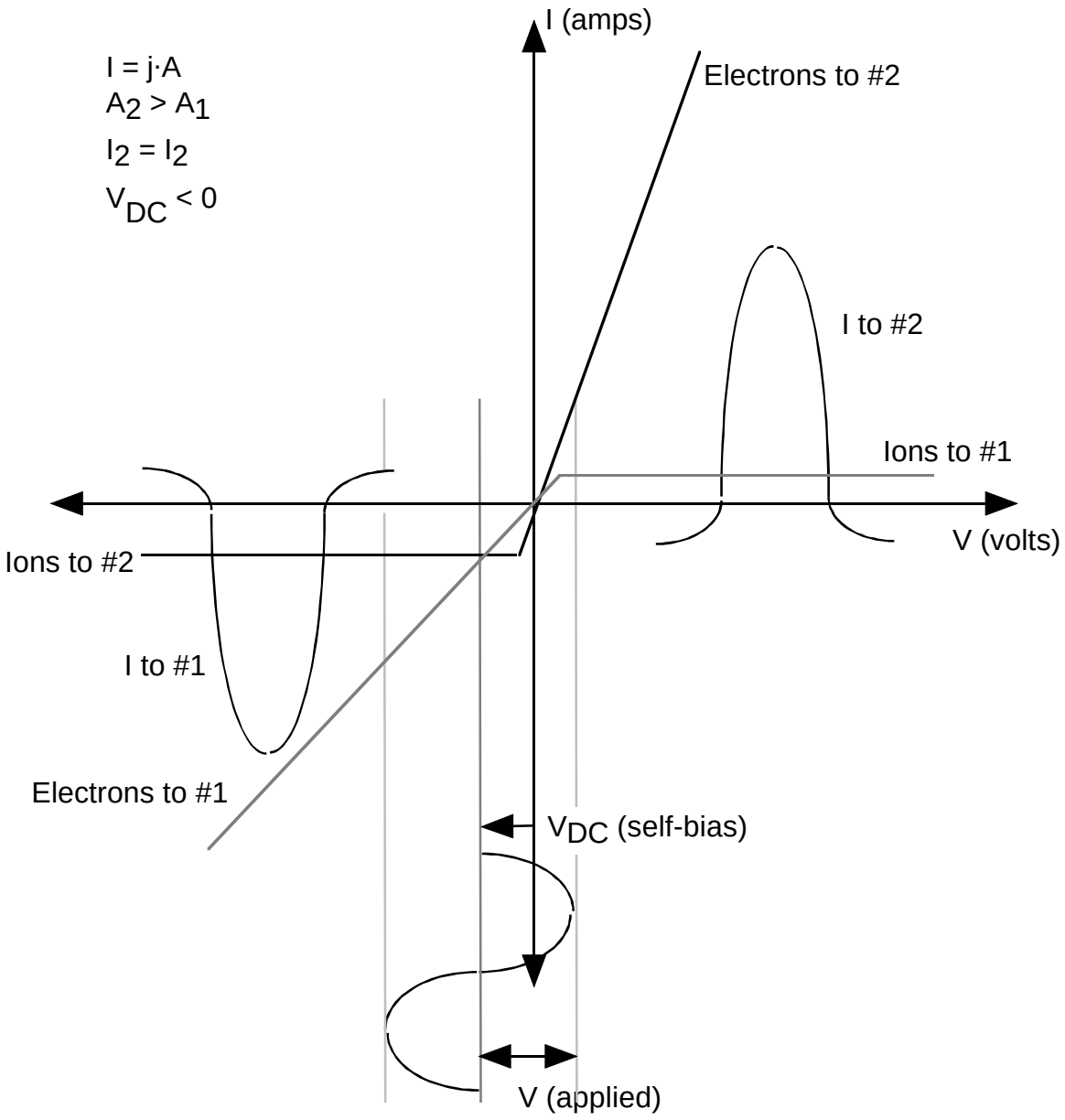

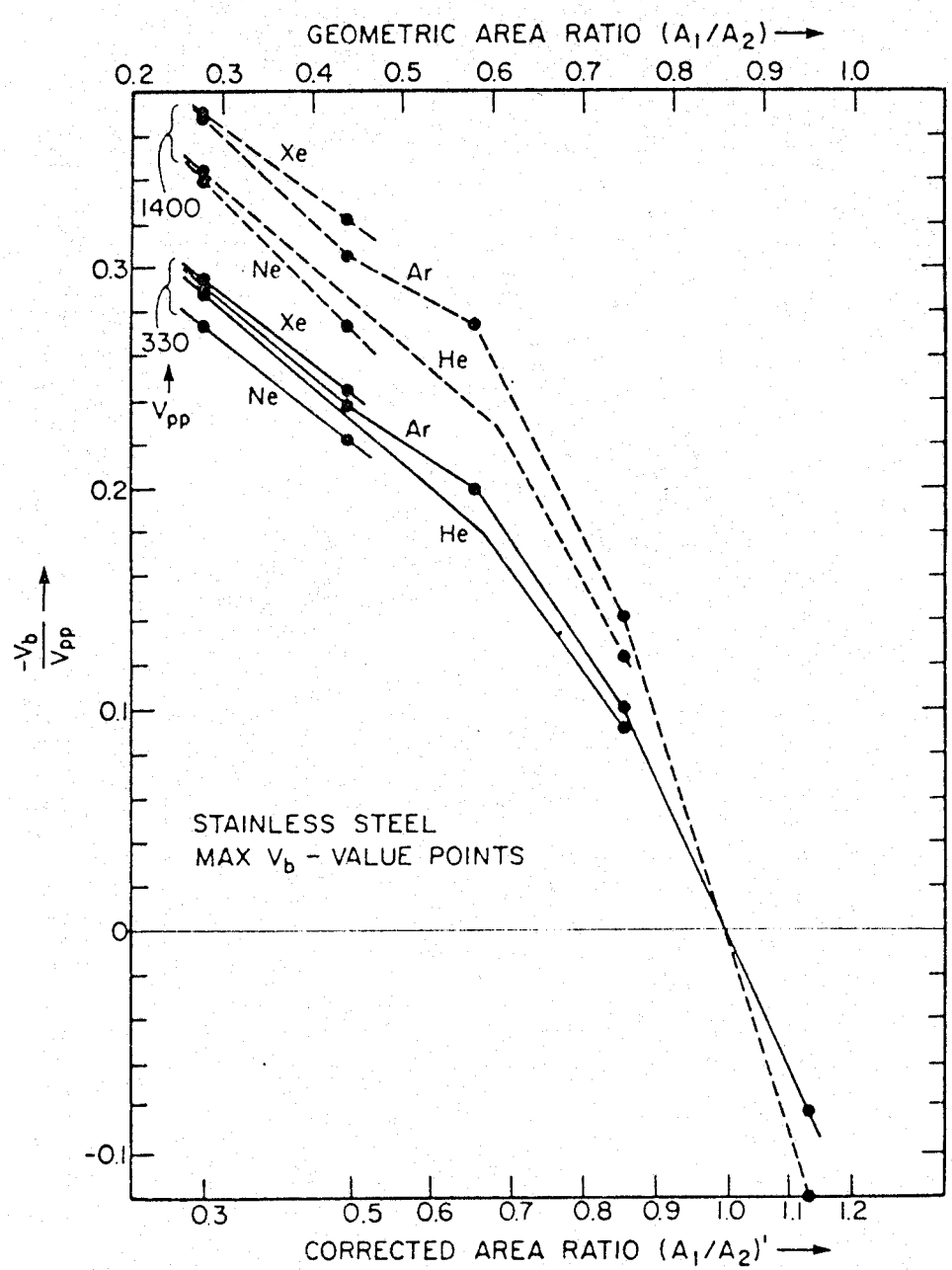

FIG. 12. Dependence of bias voltage ratio on electrode area ratio for two values of V_{pp} and several gases in a stainless steel system. Points were chosen at pressures which yield a maximum of V_b for each area ratio. For Ar, the pressure range was 0.6 to 3 Pa. The upper horizontal axis is the geometric area ratio; the lower axis is the "corrected" area ratio which would be seen by a discharge with a chamber 1.2 cm shorter in height.

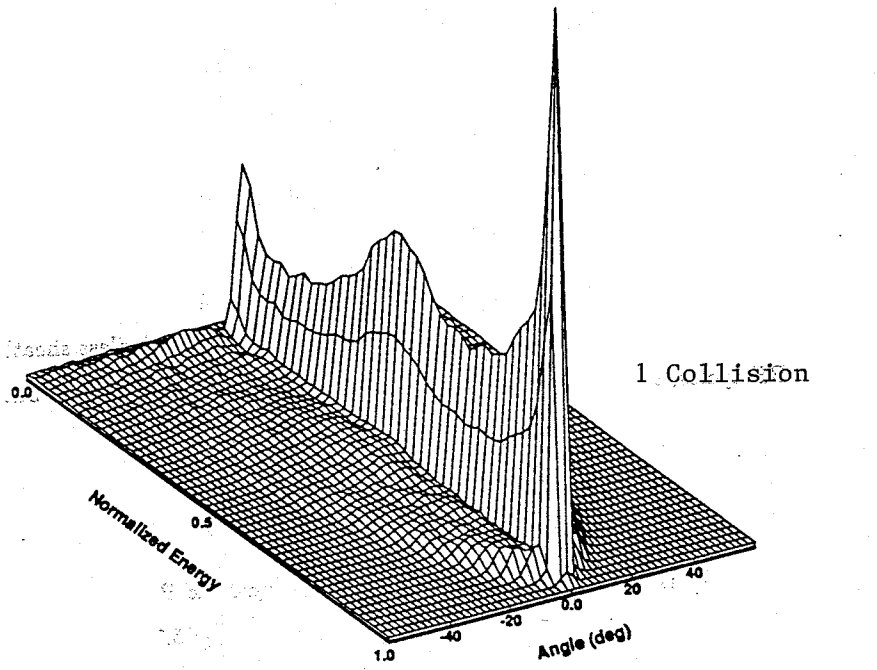

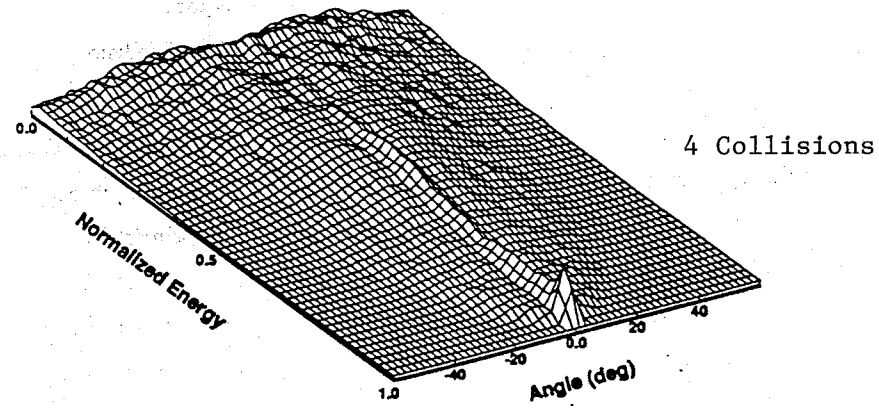

Figure 5.6. Ion-distribution functions at 1.0 (top) and 3.7 (bottom) sheath-thickness to mean-free path ratios. The x-axis corresponds to the normalized energy, the y-axis to the angle of arrival of the particle on the surface, and the z-axis to the distribution function. Note the radical change in the energy distribution function as the environment becomes more collisional.

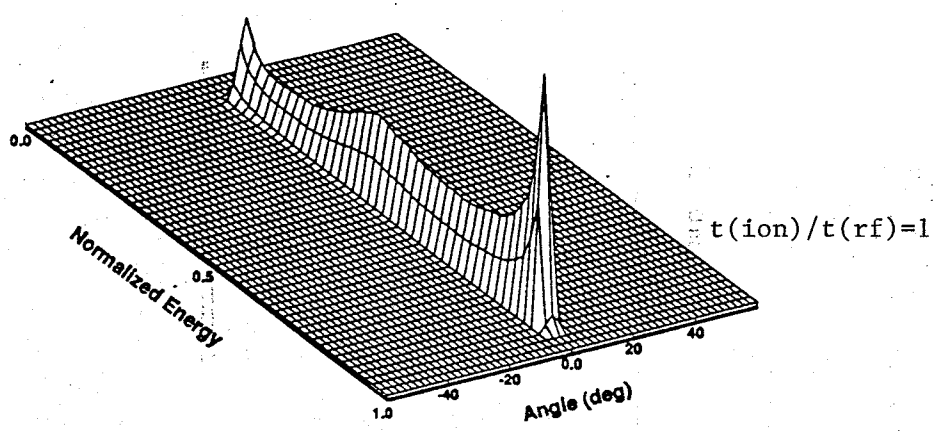

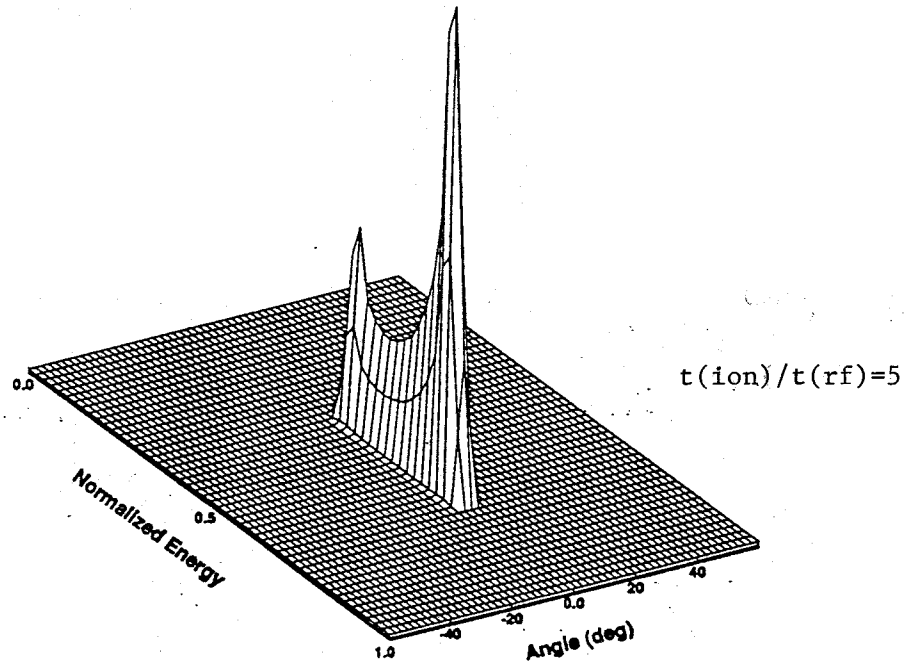

Figure 5.7. Collisionless ion-distribution functions. The particles require an average of one (top) and five RF (bottom) periods to reach the electrode, respectively. As the particle spends more time in the sheath, its energy centers on an average value. These functions are on a different scale than in Fig. 5.6.

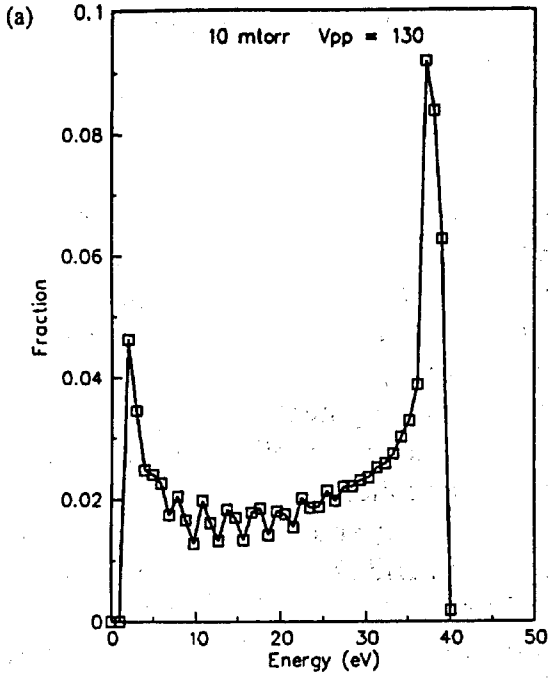

10 mTorr

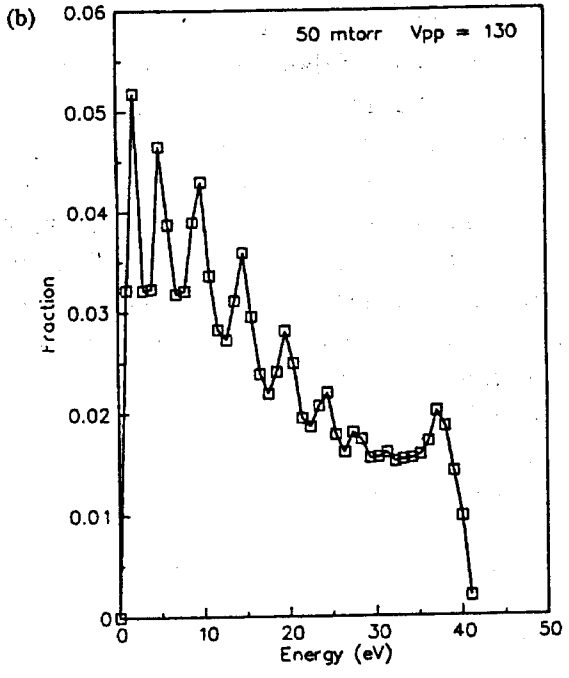

50 mTorr

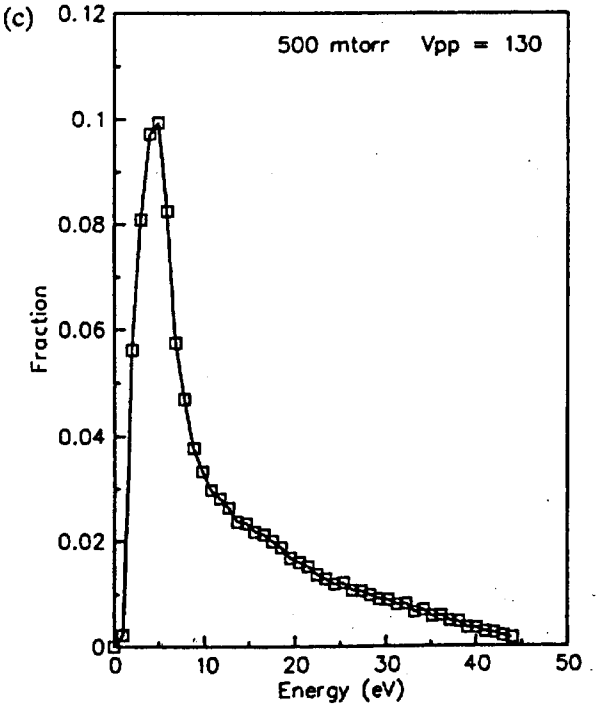

500 mTorr

FIG. 6. Total IED of argon plasmas at $V_{pp} = 130$. All graphs have been normalized so that the area under the curves are equal. (a) $P = 10$ mTorr. (b) $P = 50$ mTorr. (c) $P = 500$ mTorr.

Liu, et. al., J. Appl. Phys. 10/15/90

B. Simple Power Balance Model for RF Discharges

1. Assume $V_{sheaths} > V_{bulk}$. We control j_0, ω, dimensions

2. Power deposition is by

a. Electron heating in the bulk
b. Ion bombardment of electrodes
c. Secondary electron emission with acceleration back into the plasma
d. Stochastic heating

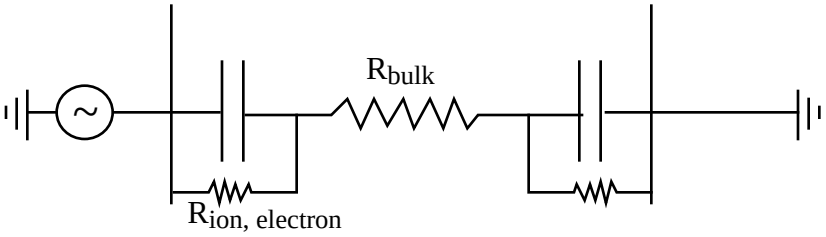

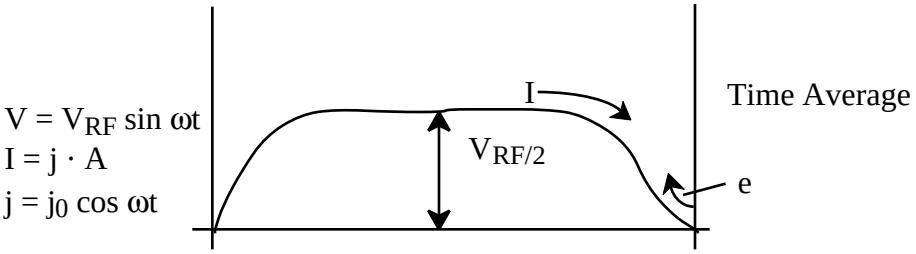

3. Current through sheaths is dominantly capacitive with

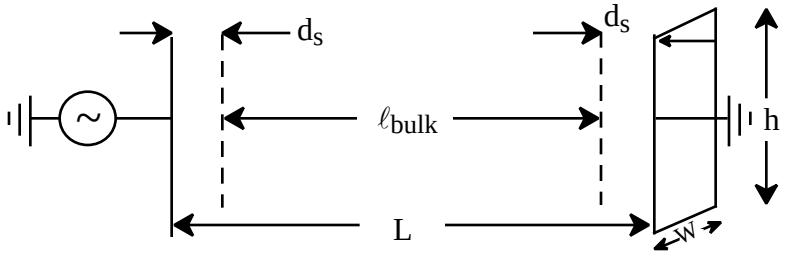

4. Bulk electron heating: P_B (Watts)

$$P_B = \int < j \cdot E >_{RMS} \cdot dV_{bulk} = \int \left(\frac{j^2}{\sigma} \right) \cdot dV_{bulk}, \quad \sigma = \text{conductivity}$$

$$= \frac{1}{2} j_0^2 \left(\frac{m_e \nu_m}{q^2 n_e} \right) \cdot l_B \cdot h \cdot w$$

5. Ion acceleration: P_I

a. Assume that there is no recombination or attachment in the bulk plasma. ($n_e = n_I$)
b. Every ion produced in the bulk is lost to the electrodes.
c. Ions enter the sheath with the Bohm speed.

$$\int (n_e \cdot k_{ion} \cdot N_{gas}) \cdot dV_{bulk} = \oint_{sheath} n_I \cdot u_{Bohm} \cdot dA_{electrodes}$$

$$n_e k_{ion} N_{gas} l_B \cdot h \cdot w = n_I u_{Bohm} \cdot w \cdot h \cdot 2$$

$$P_I = n_I \cdot u_{Bohm} \cdot w \cdot h \cdot \left(\frac{qV_{RF}}{2} + \frac{qkT_e}{2} \right) \cdot 2$$

Where the first term is the ion acceleration in the sheath, the second term is the Bohm speed contribution, and the last "2" is for 2 electrodes.

6. Secondary Electron Power: P_e

For every ion striking the electrode we get γ electrons which accelerate back into the plasma.

$$P_e = \gamma \left(\frac{qV_{RF}}{2} \right) \cdot n_I \cdot u_{Bohm} \cdot w \cdot h \cdot 2$$

where the last "2" is for two electrodes.

7. Stochastic electron heating: P_s

a. Electrons are accelerating by advancing sheath in the same manner as an elastic collision of a ball from a piston.

b.

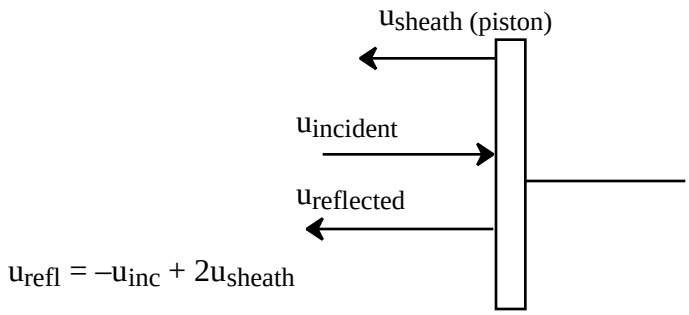

The power into the electrons for 2 sheaths is then

$$P_s = 2\int_{u_{sh}}^{\infty} \frac{1}{2} m_e \underbrace{\left(u_{refl}^2 - u_{inc}^2\right)}_{\text{energy gain}} \cdot \underbrace{\left(u_{inc} - u_{sh}\right) n_e f(u_{inc}) \cdot du_{inc}}_{\text{rate of collision}} \cdot w \cdot h$$

$$= -2 \cdot 2m_e \int_{u_{sh}}^{\infty} u_{sh} \left(u_{inc} - u_{sh}\right)^2 n_e f(u_{inc}) \cdot du_{inc} \cdot w \cdot h$$

Assume that $u_{sheath} = u_0 \sin \omega t$ and integrate over time

$$P_s \approx 2 \cdot 2m_e n_e u_0^2 \int_{u_{sh}}^{\infty} u_{inc} f(u_{inc}) du_{inc} \cdot w \cdot h$$

Since $u_{sh} << \langle u_{inc} \rangle$, then set lower limit to zero. Note that

$$\int_0^{\infty} u_{inc} f(u_{inc}) du_{inc} = \frac{\bar{v}_{th}}{4}$$

so

$$P_s = 2 \cdot \frac{m_e n_e u_0^2}{2} v_{th} \cdot w \cdot h$$

The conduction current in the bulk plasma must equal the rate at which the electrons are swept out by the sheath, so

$$j_0 = q \cdot n_e \cdot u_0$$

$$P_s = \frac{m_e \nu_{th}}{q^2 n_e} j_0^2 \cdot w \cdot h$$

8. The total power deposition is then:

$$P_{total} = P_{bulk} + P_{e-sec} + P_{ion} + P_{stochastic}$$

$$= \frac{1}{2} j_0^2 \left(\frac{m_e \nu_m}{q^2 n_e} \right) \cdot l_B \cdot h \cdot w$$

$$+ 2 \cdot n_e \cdot u_{Bohm} \cdot \left(\frac{qV_{RF}}{2}(1+\gamma) + \frac{kT_e}{2} \right) \cdot h \cdot w$$

$$+ \frac{m_e \nu_{th}}{q^2 n_e} j_0^2 \cdot h \cdot w$$

9. To complete the analysis, we need a relationship between V_{RF} and j_0, n_e and T_e.

V_{RF} If we assume that the majority of the applied voltage is across the sheaths, then on the average

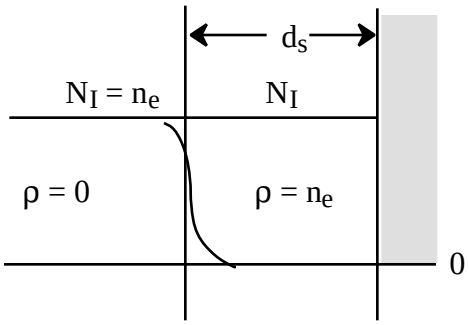

$$V_{RF} \approx \int_0^{d_s} E \cdot dx = -\frac{q n_e d_s^2}{2\varepsilon_0}$$

Since the capacitive current through the sheath is

$$I = C_s \frac{dV_{RF}}{dt}, \qquad C_s = \frac{w \cdot h \cdot \varepsilon_0}{d_s}$$

then $$j_0 = \frac{\varepsilon_0}{d_s} V_{RF}\, \omega, \qquad V_{RF} = \frac{j_0 d_s}{\varepsilon_0 \omega}$$

Since $$d_s = \left(\frac{2V_{RF}\varepsilon_0}{qn_e}\right)^{1/2} = \frac{2j_0}{\omega q n_e}$$ then

$$V_{RF} = j_0 \left(\frac{2V_{RF}\varepsilon_0}{qn_e}\right)^{1/2} \frac{1}{\varepsilon_0 \omega}, \quad V_{RF} = \frac{2j_0^2}{\varepsilon_0 q \omega^2 n_e}$$

T_e The electron temperature comes from the ion balance:

$$n_e \cdot k_{ion} \cdot N_{gas} \cdot l_B \cdot w \cdot h = n_I \cdot u_B \cdot w \cdot h \cdot 2$$

$$k_{ion}(T_e) \cdot N_{gas} \cdot l_B = u_{Bohm} \cdot 2 = \left(\frac{kT_e}{M_I}\right)^{1/2} \cdot 2$$

n_e The electron density is obtained by equating all sources of electron heating to the power dissipation

(Power into e's) = $\sum$ (elastic + inelastic losses)

$$P_B + P_{sh} + P_R = n_e N_G \left(\frac{2m_e}{M} \frac{3}{2} k_{Bolt} k_{mom}(T_e - T_g) + \sum_i \Delta\varepsilon_i k_I\right) \cdot l_B \cdot w \cdot h$$

EXAMPLE: Argon RF discharge, 100 m Torr

$w = 2\pi \cdot 13.56$ MHz

$j_0 = 25\ \frac{mA}{cm^2}$, $L = 5$ cm, $\gamma = 0.05$

$M = 40$ AMU $R_{electrode} = 10$ cm

$$k_{ion} \approx 10^{-8}\ T_e^{1/2} \left(\frac{16eV}{T_e} + 1\right) \exp\left(\frac{-16}{T_e}\right) \frac{cm^3}{s}, \qquad \Delta\varepsilon = 16 \text{ eV}$$

$$k_{exc} \approx 2 \times 10^{-8}\ T_e^{1/2} \left(\frac{12eV}{T_e} + 1\right) \exp\left(\frac{-12}{T_e}\right) \frac{cm^3}{s}, \qquad \Delta\varepsilon = 12 \text{ eV}$$

$$k_{mom} \approx 5 \times 10^{-8}\ \frac{cm^3}{s}$$

T_e If we approximate $l_B = L - 2d_s \approx L$, then

$$k_{ion} \cdot N_{gas} \cdot l_B \approx u_{Bohm} \cdot 2 = \left(\frac{kT_e}{M_I}\right)^{1/2} \cdot 2 \approx k_{ion} \cdot N_{gas} \cdot L$$

$$3.2 \times 10^{16}\ cm^{-3}\ 10^{-8}\ T_{eV}^{1/2} \left(\frac{16eV}{T_{eV}} + 1\right) \exp\left(\frac{-16eV}{T_e}\right) \cdot L = \left(\frac{1.6 \times 10^{-12} T_{eV}}{M_{ion}}\right)^{1/2} \cdot 2$$

$T_e = 1.73$ eV

n_e $P_B + P_{stochastic} + P_e =$ elastic + inelastic

(Assume $\gamma = 0$ for n_e …)

$$hw \left\lfloor \frac{1}{2}\ j_0^2 \frac{m_e \nu_m}{q^2 n_e} \cdot L + \frac{m_e V_{th}}{q^2 n_e}\ j_0^2 \right\rceil$$

$$= \left[n_e\ N_G\ \nu_m \left(\frac{2m_e}{M}\right) \frac{3}{2} k_B (T_e - T_g) + n_e N_G (\Delta\varepsilon\ k_{ion} + \Delta\varepsilon\ k_{exc}) \right] hwL$$

$n_e \approx 2.38 \times 10^{10}\ cm^{-3}$

d_s (Sheath Width)

$$d_s = \frac{2j_0}{\omega q n_e} = \frac{2 \times 25 \times 10^{-3}}{2\pi \times 13.56 \times 10^6 \times 1.6 \times 10^{-19} \times 2.38 \times 10^{10}} \frac{c - s\ cm^3}{cm^2 - s - c}$$

$$= 0.154 \text{ cm} \quad (<< L = 5 \text{ cm})$$

(Note: With the known value of d_s, you can now replace L with $l_B = L - 2d_s$ in the expression for T_e to get a more accurate temperature.)

V_{RF} $V_{RF} = \frac{j_0 d_s}{\varepsilon_0 \omega} = \frac{25 \times 10^{-3} \cdot 0.154}{8.85 \times 10^{-14} \times 2\pi\, 13.56 \times 10^6} \frac{c - cm\ J - cm - s}{cm^2 - s - c^2}$

$$= 511 \text{ V}$$

P_{total}

P_{bulk} =

$$\frac{1}{2} j_0^2 \left(\frac{m_e \nu_m}{q^2 n_e} \right) \cdot (L - 2d_s)\pi R^2 = \frac{(25 \times 10^{-3})^2\, 0.911 \times 10^{-27} \cdot 1.6 \times 10^8 (5 - 2 \times 0.154)}{2(1.6 \times 10^{-19})^2 (2.38 \times 10^{10})} \frac{ergs}{cm^2 - s} \pi R^2$$

$$= 35.1 \frac{mW}{cm^2} \cdot \pi R^2 = 11.0 \text{ W} \qquad (7.4\%)$$

$$P_{\substack{sheath \\ stochastic}} = \frac{m_e \cdot V_{th}}{q^2 n_e} j_0^2\, \pi R^2 = \frac{2 \times 0.911 \times 10^{-27} \cdot 1.12 \times 10^8 (25 \times 10^{-3})^2}{(1.6 \times 10^{-19})^2\, 2.38 \times 10^{10}} \frac{ergs}{cm^2 - s}$$

$$= 20.9 \frac{mW}{cm^2} \cdot \pi R^2 = 6.58 \text{ W} \qquad (4.4\%)$$

$$P_{\substack{ion \\ acceleration}} = 2 \cdot n_e \cdot u_{Bohm} \cdot \left(\frac{qV_{RF}}{2} + \frac{kT_e}{2} \right) \cdot \pi R^2$$

$$= 2 \times 2.38 \times 10^{10} \left(\frac{1.6 \times 10^{-12} \cdot 1.73}{40 \times 1.67 \times 10^{-24}} \right)^{1/2} \left(\frac{1.6 \times 10^{-12} \cdot 511}{2} + \frac{1.6 \times 10^{-12} \cdot 1.73}{2} \right) \pi R^2$$

$$= 397 \frac{mW}{cm^2} \cdot \pi R^2 = 125 \text{ W} \qquad (84.0\%)$$

$$P_{sec} = 2 \cdot n_e \cdot u_{Bohm} \cdot \frac{qV_{RF}}{2} \cdot \gamma \pi R^2 = 6.2 \text{ W} \qquad (4.2\%)$$

P_{total} = 148.8 W

Radio Frequency Discharge Example

Gas:	Argon
Pressure:	100 mTorr
Electrode Separation:	5 cm
Electrode Radius:	10 cm
Secondary Electron Emission Coefficient:	0.1
Frequency:	13.56 MHz

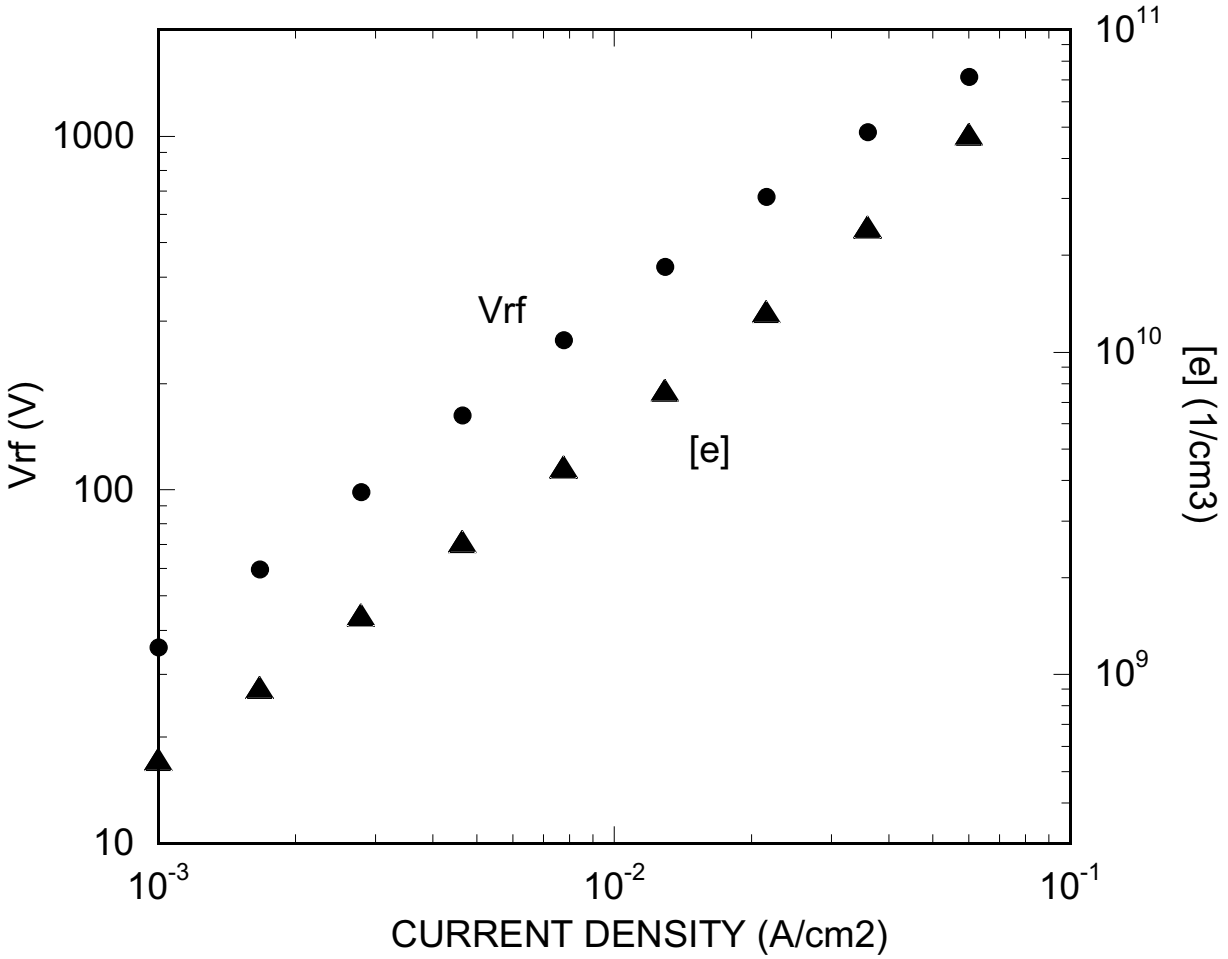

Rf_discharge_fig1

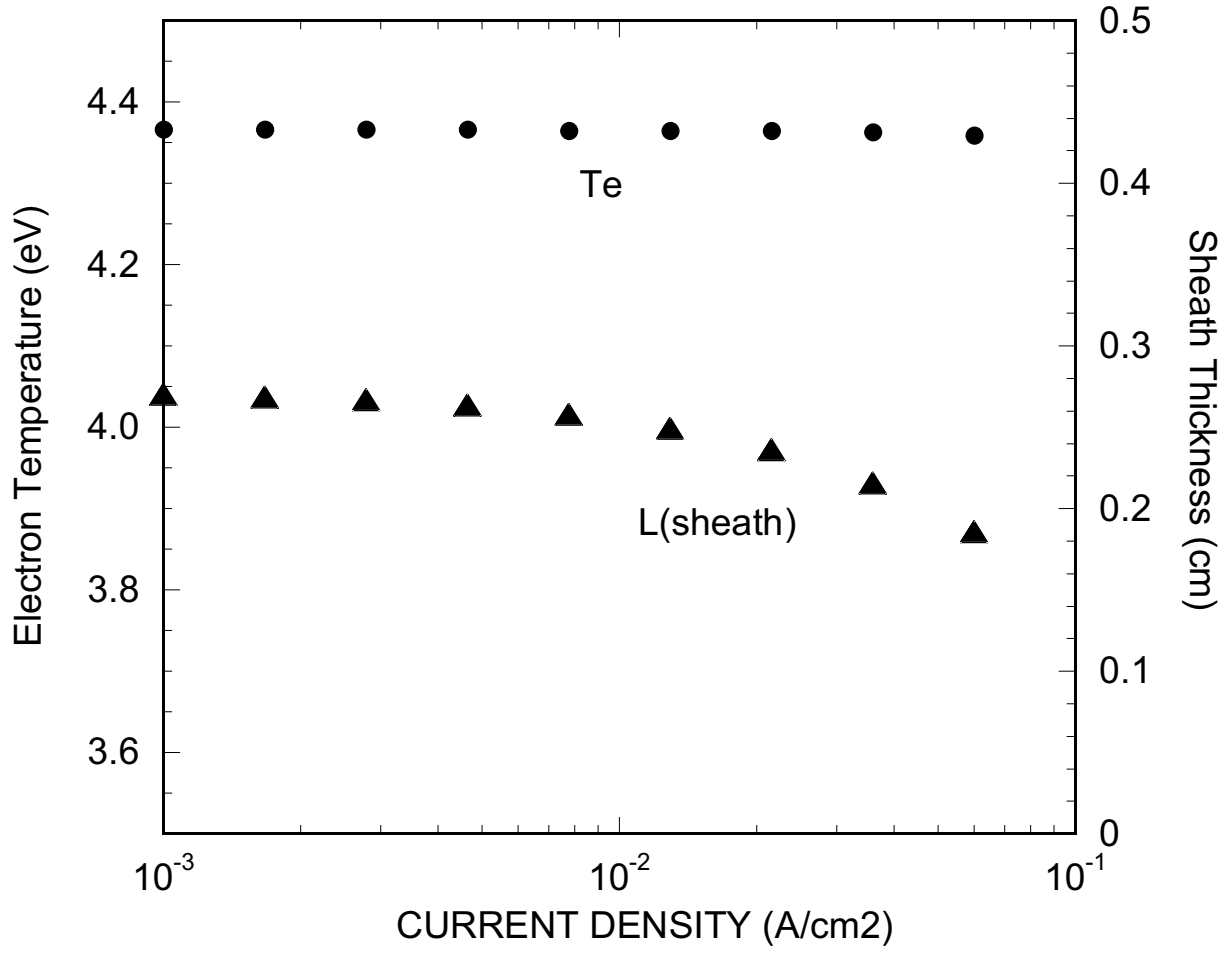

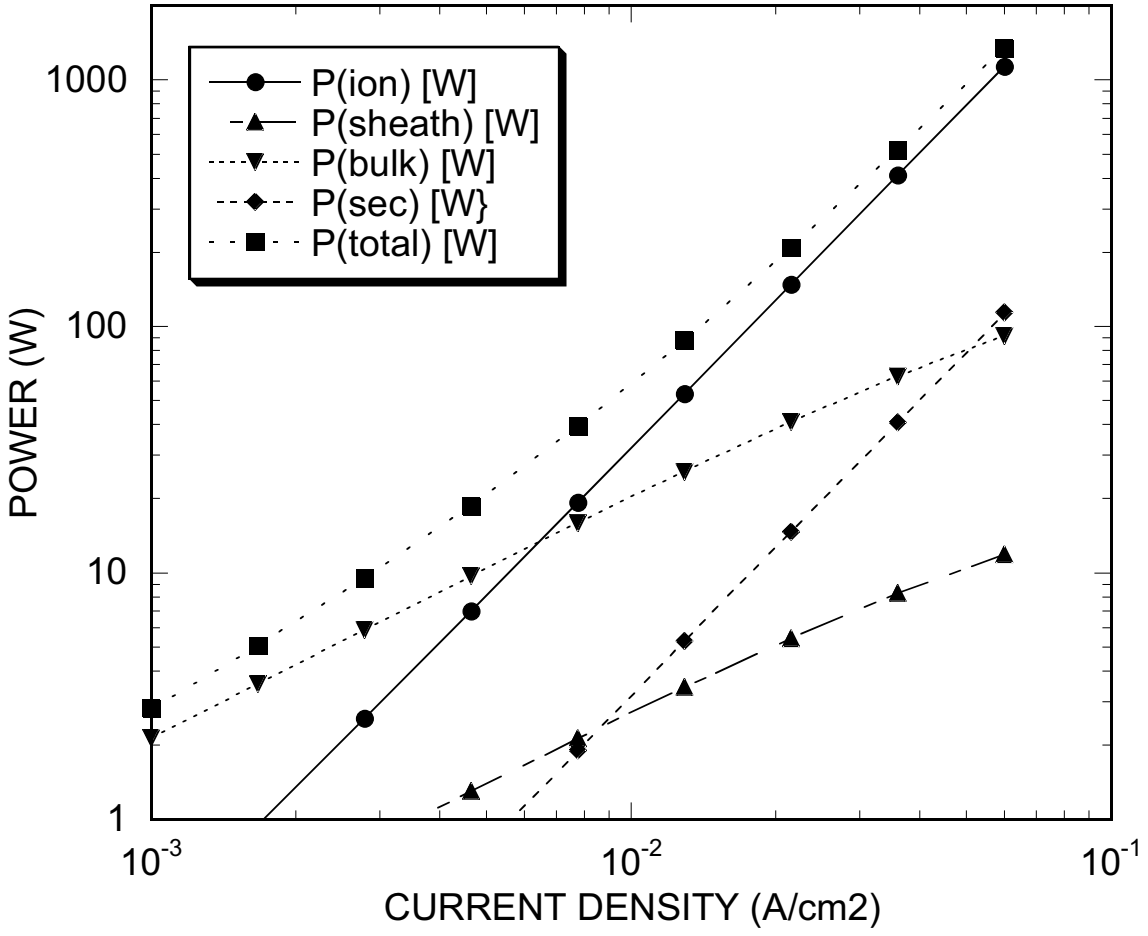

Rf_discharge_fig2

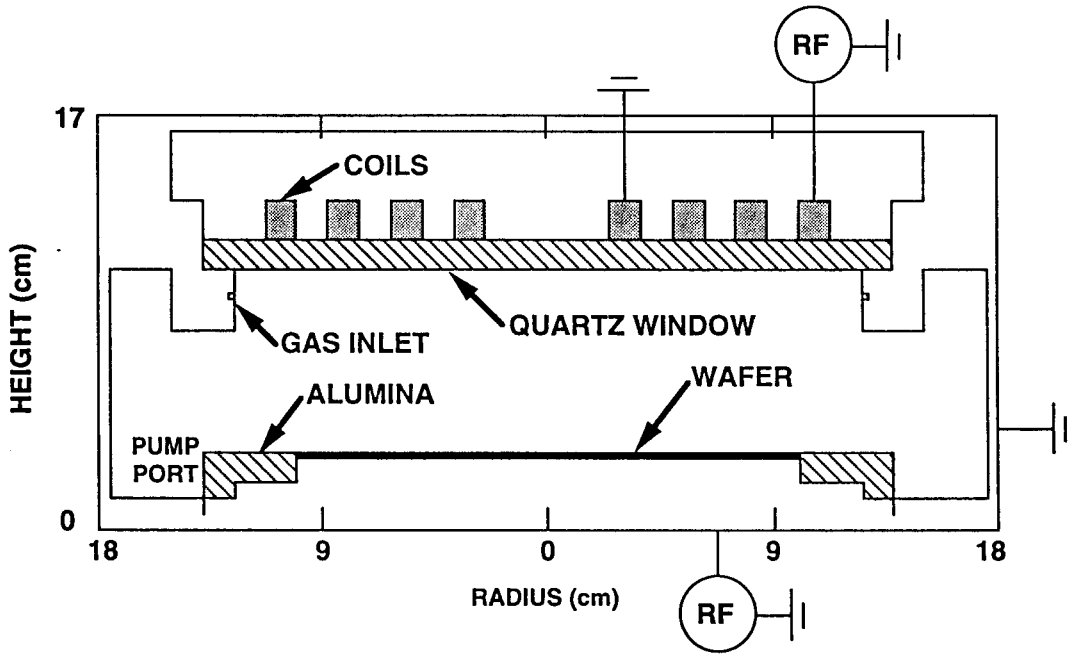
RF
17
COILS
HEIGHT (cm)
GAS INLET
QUARTZ WINDOW
ALUMINA
WAFER
PUMP
PORT
0
18
9
0
9
18
RADIUS (cm)
RF

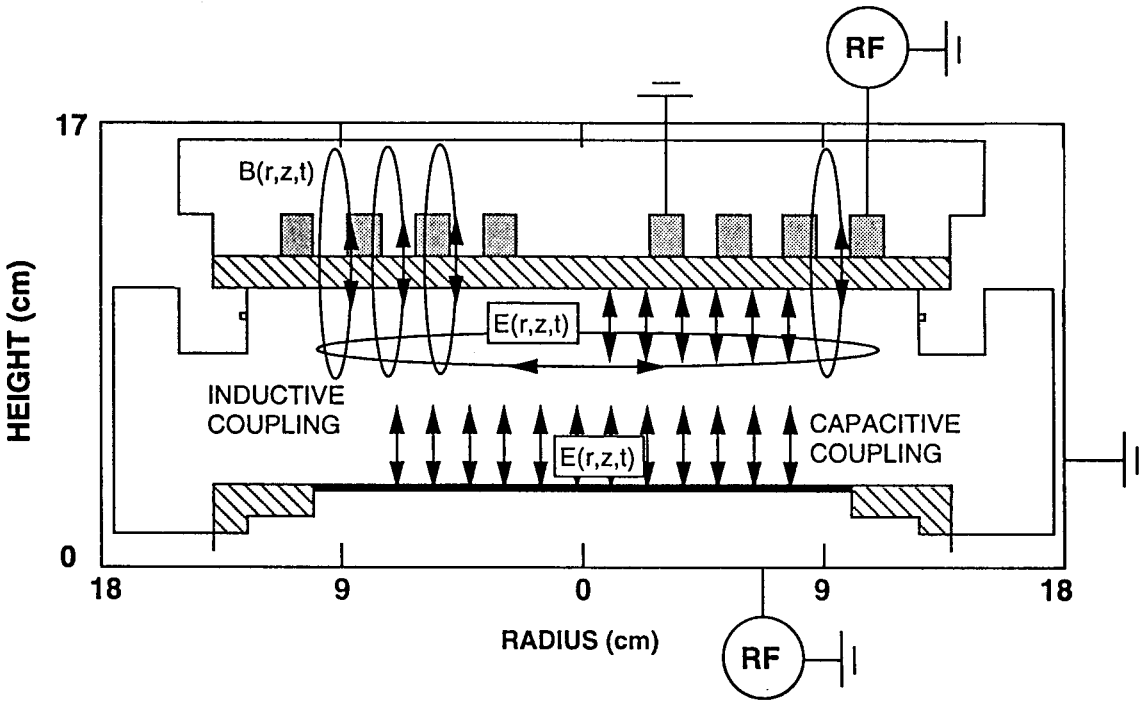
RF
17
B(r,z,t)
E(r,z,t)
INDUCTIVE
COUPLING
E(r,z,t)
CAPACITIVE
COUPLING
HEIGHT (cm)
0
18
9
0
9
18
RADIUS (cm)
RF

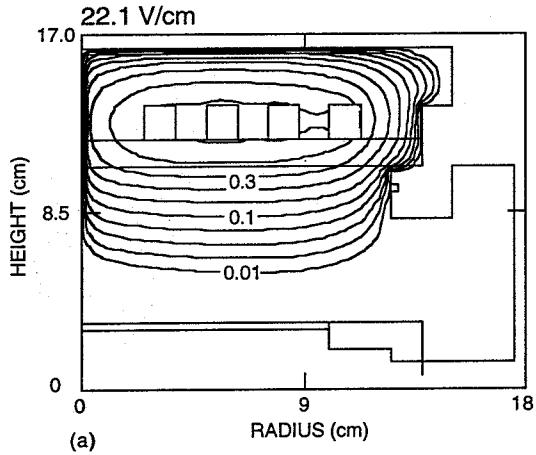

ELECTRIC FIELD

ELECTRON SOURCE (e-IMPACT)

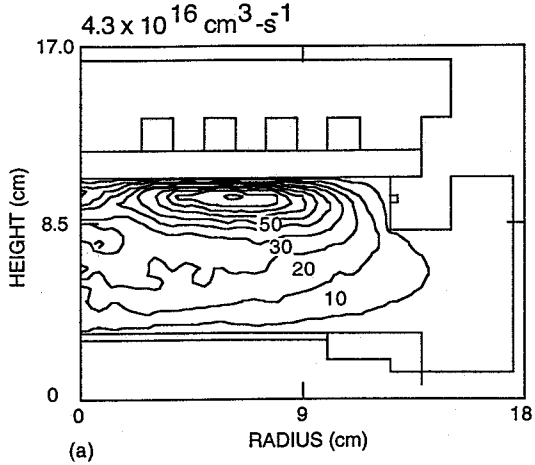

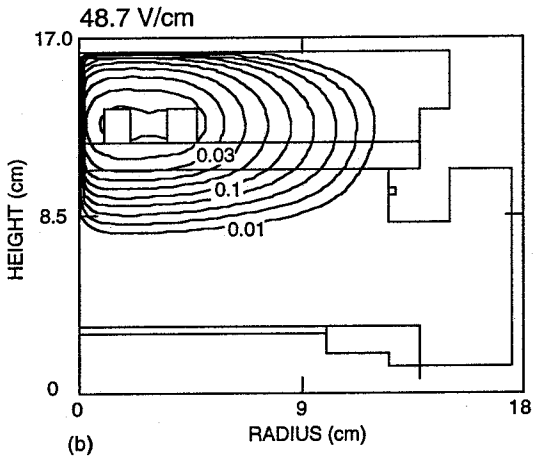

5 mTorr, 700 W
Ar/Cl2 = 70/30

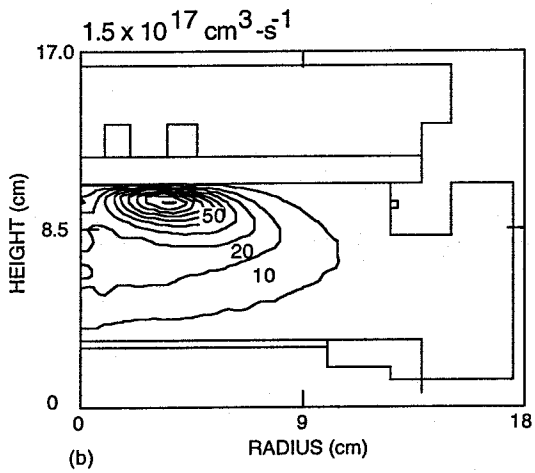

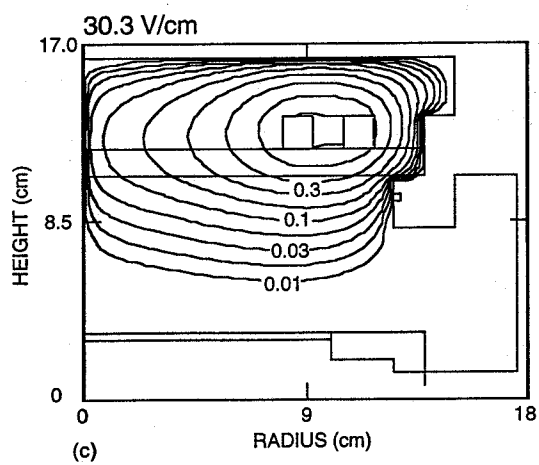

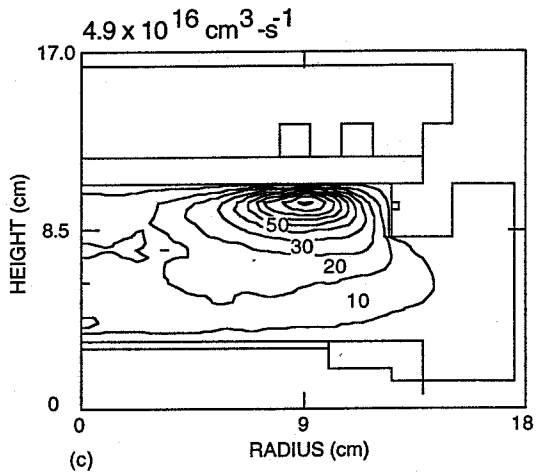

TYPICAL PLASMA PROCESSING REACTOR

- The typical low pressue (< 10s - 100s mTorr) plasma processing reactor is powered by inductive and capactive coupling, and my have auxiliary static magnetic fields.

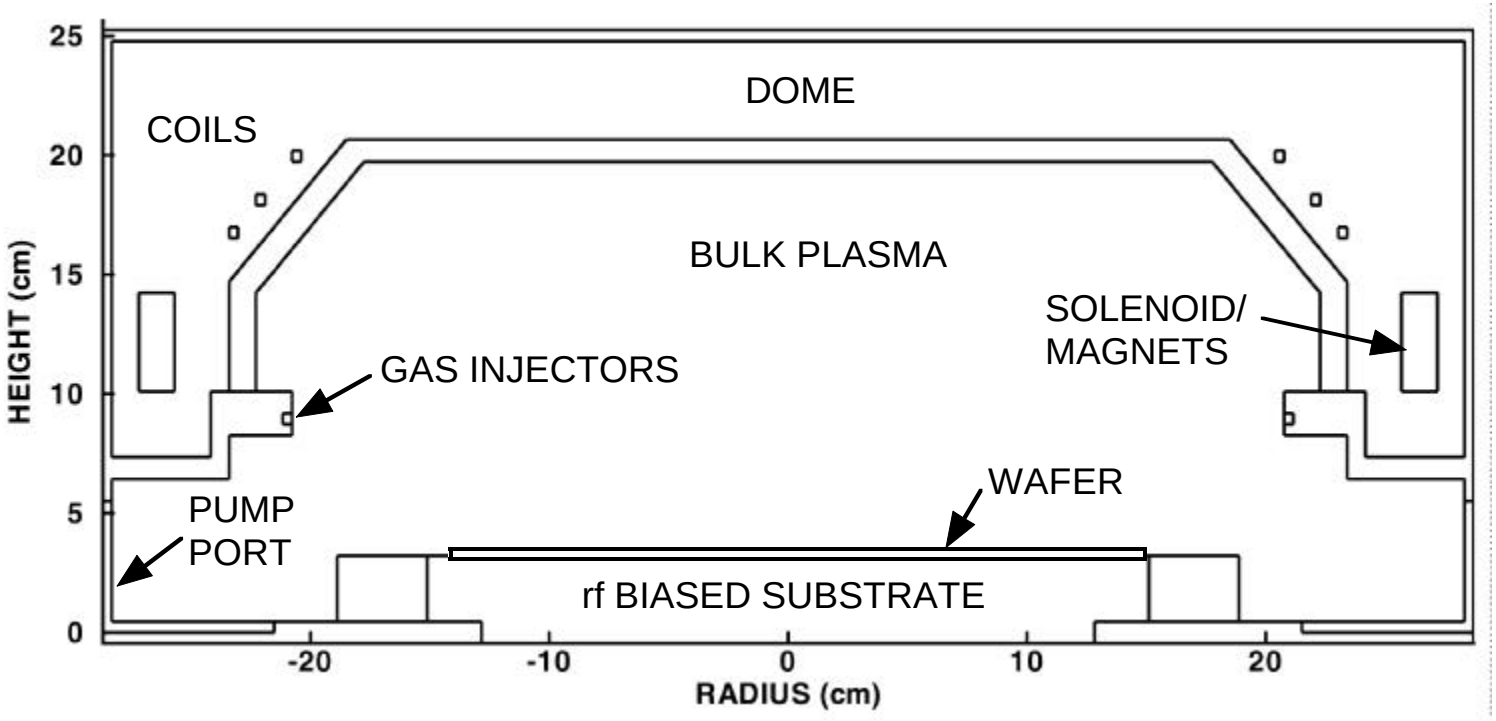

APPLIED MATERIALS DECOUPLED PLASMA SOURCE (DPS)

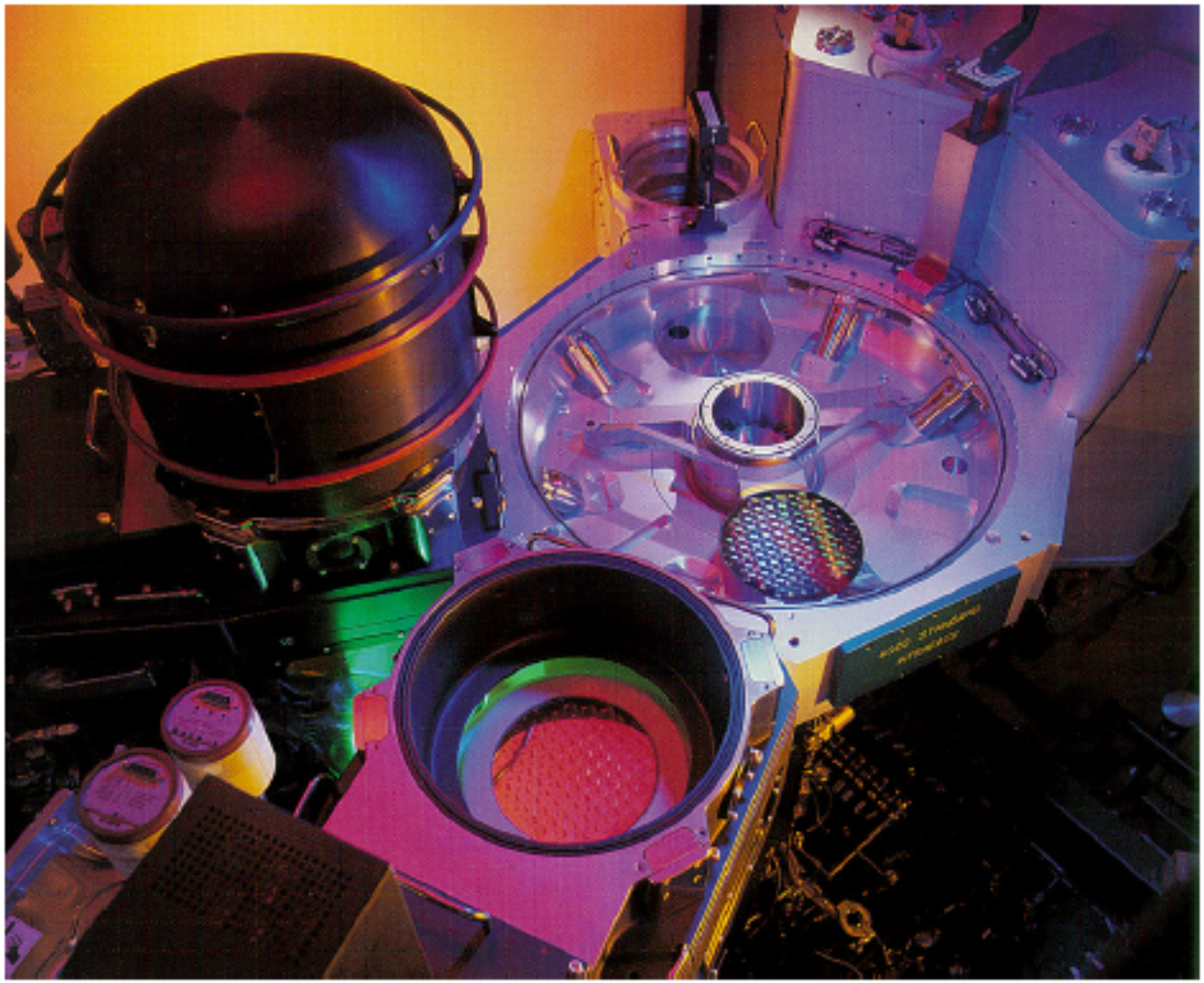

APPLIED MATERIALS DECOUPLED PLASMA SOURCE (DPS)

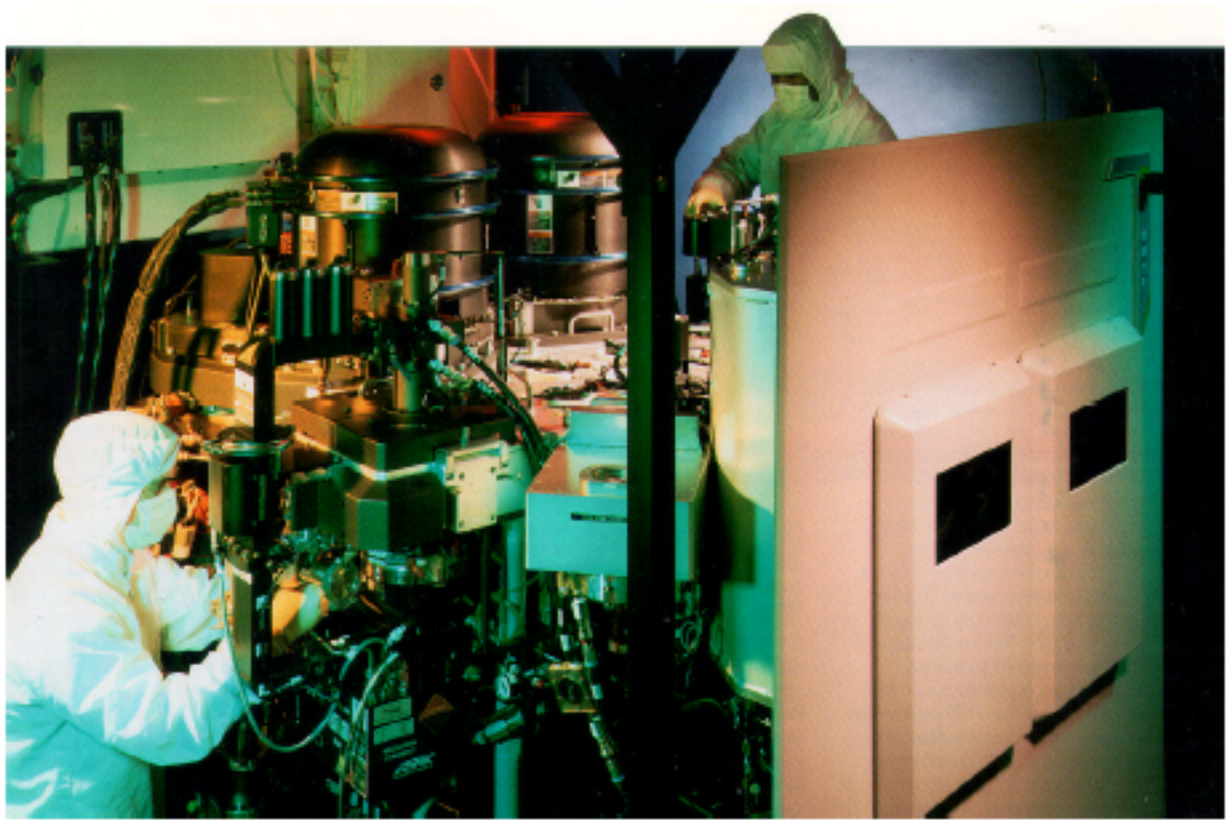

PHYSICS TO BE ADDRESSED

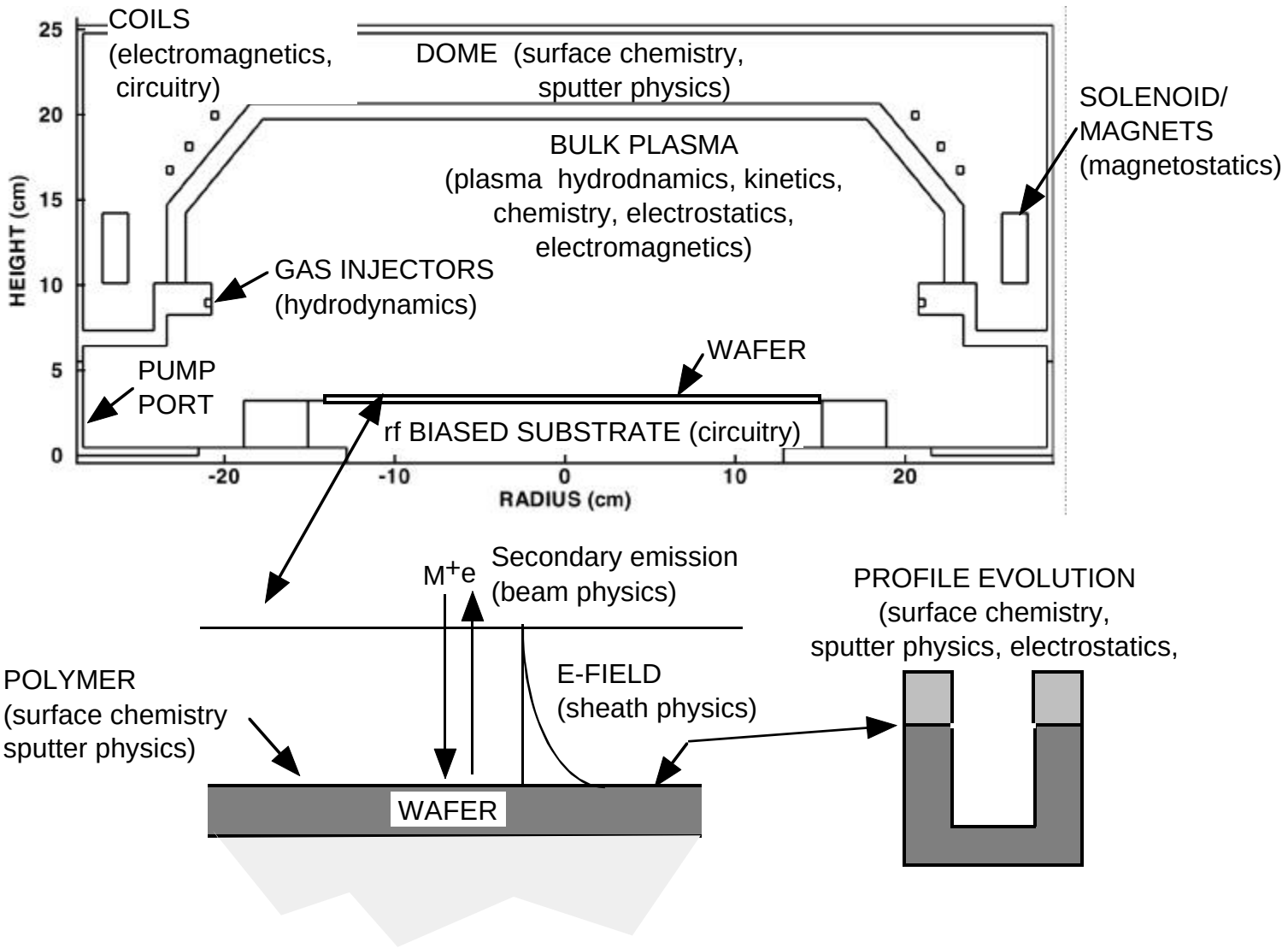

WALK THROUGH: Ar/Cl_2 ICP TOOL

- **The general properties of an Ar/Cl_2 inductively coupled plasma tool will be examined.**

- **The inductively coupled electromagnetic fields have a skin depth of 3-4 cm.**

- **Absorption of the fields produces power deposition in the plasma.**

- **Electric Field (max = 6.3 V/cm)**

- **Ar/Cl_2 = 80/20**
- **20 mTorr**
- **1000 W ICP**
- **250 V bias, 2 MHz (260 W)**

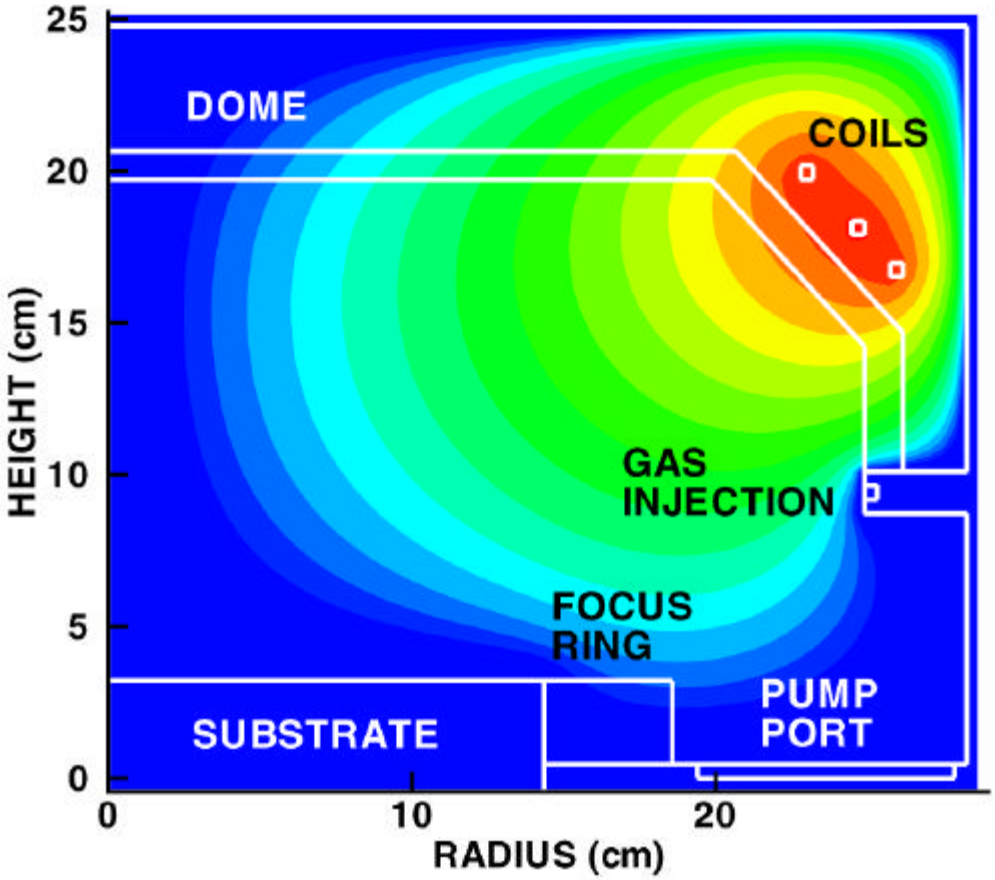

Ar/Cl_2 ICP TOOL: POWER AND ELECTRON TEMPERATURE

- **Power deposition from the inductive fields results in electron heating.**
- **At 2 MHz, power from the capacitive fields produces ion acceleration with little electron heating.**

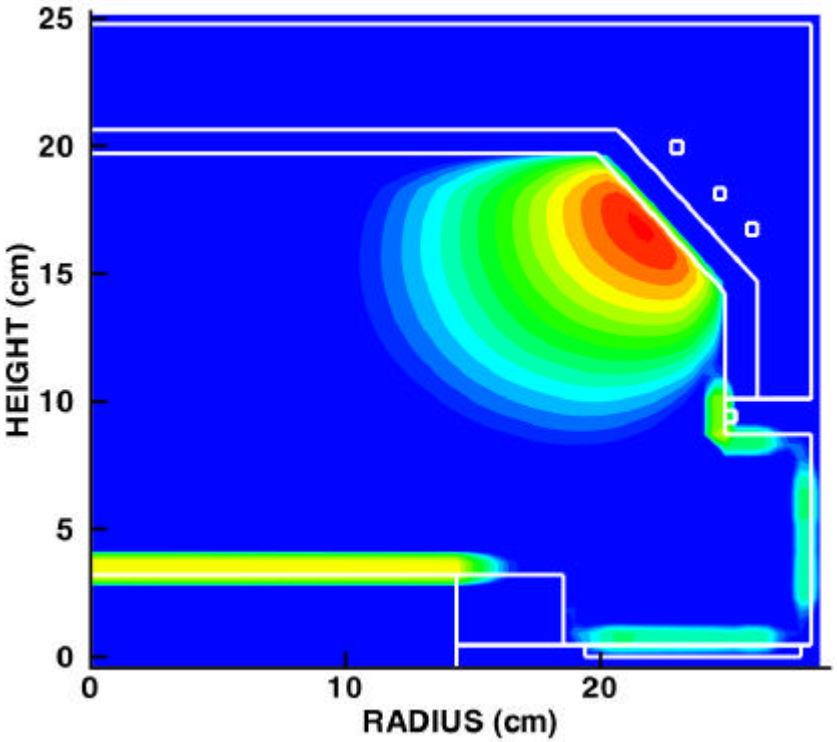

Power Deposition (max = 0.91 W/cm^3)

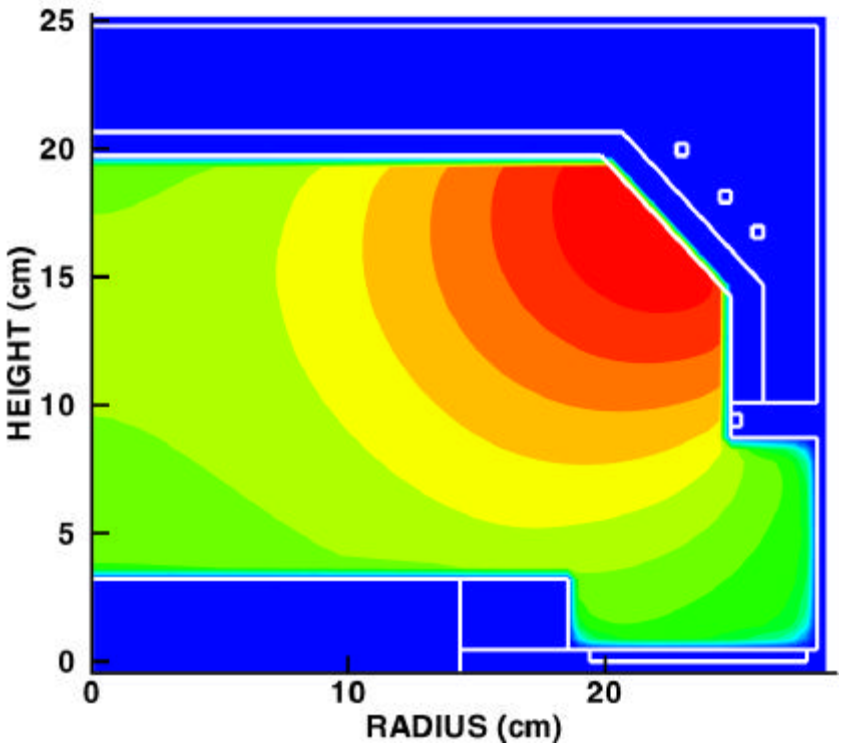

Electron Temperature (max = 5 eV)

- **Ar/Cl_2 = 80/20, 20 mTorr, 1000 W ICP, 250 V , 2 MHz bias (260 W)**

Ar/Cl_2 ICP TOOL: IONIZATION

- **Electron impact ionization by the bulk electrons heated by the inductively coupled fields dominates.**
- **Ionization by sheath accelerated beam electrons is less important due to their long mean-free-paths at the low operating pressure.**

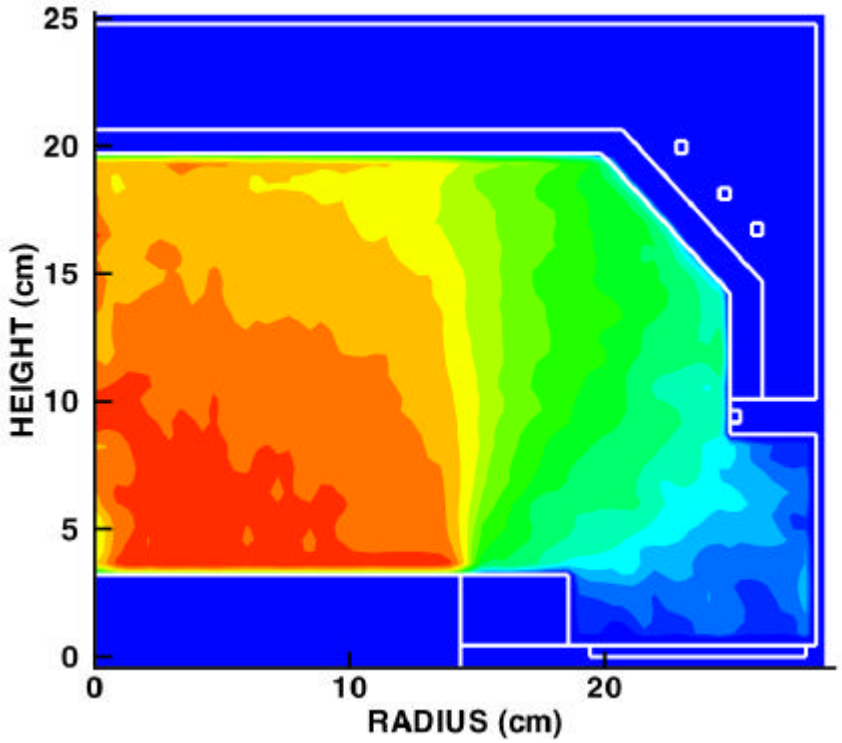

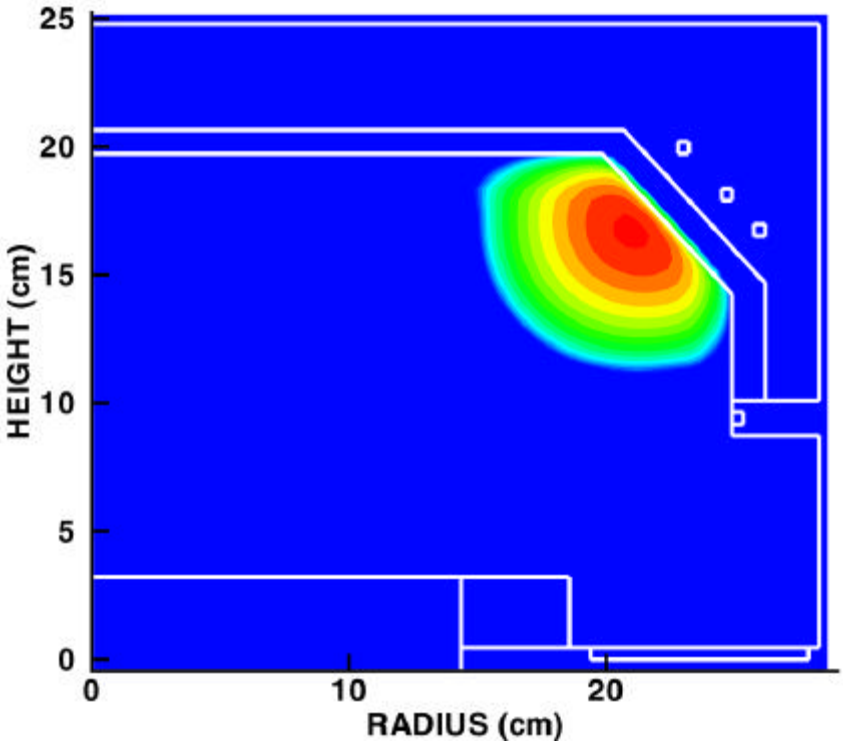

Beam ionization (max = 1.3 x 10^{14} /cm^3-s)

Bulk ionization (max = 5.4 x 10^{15} /cm^3-s)

- **Ar/Cl_2 = 80/20, 20 mTorr, 1000 W ICP, 250 V , 2 MHz bias (260 W)**

Ar/Cl_2 ICP TOOL: POSITIVE ION DENSITY

- The diffusion of plasma from the remote sources produces a fairly uniform positive ion density in the vicinity of the substrate.
- In general, better uniformity is obtained with a bias than without.

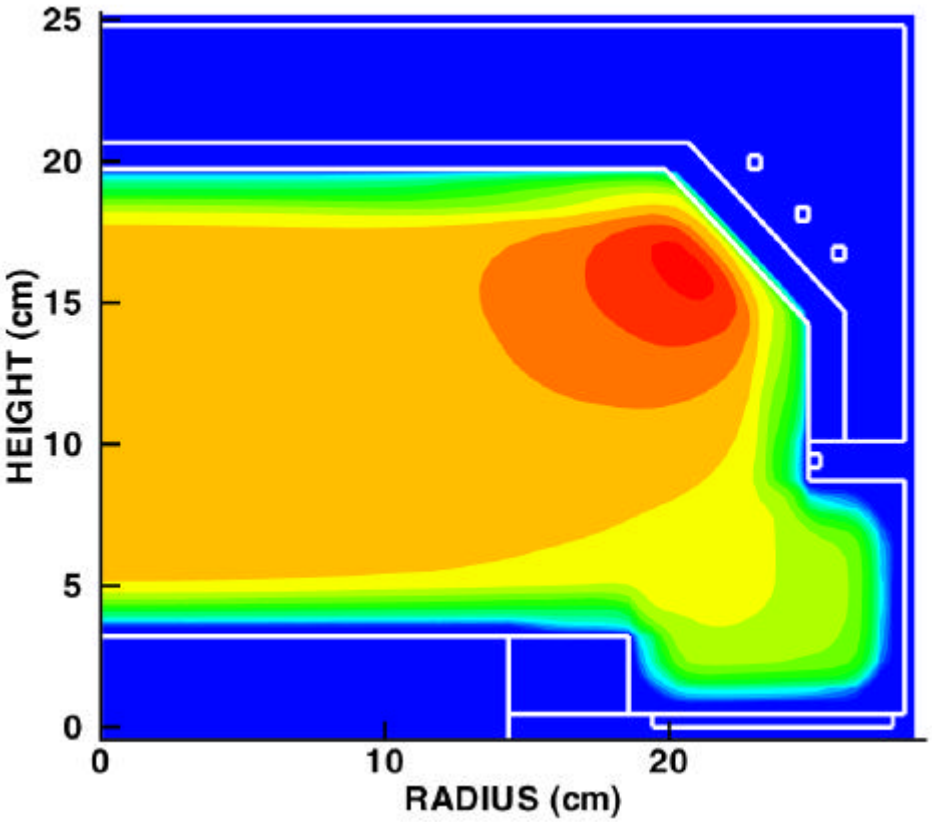

Positive Ion Density
(max = 1.8 x 10^{11} /cm^3-s)

- Ar/Cl_2 = 80/20, 20 mTorr, 1000 W ICP, 250 V , 2 MHz bias (260 W)

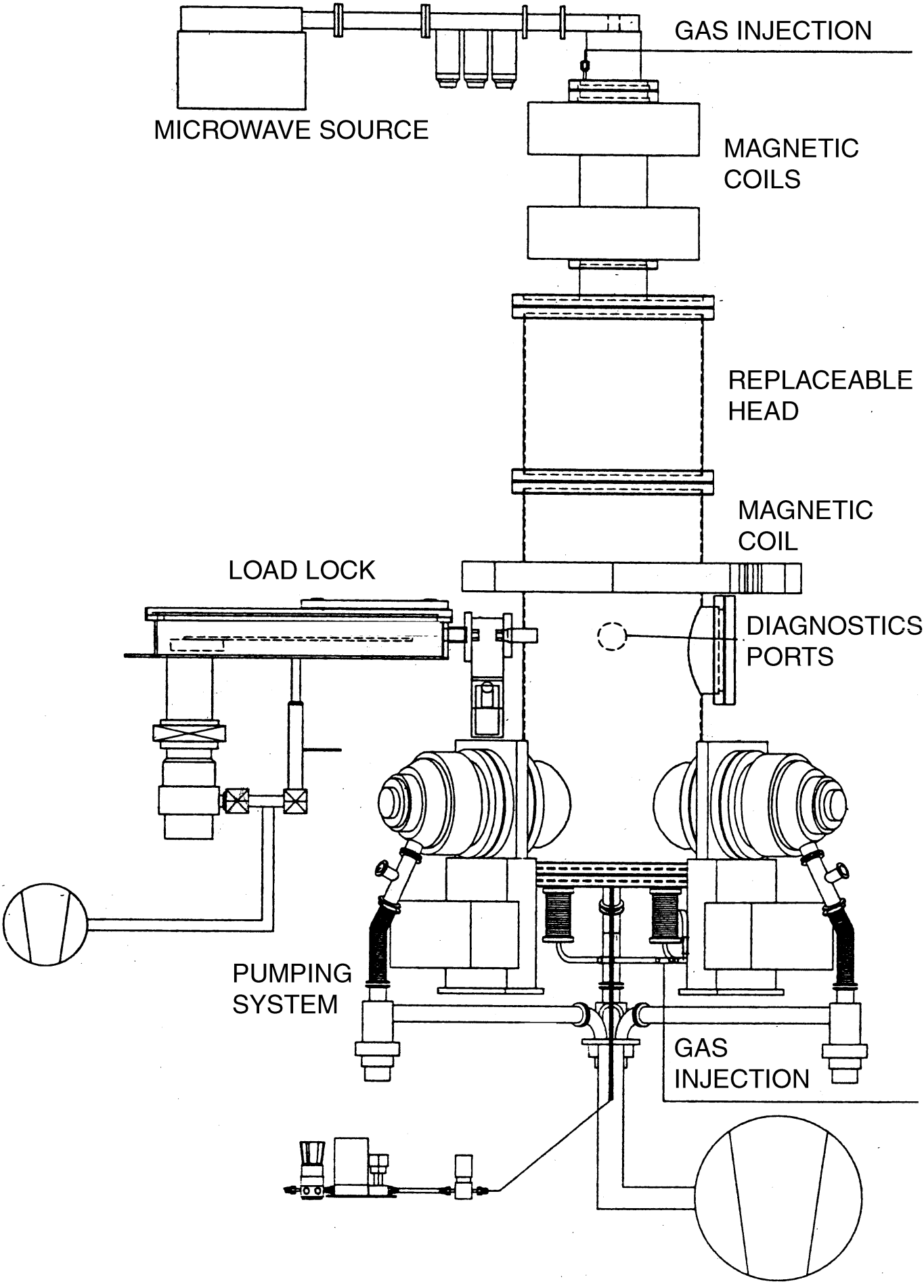
GAS INJECTION
MICROWAVE SOURCE
MAGNETIC COILS
REPLACEABLE HEAD
MAGNETIC COIL
LOAD LOCK
DIAGNOSTICS PORTS
PUMPING SYSTEM
GAS INJECTION

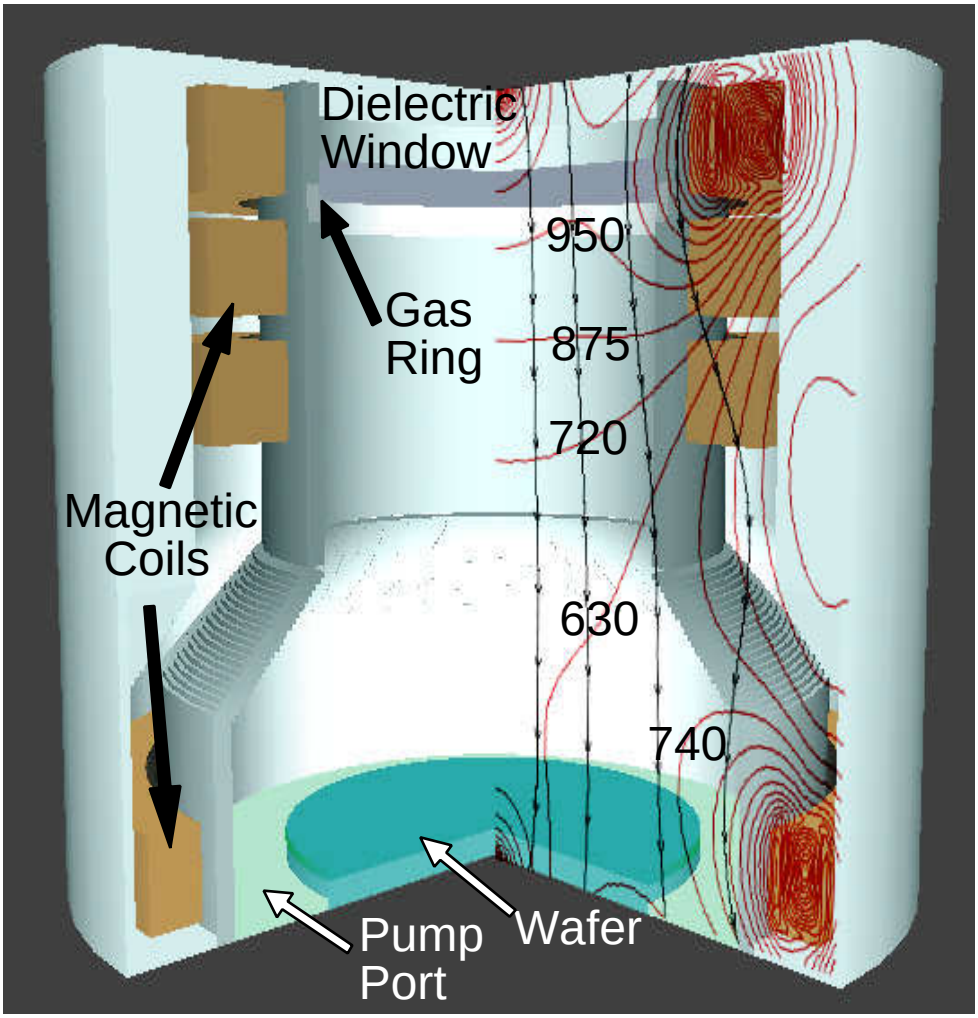
Dielectric
Window
950
Gas
Ring
875
720
Magnetic
Coils
630
740
Pump
Port
Wafer

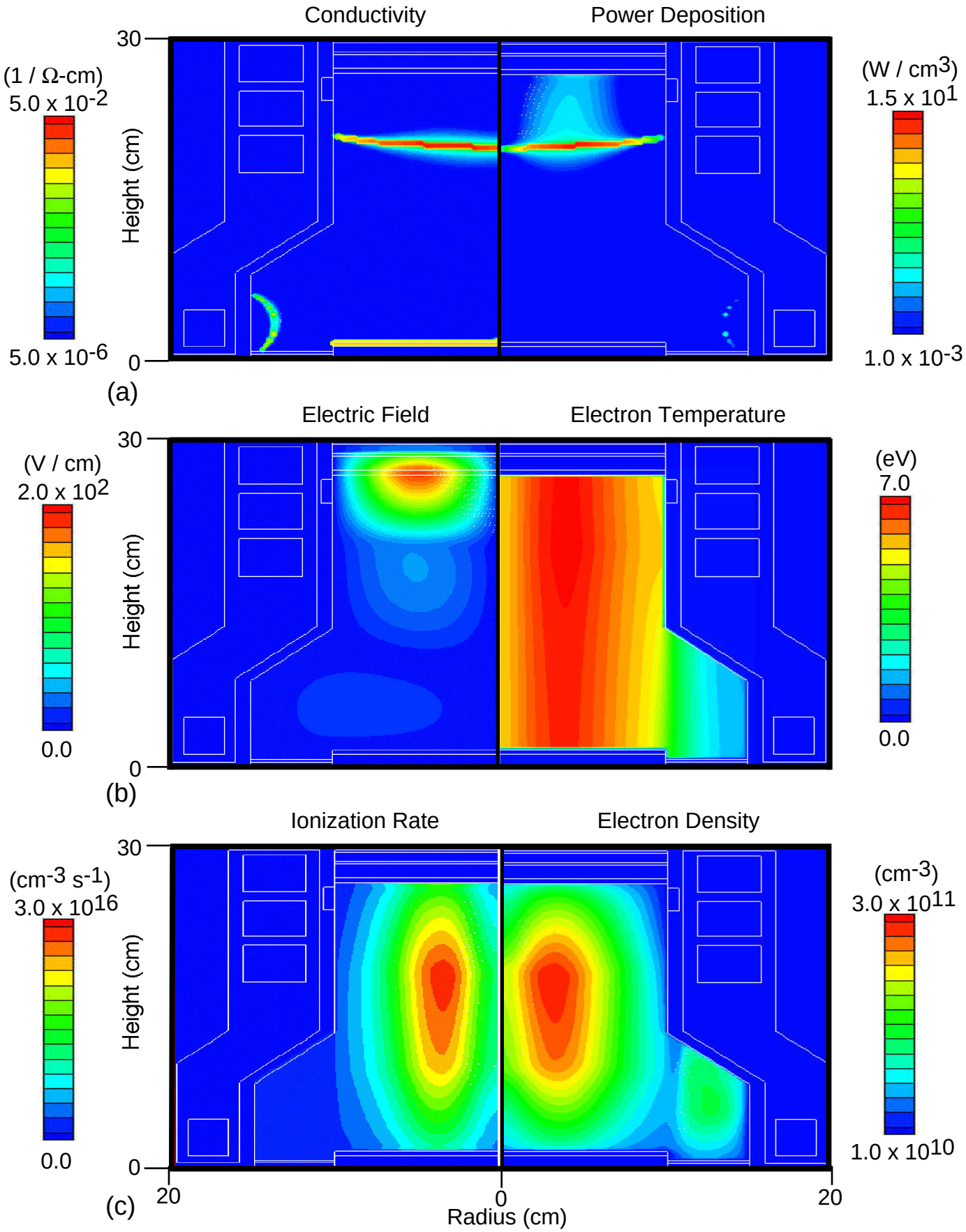
Conductivity
Power Deposition
(1 / Ω-cm)
5.0 x 10-2
5.0 x 10-6
(W / cm3)
1.5 x 101
1.0 x 10-3
30
0
Height (cm)
(a)
Electric Field
Electron Temperature
(V / cm)
2.0 x 102
0.0
(eV)
7.0
0.0
(b)
Ionization Rate
Electron Density
(cm-3 s-1)
3.0 x 1016
0.0
(cm-3)
3.0 x 1011
1.0 x 1010
20
0
Radius (cm)
(c)

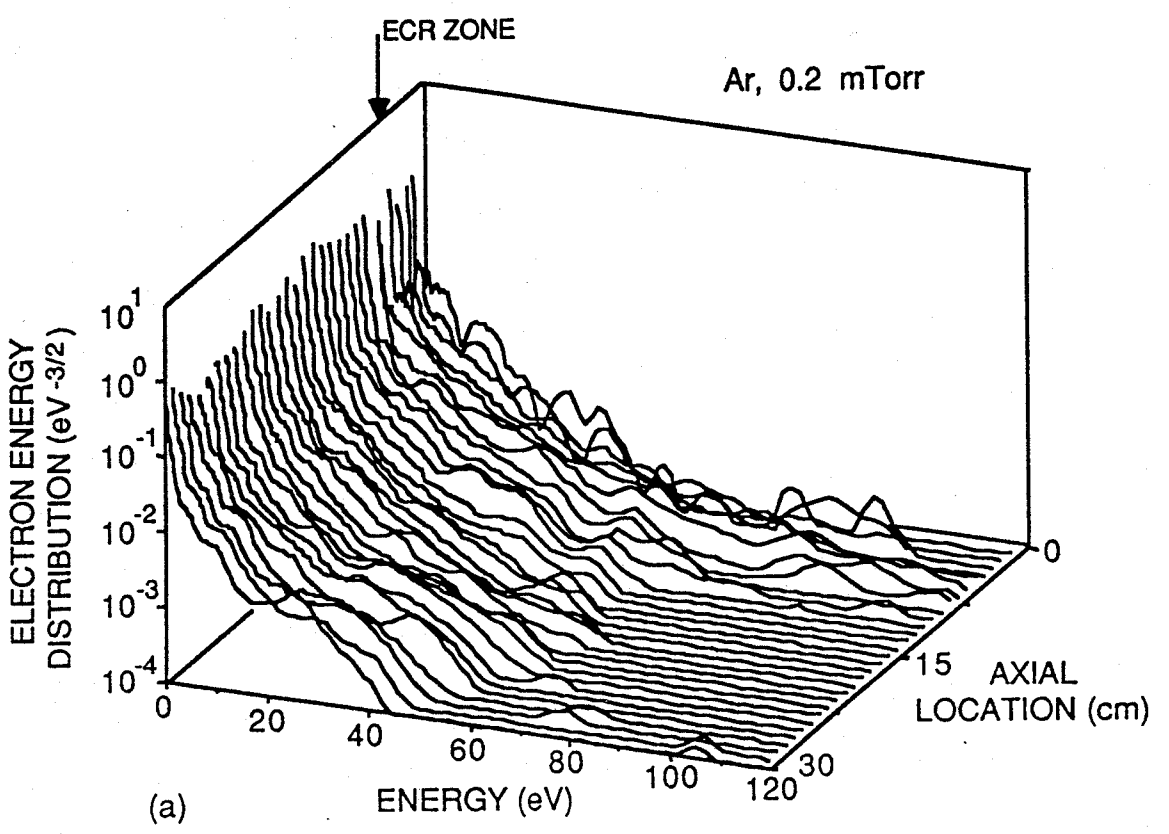
ECR ZONE
Ar, 0.2 mTorr
ELECTRON ENERGY DISTRIBUTION (eV-3/2)
10^1
10^0
10^-1
10^-2
10^-3
10^-4
0
20
40
60
80
100
120
ENERGY (eV)
0
15
30
AXIAL LOCATION (cm)
(a)

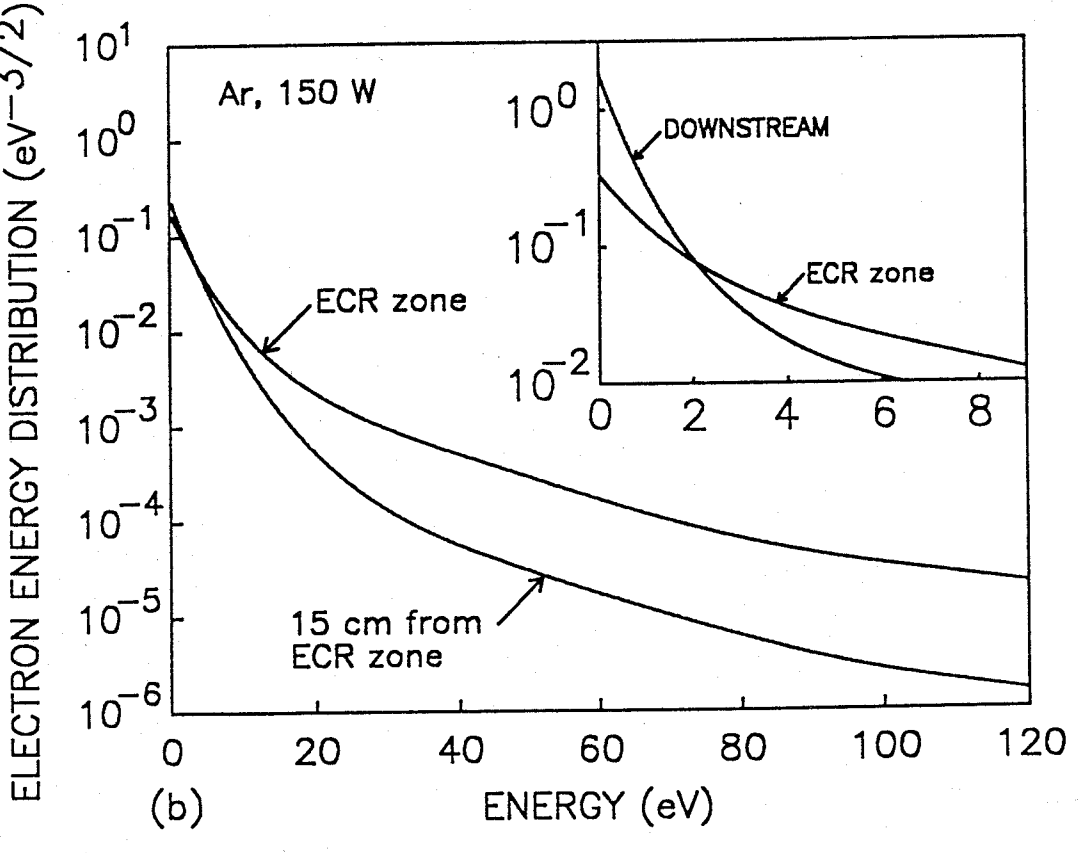
ELECTRON ENERGY DISTRIBUTION (eV−3/2)
Ar, 150 W
ECR zone
15 cm from ECR zone
DOWNSTREAM
ECR zone
10^1
10^0
10^−1
10^−2
10^−3
10^−4
10^−5
10^−6
0
20
40
60
80
100
120
ENERGY (eV)
(b)

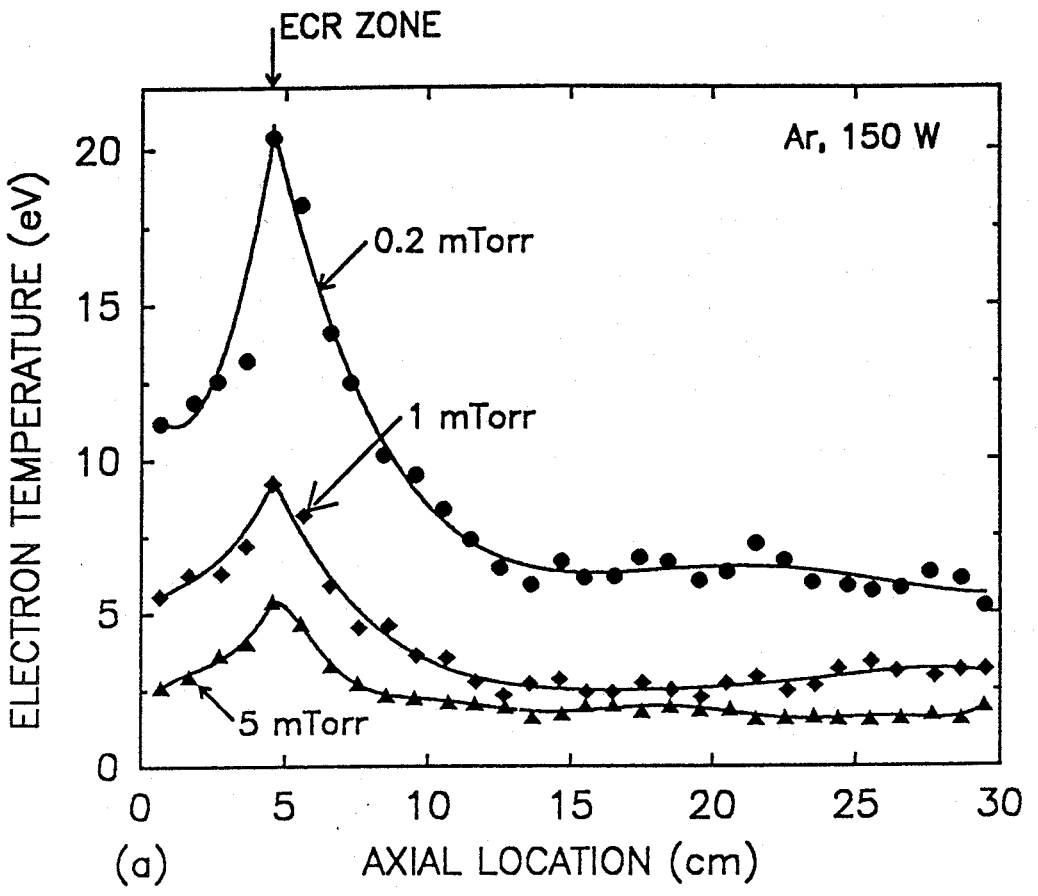
ECR ZONE
Ar, 150 W
0.2 mTorr
1 mTorr
5 mTorr
ELECTRON TEMPERATURE (eV)
0
5
10
15
20
0
5
10
15
20
25
30
(a)
AXIAL LOCATION (cm)

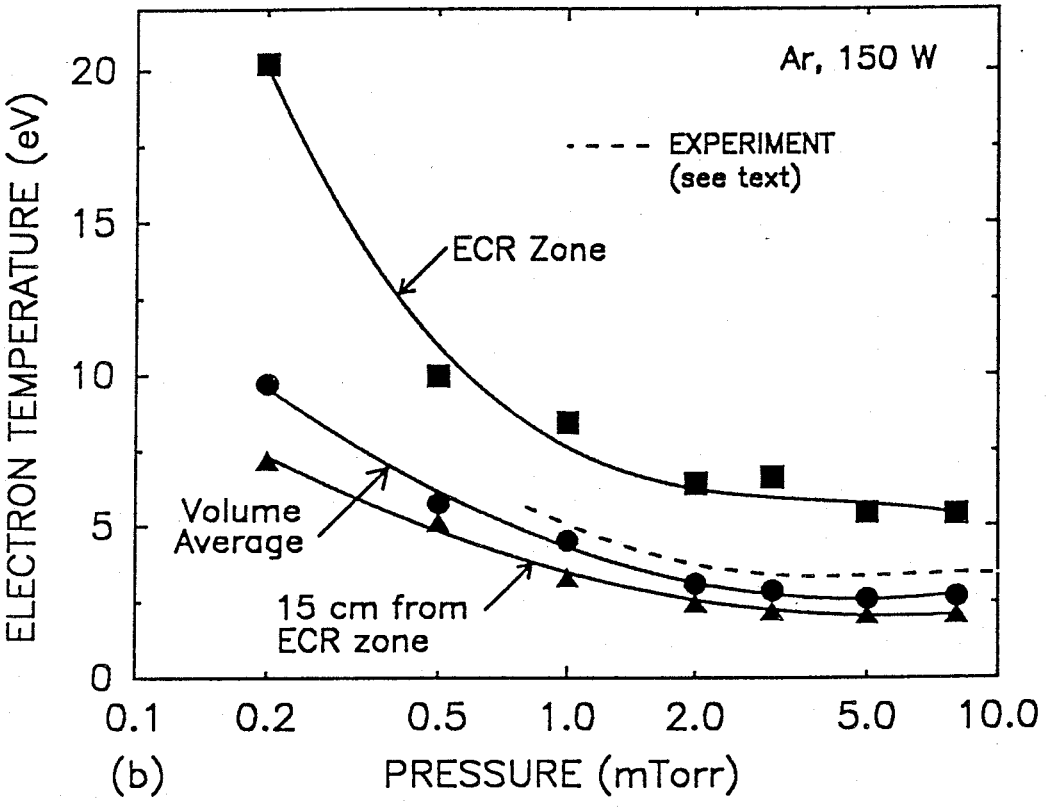
Ar, 150 W
EXPERIMENT
(see text)
ECR Zone
Volume
Average
15 cm from
ECR zone
ELECTRON TEMPERATURE (eV)
0
5
10
15
20
0.1
0.2
0.5
1.0
2.0
5.0
10.0
(b)
PRESSURE (mTorr)

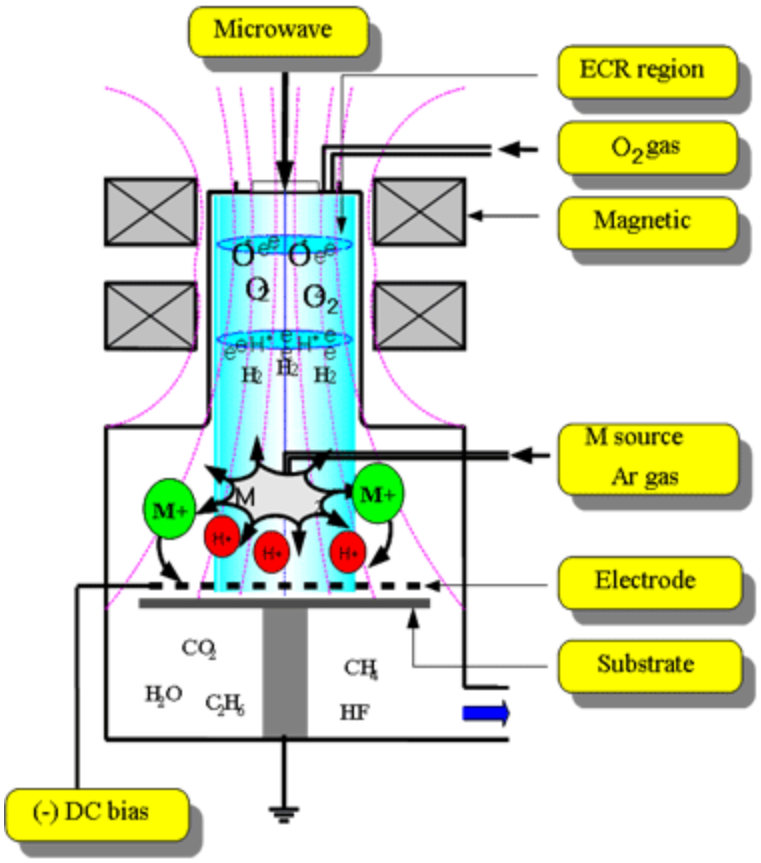

Microwave is radiated into the plasma and electrons can be heated resonantly when microwave frequency equals the cyclotron frequency, they have high energy level in this region at the same time.

Ions in the plasma are further ionized up to higher charge states through successive collisions with electrons

ECR plasma ion density $> 10^{12}$ cm^{-3}

http://www.epon.co.kr/

IRIS (Ion Source for Radioactive ISotopes)

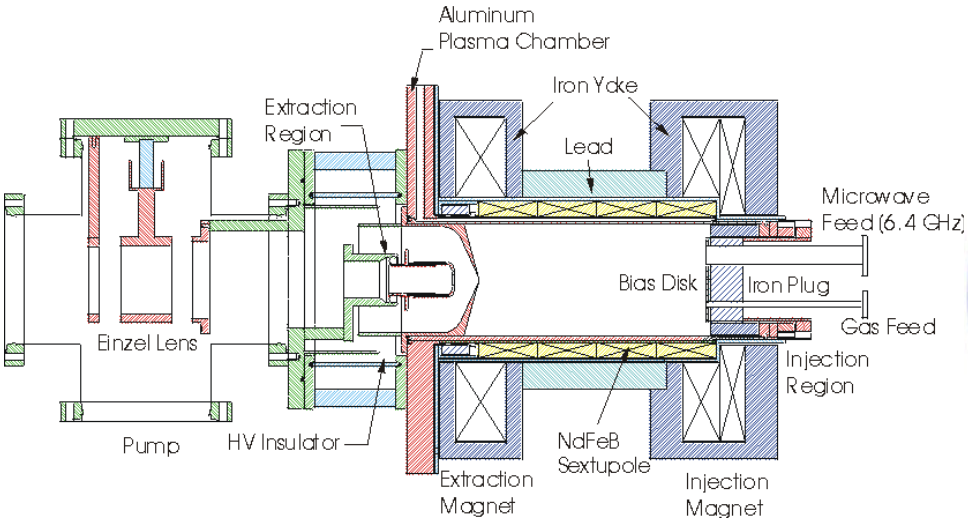

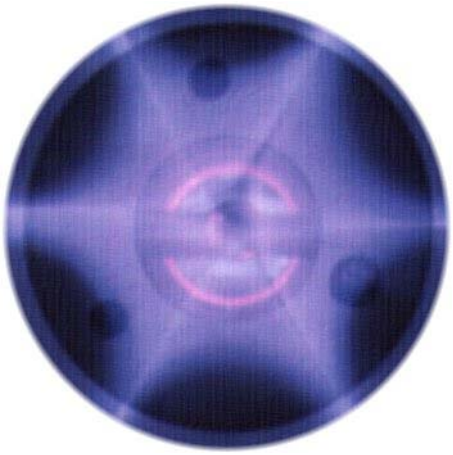

http://ecrgroup.lbl.gov/

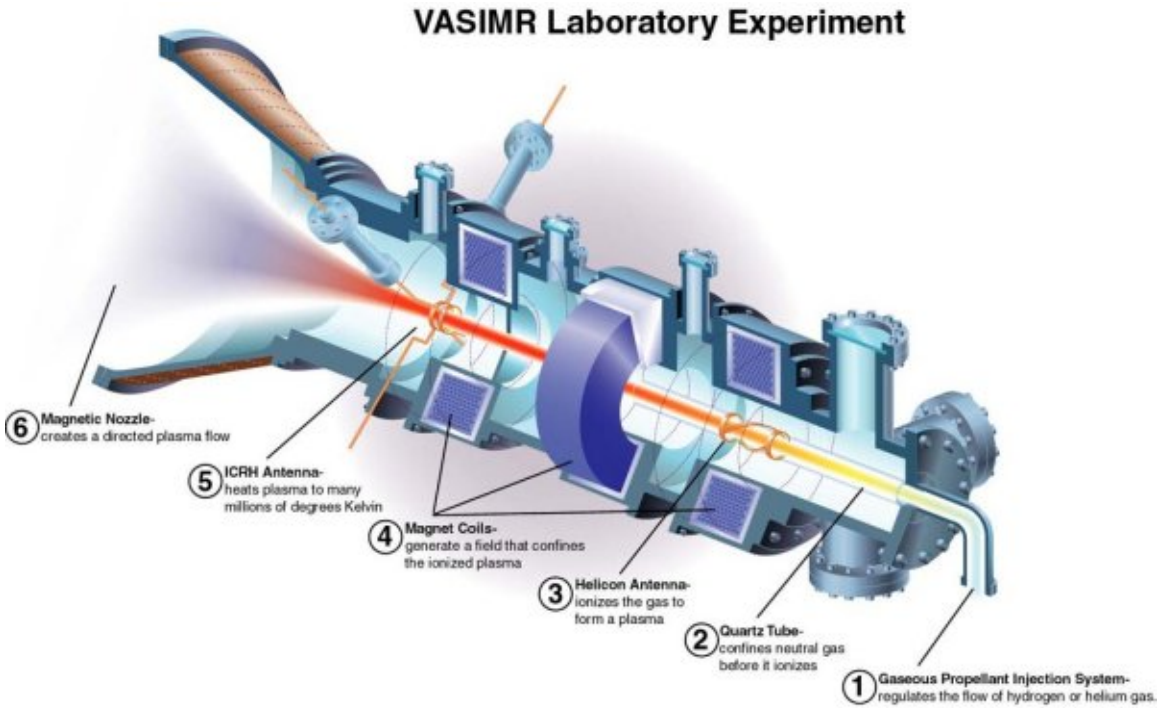

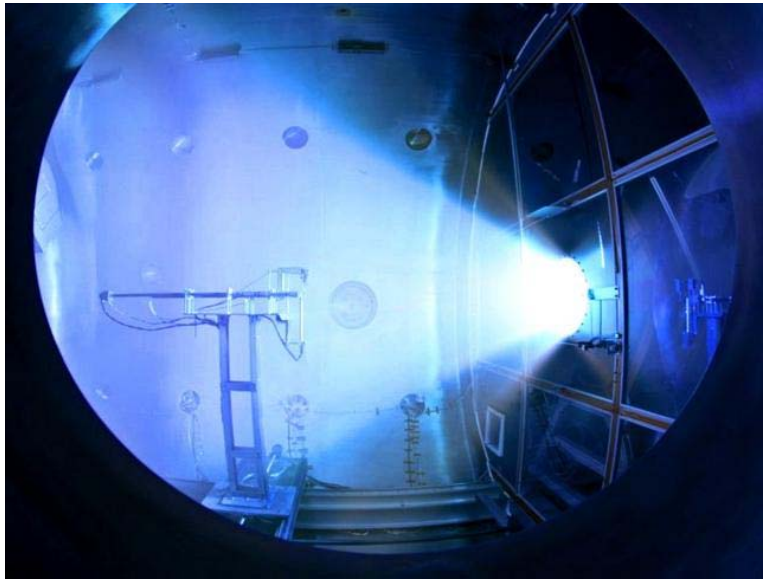

The Variable Specific Impulse Magnetoplasma Rocket (VASIMR®) http://www.adastrarocket.com/aarc/VASIMR

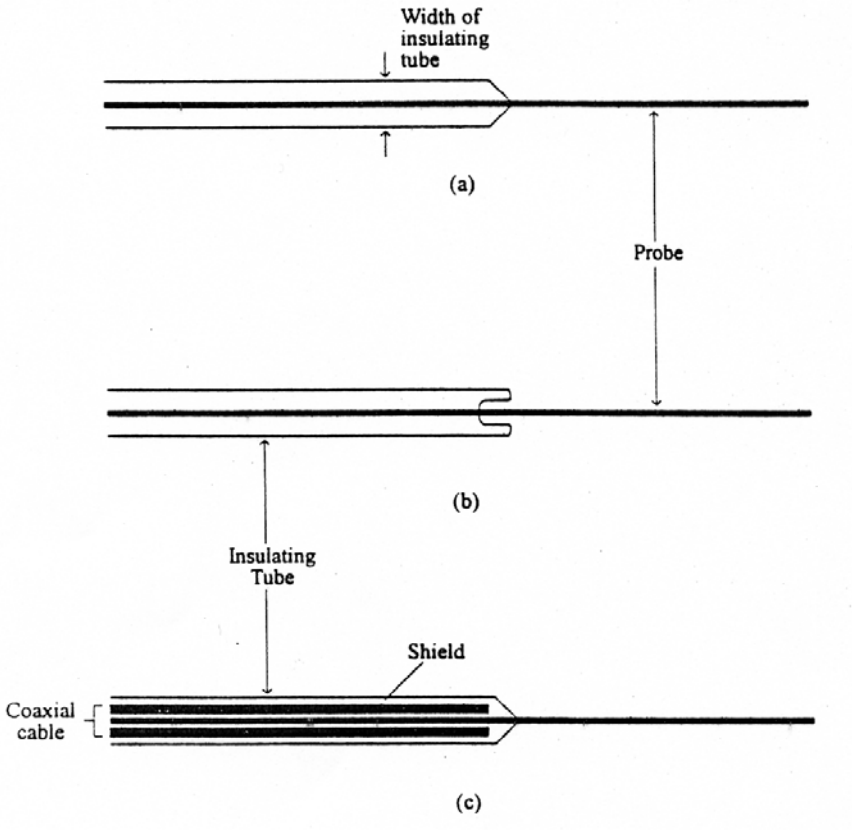

Probe Designs

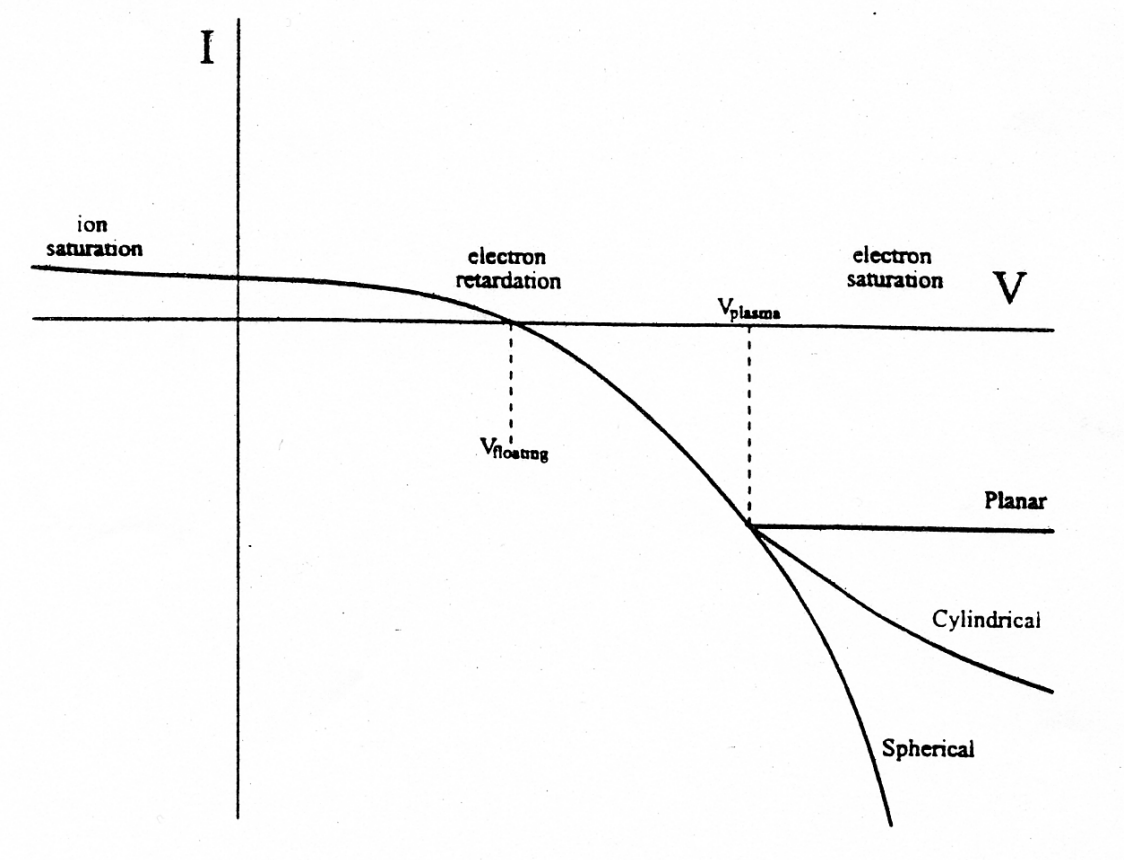

Probe Characteristics

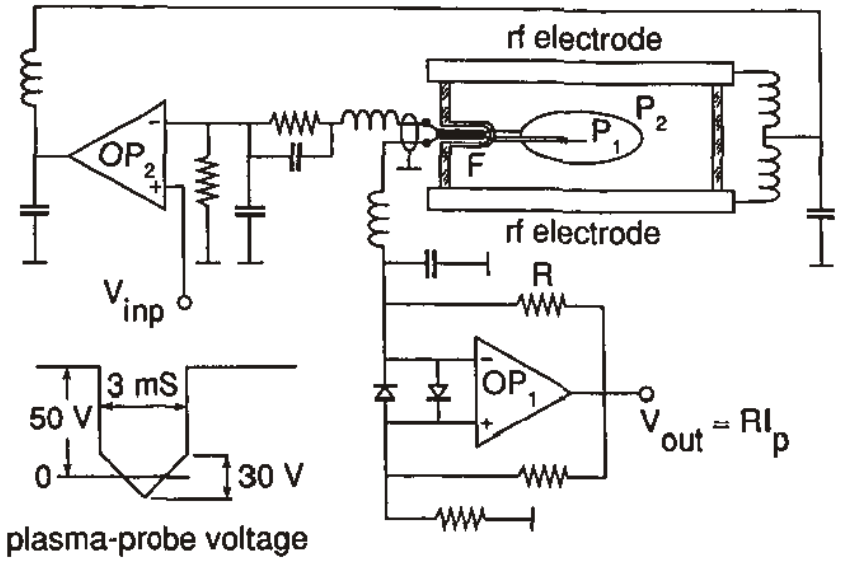

Figure 3. Simplified diagram of the probe measuring circuit.

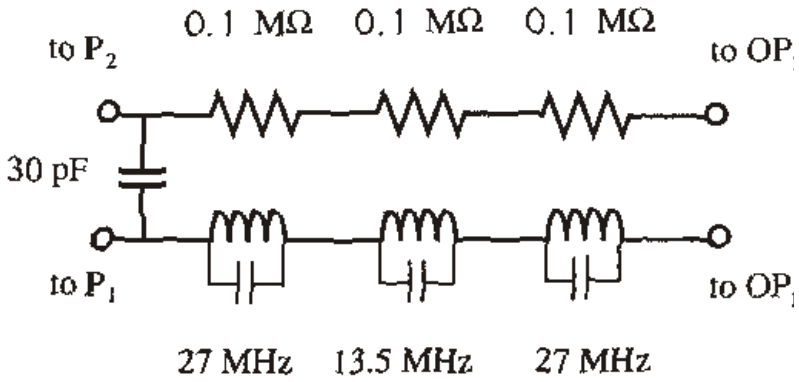

Probe compensating filters

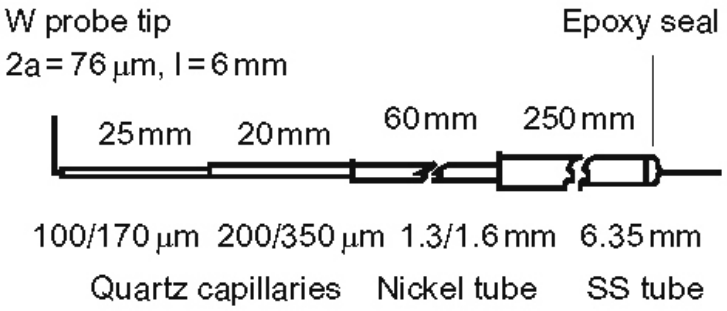

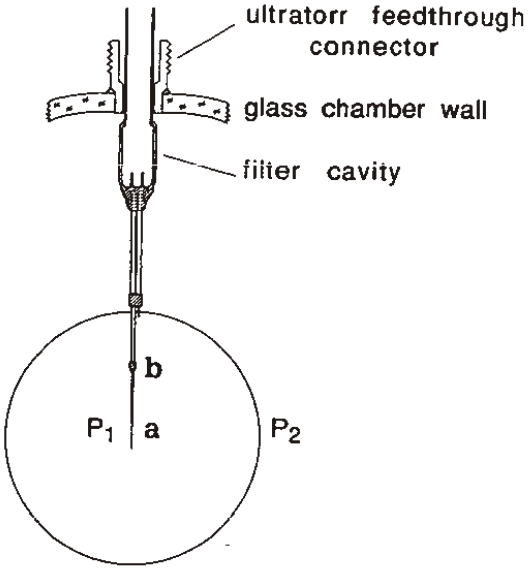

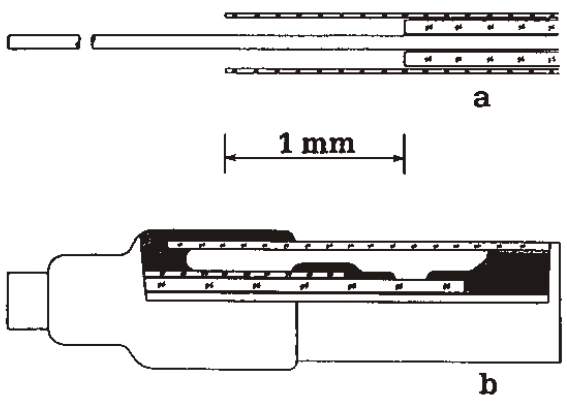

Figure 5. Probe system. The positions a and b are given magnified at the bottom to show a shielding sleeve (position a) and epoxy vacuum seals (cross hatched, position b).

V. A. Godyak, Plasma Source Sci. Technol 1, 36 (1992)
V. A. Godyak, PSST 11, 525 (2002)

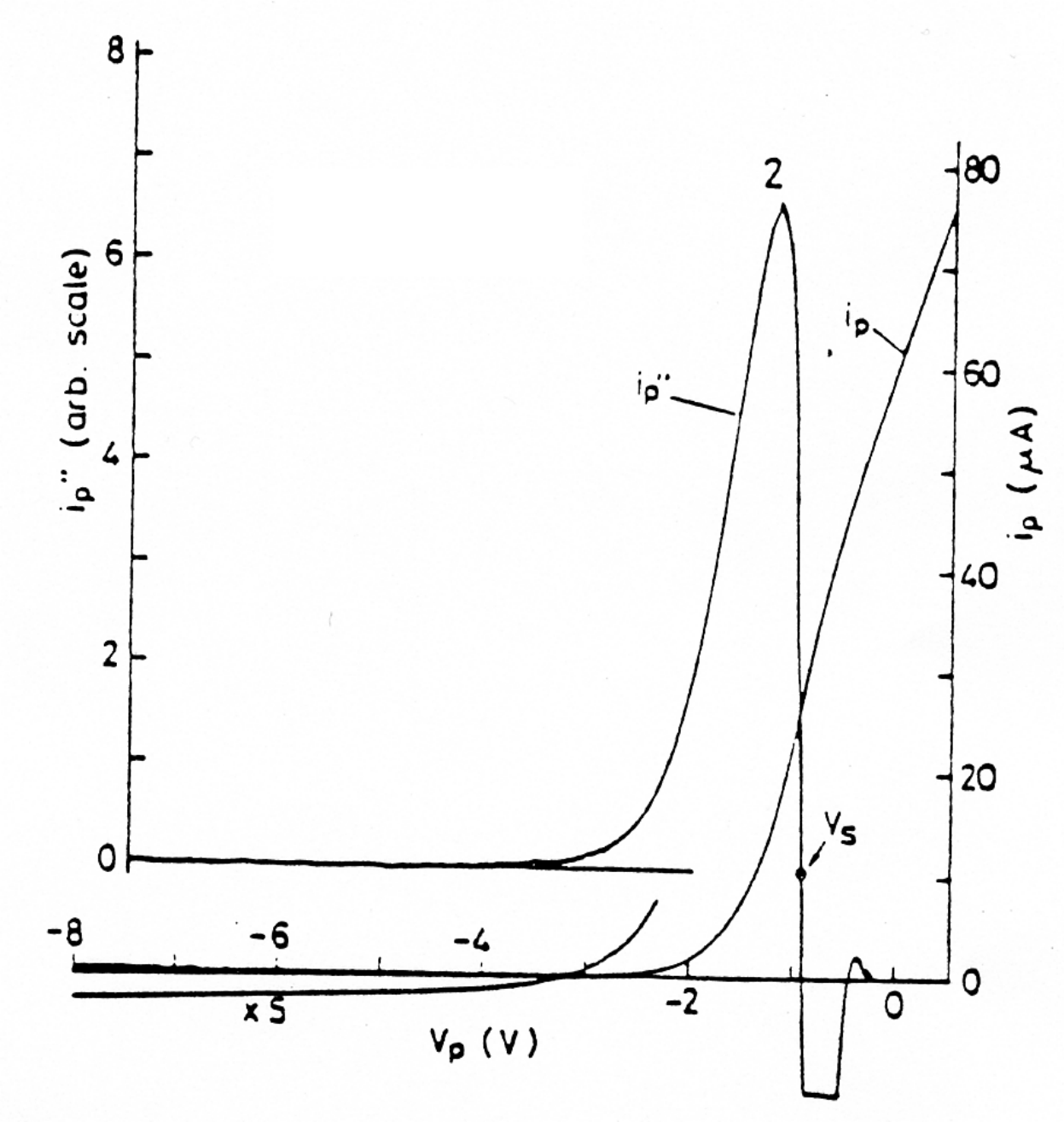

Probe Characteristic and Electron Energy Distribution

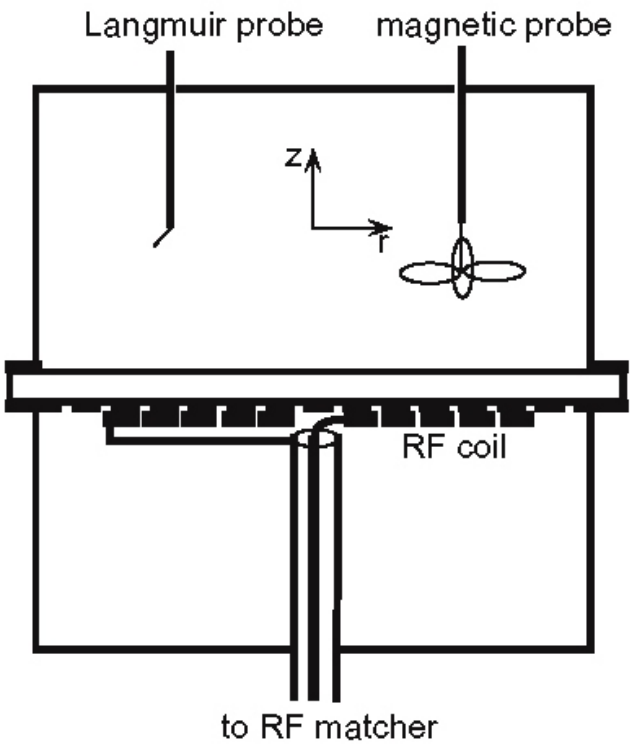

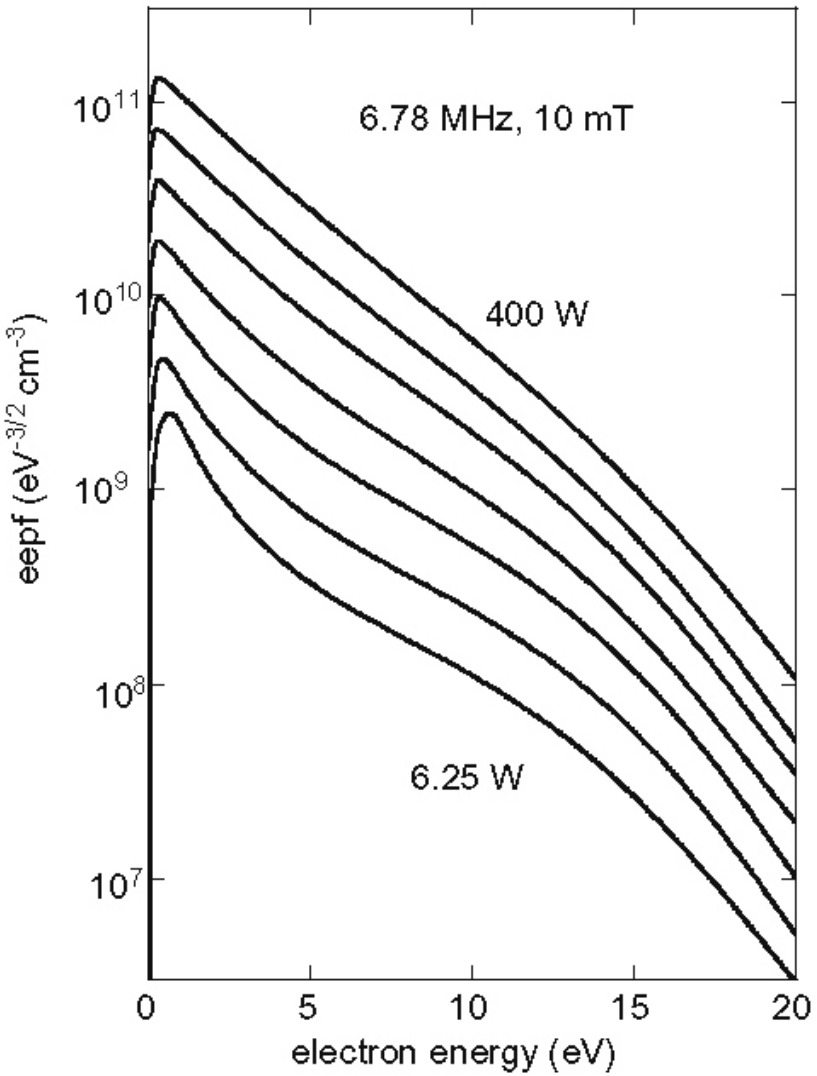

V. A. Godyak, Plasma Source Sci. Technol 11, 525 (2002)